Thesis submitted for the degree of
Doctor of Philosophy

BLACK HOLES IN HOLOGRAPHY: STRUCTURE AND EFFECTS

Nejc Čeplak

Supervisor

Prof Rodolfo Russo

August 6, 2020

Centre for Research in String Theory
School of Physics and Astronomy
Queen Mary University of London

Staršem, za vse.

Declaration

I, Nejc Čeplak, confirm that the research included within this thesis is my own work or that where it has been carried out in collaboration with, or supported by others, that this is duly acknowledged below and my contribution indicated. Previously published material is also acknowledged below.

I attest that I have exercised reasonable care to ensure that the work is original, and does not to the best of my knowledge break any UK law, infringe any third party's copyright or other Intellectual Property Right, or contain any confidential material.

I accept that the College has the right to use plagiarism detection software to check the electronic version of the thesis.

I confirm that this thesis has not been previously submitted for the award of a degree by this or any other university.

The copyright of this thesis rests with the author and no quotation from it or information derived from it may be published without the prior written consent of the author.

Signature:

Date: August 6, 2020

Details of collaboration and publications:

This thesis describes research carried out with my supervisor Rodolfo Russo in collaboration with Masaki Shigemori, which was published in [1]. This thesis also describes research carried out in collaboration with David Vegh and Kushala Ramdial, which was published in [2]. It also contains some unpublished material. Where other sources have been used, they are cited in the bibliography.

Abstract

This thesis consists of two parts.

In the first part we examine *pole-skipping*, a phenomenon observed in thermal Green's functions in quantum field theories with gravity duals. We begin by analysing the near horizon behaviour of bosonic fields in asymptotically Anti-de Sitter spacetimes before presenting the detailed analysis of fermionic fields in such backgrounds. We find that at negative imaginary Matsubara frequencies and special values of the wavenumber, there are multiple solutions to the bulk equations of motion that are ingoing at the horizon and thus the boundary Green's function is not uniquely defined. At these points in Fourier space a line of poles and a line of zeros of the correlator intersect and we derive the generic form of the Green's function near such locations. We then consider explicit examples where the correlator is known explicitly and also discuss the special case of a fermion with half-integer mass in the BTZ background.

In the second part we study the microscopic degrees of freedom of a particular black hole through the lens of the *fuzzball proposal*. In particular we construct a new class of smooth horizonless microstate geometries of the supersymmetric D1-D5-P black hole in type IIB supergravity. We first work in the $\mathrm{AdS}_3 \times S^3$ decoupling limit and use the fermionic symmetries of the theory to generate new momentum carrying perturbations in the bulk that have an explicit CFT dual description. We then use the supergravity equations to calculate the backreaction of these perturbations and find the full non-linear solutions both in the asymptotically AdS and asymptotically flat case. These new geometries have a simpler structure than the previously known superstrata solutions.

We conclude with a discussion and an outlook for possible generalizations of the results.

Acknowledgements

First and foremost, none of this would be possible without the eternal patience of my supervisor, Rodolfo Russo. I will not forget the many things I have learned from our discussions and I can only hope that one day I will be able to explain any topic with as much clarity and insight as you do. I will always be grateful for everything you have taught me.

I am also extremely thankful to be able to work with and learn from Masaki Shigemori. I hope that some of your enthusiasm, rigour, and above all knowledge has managed to permeate through to me (despite my stubborn attempts to resist). It has also been my pleasure to work with David Vegh. Thank you for introducing me to a brand new subject and leading me to a point where we could successfully finish one (and hopefully many more) project(s). I can only hope to emulate your endless supply of ideas. I would also like to thank Kushala Ramdial for the patience during our project and hope that I have not turned you away from physics.

I also had the privilege to collaborate and learn from other researchers. I would like to thank Alessandro Bombini, Andrea Galliani, Marcel Hughes and Alexander Tyukov for the discussions on projects that may not be finished yet. I would especially like to thank Stefano Giusto for his endless patience whilst tolerating my work on shared projects, despite my apparent inability to finish them. I would also like to thank Iosif Bena, Richard Davison, Sašo Grozdanov and Nick Warner for useful discussions along the way.

I would like to thank the PhD students of the CRST at Queen Mary for creating an enjoyable work environment which was both stimulating and relaxing at the same time. In particular I would like to thank Martyna Jones, Joe Hayling, Rodolfo Panerai, Arnau Koemans Collado, Zoltán Laczkó, Christopher Lewis–Brown, Ray Otsuki, Luigi Alfonsi, Nadia Bahjat–Abbas, Linfeng Li, Ricardo Stark–Muchão, Manuel Accettulli Huber, Rashid Alawadhi, Enrico Andriolo, Stefano De Angelis, Gergely Kantor, David Peinador Veiga, Rajath Radhakrishnan, Shun-Qing Zhang, George Barnes, Adrian Keyo Shan Padellaro and Sam Wikeley.

I also wish to thank other members of the CRST: David Berman, Matt Buican, Andreas Brandhuber, Gianluca Inverso, Ricardo Monteiro, Costis Papageorgakis, San-

jaye Ramgoolam, Bill Spence, Steve Thomas, Gabriele Travaglini, Congkao Wen, and Christopher White, for creating an inclusive and relaxed atmosphere in the department and their willingness to help with any issue at a moments notice.

I would also like to thank the people less related to physics for not letting me lose my grip on reality. Those include the QMBC, Giggs' bosons, and many more. Finally, a special thanks to Gemma for keeping up with me while also keeping me sane during the write up of this thesis.

Nazadnje, najlepša hvala vsem domačim. Brez vaše podpore in pomoči skozi vsa ta leta ne bi bil, kje sem danes. Hkrati pa vem, da se s tem zagovorom ne bo nič spremenilo in me boste vedno držali prizemljenega – *pa sej veš kaj mislim.*

This work was supported by a Queen Mary, University of London studentship.

Contents

1 Introduction **9**

1.1 History and Motivation . . . 9
1.2 Black Holes . . . 11
1.2.1 Entropy Puzzle . . . 15
1.2.2 Information Paradox . . . 16
1.3 String Theory and Supergravity . . . 18
1.3.1 Type IIB String theory . . . 20
1.3.2 Type IIB Supergravity . . . 22
1.4 AdS/CFT Correspondence . . . 26
1.4.1 Study of D3-Branes . . . 27
1.4.2 General Aspects of the Correspondence . . . 28
1.5 Structure of the Document . . . 33

2 Review of Pole Skipping **34**

2.1 Introduction and Motivation . . . 34
2.1.1 Retarded Green's Functions . . . 34
2.1.2 Prescription for Holographic Retarded Green's Functions . . . 36
2.1.3 Motivation for Pole-Skipping . . . 39
2.2 Pole Skipping for Scalar Fields . . . 40
2.2.1 Example: BTZ Black Hole . . . 43
2.3 Pole Skipping for Spin-2 Fields . . . 46

3 Pole Skipping for Fermion fields **50**

3.1 Motivation . . . 51
3.2 Minimally Coupled Fermion in the Bulk . . . 51
3.3 Pole-Skipping in Asymptotically AdS_3 Spaces . . . 53
3.3.1 Pole-Skipping at the Lowest Matsubara Frequency . . . 55
3.3.2 Pole-Skipping at Higher Matsubara Frequencies . . . 57
3.4 Pole-Skipping in Higher Dimensions . . . 63
3.4.1 Locating Pole-Skipping Points . . . 65
3.5 Green's Function Near the Pole-Skipping Points . . . 67

3.5.1 Near the Lowest Matsubara Frequency . . . 67
3.5.2 Near Higher Matsubara Frequencies . . . 69
3.6 Examples . . . 71
3.6.1 BTZ Black Hole . . . 71
3.6.2 Schwarzschild Black Hole in AdS_{D+2} . . . 78
3.7 Discussion . . . 79

4 Review of D1-D5-P System **82**
4.1 Brane Setup . . . 82
4.2 Gravity Description . . . 84
4.2.1 General Ansatz and System of Equations . . . 84
4.2.2 D1-D5-P Black Hole . . . 89
4.2.3 D1-D5 Black Hole . . . 92
4.3 Brane Description . . . 93
4.4 AdS/CFT Duality in the D1-D5 system . . . 97
4.5 D1-D5 CFT at the Orbifold Point . . . 98
4.5.1 Field Content . . . 98
4.5.2 Symmetry Currents and Current Algebra . . . 99
4.5.3 Twist Fields . . . 101
4.5.4 Construction of Multiplets in the NS Sector . . . 102
4.5.5 Spectral Flow . . . 104
4.5.6 AdS/CFT Dictionary . . . 105
4.6 Fuzzball Proposal . . . 107
4.6.1 Microstate Geometries . . . 109

5 Supercharging Superstrata **111**
5.1 Introduction . . . 111
5.2 CFT States . . . 112
5.3 Supergravity Setup . . . 115
5.3.1 Lunin-Mathur Geometries and the AdS/CFT Dictionary . . . 115
5.3.2 Seed solution . . . 117
5.3.3 Original Superstrata . . . 119
5.4 Killing Spinors of the $AdS_3 \times S^3$ Background . . . 122
5.4.1 Supersymmetry Variations . . . 123
5.4.2 The Killing Spinors . . . 126
5.5 Fermionically Generated Superstrata: Linear Analysis . . . 129
5.5.1 Variations of Fermionic Fields . . . 129
5.5.2 Solution-Generating Technique . . . 130
5.6 Non-Linear Completion . . . 133
5.6.1 Solving the Second-Layer Equations . . . 134

5.6.2 Regularity . . . 137
5.6.3 Asymptotically Flat Solution . . . 138
5.6.4 Conserved Charges . . . 139
5.7 Compendium of Formulas and Explicit Solutions . . . 141
5.7.1 Explicit Examples . . . 142
5.8 Conclusions . . . 144

6 Outlook **146**

A Conventions **150**
A.1 Form Conventions . . . 150
A.2 Spinor conventions . . . 151

B Details of the Pole-Skipping calculations **154**
B.1 Analysis in Asymptotically AdS_{D+2} Spacetimes . . . 154
B.2 Explicit Series Expansion Coefficients . . . 157

C Fermionic Green's Function for BTZ Black Hole **159**
C.1 Green's Function at Generic Conformal Dimension . . . 159
C.1.1 Retarded Green's Function . . . 159
C.1.2 Advanced Green's Function . . . 162
C.1.3 Equivalence at Matsubara Frequencies . . . 162
C.2 Green's Functions at Half-Integer Conformal Dimension . . . 163
C.2.1 Retarded Green's Function . . . 164
C.2.2 Advanced Green's Function . . . 165

D Explicit Results in the NS-NS Sector **166**
D.1 Identifying Killing Spinors and CFT Fermionic Generators . . . 166
D.2 Gravitino Variations Generated by $\zeta_-^{\alpha A}$ . . . 169
D.3 Fermionic Variations Generated by $\zeta_+^{\alpha A}$ . . . 170
D.4 Variations of the B-Field . . . 171

Bibliography **172**

Chapter 1

Introduction

This thesis is divided into two parts. In the first we discuss pole-skipping, a phenomenon observed in holographic thermal correlation functions. In the second part we describe the construction of a new family of microstates of a particular black hole solution in supergravity.

Both topics are fundamentally connected to black holes and their properties. Hence we use this chapter to introduce the basic concepts of black hole physics and establish the notation that is used throughout the thesis. We also discuss some problems that arise in the (semi)-classical description of black holes and present string theory, a framework where these issues are resolved. We then briefly review the AdS/CFT duality, which plays an important role in both pole-skipping and the construction of microstates, before outlining the structure of the rest of the thesis.

1.1 History and Motivation

Every course in physics inevitably begins with something along the lines of [3]:

> *"Physics is an experimental science. Physicists observe the phenomena of nature and try to find patterns that relate these phenomena."*

What is implied in this statement is that first an observation is made which then prompts a theoretical explanation of the experimental data. And historically this was the natural direction in which progress in our understanding of the world around us was (and still is) made. For example, at the end of the 19th century, the observed spectrum of black-body radiation was in conflict with the then accepted theories of nature. The resolution came in the form of Planck's law which in turn was one of the first steps in the development of the theory of quantum mechanics.

Black holes, which are the main focus of this thesis, certainly do not follow such a pattern. Even before the French revolution, John Mitchell and Pierre-Simon Laplace

were thinking about the values of the escape velocity around a very massive star [4,5]. If an object starts at a distance R from the centre of a star with mass M, then the escape velocity is given by

$$v_{esc} = \sqrt{\frac{2GM}{R^2}}\,, \tag{1.1}$$

where G is the Newton's gravitational constant. Notice that in the above expression the mass of the object is not important. Mitchell and Laplace then wondered if there exists a star that is so massive (or dense) that the escape velocity exceeds the speed of light. In this case the star would appear to emit no radiation at all – it would be a *dark star*.

The idea stayed quarantined until after Einstein proposed his general theory of relativity, when Karl Schwarzschild worked out how space and time behave around a spherically symmetric and non-rotating mass. The geometry, which we now call the Schwarzschild solution and is discussed in more detail below, includes a region where the gravitational potential is so high that not even light can escape. The boundary of the region, called the *event horizon*, is one of the main objects of this thesis. The event horizon of a Schwarzschild solution with mass M is located at a distance R_s, called the *Schwarzschild radius*, and is given by

$$R_s = \frac{2GM}{c^2}\,, \tag{1.2}$$

where c is the speed of light. Remarkably, this value coincides with the value obtained from (1.1), if we take $v_{esc} = c$. General relativity allows for dark star-like solutions, which in this context are better known as *black holes*. Yet the question whether such objects exist in our universe was still open. After all, how can you observe something you cannot see (or hear, touch, smell, or taste for that matter)?

Fast forward a hundred years and we have been able to gather a huge amount of experimental evidence that point to black holes. For example, studies of the motion of stars around galactic centres, such as our own Milky Way galaxy, hint that there is a supermassive black hole around which nearby objects are orbiting [6]. More recently, the observation of gravitational waves [7] is consistent with the merger of two black holes into a more massive one. And, perhaps most convincingly, the Event Horizon Telescope collaboration has reported the first direct observation of the accretion disk surrounding a supermassive black hole [8].

Furthermore, our understanding of the nature of massive objects has increased dramatically. For example, theoretical results [9–11] have shown that in general relativity the formation of singularities is a generic feature of well behaved systems.

Today, the existence of black holes is widely accepted. Yet despite the head start

that theory had over experiment, a complete understanding of black holes and their properties is still lacking. New and exciting properties are being discovered even over two hundred years after their first conception. In this thesis some of these results are presented.

1.2 Black Holes

We use Einstein's general relativity as a framework to describe black holes. The central idea of this theory is that the space *and* time are not rigid but are malleable. Most importantly, spatial distances and the rate at which time flows are distorted by presence of energy and matter. The equation describing the evolution of space and time is the Einstein's equation [12]

$$R_{MN} - \frac{1}{2} R\, g_{MN} + \Lambda\, g_{MN} = 8\pi G\, T_{MN}\,. \tag{1.3}$$

The matter appears in the equation through the energy-momentum tensor T_{MN}, while the structure of spacetime is encoded in the metric g_{MN}, the Ricci tensor R_{MN}, and the Ricci scalar R. Throughout the thesis the spacetime indices are denoted by upper-case Latin letters, such as M, N. In (1.3) we have set the speed of light c to be equal to 1, while leaving the Newton's gravitational constant G explicit. Furthermore, we allow for a term with a cosmological constant Λ.

Let us begin by setting $\Lambda = 0$. We look for *vacuum* solutions of (1.3) which have $T_{MN} = 0$ and describe spacetimes with no matter. The simplest vacuum solution with vanishing cosmological constant is the flat Minkowski spacetime which is described by the line element

$$ds^2 = \eta_{MN}\, dx^M\, dx^N = -dt^2 + dx^2 + dy^2 + dz^2\,, \tag{1.4}$$

where we have introduced the Minkowski metric $\eta_{MN} = \mathrm{diag}(-1, 1, 1, 1)$. At the moment we only consider four dimensional spacetimes, however most of the ideas are readily generalised to higher dimensions.

Another more interesting vacuum solution is the aforementioned Schwarzschild solution, given by the metric

$$ds^2 = -\left(1 - \frac{2GM}{r}\right) dt^2 + \frac{dr^2}{\left(1 - \frac{2GM}{r}\right)} + r^2 \left(d\theta^2 + \sin^2\theta d\phi^2\right)\,. \tag{1.5}$$

where the spatial part is described by the coordinates (r, θ, ϕ) with $0 \leq \theta \leq \pi$ and $0 \leq \phi < 2\pi$. The coordinate time is given by $t \in \mathbb{R}$. This metric personifies the essence of general relativity. Not only does the presence of mass affect space, as is seen by the

coefficient multiplying the term dr^2, but it also alters the passage of time, as is seen by the term multiplying dt^2.

This metric describes the spacetime outside any spherically symmetric non-rotating object with mass M, for example the exterior of a non-rotating star with radius $R_* > 2GM$, in which case the range of the radial coordinate in the metric (1.5) is $r > R_*$.[1] We observe that as we approach the star by decreasing r, the value of the factor $(1-2GM/r)$ decreases until it reaches its minimum at the star's surface.[2] From (1.5) it then follows that closer to a star radial distances are longer and time passes more slowly than further away.

By taking the limit $r \to \infty$, we see that the Schwarzschild metric simplifies to the flat metric given in (1.4). We say that (1.5) is *asymptotically flat* – at spatial infinity it approaches the Minkowski solution "fast enough".[3]

In fact, according to Birkhoff's theorem, (1.5) is the *unique* spherically symmetric solution of the vacuum Einstein's equation [11]. This is important because this metric also describes the spacetime of a non-rotating black hole. However, in this case we need to be more careful as the range of the radial coordinate now extends to $r \to 2GM$, where some components of the metric and its inverse diverge. To further investigate what happens at this point, we calculate the Kretschmann scalar, a curvature invariant of the metric, which in the case of (1.5) is

$$K(r) \equiv R_{MNPQ}\, R^{MNPQ} = \frac{48G^2M^2}{r^6}\,. \tag{1.6}$$

Evaluating this invariant at the Schwarzschild radius yields $K(r = R_s) \approx (GM)^{-4}$. Not only is this finite, but it can be made arbitrary small by increasing the mass. The fact that the metric (1.5) diverges while the curvature remains finite is attributed to a bad choice of coordinates, hence the point $r = R_s$ is called a *coordinate singularity*. It can eliminated by introducing a so called "tortoise" coordinate

$$dr_* = \frac{dr}{1-\frac{2GM}{r}}\,, \qquad r_* = r + 2GM \log\left|\frac{r}{2GM} - 1\right| \tag{1.7}$$

Notice that $r_* \to \infty$ as $r \to \infty$, but on the other hand $r_* \to -\infty$ as $r \to 2GM$. Now

[1] Since the metric (1.5) is a vacuum solution, it cannot describe the interior of the star ($r < R_*$) where the value of the energy-momentum tensor is non-vanishing due to the presence of matter. In this region other solutions to (1.3) need to be considered, but we are not interested in those here. Note that at the surface $r = R_*$ we need to impose appropriate boundary conditions (see for example [13] for more details).

[2] Note that for stars $R_* > 2GM$ meaning that the factor $(1-2GM/r)$ is positive for all $r > R_*$ and most importantly never vanishes.

[3] For a more precise definition, see for example [12].

let us introduce a new coordinate

$$v = t + r_* \,, \tag{1.8}$$

and rewrite Schwarzschild metric using the so-called the *ingoing Eddington-Finkelstein coordinates*

$$ds^2 = -\left(1 - \frac{2GM}{r}\right) dv^2 + 2\, dr\, dv + r^2 \left(d\theta^2 + \sin^2\theta d\phi^2\right) \,. \tag{1.9}$$

In this coordinate system the point $r = R_s$ is completely regular as all components of the metric and its inverse are non-divergent. We can now use this coordinate system to investigate the region $0 < r < R_s$. At the event horizon the causal structure of spacetime changes. In the region $r < R_s$ all future light cones are directed towards $r = 0$. This means that no causal curve can cross from the region $0 < r < R_s$ to $r > R_s$ or, in other words, no information can escape this region of spacetime.

Our current understanding of black holes suggests that the matter inside them is so dense that there is no force that can withstand the gravitational collapse and thus all matter is concentrated in a very small region around $r = 0$. Using the new coordinates we gain access to this point. There matter highly distorts the spacetime as can be seen from (1.6) which diverges at the origin. Since this result is coordinate independent, it suggests that as $r \to 0$, the curvature of the spacetime diverges – this point is a *curvature singularity*.

At such singularities general relativity breaks down. From a physical point of view this may be expected as general relativity is a classical theory that works well over large distances at which quantum effects are negligible. But at a singularity we expect these effects to be important. So it should not be a surprise that a classical theory cannot fully describe a black hole and a new, more complete theory, which reconciles quantum and gravitational effects, should be used.

The indication that a full theory of quantum gravity is needed can also be seen by considering the thermodynamic properties of black holes. There exist a set of results, commonly referred to as the laws of black hole mechanics, that closely resemble the usual laws of thermodynamics [14, 15]. The first law of black hole mechanics is the analogue of energy conservation. It states that a change of the mass of a black hole

δM is related to the change in the horizon area δA by[4]

$$\delta M = \frac{\kappa}{8\pi}\,\delta A\,, \tag{1.10}$$

with κ being the surface gravity of the black hole, which can be interpreted as the tension of the string that an observer measures at infinity for a test mass suspended at rest just above the horizon.[5] This expression closely resembles the first law of thermodynamics where the change of internal energy is given by $dU = TdS$ if we assume that no work or charges were changed. This is further strengthened by both the zeroth law of black hole mechanics, which states that the surface gravity is constant across the event horizon, and by the second law stating that classically the area of the event horizon of a black hole cannot decrease. Both of these laws are have their analogues in thermodynamics, dealing with temperature and entropy respectively. This led Bekenstein to propose that black holes have an associated entropy that is proportional to the area of the event horizon [16].

The exact expression was derived by Hawking [17] who analysed the behaviour of quantum fields in a spacetime created by collapsing matter that eventually forms a black hole. He observed a constant flux of particles, which is now known as *Hawking radiation*, originating from the region near the horizon, and furthermore he showed that the spectrum of these particles is thermal[6] with the temperature given by the *Hawking temperature*

$$T_H = \frac{\hbar\kappa}{2\pi}\,, \tag{1.11}$$

where we have set $c = k_B = 1$ while $\hbar$ and G are kept explicit. Inserting this into (1.10), one can read of the corresponding entropy of a black hole, called the *Bekenstein-*

[4] In the case of a charged and rotating black hole we also include the change in the angular momentum δJ and electric charge δQ

$$\delta M = \frac{\kappa}{8\pi}\,\delta A + \Omega\,\delta J + \Phi\,\delta Q\,,$$

where Ω is the angular velocity of the black hole as measured by an observer at infinity, and Φ is the electrostatic potential. This form makes it more apparent that the first law of black hole mechanics and first law of thermodynamics are analogous.

[5] On a more technical note, a theorem by Hawking showed that in a stationary, analytic, and asymptotically flat spacetime describing a black hole, the event horizon is a Killing horizon, meaning that in the neighbourhood of the horizon there exist a Killing vector field k^M normal to the horizon. The surface gravity can then be defined through the equation

$$k^M \nabla_M k^N = \kappa\, k^N\,,$$

where ∇_M is the covariant derivative on the spacetime and the left hand side of the equation is evaluated on the horizon. The surface gravity thus measures the failure of the integral curves of k^M to be affinely parametrised. For more details see [11, 12]

[6] In fact, this is the same spectrum that Planck was analysing some 70 years prior.

Hawking entropy (reinstating G)

$$S_{BH} = \frac{A_H}{4G\hbar}\,. \tag{1.12}$$

By retaining $\hbar$ we can observe the "quantumness" of these results, as classical expressions are obtained by taking the formal limit $\hbar \to 0$, where the entropy diverges and the temperature vanishes.

To give a sense of the magnitude these values take, we can evaluate them for the Schwarzschild black hole. The entropy scales with the square while the temperature scales with the inverse of the mass. Reinstating all the constants, we obtain

$$S_{BH} \approx 10^{77} \left(\frac{M}{M_\odot}\right)^2 \times k_B\,, \qquad T_H \approx 6 \times 10^{-8} \left(\frac{M_\odot}{M}\right) K\,. \tag{1.13}$$

While the precise values vary between different types of black holes (*e.g.* rotating, charged), we can gain some intuition about the magnitude of the values. The temperature of a black hole is typically very close to the absolute zero, whereas the entropy of a black hole is *enormous*.

The above results are not without their problems. They offer us a glimpse into the quantum nature of space and time without the proper understanding of the full theory, so it should not be surprising that we run into paradoxical results. Two problems that arise if we try to understand the consequences of (1.11) and (1.12) are the *entropy puzzle* and the *information paradox*. They are related to the apparent inconsistencies of the encoding of information in a black hole, at least when we treat the problem classically.

1.2.1 Entropy Puzzle

The only parameter in the Schwarzschild solution (1.5) is the mass. More complicated metrics, such as the Kerr-Newman that describe the spacetimes of rotating and (electrically and magnetically) charged black holes, depend also on the electric and magnetic charges, and angular momentum. In all such cases, there exist uniqueness theorems [18, 19] which state that a black hole geometry is *uniquelly* specified by only a finite number of parameters.

On the other hand, the entropy of a black hole with a non-vanishing horizon area is non-zero. This implies that there should exists a set of microstates whose ensemble averages reproduce the macroscopical observables of a black hole. Recall that the relation between the entropy and the number of microstates Ω_μ in a microcanonical ensemble is given by Boltzmann's law ($k_B = 1$)

$$S = \log \Omega_\mu\,. \tag{1.14}$$

Combining this with the Bekenstein-Hawking entropy suggests that a black hole should have $e^{S_{BH}}$ microstates. In the case of a Schwarzschild solution with a mass equal to that of the Sun this amounts to roughly $\Omega_\mu \approx 4 \times 10^{76}$.

The two results are at odds. If the spacetime is determined uniquely, then there is no room for microstates. But the non-zero entropy suggests that some microscopical description may exist. Our current understanding is that to resolve this puzzle one needs a consistent theory of quantum gravity, after all, the uniqueness theorems are classical results, whereas the Bekenstein-Hawking entropy is a quantum (or at least semi-classical) expression.

1.2.2 Information Paradox

Quantum mechanics teaches us that in physical systems time evolution is unitary, meaning that information is neither spontaneously destroyed nor spontaneously created. Black holes seem to violate this principle, as can be seen from the following scenario (see left panel of figure 1).

Start with matter in a *pure state* so that information about the initial configuration is completely known and let this matter collapse into a black hole. According to the uniqueness theorems, once the spacetime settles it is parametrised only by a few charges. Furthermore, classically the black hole can only increase in size and the information about the initial state is forever hidden behind the horizon, inaccessible to an outside observer.

However, semi-classically black holes lose mass through Hawking's radiation. Assume that the black hole evaporates completely so that the final system consists only of Hawking radiation. The information paradox arises because the spectrum of the emitted particles is thermal [11], which is described by a *mixed state*. Thus we have described a process in which a pure state evolved into a mixed state. This is not allowed in a unitary theory, as in such a process information is lost forever.[7]

A heuristic picture of Hawking radiation is the following (see right panel of figure 1) [22]. By turning on quantum effects, we allow for quantum fluctuations of the fields around the vacuum. This allows for particle–anti-particle pairs to jump in and out of existence for a short period of time, according to the uncertainty principle. At a generic point in space the two particles are pair-created and annihilated in quick succession. However, if the pair-creation occurs near the horizon, one of the particles can cross into the black hole region and is thus unable to recombine with its partner. The outside particle is thus free escape the gravitational potential and is emitted as

[7] There are other, equivalent ways to state the information paradox. For example, one can analyse the entanglement between the radiation and the evaporating black hole. The entanglement entropy of the radiation rises monotonically, while in a unitary theory one expects the entanglement entropy to eventually start decreasing and follow the Page curve [20, 21].

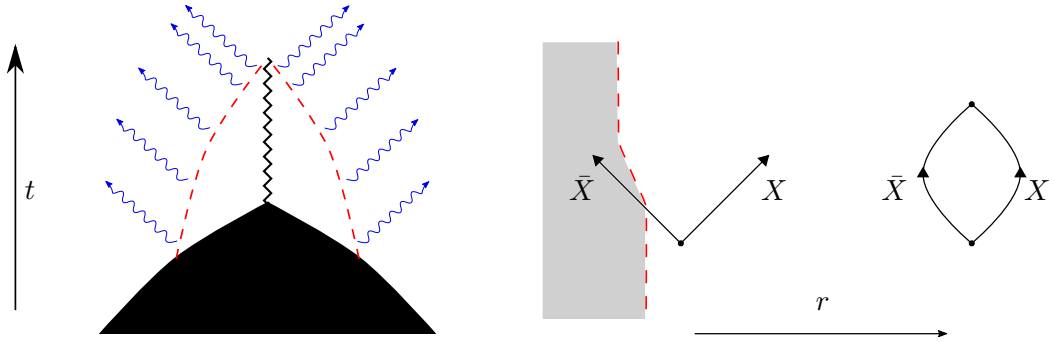

Figure 1: (Left): The schematical depiction of a black hole collapse and subsequent radiation. Some matter (black) collapses and at some point forms the horizon (red dashed) and a singularity (zigzag black line). The black hole emits thermal Hawking radiation (blue wavy curves) and decreases in size until it evaporates completely. In such a process an initial pure state (matter) evolves into a mixed state (thermal radiation) which violates unitarity. (Right): The pair-production of a particle X and its anti-particle $\bar{X}$. Away from the black hole (gray with dashed boundary representing the horizon), the pair quickly annihilate. Near the horizon, the anti-particle crosses the horizon, thereby lowering the mass and decreasing the horizon area, while the particle escapes to infinity.

Hawking radiation.

One important aspect of the above process is that Hawking particles get created at the horizon and thus can carry information only about that region of spacetime. As we discussed, the curvature at the horizon is small for black holes with high mass. Therefore we expect that in such a region (effective) quantum field theory is a good approximation to the full physical theory, or in other words, quantum gravitational effects should not make significant contributions, so perhaps then it should not be surprising that there is no information encoded in the Hawking radiation

The above argument is not completely sound proof. It was shown in [23] that for a sufficiently old black hole under reasonable conditions the following three statements *cannot* be simultaneously true

1. Hawking radiation is in a pure state, thus allowing for preservation of unitarity.
2. The radiation originates at the horizon where no new physics is necessary.
3. An observer passing through the horizon experiences nothing out of the ordinary.

This suggests that we either need to accept the loss of information, assume new non-trivial physics already at the horizon scale, or let an observer burn in a firewall as they cross the horizon.

It seems that the resolution of the paradox requires a full quantum theory of gravity. Yet combining quantum field theory and general relativity famously runs into troubles (see for example [12]). However, a unified framework where these two theories emerge consistently in the low energy limit is *string theory*.

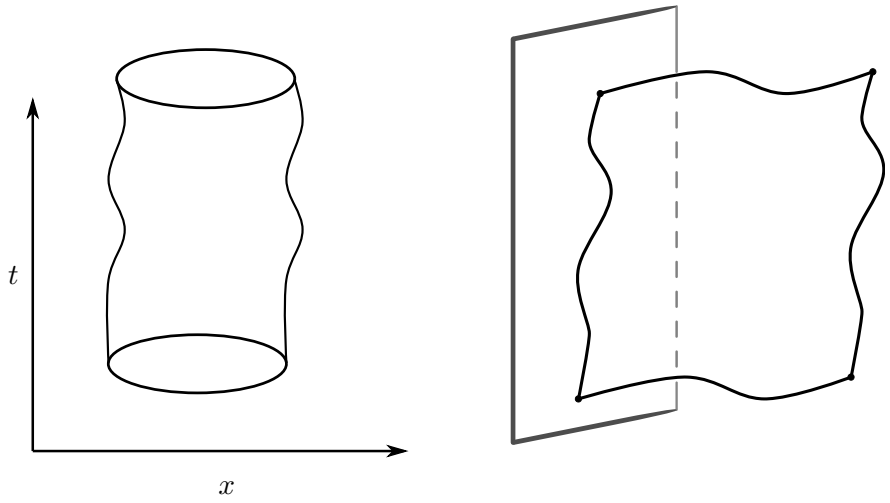

Figure 2: A schematic depiction of the world-sheets of a closed string (left) and an open string (right) whose left endpoint is fixed on a flat brane, while the right endpoint is free to move. The extended nature of the fundamental objects resolves many problems of conventional theories where the funamental objects are point-like. Different species of fields (particles) arise as excitations on these strings.

1.3 String Theory and Supergravity

Here we only introduce concepts which are of relevance for the thesis. In doing so, we mainly follow [22, 24–26].

The main idea of string theory is that the fundamental objects are one-dimensional *strings* that get resolved at the length scale l_s called the *string length*.[8] Particles of different masses are manifested as vibrational excitations of the string. We typically assume that the string length is much smaller than the experimentally accessible length scales, hence the stringy nature of fundamental particles remains unresolved which is why they effectively behave as point-like objects.

As strings propagate in spacetime, they trace out a two-dimensional *world-sheet* and depending on its topology, we can distinguish two types of strings. *Closed strings* are loops propagating in time and form a cylinder in spacetime, while the world-sheets of *open strings* have the topology of a sheet, as they can be seen as finite open lines evolving in time (see figure 2 for a schematic depiction).

Open strings have two endpoints at which we need to specify the boundary conditions, which needs to be done in every spatial direction. If we impose the Neumann boundary condition (N), the endpoint is allowed to move freely along the chosen direction at the speed of light. If we impose the Dirichlet boundary conditions (D), the endpoint is fixed at a certain position in the chosen direction. Such boundary condi-

[8] We use the string length l_s as the free parameter of string theory. One could equivalently use the Regge slope α'. We set the relation between them as $l_s = \sqrt{\alpha'}$. Note that in some of the literature $l_s = 2\pi\sqrt{\alpha'}$ can be used.

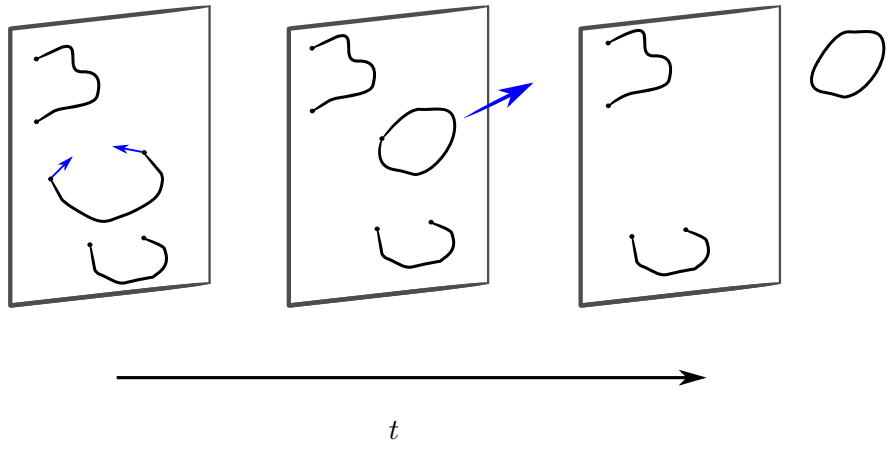

Figure 3: An example of a process where open and close strings interact – the emission of a closed string from a brane. In this process the endpoints of an open string on the brane combine to form a close string which gets emitted. Since close strings contain the gravitational part of the spectrum, the strength of such an interaction determines the extend to which the branes "gravitate", meaning whether they backreact on the geometry and cause a bending of surrounding spacetime.

tions describe dynamical hypersurfaces in spacetime, called *Dp-branes* [27], which are $(p+1)$-dimensional objects extended in the directions where N boundary conditions are imposed and localised in the directions where D boundary conditions are imposed (see right panel of figure 2).

One of the motivations for using string theory is that it provides a framework where quantum field theory and gravity are combined in a consistent way. For example, the closed string spectrum contains a massless spin-2 field which can be identified with the graviton. On the other hand, the spectrum of an open string ending on a stack of N Dp-branes contains a massless vector field living on the world-volume of the brane transforming under the gauge group $U(N)$. This way the spectrum of string theory naturally contains both gravitational and gauge fields.

The spectrum also contains other fields depending on the type of string theory. We always find additional massless fields and we review the massless spectrum of Type IIB superstring theory below. Furthermore, there exists an infinite tower of massive fields for both the closed and open strings with the mass of all states scaling with $m^2 \sim l_s^{-2}$.

String theory also has a well defined perturbation theory where open and closed strings are able to interact. For example, an open (closed) string can separate into two new open (closed) strings which is the process of particle decay. Similarly, a pair of open strings can join up and form a closed string or vice versa (see figure 3).

The strength of these interactions is controlled by a dimensionless parameter g_s, called the *string coupling* constant. We will be mostly interested in the *classical string limit* $g_s \ll 1$ in which string perturbation theory is valid and stringy loop effects are

suppressed.

A small value for g_s is sometimes not enough to ensure a valid perturbation theory. Consider a system where open strings end on a stack of N coincident Dp-branes. The effective string coupling for open string scattering is then given by g_sN which is also the strength of interaction between open and closed strings. However, the interaction between closed strings is still determined only by g_s. It is this combination of factors g_s and N that allow us to interpolate between different descriptions of the same theory and is one of the main ingredients of the AdS/CFT duality.

String theory has its own problems. For a well defined theory of the bosonic string we need to work in 26 dimensions. This number is lowered to 10 if we introduce fermions and make the theory supersymmetric. A string theory with world-sheet supersymmetry is called *superstring theory* and from now on we assume we work with such a theory.[9]

1.3.1 Type IIB String theory

In particular, we work with *Type IIB* string theory in 10 dimensions with $\mathcal{N} = 2$ supersymmetry. This means that there are two fermionic symmetry generators corresponding to the left and right moving excitations on the string. Each generator is a Majorana-Weyl spinor, containing 16 real degrees of freedom and we commonly refer to the components of these Majorana-Weyl spinors as the 32 supercharges of the theory. In Type IIB theory, the spinors have the same chirality, whereas in Type IIA string theory, the supersymmetry generators have opposite chirality.[10]

The solutions of the equations of motion may not be invariant under all fermionic symmetries and we say that such solutions break some supersymmetry. An object which preserves only $32/n$ of all possible supercharges is called $1/n$-BPS. For example, an object that preserves 16 supercharges breaks half of the supersymmetry and is thus called 1/2-BPS.

There is a variety of objects appearing in this theory allowing for a rich microscopic structure. The massless spectrum of the closed string includes a graviton g_{MN}, a dilaton ϕ, and an anti-symmetric two-tensor B_{MN}, which can be written in terms of a differential form B, called the NS-NS two-form. The spectrum in type IIB also contains RR gauge fields – the axion C_0, the two-form C_2, and a four-form C_4.

Since the theory is supersymmetric, the massless spectrum also includes fermionic excitations. There are two pairs of Majorana-Weyl spinors: two gravitinos ψ^I_M with positive chiralities and two dilatinos λ^I with negative chiralities, where $I = 1, 2$, and

[9] In what follows any string theory mentioned is assumed to be supersymmetric. We omit the "super" in superstring theory, except where the clear distinction between the bosonic string and superstring is needed.

[10] We discuss Majorana and Weyl conditions and the conventions on the form notation in more detail in Appendix A

Field	Object
Metric	g_{MN}
Dilaton	ϕ
NS-NS two-form	B_2
Axion	C_0
RR two-form	C_2
self-dual four-form	C_4
Gravitinos	$\psi^I_M\,, \quad I=1,2$
Dilatinos	$\lambda^I\,, \quad I=1,2$

Table 1: The massless spectrum of closed strings in type IIB superstring theory or equivalently the spectrum of type IIB supergravity [24, 25]. The number of bosonic and fermionic degrees of freedom are equal. The gravitino and dilatino fields come in a doublet of Majorana-Weyl spinors (we suppressed the spinor index). The two gravitinos have equal chirality which is opposite to the chirality of both dilatinos. The massless spectrum of open strings depends on the boundary conditions at the endpoints. In general it is that of a supersymmetric gauge theory on the worldvolume of the brane on which the string ends.

the spinor indices are suppressed. The massless spectrum of the closed string in type IIB string theory is summarised in table 1.

Open strings end on Dp-branes on which left and right moving excitations of the string are identified and thus at least half of the supersymmetries are broken. In type IIB string theory only branes with p *odd* are allowed and are all 1/2-BPS objects, breaking exactly half of the supersymmetry of the full theory. As discussed above, the massless spectrum of open string excitations gives a vector field A_μ, with μ running along the directions of the brane world-volume, which transforms under the gauge group $U(N)$, with N being the number of coincident branes. On the world-volumes of the branes there are other fields which transform as a scalar under $U(N)$ and fermion fields that ensure supersymmetry, but the precise details of the open string spectrum are not important for our purposes. We only use the general notion that on a brane, the massless spectrum of open strings reproduces a gauge theory.

Branes are also coupled to the closed strings and their massless excitations. Firstly, branes of different dimensions couple to appropriate RR form fields. In addition, all Dp-branes couple to the graviton and the dilaton. The coupling is such that there is no net force between two branes of the same type, as the repulsion due to the form fields is exactly cancelled by the attraction due to the graviton and dilaton exchange. The repulsion–attraction equality is the analogue of the cancellation between the electro-

Object	Coupled Field	Type of coupling
F1-string	B_2	E
NS5-brane	B_2	M
D(-1)-brane	C_0	E
D1-brane	C_2	E
D3-brane	C_4	E *and* M
D5-brane	C_2	M
D7-brane	C_0	M

Table 2: The content of Type IIB superstring theory and the fields that these objects couple to [22, 24]. The F1-string is the fundamental string while the NS5-brane is a solitonic (5+1)-dimensional object that we do not consider in the main text. The D(-1)-brane is localised in space and time and should be seen as an instanton. It is also not discussed in the main text. The couplings "E" and "M" refer to whether the field couples to the brane electrically or magnetically, in analogy with the coupling of electric and magnetic point charges in electromagnetism. The D3-brane is *dyonic*, as it couples to C_4 both electrically and magnetically.

magnetic repulsion and gravitational attraction of extremal Reissner–Nordström black holes which leads to Majumdar-Papapetrou solutions [28, 29]. Finally, the NS-NS two-form B couples only to the fundamental string and the NS5-brane. The brane content and the fields that the branes couple to are summarized in table 2.

1.3.2 Type IIB Supergravity

Massive excitations in string theory scale as $m^2 \sim l_s^{-2}$. If the string length is negligible compared to the length scale associated to our experiment, then the massive states are inaccessible and we can work with the theory of massless excitations – *supergravity*. In this section we introduce the basics of the low energy limit of Type IIB string theory, called Type IIB supergravity and present extremal p-brane geometries, the gravitational description of Dp-branes [26, 30].

Supergravity describes the fields found in the massless spectrum of the closed string. In type IIB the low energy theory also has 32 supercharges distributed in two Majorana-Weyl spinors with equal chiralities. We focus on the bosonic sector of the theory, as we are interested in classical solutions which have vanishing fermionic fields. The relevant part of the action in the string frame is given by [24]

$$S^{(0)}_{IIB} = \frac{1}{2\kappa_{10}^2}\int d^{10}x\,\sqrt{-g}\Big[e^{-2\phi}\left(R + 4\nabla_M\phi\nabla^M\phi - \frac{1}{2}\left|H\right|^2\right) - \frac{1}{2}\left|F_1\right|^2 - \frac{1}{2}\left|F_3\right|^2 - \frac{1}{4}\left|F_5\right|^2\Big] - \frac{1}{4\kappa_{10}^2}\int C_4\wedge H_3\wedge F_3\,, \tag{1.15}$$

where the ten dimensional gravitational coupling is related to the string length as $4\pi\kappa_{10}^2 = (2\pi l_s)^8$. In the above we have introduced form field-strengths defined as

$$H = dB\,, \qquad F_1 = dC_0\,, \qquad F_3 = dC_2 - HC_0\,,$$
$$F_5 = dC_4 - \frac{1}{2}C_2 \wedge H + \frac{1}{2}B \wedge dC_2 \tag{1.16}$$

and have used the notation

$$|F_p|^2 = \frac{1}{p!}F_{M_1\ldots M_p}F^{M_1\ldots M_p}\,. \tag{1.17}$$

Note that the last term in the action is the Chern-Simons term. In addition to the equations of motion derived from this action, we have to impose the self-duality condition for the field F_5

$$F_5 = *F_5\,, \tag{1.18}$$

where the $*$-operator is the hodge dual in ten dimensions.

The *extremal p-brane solutions* are higher dimensional generalisations of the extremal Reissner–Nordström black hole and correspond to objects that are extended in p-spatial dimensions and localised in the remaining transverse directions. They are called extremal because they preserve half of the supercharges and are thus 1/2-BPS solutions and are the supergravity description of Dp-branes found in full string theory. They are given by the ansatz [25, 26, 30]

$$ds^2 = H_p^{-\frac{1}{2}}\,\eta_{\mu\nu}dx^\mu\,dx^\nu + H_p^{\frac{1}{2}}\,\delta_{ij}\,dy^i dy^j\,, \tag{1.19a}$$
$$e^{2\phi} = g_s^2 H_p^{\frac{3-p}{2}}\,, \tag{1.19b}$$
$$C_{p+1} = g_s^{-1}\left(H_p^{-1} - 1\right)dx^0 \wedge dx^1 \wedge \ldots \wedge dx^p\,, \tag{1.19c}$$
$$B = 0\,, \tag{1.19d}$$

where x^μ are the coordinates of the dimensions in which the brane is extended, with $\mu = 0, 1, \ldots p$, and y^i, with $i = p+1, \ldots 9$, are the coordinates in the transverse directions in which the object is localised.

The equations of motion are satisfied if the function H_p is a harmonic function in the transverse directions

$$\Box_{(9-p)}H_p = 0\,, \tag{1.20}$$

and thus takes the form

$$H_p(r) = 1 + \left(\frac{L_p}{r}\right)^{7-p} , \tag{1.21}$$

where $r^2 = \sum_{i=p+1}^{9} y^i y^i$, and we have set the constant of integration to "1", which makes the metric (1.19a) asymptotically flat. Furthermore, as $r \to 0$, the Harmonic function H_p and thus some components of the metric diverge. By studying (1.19) as a limit of non-extremal solutions, one finds that at this point a horizon with vanishing area coincides with a curvature singularity.

The solution also has a characteristic length scale L_p given by

$$L_p^{7-p} = (4\pi)^{\frac{5-p}{2}} \, \Gamma\left(\frac{7-p}{2}\right) g_s N \, l_s^{7-p} , \tag{1.22}$$

where $\Gamma(x)$ is the Euler Gamma function. This relation is obtained by equating the charge carried by the supergravity solution to charge of N coincident Dp-branes in string theory.

Particularly important is the 3-brane solution ($p = 3$). If we take the *near horizon* or *decoupling* limit $r \ll L_3$, where $H_3 \approx (L_3/r)^4$, then to leading order the metric takes the form

$$ds^2 \approx \frac{L_3^2}{r^2} \, dr^2 + \frac{r^2}{L_3^2} \, \eta_{\mu\nu} dx^\mu \, dx^\nu + L_3^2 d\Omega_5^2 , \tag{1.23}$$

where $\mu = 0, 1, 2, 3$, and we have introduced polar coordinates for the six dimensional space transverse to the branes so that $d\Omega_5^2$ denotes the differential area element of a unit 5-sphere. This metric describes Anti-de Sitter spacetime in five dimensions multiplied by a five-sphere, which we denote by $\mathrm{AdS}_5 \times S^5$, with the radius of the AdS space and the radius of the sphere both being equal to L_3. Another way of writing this metric is by introducing a new coordinate $z = L_3^2/r$ so that

$$ds^2 \approx \frac{L_3^2}{z^2} \left(dz^2 + \eta_{\mu\nu} \, dx^\mu dx^\nu\right) + L_3^2 d\Omega_5^2 . \tag{1.24}$$

As an aside, the above metric actually describes the *Poincaré* patch of AdS_5 space which covers only a part of the entire spacetime. The whole of AdS can be described by the use of *global* coordinates in which the metric takes form (see for example [25,31])[11]

$$ds^2 = L_3^2 \left(-\cosh^2 \rho \, d\tau^2 + d\rho^2 + \sinh^2 \rho \, d\Omega_3^2\right) , \tag{1.25}$$

[11] In this discussion we consider for concreteness only AdS_5 while the generalisation to Anti-de Sitter spacetimes of other dimensions is trivial. Additional care needs to be taken when dealing with AdS_2, however we will not discuss such a low-dimensional spacetime in this thesis.

where $d\Omega_3^2$ denotes the differential area element of a unit 3-sphere and $\rho \geq 0$. If one uses these coordinates to parametrise the surface of a hyperboloid embedded in a six dimensional space with signature $(-,-,+,+,+,+)$, then $0 \leq \tau < 2\pi$, however such a spacetime contains closed timelike curves which we would like to avoid. Hence we usually consider the universal cover AdS in which the τ direction is "unwrapped" so that $\tau \in \mathbb{R}$ and is understood to be the usual temporal direction.[12] Note that we encounter global AdS_3 in equation (5.3.13) in section 5.3 albeit expressed in a different set of coordinates.

The metric in the form of (1.25) slightly conceals the nature of the boundary of global AdS. If we perform a coordinate transformation with $\tan\theta = \sinh\rho$, where $0 \leq \theta < \pi/2$, then the metric takes the form

$$ds^2 = \frac{L_3^2}{\cos^2\theta}\left(-d\tau^2 + d\theta^2 + \sin^2\theta\, d\Omega_3^2\right) . \tag{1.26}$$

The boundary of this metric is located at $\theta = \pi/2$ where we find a double pole. To extend the metric to this boundary we need to multiply (1.26) by a function which cancels out divergence. In doing so we define the metric at the boundary up to conformal transformations[13] [32]. Ignoring this conformal factor, we find that the metric of the boundary of global AdS is given by

$$ds^2 = -d\tau^2 + d\Omega_3^2 , \tag{1.27}$$

which is just $\mathbb{R} \times S^3$.

We can also extract the boundary metric for the Poincaré patch of AdS. The boundary is in this case located at $r \to \infty$ (or equivalently $z = 0$) and the metric, up to a conformal factor, is simply the four dimensional Minkowski metric on flat space $\mathbb{R}^4$

$$ds^2 = \eta_{\mu\nu}\, dx^\mu\, dx^\nu = -dt^2 + d\vec{x}^2 . \tag{1.28}$$

The two boundaries are related by a conformal transformation. To see this we can Wick rotate the flat metric to its Euclidean counterpart with $t_E = -it$ and obtain [31]

$$ds^2 = dt_E^2 + d\vec{x}^2 = d\tilde{r}^2 + \tilde{r}^2 d\Omega_3^2 = e^{2\tau_E}\left(d\tau_E^2 + d\Omega_3^2\right) , \tag{1.29}$$

where in the last equality we introduced $\tau_E = \log\tilde{r}$. The resulting metric equals to the Euclidean version of (1.27) (we use $\tau_E = -i\tau$) up to an overall prefactor.

For a generic Dp-brane the length scale of the curvature of (1.19) is L_p, which needs to be much larger than the string length in order for the geometry to be a

[12] Note that the Poincaré coordinates cover only a half of the hyperboloid, while the global coordinates cover the entire surface. See for example [25] for more details.

[13] Transformations which leave the metric invariant up to an overall factor.

valid description of Dp-branes. Through (1.22) this is equivalent to $g_s N \gg 1$, which is also the regime where open strings are strongly coupled to closed strings. There the Dp-branes are gravitating which creates a curved geometry. Furthermore, classical supergravity is valid only if all loop corrections in the closed string perturbation theory are suppressed. Since this expansion is controlled by the string coupling, we work in the regime $g_s \ll 1$. All in all, (1.19) is a valid description of Dp-branes in the regime

$$1 \ll g_s N \ll N \,. \tag{1.30}$$

which, from a string theory point of view, requires a large number N of coincident branes *and* tuning the value of g_s to be small, yet large enough to ensure strong interactions between open and closed strings.

One has to remember that the metric (1.23) is a solution to the equations of motion obtained from the supergravity action (1.15) which is the low-energy limit of string theory. If one considers stringy corrections to the action, then the metric needs to be amended. For type IIB string theory the first corrections come at order $\alpha'^3 = l_s^6$ [33–35] and include terms which involve are the contraction of four factors of the Weyl tensor C_{ABCD}[14] [36, 37] and are schematically denoted as R^4 terms.[15] The metric (1.23) is only a valid solution as long as these stringy corrections to the action are negligible, otherwise a α'-corrected metric of $\mathrm{AdS}_5 \times S^5$, which was worked out in [39, 40], needs to be used.

1.4 AdS/CFT Correspondence

Dp-branes have multiple roles in string theory. They serve as endpoints of open strings and the world-volumes for the resulting effective gauge theories. They are also the sources of closed strings.

For a stack of N branes, the effective coupling that determines the strength of interaction between strings is $g_s N$. As we have seen, in the regime (1.30) the branes produce the geometry given by (1.19). On the other hand, in the limit

$$g_s N \ll 1 \tag{1.32}$$

open and closed strings decouple, and open strings become effectively free. Hence in

[14] The Weyl tensor C_{ABCD} in D dimensions is given by [36]:

$$C_{ABCD} \equiv R_{ABCD} - \frac{2}{3}\left(g_{A[C}R_{D]B} - g_{B[C}R_{D]A}\right) + \frac{1}{6}R\, g_{A[C}g_{D]B} \,. \tag{1.31}$$

[15] There are other correction terms at order l_s^6 in the type IIB action, but it was argued in [38] that for specific spacetimes, such as $\mathrm{AdS}_5 \times S^5$, only the R^4 correction terms are important while the correction terms involving other fields, such as F_5 gauge fields, do not contribute at this order.

this regime, the branes can be seen infinite objects in flat space on which we have a system of non-interacting open strings.

Discarding all massive stringy excitations, the resulting theory living on the world-volume of the brane becomes a weakly-coupled (supersymmetric) $U(N)$ gauge theory in flat space. This is in stark contrast to the limit (1.30) where open strings are strongly coupled, but the branes admit a supergravity description. One of the remarkable results of the last 25 years is that the two descriptions are in fact related.

1.4.1 Study of D3-Branes

In [41] Maldacena studied a stack of N D3-branes in the limit where N is large. He noticed that in taking the near horizon limit

$$l_s^2 \to 0\,, \quad \text{with} \quad U = \frac{r}{l_s^2} \quad \text{fixed}\,, \tag{1.33}$$

the dynamics near the brane completely decouples from the dynamics of the asymptotic spacetime. Let us consider only the massless spectrum of the theory. On one hand, the low energy theory of open strings is $\mathcal{N} = 4$ Super Yang-Mills (SYM) theory living on the flat world-volume of the D3-branes, with the gauge group $U(N)$. On the other hand, the gravitational physics near the brane is described by type IIB supergravity on the $\mathrm{AdS}_5 \times S^5$. Maldacena proposed that these two theories are dynamically equivalent – the two pictures describe the same physics.

What is more, he conjectured that the correspondence is not limited to the low energy limit, and thus [41] $\mathcal{N} = 4$ *Super Yang-Mills theory with gauge group* $U(N)$ *is dual to type IIB superstring theory on* $AdS_5 \times S^5$ *with additional fluxes on* S^5.[16] The duality states that each physical object on one side has a corresponding term in the dual theory. Let us begin by analysing the relations between the free parameters of the two theories. In the gauge theory we have the Yang-Mills coupling g_{YM} and the number of colours N, while on the gravity side we have the string coupling g_s and the ratio between the radius of curvature of AdS R_{AdS} and the string length l_s. It is convenient to introduce the 't Hooft coupling

$$\lambda \equiv g_{YM}^2 N \tag{1.34}$$

which serves as an effective perturbative expansion parameter in the SYM theory. One then identifies

$$\frac{\lambda}{N} = 2\pi g_s\,, \qquad 2\lambda = \frac{R_{\mathrm{AdS}}^4}{l_s^4}\,. \tag{1.35}$$

[16] The correct gauge group should be $SU(N)$, however we do not need the distinction here.

By taking the limit $g_s \to 0$, we can neglect stringy loop contributions and work with the classical string. This corresponds to taking $N \to \infty$ while holding λ fixed. Classical string theory is thus dual to large N gauge theory. Since our knowledge of the quantum string is limited, we almost always assume that we work in this limit.

According to the second relation in (1.35), taking $R_{\text{AdS}} \gg l_s$, where supergravity is a good approximation, corresponds to $\lambda \to \infty$. In contrast, by setting $\lambda < 1$, in which case the gauge theory is weakly coupled, we require $l_s \approx R_{\text{AdS}}$. In this case the curvature scale of spacetime is of the string length, meaning that stringy states become important and supergravity is not a valid approximation any more.

These relations highlight the importance of the duality – a difficult theory (such as a strongly coupled gauge theory or a string theory) has a known, and usually tractable dual.

1.4.2 General Aspects of the Correspondence

A stack of D3-branes is only one of many configurations in string theory that, in a certain limit, admits two equivalent descriptions in terms of dual theories. Some examples were already discussed in [41] and by now it is understood that such dualities occur more generically. So let us now focus on the general correspondence between a classical gravitational theory and a strongly coupled gauge theory.

The duality emerging from the analysis of D3-branes is not the only instance where a string theory in a curved spacetime is related to a field theory. Other examples include [41]: M-theory on $\text{AdS}_7 \times S^4$ being dual to a supersymmetric field theory in six dimensions, which arises from the study of a large number of coincident M5-branes;[17] M-theory on $\text{AdS}_4 \times S^7$ being dual to a three dimensional field theory (a perhaps better studied example might be the $\text{AdS}_4 \times \mathbb{CP}^3$/ABJM duality [42]); and string theory on $\text{AdS}_3 \times S^3 \times M$, where M is either T^4 or $K3$, which is dual to a two-dimensional superconformal field theory – we study this duality in more detail in chapter 4. These examples all arise in the *top-down* approach, where we identify a suitable system in string theory, take the appropriate decoupling limit, and study the dual descriptions. While this approach usually allows us to identify the two theories that are involved in the duality and test the conjecture, it can also limit the applicability.

To extend the range in which one can use holography, one can take all the lessons learned from the explicit, top-down, examples and construct either a gravitational theory or a field theory and assume that it admits a dual description. The principle of this *bottom-up* approach is that the duality itself is more fundamental and should exist even outside the systems derived from string theory. In [43] it was even argued that a generic large N field theory with a gap in the spectrum of states should have a dual

[17] M-theory is an eleven dimensional theory which includes M2-branes and M5-branes as objects in the theory and can be seen as type IIA string theory at strong coupling [31].

gravity description. This approach, which we are going to take in chapter 2, allows us to isolate the individual ingredients of the theory and infer results that should hold for all holographic systems.

It is also important to identify the ingredients which are common to the top-down examples and assume that they are found in the conjectured bottom-up models as well [31]. For example, the duality should relate a gravitational theory on a negatively curved bulk spacetime to a field theory in one dimension lower, which we can imagine to reside at the boundary of the bulk. A large number of degrees of freedom is needed at the boundary to ensure a gravitational (and not a stringy) description which is usually achieved by choosing a large gauge symmetry group for the field theory (for example $SU(N)$ with $N \to \infty$). Furthermore, as we will discuss below, it is important that the symmetries of both systems are identified (see table 3). For example in the cases mentioned above, the gauge symmetry in the bulk arises from the isometry of a compact manifold multiplying the AdS, (for example S^5 in $\mathrm{AdS}_5 \times S^5$) with the size of the compact manifold being comparable to the size of the negatively curved spacetime.

Both approaches have their advantages and disadvantages. In what follows we present some of the principles which are commonly assumed. Our presentation is a combination of the following reviews [25, 26, 44–46], where a more detailed analysis is presented and original sources are cited.

Symmetries

We first match the symmetries of the two theories which also allows us to identify the fields on the gravity side with the operators of the CFT.

The spacetime symmetry of the CFT is the conformal group in $D+1$ dimensions, $SO(D+1,2)$, which exactly matches the isometry group of AdS in $D+2$ dimensions. To see the precise identification, look for example at AdS part of the metric (1.23), where at each fixed value of r, we get a Poincaré invariant $(D+1)$-dimensional Minkowski spacetime. The additional dilatation symmetry of the CFT is manifested by the isometry

$$x^\mu \to \lambda x^\mu \,, \qquad r \to \frac{r}{\lambda} \,, \tag{1.36}$$

with the first part being the usual flat space dilatation, while the r transformation ensures the preservation of the metric. Thus the dilatation symmetry is associated with a change of the scale in the radial direction of AdS.[18] By introducing an object with an associated length scale r_0 into the latter space, we break the dilatation symmetry

[18] Note that in this analysis we are using the Poincaré patch of AdS to describe the gravitational part of the duality. However the duality is *not* limited only to a part of AdS, but holds for the entire spacetime. So the correct statement is that string theory in global AdS_{D+2} is dual to a CFT defined on $\mathbb{R} \times S^D$ [31].

Symmetry on the Boundary	Symmetry in the Bulk
Conformal Spacetime Symmetry	Isometry of AdS
Global Symmetry (*e.g.* $\mathcal{R}$-Symmetry)	Gauge Symmetry (Symmetry of S^n)
Gauge Symmetry	*No analogue*

Table 3: The matching of the bosonic symmetries between the gauge theory (left column) and the dual gravitational theory (right column) [26, 44]. In addition the supersymmetries must match as well.

in the CFT, for example, an asymptotically AdS black hole, whose length scale is set by the horizon, breaks the the dilatation symmetry of the dual CFT by introducing a temperature whose value is given by the Hawking temperature of the black hole [47].

Next, a global symmetry of the quantum field theory gets translated into a gauge theory in the gravity picture. The global symmetry is usually a flavour symmetry or an $\mathcal{R}$-symmetry under which the theory is invariant. On the gravity side this corresponds to the symmetry of the S^n part, which can be dimensionally reduced generating a gauge theory (this is the Kaluza-Klein procedure).

If the theories are supersymmetric, the fermionic symmetries must match as well. A specific example of such an identification is discussed in chapter 4.

Finally, the gauge symmetry of the field theory has no analogue on the gravity side, since it is not a physical symmetry, but rather redundancy in the description. As a consequence, only *gauge invariant* operators, which represent physical observables, are mapped onto fields found in gravity. A summary of symmetry identifications is found in table 3.

Field-Operator Map and Correlation functions

There exist a precise prescription of how to map fields on the gravity side to the gauge invariant operators of the dual CFT, and as is often the case the physics lies in the boundary conditions. The precise prescription for computing Euclidean correlators was first given in [32, 48] and was generalised to correlators in Minkowski spacetime in [49] (see also [50–59]).

We present the prescription through the analysis of a minimally coupled massive scalar field. Assume that the metric is asymptotically AdS_{D+2} with radius R_{AdS}, so that the near boundary expansion $r \to \infty$ at leading order takes the form

$$ds^2 = g_{MN}\, dx^M dx^N \approx \frac{R^2_{\mathrm{AdS}}}{r^2}\, dr^2 + \frac{r^2}{R^2_{\mathrm{AdS}}}\, \eta_{\mu\nu}\, dx^\mu dx^\nu\,, \tag{1.37}$$

where $\mu = 0, 1, \ldots D$. The equation of motion for a scalar field $\phi(r, x^\mu)$ with mass m is

given by the Klein-Gordon equation

$$\partial_M \left(\sqrt{-g} g^{MN} \partial_N \phi(r, x^\mu)\right) - m^2 \sqrt{-g}\, \phi(r, x^\mu) = 0\,. \tag{1.38}$$

This is a second order ordinary differential equation, so it has two independent degrees of freedom that we need to fix to fully specify the solution. Near the boundary, there are two independent terms

$$\phi(r) = \frac{R_{\text{AdS}}^{2\Delta_-}}{r^{\Delta_-}} \phi_{(nn)}(x^\mu)\,(1 + \ldots) + \frac{R_{\text{AdS}}^{2\Delta_+}}{r^{\Delta_+}} \phi_{(n)}(x^\mu)\,(1 + \ldots) \tag{1.39}$$

where $\ldots$ denotes subleading terms that are uniquely determined in terms of $\phi_{(nn)}(x^\mu)$ and $\phi_{(n)}(x^\mu)$, and

$$\Delta_\pm = \frac{D+1}{2} \pm \sqrt{\left(\frac{D+1}{2}\right)^2 + m^2 R_{\text{AdS}}^2}\,, \tag{1.40}$$

so that $\Delta_+ = D + 1 - \Delta_-$ and $\Delta_+ > \Delta_-$. The solution corresponding to the free parameter $\phi_{(n)}(x^\mu)$ is called *normalisable*, whereas the solution with the degree of freedom $\phi_{(nn)}(x^\mu)$ is called *non-normalisable*, because if we evaluate the scalar field action on these solutions, the resulting value is normalisable and non-normalisable respectively.

The prescription [32, 48] states that the non-normalisable solution is identified with the source $J(x^\mu)$

$$\phi_{(nn)}(x^\mu) = J(x^\mu)\,, \tag{1.41}$$

while the normalisable solution is identified with the expectation value (or one-point function) $\langle \mathcal{O}(x^\mu) \rangle$ of the dual boundary operator $\mathcal{O}(x^\mu)$, whose conformal dimension is given by

$$\Delta_{\mathcal{O}} = \Delta_+ = \frac{D+1}{2} + \sqrt{\left(\frac{D+1}{2}\right)^2 + m^2 R_{\text{AdS}}^2}\,. \tag{1.42}$$

Since the identification between operators and gravitational fields is done at $r \to \infty$, we often refer to the CFT as the boundary theory with the asymptotically AdS spacetime considered the bulk.

Equation (1.42) expresses the conformal dimension of a boundary operator $\mathcal{O}$ in terms of the mass of its dual field ϕ in the bulk.[19] This relation changes for operators

[19] For certain ranges of the mass m, $\phi_{(n)}$ and $\phi_{(nn)}$ are both normalisable in which case either can be identified with the operator dual to the gravity field. Taking the former is called *regular quantisation*, while taking the latter is called *alternate quantisation*, in which case the conformal dimension of the dual CFT operator is given by $\Delta_{\mathcal{O}} = \Delta_-$. Special care needs to be taken if $\Delta_+ = \Delta_-$, but we do not

Bulk Fields	Conformal Dimension of Dual Operator
scalar fields	$\Delta_{\pm} = \frac{1}{2}\left(D+1 \pm \sqrt{(D+1)^2 + 4m^2 R_{\text{AdS}}^2}\right)$
spinor fields	$\Delta = \frac{1}{2}\left(D+1+2\lvert m\rvert R_{\text{AdS}}\right)$
vector fields	$\Delta_{\pm} = \frac{1}{2}\left(D+1 \pm \sqrt{(D-1)^2 + 4m^2 R_{\text{AdS}}^2}\right)$
p-form fields	$\Delta = \frac{1}{2}\left(D+1 \pm \sqrt{(D+1-2p)^2 + 4m^2 R_{\text{AdS}}^2}\right)$
spin-$\frac{3}{2}$ fields	$\Delta = \frac{1}{2}\left(D+1+2\lvert m\rvert R_{\text{AdS}}\right)$
massless spin-2 fields	$\Delta = D+1$

Table 4: The relation between the mass of a field in AdS and the conformal dimension of its dual boundary operator [26]. Where the conformal dimension is denoted by $\Delta_{\pm}$, one encounters two possible quantisations that cover the spectrum of boundary operators.

with non-zero spin, and the results are summarised in table 4. Combining the results of table 3 and table 4 allows us to identify duals of important bulk excitations. For example, metric excitations are identified with the energy-momentum tensor of the dual theory, while the excitations of the gauge field in the bulk are related to the globally conserved current in the CFT. These two identifications are universal in all holographic theories.

To uniquely determine the solution to the bulk equations of motion, we need to specify a boundary condition in the interior. In the case of Euclidean AdS space (after Wick rotating the time coordinate) it is sufficient to demand that the fields are regular in the interior. The correspondence then states that the exponent of the gravitational action evaluated on the regular solution with the boundary identification (1.41) is equivalent to the CFT path integral with a source. For a scalar field this gives

$$e^{-S_{grav}[\phi]}\Big|_{\phi_{(nn)}=J} = \left\langle e^{-\int d^{D+1}x\, J(x^\mu)\mathcal{O}(x^\mu)} \right\rangle_{CFT} , \tag{1.43}$$

or in other words, the on-shell gravitational action acts as a generating functional for the correlators of the dual CFT. The calculation of correlation functions in Lorentzian time contains additional subtleties which are discussed in chapter 2.

With this we conclude our brief review of the AdS/CFT duality. We have glossed over many important details, such as the renormalisation procedure which makes the equation (1.43) well defined, nonetheless we have introduced the relevant concepts that

consider such details here.

are used throughout the thesis.

1.5 Structure of the Document

The structure of the remainder of the document is as follows.

In chapter 2 we begin by stating the prescription for calculating the retarded Green's function in holographic theories. We then review pole-skipping, a phenomenon in which a pole and a zero of holographic correlation functions coincide, by studying bulk scalar fields in section 2.2 and excitations of the bulk metric in section 2.3. In the latter case we also discuss a potential relation to chaotic properties of such theories.

In chapter 3 we show that pole skipping is generically observed for fermionic fields as well. We start by analysing the equations of motion in asymptotically AdS_3 spaces for which some of the Green's functions are explicitly known. Higher dimensional spacetimes are considered in section 3.4, while in section 3.5 we show that near the pole-skipping points the correlator is infinitely multivalued. In section 3.6 explicit examples are considered before we end with some concluding remarks.

In chapter 4 we introduce the D1-D5-P system by studying its gravitational description and the corresponding brane picture in section 4.2 and section 4.3 respectively. We then review the AdS_3/CFT_2 duality and give a brief overview of the D1-D5 CFT at the orbifold point where the field theory is described by a collection of free fields. We then present the fuzzball proposal in section 4.6, which says that one should treat classical black holes as a course-grained average over many horizonless microstates. Finally, we introduce the microstate geometries programme whose aim is it to construct smooth and horizonless solutions within supergravity that have the same charges as a given black hole.

In chapter 5 we present the construction of a new family of superstrata – microstates of the D1-D5-P black hole for which the dual CFT description is explicitly known. The procedure relies on the construction of Killing spinors of global $AdS_3 \times S^3$ presented in section 5.4. These are then used as generators of a new perturbation around $AdS_3 \times S^3$ whose non-linear completion, calculated in section 5.6, is the new superstratum family.

We conclude in chapter 6 with an outlook on future research directions.

The appendices contain some technical details that are omitted from the main text. In Appendix A we collect the conventions used throughout the document. Appendix B and Appendix D contain some explicit calculations for the results presented in chapter 3 and chapter 5 respectively. The exact Green's function for fermion fields in the BTZ black hole background is calculated in Appendix C.

Chapter 2

Review of Pole Skipping

In this chapter we define different two-point functions appearing in thermal quantum field theories and present the prescription for calculating the retarded Green's functions in theories with gravity duals, by studying scalar fields in asymptotically AdS spacetimes.

We then turn to pole-skipping, a phenomenon where at certain (imaginary) values of the frequency and momentum, the value of the retarded Green's function of a holographic theory is infinitely multivalued. We introduce the basic principles through the analysis of scalar fields in the bulk, before reviewing the results for the energy-density correlator and comment on the connection to chaos.

Parts of this chapter have been reviewed in [2].

2.1 Introduction and Motivation

2.1.1 Retarded Green's Functions

In this and the following chapter we are interested in retarded Green's functions in theories at finite temperature. Our main motivation is to understand the behaviour of strongly coupled holographic quantum field theories which, through the AdS/CFT correspondence, have an equivalent description in terms of classical gravitational theories on curved backgrounds.

We consider field theories in a state at a finite temperature $T = \beta^{-1}$. In such theories the expectation values of an operator $\mathcal{O}$ is defined to be

$$\langle \mathcal{O} \rangle \equiv \mathrm{tr}\left(\rho \mathcal{O}\right) , \tag{2.1}$$

with the trace operator going over the Hilbert space of the field theory, and ρ is the

density matrix given by

$$\rho \equiv \frac{\exp\left(-\beta\mathcal{H}\right)}{\mathrm{tr}\left[\exp\left(-\beta\mathcal{H}\right)\right]}\,, \tag{2.2}$$

where for the canonical ensemble $\mathcal{H} = H$ is just the Hamiltonian, while for the grand-canonical ensemble $\mathcal{H} = H - \mu_i Q_i$, with Q_i being the operators measuring the conserved charges and μ_i the associated chemical potentials.

The fundamental objects of interest are retarded Green's functions. For a bosonic operator $\mathcal{O}_B(t,\vec{x})$ these can be written as (we follow the conventions of [55])

$$G^R_{(B)}(t,\vec{x}) \equiv i\theta(t)\ \langle[\mathcal{O}_B(t,\vec{x}),\mathcal{O}_B(0)]\rangle \tag{2.3}$$

where $\theta(t)$ is the step function and the brackets denote the expectation value of the commutator. Similarly, the advanced Green's function can be defined as

$$G^A_{(B)}(t,\vec{x}) \equiv -i\theta(-t)\ \langle[\mathcal{O}_B(t,\vec{x}),\mathcal{O}_B(0)]\rangle\ . \tag{2.4}$$

One can also define other two-point functions, such as the Feynman propagator or the (symmetrized) Wightman function [49, 60], however these can be determined once the retarded Green's function is known (see for example (2.7) of [49] for a relation between the Feynman propagator and the retarded Green's function in momentum space).

In Euclidean signature ($\tau_E \equiv it$) we usually deal with only a single correlator defined by

$$G^E_{(B)} \equiv \langle T_E \mathcal{O}_B(\tau_E,\vec{x})\mathcal{O}_B(0)\rangle\ , \tag{2.5}$$

where T_E denotes Euclidean time ordering.

If the operator $\mathcal{O}_F(t,\vec{x})$ is a complex fermion field, then the commutator has to be replaced with an anti-commutator and the analogous Green's functions are defined as [55]

$$G^R_{(F)}(t,\vec{x}) \equiv i\theta(t)\ \left\langle\left\{\mathcal{O}(t,\vec{x}),\mathcal{O}^\dagger(0)\right\}\right\rangle\ , \tag{2.6a}$$

$$G^A_{(F)}(t,\vec{x}) \equiv -i\theta(-t)\ \left\langle\left\{\mathcal{O}(t,\vec{x}),\mathcal{O}^\dagger(0)\right\}\right\rangle\ , \tag{2.6b}$$

$$G^E_{(F)}(\tau_E,\vec{x}) \equiv \left\langle T_E\mathcal{O}(\tau_E,\vec{x})\mathcal{O}^\dagger(0)\right\rangle\ , \tag{2.6c}$$

where the $\mathcal{O}^\dagger$ denotes the hermitian conjugate.

By performing a Fourier transformation one can obtain correlators in momentum

space, which in the Euclidean and Lorentzian signature are given by [49]

$$G^E\left(\omega_E, \vec{k}\right) = \int dx_E^4\, G^E(\tau_E, \vec{x})\, e^{-i\omega_E \tau_E - i\vec{k}\cdot\vec{x}}\,, \tag{2.7a}$$

$$G^{R,A}\left(\omega, \vec{k}\right) = \int dx^4\, G^{R,A}(t, \vec{x})\, e^{i\omega t - i\vec{k}\cdot\vec{x}}\,, \tag{2.7b}$$

where the Green's functions can involve either bosonic or fermionic operators.

2.1.2 Prescription for Holographic Retarded Green's Functions

Our aim is to calculate retarded Green's functions in holographic theories at finite temperature. The prescription (1.43) is formulated in Euclidean space and thus can be used to obtain Euclidean correlation functions. Lorentzian time correlators can in principle be obtained from their Euclidean counterparts by an appropriate analytic continuation, however as discussed in for example [49] or [51], this procedure is only possible if the Euclidean correlator is known exactly for all Matsubara frequencies. In practice the Euclidean correlator is often obtained only in some approximation or only at some, but not all, Matsubara frequencies. Thus in most cases we prefer a direct method to a Green's function in Lorentzian signature, which was formulated in [49] (see also [50–59]).

Assume that the bulk gravitational theory is described by the Einstein-Hilbert action with a negative cosmological constant term. We allow for additional matter content that can also contribute to the curvature of spacetime, thus the total action is given by

$$S = \int d^{D+2}x\sqrt{-g}\,(R - 2\Lambda) + S_{matter}\,, \tag{2.8}$$

where $\Lambda = -D(D+1)/2R_{\text{AdS}}^2$ is the cosmological constant, R_{AdS} is the AdS radius, which we henceforth set to $R_{\text{AdS}} = 1$, and S_{matter} denotes the matter contribution to the action.

As initially proposed in [47], the gravity dual of a thermal state is a black hole in AdS whose Hawking temperature matches the temperature of the boundary theory. In our case we assume that there exist a generic planar black hole solution which is asymptotically AdS and whose metric is given by

$$ds^2 = -r^2 f(r) dt^2 + \frac{dr^2}{r^2 f(r)} + h(r) d\vec{x}^2\,, \tag{2.9}$$

with r denoting the radial direction and the boundary is located at $r \to \infty$. Furthermore, t denotes time, and x_i with $i = 1 \ldots D$ are the coordinates of the D spatial dimensions, thus making $(t, \vec{x}) \in \mathbb{R}^{1,D}$ the spacetime on which we find the boundary theory.

The precise form of the two functions $f(r)$ and $h(r)$ is determined by the additional matter, yet their near-boundary behaviour is constrained to be

$$\lim_{r\to\infty} f(r) \to 1\,, \qquad \lim_{r\to\infty} h(r) \to r^2\,, \tag{2.10}$$

by demanding that the spacetime is asymptotically anti-de Sitter. We also assume that the geometry has a non-degenerate horizon at $r = r_0$, *i.e.* $f(r_0) = 0$ with $f'(r_0) \neq 0$, so that the corresponding Hawking temperature is given by

$$4\pi T = r_0^2\, f'(r_0)\,. \tag{2.11}$$

The simplest solutions of the this type are planar AdS-Schwarzschild black holes with

$$f(r) = 1 - \left(\frac{r_0}{r}\right)^{D+1}\,, \qquad h(r) = r^2\,, \tag{2.12}$$

which in the case of $D = 1$ becomes the BTZ black hole [61,62], and occur when there is no additional matter in the system.

The horizon plays a central role in our analysis. Thus it is convenient to switch to the ingoing Eddington-Finkelstein coordinates, which we now define more generally as

$$v = t + r_*\,, \qquad \frac{dr_*}{dr} = \frac{1}{r^2 f(r)}\,, \tag{2.13}$$

with the metric taking the form

$$ds^2 = -r^2 f(r) dv^2 + 2dv\, dr + h(r) d\vec{x}^2\,. \tag{2.14}$$

In these coordinates the horizon is a regular surface where the components of the metric do not diverge.

Let us now review the prescription of Son and Starinets using a bulk scalar field φ and its dual boundary operator $\mathcal{O}$. Assume that the action of the bulk scalar is given by

$$S_\varphi = -\frac{1}{2}\int d^{D+2}x\sqrt{-g}\left(g^{MN}\partial_M\varphi\,\partial_N\varphi + m^2\varphi^2\right)\,, \tag{2.15}$$

resulting in equation of motion

$$\partial_M(\sqrt{-g}g^{MN}\partial_N\varphi) - m^2\sqrt{-g}\varphi = 0\,. \tag{2.16}$$

Assume that the backround metric is given by (2.14). Since the metric components depend only on the variable r, we can consider the plane-wave ansatz $\varphi = \phi(r)e^{-i\omega v + i\vec{k}\cdot\vec{x}}$

which reduces the differential equation to

$$\frac{d}{dr}\left[h^{\frac{D}{2}}\left(r^2 f\partial_r\phi - i\omega\phi\right)\right] - i\omega h^{\frac{D}{2}}\partial_r\phi - h^{\frac{D}{2}-1}\left(k^2 + m^2 h\right)\phi = 0. \tag{2.17}$$

Next we expand this equation around the horizon. In the ingoing Eddington-Finkelstein coordinates the horizon is a regular point, so we assume that the series expansions of $f(r)$ and $h(r)$ around this point have finite radii of convergence, and look for the solutions that are regular at the horizon and can thus be written as

$$\phi(r) = \sum_{j=0}^{\infty} \phi_j (r - r_0)^j \,, \tag{2.18}$$

Near the horizon, there exist two power law solutions $\phi = (r - r_0)^\alpha$ with

$$\alpha_1 = 0, \qquad \alpha_2 = \frac{i\omega}{2\pi T}. \tag{2.19}$$

For generic values of ω, only the solution with exponent α_1 is regular and is therefore taken to be the ingoing solution, while the solution with exponent α_2 corresponds to the outgoing solution.[20]

The prescription [49] states that in order to calculate the retarded Green's function only the ingoing solution (which we call ϕ_R) needs to be retained while the outgoing solution is set to 0. The chosen solution is then evolved in the radial direction outwards to the boundary of AdS where it can be expanded into a normalisable and non-normalisable part

$$\phi_R = \phi^{(nn)}(\omega, k) r^{\Delta_\mathcal{O} - D - 1} + \phi^{(n)}(\omega, k) r^{-\Delta_\mathcal{O}} + \dots \,, \tag{2.20}$$

where $\Delta_\mathcal{O}$ is given in (1.42). The non-normalisable solution is again identified with the source field, while the normalisable solution is identified with the expectation value of the dual operator. The retarded Green's function of the dual operator is then given by

$$G^R(\omega, k) \propto \frac{\phi^{(n)}(\omega, k)}{\phi^{(nn)}(\omega, k)} \,, \tag{2.21}$$

up to possible contact terms. The constant prefactor can be obtained from a more careful analysis of the action near the boundary, but plays no role in this thesis.

The above is reminiscent of linear response theory where upon the introduction of an external source $J(x)$ of a field $\psi(x)$, the relation to linear order in the interaction is

[20] The exponent α_1 has to be zero, because the horizon is not a special point in the ingoing Eddington-Finkelstein coordinates. In the coordinate system of (2.9), the two exponents take the values $\alpha_\pm = \pm\frac{i\omega}{4\pi T}$. The solution with α_- is ingoing, while α_+ is related to the outgoing solution.

given in Fourier space by (see for example [63])

$$\delta \langle \psi(\omega, k) \rangle = -G^R(\omega, k)\, J(\omega, k)\,, \tag{2.22}$$

with the additional minus sign being due to our choice of conventions, and $\delta \langle \psi(\omega, k) \rangle$ denotes a small change in the expectation value of the field evaluated in the equilibrium ensemble. In holographic theories, we associate the one-point function with the normalised bulk solution and the source with the non-normalisable bulk solution, thus we see that (2.21) and (2.22) are analogous. This is why retarded Green's functions are one of the basic quantities of interest in quantum field theories, as they measure how the system in equilibrium responds to small perturbations.

2.1.3 Motivation for Pole-Skipping

In principle the prescription for calculating the retarded Green's function is straightforward. However, evolving the ingoing solution from the horizon to the boundary turns out to be computationally challenging. While it can be done explicitly in the simplest cases (e.g. the BTZ black hole [49, 55, 64–66]), typically one has to use numerical methods to obtain full solutions.

Generically, the retarded Green's function depends in a complicated way on the details of the state in the quantum field theory which by the holographic dictionary means an equally complicated dependence on the full bulk profile of the dual field. Thus obtaining a complete solution of the bulk equations of motion is paramount to uncover all the details of the Green's functions.

Simplifications occur in the low-frequency and low-wavenumber limit, where the form of the correlator is dictated by near-horizon physics in the bulk and its qualitative features are independent of the rest of the geometry. For example, the value of the ratio between the shear viscosity and entropy density is determined only by the horizon geometry and is independent of the value of the bulk field couplings [67].

Recently it has been observed that certain properties of the correlators *away from the* $\omega = 0$, $k = 0$ *point in Fourier space* can already be seen in the near horizon behavior of the solutions [68–75]. At certain finite imaginary values of the frequency and momentum there is no unique ingoing solution at the horizon. As a consequence, near these points in Fourier space the holographic retarded Green's function ceases to be uniquely defined and takes on a form that explicitly depends on a parameter determining the direction in which we approach the special point. Such behaviour was dubbed "pole-skipping" as it occurs where a line of poles intersects a line of zeros of the Green's function of the dual boundary operator.

2.2 Pole Skipping for Scalar Fields

Let us start by analysing pole-skipping for a minimally coupled scalar field with the action (2.15). We closely follow [72] where these calculations were initially performed. See that paper and the references therein for more details.

Working in the ingoing Eddington-Finkelstein coordinates, we saw that the equation of motion (2.17) has two power law solutions at the horizon with the exponents given by (2.19). For generic values of ω, the solution with the exponent α_2 cannot be expanded in a regular series around the horizon, hence the solution with α_1 is the unique ingoing solution.

However, at the special values of frequency $\omega_n = -2i\pi Tn$ with $n = 1, 2, \ldots$, the second exponent becomes $\alpha_2 = n$, and naïvely both solutions seem to be regular at the horizon. But in fact, the solution with the exponent α_1 becomes logarithmically divergent as the full near-horizon expansion now takes the form

$$\begin{aligned}\phi(r) = \phi_0 \left[1 + A_1(r-r_0) + \ldots + (r-r_0)^n \log(r-r_0)\left(B_0 + B_1(r-r_0) + \ldots\right)\right] \\ + \phi_n (r-r_0)^n \left[1 + C_1(r-r_0) + \ldots\right] ,\end{aligned} \tag{2.23}$$

where ϕ_0 and ϕ_n are the free parameters associated with the two solutions near the horizon, and the coefficients A_i, B_i, and C_i are completely determined in terms of the scalar field mass and the background metric evaluated at the horizon. Since the ingoing solution is regular in the ingoing Eddington-Finkelstein coordinates, we are prescribed to set $\phi_0 = 0$ which eliminates the divergent parts. Thus even at such special values of the frequency, there exists a unique ingoing solution at the horizon, albeit with a different leading near-horizon behaviour.

However, for certain values of the momentum k, *all* B_i coefficients vanish, rendering all solutions regular at the horizon. Therefore, for finely tuned values of ω and k, there are two independent ingoing solutions. Thus when using the prescription of [49], selecting the ingoing solution does not sufficiently constrain the solution to yield a uniquely defined retarded Green's function.

To see this explicitly, insert the field expansion (2.18) into the equations of motion (2.17), expand them around the horizon as

$$\mathcal{S} = \sum_{j=0}^{\infty} \mathcal{S}_j (r-r_0)^j , \tag{2.24}$$

and solve the resulting system of algebraic equations $\mathcal{S}_j = 0$ order by order for each j. The first relation imposes a constraint between ϕ_0 and ϕ_1

$$\mathcal{S}_0 = (4\pi T - 2i\omega)\, h(r_0)\, \phi_1 - \left(k^2 + m^2 h(r_0) + \frac{i\omega D h'(r_0)}{2}\right) \phi_0 = 0, \tag{2.25}$$

which, for generic values of k and ω, can be used to determine ϕ_1 in terms of ϕ_0. The next equation, $\mathcal{S}_1 = 0$, relates ϕ_2, ϕ_1 and ϕ_0, which combined with (2.25), determines ϕ_2 as a function of only ϕ_0. This procedure is then repeated indefinitely until all coefficients are uniquely determined in terms of only ϕ_0, which serves as the undetermined overall normalisation, or equivalently, the free parameter of the ingoing solution.

If we evaluate (2.25) at $\omega = \omega_1 = -2i\pi T$, which is the first bosonic Matsubara frequency,[21] the equation becomes

$$\left(k^2 + m^2 h(r_0) + \pi D T h'(r_0)\right)\, \phi_0 = 0, \tag{2.26}$$

which for generic values of k imposes $\phi_0 = 0$ while leaving ϕ_1 unconstrained. Higher order equations $\mathcal{S}_j = 0$ are then used to express all other coefficients ϕ_n uniquely in terms of ϕ_1, which in this case serves as the free parameter of the solution. This result is consistent with the analysis of the divergences in (2.23), as when $\omega = \omega_1$ the exponents (2.19) take the values $\alpha_1 = 0$ and $\alpha_2 = 1$, with the solution associated with the former being divergent due to the logarithmic terms.

Finally, the equation (2.25) becomes trivially satisfied, leaving ϕ_0 and ϕ_1 unconstrained, if the frequency and the wavenumber are tuned to be equal to

$$\omega_1 = -2i\pi T, \qquad k_1^2 = -m^2 h(r_0) - \pi D T h'(r_0)\,. \tag{2.27}$$

Higher order constraints $\mathcal{S}_j = 0$ allow us to express ϕ_j, with $j = 2, 3, \ldots$, as a linear combination of ϕ_0 and ϕ_1, in which case we obtain an explicit ingoing solution with two independent free parameters. Due to the lack of a unique ingoing solution, the retarded Green's function of the operator dual to the scalar field is infinitely multivalued at this point in Fourier space.

Furthermore, it was shown in [72] that there are infinitely many additional pole-skipping points located at higher Matsubara frequencies $\omega = \omega_n = -2\pi i T n$. To locate these, we arrange the system of equations $\mathcal{S}_j = 0$ for $j = 0, 1, 2, \ldots$ in matrix form

$$M(\omega, k^2) \cdot \phi \equiv \begin{pmatrix} M_{11} & 2\pi T - i\omega & 0 & 0 & \ldots \\ M_{21} & M_{22} & 4\pi T - i\omega & 0 & \ldots \\ M_{31} & M_{32} & M_{33} & 6\pi T - i\omega & \ldots \\ \ldots & \ldots & \ldots & \ldots & \ldots \end{pmatrix} \begin{pmatrix} \phi_0 \\ \phi_1 \\ \phi_2 \\ \vdots \end{pmatrix} = 0\,, \tag{2.28}$$

where the coefficients are generically of the form $M_{ij}(\omega, k^2) = i\omega\, a_{ij} + k^2 b_{ij} + c_{ij}$, with a_{ij}, b_{ij}, and c_{ij} determined by the background metric at the horizon and the mass of

[21] Euclidean Green's functions are defined at Matsubara frequencies which are real numbers. With an abuse of language, we refer to the purely imaginary frequencies $\omega_n = -2\pi i n$ ($n \in \mathbb{Z}^+$) as Matsubara frequencies as well.

the scalar field. Due to the almost-lower triangular form of the matrix $M(\omega, k^2)$, the system is easily solved iteratively with all ϕ_n expressed in terms of only one parameter, which is usually taken to be ϕ_0, as we have discussed above.

Such a solution exists only if the frequency is not equal to one of the bosonic Matsubara frequencies, in which case exactly one of the elements above the main diagonal of M vanishes. If we assume that $\omega = \omega_n$, we obtain a closed set of equations for the coefficients $\tilde{\phi} = (\phi_0, \ldots, \phi_{n-1})$, which is of the form

$$\mathcal{M}^{(n)}(\omega_n, k^2) \cdot \widetilde{\phi} = 0\,, \tag{2.29}$$

where $\mathcal{M}^{(n)}(\omega_n, k^2)$ is the submatrix of $M(\omega, k^2)$ consisting of the first n rows and first n columns. For generic values of k, the matrix $\mathcal{M}^{(n)}(\omega_n, k^2)$ is invertible, setting $\tilde{\phi} = 0$. Inserting this into (2.28) allows us to solve the remaining system of equations iteratively with ϕ_n as the free parameter.

If the value of k is such that the matrix $\mathcal{M}^{(n)}(\omega_n, k^2)$ is not invertible, then the regular solution of (2.28) has two free parameters, for example ϕ_0 and ϕ_n. This occurs at the following locations in Fourier space

$$\omega_n = -2\pi i T n, \qquad k^2 = k_n^2, \qquad \det \mathcal{M}^{(n)}(\omega_n, k_n^2) = 0\,, \tag{2.30}$$

which at each order n, due to the determinant being a polynomial function of k^2 with degree n, gives in general $2n$ pole-skipping points. Similar to before, at these locations imposing the ingoing boundary condition at the horizon does not yield a unique value for the retarded Green's function.

Near such points in momentum space the correlator takes on the *pole-skipping form* [70, 72], given by

$$G^R(\omega_n + \delta\omega, k_n + \delta k) \propto \frac{\delta\omega - \left(\frac{\delta\omega}{\delta k}\right)_z \delta k}{\delta\omega - \left(\frac{\delta\omega}{\delta k}\right)_p \delta k}\,, \tag{2.31}$$

where $(\delta\omega/\delta k)_p$ is the direction at which we obtain a normalizable solution, corresponding to the poles in the boundary Green's function, while $(\delta\omega/\delta k)_z$ denotes the direction of the non-normalisable solution associated with the slope of the line of zeros of the correlator. This form shows that generically pole-skipping points are intersections of lines of zeros and lines of poles of the retarded Green's function. This is the motivation behind the name "pole-skipping", because at such points the expected divergence coming from the vanishing denominator of (2.31), is cancelled out by a coinciding zero of the numerator of the correlator [68–71].

There also exist *anomalous* points [72] which are locations that appear as possible pole-skipping points from the near-horizon analysis, but the Green's function near them

does not take the pole-skipping form (2.31). For the scalar field a location is called anomalous if, in addition to (2.30), it satisfies [72]

$$\partial_k \det \mathcal{M}^{(n)}(\omega_n, k_n^2) = 0\,, \tag{2.32}$$

which means that anomalous points correspond to locations of coinciding pole-skipping points. We discuss the appearance and meaning of such locations in much more detail in the next chapter when we study pole-skipping for fermionic fields.

2.2.1 Example: BTZ Black Hole

As an illustration of the above concepts, we can analyse the example of a massive minimally coupled scalar field (with action (2.15)) propagating in the non-rotating BTZ black hole background with the metric [61, 62]

$$ds^2 = -(r^2 - r_0^2)dt^2 + \frac{dr^2}{(r^2 - r_0^2)} + r^2 dx^2\,, \tag{2.33}$$

with $0 \leq x < 2\pi$ and r_0 denoting the location of the horizon which is related to the mass and the temperature of the black hole as

$$2\pi T = r_0\,, \qquad 8MG_N = r_0^2\,, \tag{2.34}$$

where G_N is the Newton's constant.

In this case the retarded correlation function of the dual boundary operator is known explicitly [49] and can be (up to some constant prefactors) written as [72]

$$G^{\mathrm{R}}(\omega, k) \propto \frac{\Gamma\left(\frac{\Delta}{2} + \frac{i(k-\omega)}{4\pi T}\right)\Gamma\left(\frac{\Delta}{2} - \frac{i(k+\omega)}{4\pi T}\right)}{\Gamma\left(1 - \frac{\Delta}{2} + \frac{i(k-\omega)}{4\pi T}\right)\Gamma\left(1 - \frac{\Delta}{2} - \frac{i(k+\omega)}{4\pi T}\right)}\,, \tag{2.35}$$

where we have used the conformal dimension of the dual operator Δ, which is related to the mass m of the bulk field through $m^2 = \Delta(\Delta - 2)$. In the standard quantisation method the larger root is taken and in the alternative quantisation the smaller root of the equation is chosen. Importantly, we need to note that (2.35) is valid only if Δ takes on a non-integer value. In the special case of integer conformal dimensions additional care needs to be taken and we discuss such occasions later.

With the exact expression for the retarded Green's function known, we can explicitly check the pole-skipping structure of the correlator. This analysis was first performed in [73] and [72] with our analysis closely following the latter presentation. Following the systematic procedure described above, the near-horizon analysis of the bulk scalar equations of motion on (2.33) (using the ingoing Eddington-Finkelstein coordinates)

shows that the determinant of the (sub)matrix $\mathcal{M}^{(n)}(\omega_n, k^2)$ (evaluated at the n-th bosonic Matsubara frequency $\omega_n = -2\pi i n T$) is given by [72]

$$\det \mathcal{M}^{(n)}(\omega_n, k^2) = C_n \prod_{q_1=1}^{n} (k^2 - k_{n,q_1}^2)\,, \qquad k_{n,q_1}^2 = -r_0^2(n - 2q_1 + \Delta)^2\,, \tag{2.36}$$

with C_n denoting some constant numbers and $q_1 \in \{1, \ldots, n\}$. This means that the bulk prediction for locations of pole-skipping points is given by

$$\omega = \omega_n = -2\pi i n T\,, \qquad k_{n,q_1} = \pm 2\pi i T(n - 2q_1 + \Delta)\,, \tag{2.37}$$

with $n = 1, 2, \ldots$ and $q_1 \in \{1, \ldots, n\}$.

Let us now compare these results with the analysis of the exact correlator (2.35). The Green's function has a pole whenever an argument of a gamma function in the numerator equals a non-positive integer and a zero whenever an argument of a gamma function in the denominator is a non-positive integer. One thus finds that there are two families of poles, given by

$$\omega_{q_2}^{p}(k) = \pm k - 2\pi i T(\Delta + 2q_2)\,, \tag{2.38}$$

and similarly two sets of lines of zeros parametrised by

$$\omega_{q_2}^{z}(k) = \pm k - 2\pi i T(2 - \Delta + 2q_2)\,, \tag{2.39}$$

where in both cases $q_2 = 0, 1, 2, \ldots$. As the name suggests, we expect pole-skipping whenever a pole and a zero of the correlator coincide which in this case occurs at the intersections between the lines given by equations (2.38) and (2.39). These locations are

$$\omega = \omega_n = -2\pi i T n\,, \qquad k_{n,q_2} = \pm 2\pi i T(n - 2q_2 + \Delta)\,, \tag{2.40}$$

with $n = 1, 2, \ldots$ and $q_2 \in \{1, 2, \ldots n\}$. Comparing these locations with the near-horizon prediction (2.37), we observe that the two locations match perfectly (see figure 4 for a graphical representation of these results).

Should the conformal dimension of the dual field be an integer then the correlator

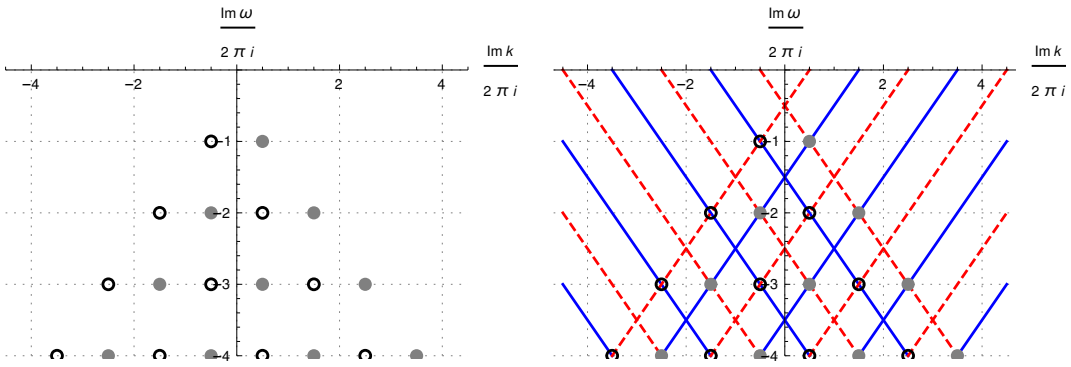

Figure 4: Plots of the locations of pole-skipping points for the scalar Green's function in the BTZ black hole background with $\Delta = 3/2$. The left plot shows only the locations of the pole-skipping points as predicted from the near horizon analysis. The gray points correspond to the the momentum values with a positive sign in and the hollow points correspond to the momenta with a negative sign as written (2.37). The right plot has superimposed the lines of zeros (red, dashed) from (2.39) and lines of poles (blue) from (2.38). The near-horizon analysis predicts the location of the intersections of lines of zeros and lines of poles.

takes on a slightly different form, given by [72, 73][22]

$$G^{\mathrm{R}}(\omega,k) \propto \frac{\Gamma\left(\frac{\Delta}{2}+\frac{i(k-\omega)}{4\pi T}\right)\Gamma\left(\frac{\Delta}{2}-\frac{i(k+\omega)}{4\pi T}\right)}{\Gamma\left(1-\frac{\Delta}{2}+\frac{i(k-\omega)}{4\pi T}\right)\Gamma\left(1-\frac{\Delta}{2}-\frac{i(k+\omega)}{4\pi T}\right)}\times \left[\psi\left(\frac{\Delta}{2}+\frac{i(k-\omega)}{4\pi T}\right)+\psi\left(\frac{\Delta}{2}-\frac{i(k+\omega)}{4\pi T}\right)\right], \tag{2.41}$$

with $\psi(z) \equiv \Gamma'(z)/\Gamma(z)$ denoting the digamma function. This change of the correlator has a signature in the near-horizon analysis in the form of anomalous pole-skipping locations. Here we will merely state the results, while the detailed analysis can be found in Appendix C of [72]. Let us limit ourselves to the case where $\Delta > 1$ (and still an integer).[23] At frequencies $\omega_n = -2\pi i n T$ with $n < \Delta$ the pole-skipping points are located at the standard positions (2.37) whereas for $n \geq \Delta$ the pole-skipping points can be found at [72]

$$\omega_n = -2\pi i n T\,, \qquad k_{n,q} = \pm 2\pi i T(n-2q+\Delta)\,, \tag{2.42}$$

where $n = 1, 2, \ldots$, but now $q \in \{1, \ldots \min(n, \Delta-1)\}$.

Let us now analyse the exact form of the correlator (2.41). Since Δ is now an integer, the ratio of gamma functions can be pairwise replaced by a product of a finite

[22] See Appendix D of [72] for the explicit derivation of this form for the correlator.

[23] The case for $\Delta = 1$ is special as there are no non-anomalous pole-skipping points [72, 73], so we do not consider it here.

number of simple factors, for example

$$\frac{\Gamma\left(\frac{\Delta}{2}+\frac{i(k-\omega)}{4\pi T}\right)}{\Gamma\left(1-\frac{\Delta}{2}+\frac{i(k-\omega)}{4\pi T}\right)}=\left(1-\frac{\Delta}{2}+\frac{i(k-\omega)}{4\pi T}\right)\left(2-\frac{\Delta}{2}+\frac{i(k-\omega)}{4\pi T}\right)\cdots\left(\frac{\Delta}{2}-1+\frac{i(k-\omega)}{4\pi T}\right), \tag{2.43}$$

where the right hand side contains $\Delta-1$ factors. An analogous expression can be obtained for the other pair of gamma functions.

We see that these products contain the lines of zeros of the correlator, which are located at

$$\omega^z_{q_1}=\pm k-2\pi iT(2-\Delta+2q_1)\,, \tag{2.44}$$

with $q_1\in\{0,1,\ldots,\Delta-2\}$. The poles of the correlator are contained within the digamma functions – the Green's function diverges whenever an argument of either function is a non-positive integer. This yields two infinite families of lines of poles with dispersion relations

$$\omega^p_{q_2}=\pm k-2\pi iT(\Delta+2q_2)\,, \tag{2.45}$$

with $q_2\in\{0,1,2,\ldots\}$. Comparing the lines of zeros (2.44) with the lines of poles (2.45) we find intersections at

$$\omega=\omega_n=-2\pi inT\,,\qquad k_{n,q_2}=\pm 2\pi iT(n-2q_2+\Delta)\,, \tag{2.46}$$

with $n=1,2,\ldots$ and $q\in\{1,\ldots\min(n,\Delta-1)\}$. Again these locations coincide precisely with the predictions from the near-horizon analysis (2.42) (see figure 5 for an example of pole-skipping points at integer Δ).

2.3 Pole Skipping for Spin-2 Fields

Let us briefly review pole-skipping in the energy density correlator where this phenomenon was initially observed [68–71]. We closely follow [70], assume that the background metric is given by (2.14), and let the metric perturbations take the plane wave form $\delta g_{MN}e^{-i\omega v+i\vec{k}\cdot\vec{x}}$, with a similar ansatz for any matter fields.

The equations of motion for such perturbations are the linearised Einstein's equations which we separate into two parts; let $E_{vv}=0$ denote the vv component while $X=0$ schematically represents all other equations. Expand the perturbations in a

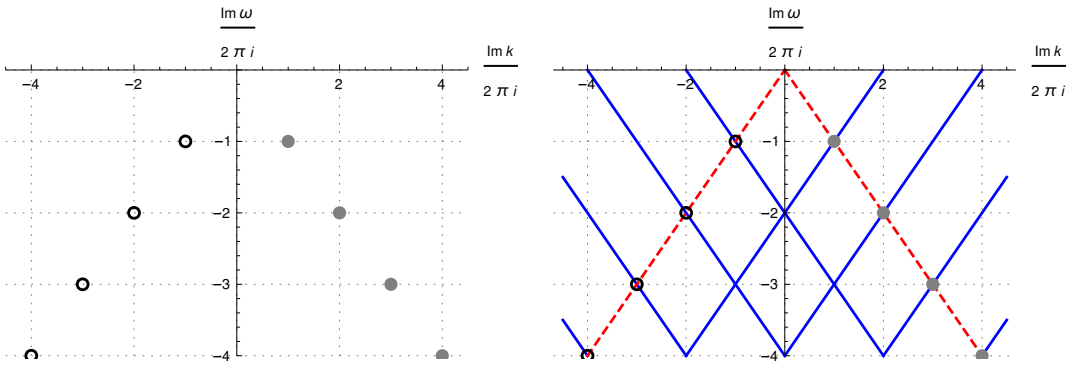

Figure 5: Plots of the locations of pole-skipping points for the scalar Green's function in the BTZ black hole background with $\Delta = 2$. The left plot shows only the locations of the pole-skipping points as predicted from the near horizon analysis, taking anomalous pole-skipping points into account. The gray points correspond to the the momentum values with a positive sign in and the hollow points correspond to the momenta with a negative sign as written (2.42). The right plot has superimposed the lines of zeros (red, dashed) from (2.44) and lines of poles (blue) from (2.45). The near-horizon analysis predicts the location of the intersections of lines of zeros and lines of poles.

series around the horizon as

$$\delta g_{MN} = \sum_{k=0}^{\infty} \delta g_{MN}^{(k)} \, (r - r_0)^k \,, \tag{2.47}$$

with $\delta g_{MN}^{(k)}$ being constant expansion coefficients. Evaluating the equations of motion at the horizon, $X = 0$ introduce non-trivial relations between different perturbation components, while $E_{vv} = 0$ reads [70][24]

$$\left(-i \frac{D\omega h'(r_0)}{2} + k^2 \right) \delta g_{vv}^{(0)} - i \, (2\pi T + i\omega) \left[\omega, \delta g_{x^i x^i}^{(0)} + 2k \, \delta g_{vx}^{(0)} \right] = 0 \,. \tag{2.48}$$

If $\omega = +2\pi i T$ while k is generic, this equation implies that $\delta g_{vv}^{(0)}$ vanishes. If in addition $k^2 = -D\pi T h'(r_0)$, then (2.48) is trivially satisfied and does not impose any constraints. In this case the ingoing condition at the horizon again does not restrict the solution enough to uniquely determine the Green's function.

Thus for the energy density correlator, unlike for the scalar field, the first pole-skipping point is located in the upper complex plane for the frequency at

$$\omega = +i\lambda_L \,, \qquad k = ik_0 \,, \tag{2.49}$$

[24] In (2.48) we omitted a term on the right hand side coming from the variation of the matter fields. However, in [70] it was shown that this term vanishes identically at the horizon for a class of theories called the Einstein-Maxwell-Dilaton-Axion gravity (see Appendix A of that paper).

with

$$\lambda_L = 2\pi T\,, \qquad k_0^2 = \frac{\lambda_L^2}{v_B^2} = \pi D T h'(r_0)\,, \tag{2.50}$$

where v_B denotes the butterfly velocity and λ_L the Lyapunov exponent of holographic theories [76]. So it seems that this pole-skipping point contains information about the chaotic properties of the theory, which is further substantiated by inserting (2.49) into the plane wave ansatz. Assuming isotropic spreading in the spatial directions with momentum k_0, the resulting profile $e^{\lambda_L(t-|x|/v_B)}$ shows the exponential growth typically observed in the out-of-time ordered correlation functions (OTOCs) of chaotic systems [76–80]. But is this relation a generic feature of pole-skipping or only a peculiarity?

The point (2.49) seems to be robustly related to chaos. For example, in [70] they studied a specific axion model with a parameter that controls the momentum dissipation in the boundary theory [81, 82]. The pole-skipping point (2.49) remained a reliable prediction of chaos, despite the physics being fundamentally distinct for different values of the parameter which was confirmed both analytically and numerically. Similar results hold for a pure gravity system on AdS_5 [68]. Furthermore, [71] showed that this pole-skipping location correctly predicts the chaotic properties of a system with large N and t'Hooft coupling corrections.

A possible explanation was provided in [69], where they proposed that pole-skipping is a generic feature of holographic systems due to the dual role of an effective "chaotic" mode which is responsible for both the chaotic properties and energy transport. In addition, a *shift symmetry* prevents the 2-point function to exhibit generic chaotic behaviour, while also predicting the exponential growth of the OTOC.[25] This provides an explicit mechanism to explain the observation that microscopic chaotic behaviour and the hydrodynamics of holographic systems seem to be intimately connected.[26]

On the contrary, the relation to chaos is not clear for other pole-skipping points. For example, it was shown in [72] that the energy density correlator, in addition to (2.49), contains an infinite tower of pole-skipping points at negative imaginary values of the frequency. Also, the momentum values at these locations depend on the background geometry in a complicated manner and seem to have no clear connection to the butterfly velocity. Furthermore, other components of the energy-momentum tensor have pole-skipping points only at negative imaginary values of the frequency with the momentum values showing no direct relation to chaos.

Similarly, no scalar pole-skipping point is located on the upper complex plane of the frequency while the momentum also explicitly depends on the mass of the field, as

[25] A similar effective approach was taken in [83] where they studied two-dimensional CFTs at large central charge and also found pole-skipping

[26] See [84–89] for some concrete results, where for example the butterfly velocity appears in hydrodynamic quantities such as diffusion constants.

can be seen even from the simplest expression (2.27), thus showing no clear connection to the butterfly velocity in general. But notice that at $m = 0$, the momentum location is the same as for the energy density correlator (2.50).

To summarize, the relation between chaos and pole-skipping seems to be somewhat clear only in the case of the special pole-skipping point in the energy density correlator while being obscured in the case of other correlators. Resolving this relation, together with the physical interpretation of these results, is the central problem of pole-skipping.

Chapter 3

Pole Skipping for Fermion fields

In this chapter we generalise the results of [72] by studying the retarded Green's functions of fermionic fields. We present a systematic procedure to extract the pole-skipping points which are now located at fermionic Matsubara frequencies, and show that near these locations the correlator takes on the pole-skipping form. Explicit examples are considered and complete agreement is found where the Green's function is known.

The plan of the chapter is as follows. We begin by defining a minimally coupled fermion field on an anti-de Sitter background and review the prescription to calculate the retarded Green's function for fermion fields in holography [55]. Then in section 3.3 we look at pole-skipping in 3-dimensional spacetimes while the generalization to higher dimensions is given in section 3.4. In section 3.5 we examine the form of the Green's function near a pole-skipping point in momentum space and discuss the appearance of anomalous locations. In section 3.6 we consider some explicit examples, such as the BTZ black hole, and compare the results with the known Green's function. We also examine the special case of boundary operators with half-integer conformal dimensions. We conclude with a discussion where we also comment on pole-skipping for spin-3/2 fields.

Details of some of the calculations omitted in the main text are collected in Appendix B, and we examine the exact Green's function for the BTZ black hole in Appendix C. There we uncover the equivalence of the retarded and advanced Green's function at Matsubara frequencies and further consider the special case of a spinor with half-integer conformal dimension.

The original work presented in this chapter is published in [2]. The analysis of pole-skipping for spin-3/2 fields will be presented in future work [90].

3.1 Motivation

As with scalar fields, the exact Green's functions for fermion fields are hard to obtain. An example where an explicit expression is known is the minimally coupled fermion field with mass m propagating in a BTZ black hole background [55][27]

$$G^R(\omega,k) = -i\,\frac{\Gamma\left(\frac{1}{2}-m\right)\Gamma\left(\frac{m}{2}+\frac{1}{4}+\frac{i(k-\omega)}{4\pi T}\right)\Gamma\left(\frac{m}{2}+\frac{3}{4}-\frac{i(k+\omega)}{4\pi T}\right)}{\Gamma\left(\frac{1}{2}+m\right)\Gamma\left(-\frac{m}{2}+\frac{3}{4}+\frac{i(k-\omega)}{4\pi T}\right)\Gamma\left(-\frac{m}{2}+\frac{1}{4}-\frac{i(k+\omega)}{4\pi T}\right)}\,, \tag{3.1}$$

It was observed in [72] (see also section 3.6) that this correlator contains two lines of zeros and two lines of poles which intersect at

$$\begin{aligned} \omega_n = -i\pi T(2n+1), \qquad k_{n,q_1} &= 2\pi i T(m+n-2q_1), \\ k_{n,q_2} &= -2\pi i T(m+n+1-2q_2), \end{aligned} \tag{3.2}$$

for any $n \in \{0,1,\ldots\}$ and with $q_1 \in \{0,\ldots,n\}$, $q_2 \in \{1,\ldots,n\}$. This example shows explicitly that pole-skipping exists even for fermions. In this chapter we provide the gravitational origin of this result and show that such behaviour is not limited to the BTZ black hole, but appears generically in holographic theories. As in the above example, pole-skipping for fermions occurs at fermionic Matsubara frequencies[28]

$$\omega = \omega_n^F := -2\pi i T\left(n+\frac{1}{2}\right)\,, \qquad n = 0,1,2,\ldots\,, \tag{3.3}$$

which nicely complements the fact that scalar and energy-momentum pole-skipping occur at bosonic Matsubara frequencies $\omega = \omega_n^B = -2\pi i T\tilde{n}$, with $\tilde{n} = 1,2,3,\ldots$.

3.2 Minimally Coupled Fermion in the Bulk

Assume that the action of the fermion field with mass m is given by [91,92]

$$S_f = \int d^{D+2}x\sqrt{-g}\,i\overline{\psi}\left(\Gamma^M\nabla_M - m\right)\psi + S_{bdy}\,, \tag{3.4}$$

which we add to the action (2.8). We included a boundary term S_{bdy} that does not alter the equations of motion, but is important for a well defined variational problem. The fermion conjugate is defined as $\overline{\psi} = \psi^\dagger\Gamma^0$, and the covariant derivative acting on

[27] As we discuss in more detail in Appendix C, the result (3.1) is correct only if the mass of the fermion is not a half-integer number (recall that we have set the AdS radius R_{AdS} to 1).

[28] As in the previous chapter, we refer to the purely imaginary ω_n^F frequencies as fermionic Matsubara frequencies.

fermions is defined by

$$\nabla_M = \partial_M + \frac{1}{4}\left(\omega_{ab}\right)_M \Gamma^{ab}\,, \tag{3.5}$$

with ω_M denoting the spin connection one-form and Γ^{ab} is the anti-symmetrised product of flat space gamma matrices, with flat space indices denoted by lower-case Latin letters.[29] The equation of motion for the spinor ψ is the Dirac equation

$$\left(\Gamma^M \nabla_M - m\right)\psi = 0\,. \tag{3.6}$$

A spinor in $D+2$ dimensions has

$$N_F = 2^{\lfloor \frac{D}{2} \rfloor + 1} \tag{3.7}$$

components, where $\lfloor q \rfloor$ denotes the highest integer that is less than or equal to q, meaning that the Dirac equation (3.6) is a system of N_F coupled first order differential equations for the components of the spinor. We do not impose any additional constraints on the spinor, such as the Majorana or Weyl conditions, so that in general its components are complex numbers. Our analysis is independent of whether the degrees of freedom are real or complex, hence we refer to the N_F components of the fermion as its degrees of freedom.

To calculate the retarded Green's function we follow the prescription of [55]. Assume that the metric takes the form (2.9) for which we can choose a "diagonal" orthonormal frame with components $E^a{}_M$. We then use the radial tangent space direction gamma matrix $\Gamma^{\underline{r}}$ to decompose the spinor in terms of

$$\begin{aligned} \psi &= \psi_+ + \psi_-\,, \\ \psi_\pm \equiv P_\pm\,\psi\,, &\qquad P_\pm \equiv \frac{1}{2}\left(1 \pm \Gamma^{\underline{r}}\right)\,, \end{aligned} \tag{3.8}$$

so that $\Gamma^{\underline{r}}\psi_\pm = \pm\psi_\pm$, and each of $\psi_\pm$ contains exactly half of the total degrees of freedom.

Since the metric components depend only on the r coordinate, we make the plane wave ansatz $\psi = \psi(r)e^{-i\omega t + i\vec{k}\cdot\vec{x}}$ and solve the Dirac equation in momentum space. We are advised to pick the ingoing solution at the horizon, which, for generic values of the frequency and momentum, halves the number of the degrees of freedom of the spinor. The ingoing solution is then evolved to the boundary of AdS ($r \to \infty$) where its leading

[29] A general flat space tensor has lower-case Latin letter indices, but particular values for the indices are underlined, for example $\underline{v}, \underline{r}$, or $\underline{x}$. This is to distinguish them from curved space indices where a generic tensor has upper-case Latin letters, but a particular value is lower-case letter that is not underlined, for example u, v, or x. More details on the conventions used, such as the Clifford algebra, is presented in Appendix A.

behaviour is given by

$$\psi_+ = \zeta_+(k) r^{-\frac{D+1}{2}+m} + \chi_+(k) r^{-\frac{D+1}{2}-m-1}\,, \tag{3.9a}$$

$$\psi_- = \zeta_-(k) r^{-\frac{D+1}{2}+m-1} + \chi_-(k) r^{-\frac{D+1}{2}-m}\,, \tag{3.9b}$$

where $\zeta_\pm(k)$ and $\chi_\pm(k)$ are spinors with a definite chirality with respect to $\Gamma^{\underline{r}}$ and by inserting (3.9) into the Dirac equation we find that it relates the spinor $\chi_+(k)$ with $\chi_-(k)$, and $\zeta_+(k)$ with $\zeta_-(k)$.

Assume that $m \geq 0$. The dominant, non-normalisable term in the expansion is the term multiplied by $\zeta_+(k)$ which thus is identified with the source in the boundary field theory. According to [55], the response is given by $\chi_-(k)$, the normalisable term, meaning that the conformal dimension Δ of the dual operator is[30]

$$\Delta = \frac{D+1}{2} + m\,. \tag{3.10}$$

The retarded Green's function is given by

$$G_R(k) \propto i\mathcal{R}(k)\,, \tag{3.11}$$

where $\mathcal{R}(k)$ is a matrix in spinor space that relates the spinors $\zeta_+(k)$ and $\chi_-(k)$ after imposing the ingoing condition at the horizon

$$\chi_-(k) = \mathcal{R}(k)\,\zeta_+(k)\,. \tag{3.12}$$

3.3 Pole-Skipping in Asymptotically AdS$_3$ Spaces

We begin with a three-dimensional ($D = 1$) bulk theory and a corresponding two-dimensional dual in which case both bulk and boundary spinors have two components.

Let the background metric be given by

$$ds^2 = -r^2 f(r) dv^2 + 2dv\,dr + h(r) dx^2 \tag{3.13}$$

where $f(r)$ and $h(r)$ satisfy the properties described in section 2.1.2. Choose the orthonormal frame

$$E^{\underline{v}} = \frac{1+f(r)}{2}\, r dv - \frac{dr}{r}\,, \qquad E^{\underline{r}} = \frac{1-f(r)}{2}\, r dv + \frac{dr}{r}\,, \qquad E^{\underline{x}} = \sqrt{h(r)}\, dx\,, \tag{3.14}$$

[30] There are some subtleties when the mass is in the ranges $0 \leq m \leq \frac{1}{2}$ or $m \leq 0$ and they are considered in [55], but conceptually the prescription does not change. In these cases the relation between the mass and the conformal dimension can be different due to the alternative quantisation.

for which

$$ds^2 = \eta_{ab} E^a E^b\,, \qquad \eta_{ab} = \mathrm{diag}(-1,1,1) \tag{3.15}$$

We choose this frame because neither the vielbein nor any its derivatives diverge at the horizon (assuming $\sqrt{h(r)}$ is regular) and we avoid any square roots of $f(r)$. The spin connections are given by

$$\begin{aligned}
\omega_{\underline{vr}} &= \frac{dr}{r} - \frac{2rf(r) + r^2 f'(r)}{2}\, dv, \\
\omega_{\underline{vx}} &= \frac{r\, h'(r)\ (1 - f(r))}{4\sqrt{h(r)}}\, dx, \\
\omega_{\underline{rx}} &= -\frac{r\, h'(r)\, (1 + f(r))}{4\sqrt{h(r)}}\, dx
\end{aligned} \tag{3.16}$$

with all other components, which are not related by symmetry to the ones above, vanishing. The Dirac equation is then

$$\begin{aligned}
\Bigg[&\left(\frac{r(1+f(r))}{2}\, \Gamma^{\underline{r}} - \frac{r(1-f(r))}{2}\, \Gamma^{\underline{v}} \right) \partial_r + \frac{\Gamma^{\underline{r}} + \Gamma^{\underline{v}}}{r} \partial_v + \frac{\Gamma^{\underline{x}}}{\sqrt{h(r)}}\, \partial_x \\
&+ \frac{1 + f(r) + r f'(r)}{4}\, \Gamma^{\underline{r}} - \frac{1 - f(r) - r f'(r)}{4}\, \Gamma^{\underline{v}} - \frac{r\,(1-f(r)) h'(r)}{8h(r)}\, \Gamma^{\underline{v}} \\
&+ \frac{r\,(1+f(r)) h'(r)}{8h(r)}\, \Gamma^{\underline{r}} - m \Bigg] \psi(r,v,x) = 0\,.
\end{aligned} \tag{3.17}$$

Since the metric is independent of the coordinates v and x, we introduce the plane wave ansatz $\psi(r,v,x) = \psi(r) e^{-i\omega v + ikx}$, and furthermore we use the decomposition (3.8). In this case, $\psi_\pm$ are two-component objects, but each contain only one independent degree of freedom. After some algebra one can write the two independent equations as

$$\begin{aligned}
\mathcal{S}_+ \equiv &\left[\frac{r^2 f'(r)}{4} + \frac{r f(r)}{4} \left(2 + \frac{r\, h'(r)}{h(r)} \right) - \frac{m\, r(1+f(r))}{2} - \frac{ikr(1-f(r))}{2\sqrt{h(r)}} - i\omega \right] \psi_+ \\
&+ \Gamma^{\underline{v}} \left[\frac{r^2 f'(r)}{4} + \frac{m\, r(1-f(r))}{2} + \frac{ikr(1+f(r))}{2\sqrt{h(r)}} - i\omega \right] \psi_- + r^2 f(r)\, \partial_r \psi_+ = 0\,,
\end{aligned} \tag{3.18a}$$

$$\begin{aligned}
\mathcal{S}_- \equiv &\left[\frac{r^2 f'(r)}{4} + \frac{r f(r)}{4} \left(2 + \frac{r\, h'(r)}{h(r)} \right) + \frac{m\, r(1+f(r))}{2} + \frac{ikr(1-f(r))}{2\sqrt{h(r)}} - i\omega \right] \psi_- \\
&- \Gamma^{\underline{v}} \left[\frac{r^2 f'(r)}{4} - \frac{m\, r(1-f(r))}{2} - \frac{ikr(1+f(r))}{2\sqrt{h(r)}} - i\omega \right] \psi_+ + r^2 f(r)\, \partial_r \psi_- = 0\,.
\end{aligned} \tag{3.18b}$$

We have used the fact that the set of matrices $(\mathbb{I}, \Gamma^{\underline{v}}, \Gamma^{\underline{x}}, \Gamma^{\underline{r}})$ forms a complete basis for

all 2×2 matrices, hence any product of two or more gamma matrices can be written as a linear combination of the elements from this set, and we have chosen a representation such that $\Gamma^{\underline{vx}} = \Gamma^{\underline{r}}$.

It is straightforward to transform (3.18) into two decoupled second order differential equations for $\psi_\pm$. The leading behaviour at the horizon is found by using an ansatz

$$\psi_\pm \sim (r - r_0)^\alpha \xi_\pm \,, \tag{3.19}$$

where $\xi_\pm$ are constant spinors satisfying $\Gamma^{\underline{r}} \xi_\pm = \pm \xi_\pm$, and the exponents are given by

$$\alpha_1 = 0 \,, \qquad \alpha_2 = -\frac{1}{2} + \frac{i\omega}{2\pi T} \,. \tag{3.20}$$

For generic values of the frequency, the solution with the exponent α_1 represents the ingoing solution while the exponent α_2 corresponds to the outgoing solution. If ω is equal to a fermionic Matsubara frequency given by

$$\omega = \omega_n \equiv -2\pi i T \left(n + \frac{1}{2} \right) \,, \qquad n = 1, 2, 3, \ldots \,, \tag{3.21}$$

then $\alpha_2 = n$ and both solutions would seem to be regular at the horizon. However, similar to the scalar field there is still a unique ingoing solution due to logarithmic divergences in the series expansion of the solution with exponent α_1. But at particular values of the momentum, these logarithmic divergences vanish in which case we indeed find two independent ingoing solutions. These values of ω and k are the pole-skipping points for fermions.

3.3.1 Pole-Skipping at the Lowest Matsubara Frequency

The exponents (3.20) suggest that there is no pole-skipping at the lowest fermionic Matsubara frequency $\omega_0 = -\pi i T$. However, this result is an artefact of working with second order differential equations. Pole-skipping does occur at such a frequency and is a consequence of the interplay between different components of the spinor.

Let us assume that the spinors admit a series expansion around the horizon

$$\psi_+ = \sum_{l=0}^{\infty} \psi_+^{(l)} (r - r_0)^l \,, \qquad \psi_- = \sum_{l=0}^{\infty} \psi_-^{(l)} (r - r_0)^l \,, \tag{3.22}$$

where $\psi_\pm^{(l)}$ are constant spinors with definite $\Gamma^{\underline{r}}$ eigenvalues. We insert these into (3.18) and expand as

$$\mathcal{S}_+ = \sum_{l=0}^{\infty} \mathcal{S}_+^{(l)} (r - r_0)^l = 0 \,, \qquad \mathcal{S}_- = \sum_{l=0}^{\infty} \mathcal{S}_-^{(l)} (r - r_0)^l = 0 \,, \tag{3.23}$$

so that solving the equations of motion is translated into solving a system of algebraic equations $\mathcal{S}_\pm^{(l)} = 0$ for the variables $\psi_\pm^{(l)}$.

The equations (3.23) can be solved in succession and the first instance of pole-skipping is already visible by evaluating the equations at the horizon. We obtain

$$\begin{aligned}\mathcal{S}_+^{(0)} = \Gamma^{\underline{v}} &\left[\frac{r_0^2 f'(r_0)}{4} + \frac{m\, r_0}{2} + \frac{ikr_0}{2\sqrt{h(r_0)}} - i\omega\right]\psi_-^{(0)} \\ &+\left[\frac{r_0^2 f'(r_0)}{4} - \frac{m\, r_0}{2} - \frac{ikr_0}{2\sqrt{h(r_0)}} - i\omega\right]\psi_+^{(0)} = 0\,, \qquad (3.24a)\\ \mathcal{S}_-^{(0)} = -\Gamma^{\underline{v}} &\left[\frac{r_0^2 f'(r_0)}{4} - \frac{m\, r_0}{2} - \frac{ikr_0}{2\sqrt{h(r_0)}} - i\omega\right]\psi_+^{(0)} \\ &+\left[\frac{r_0^2 f'(r_0)}{4} + \frac{m\, r_0}{2} + \frac{ikr_0}{2\sqrt{h(r_0)}} - i\omega\right]\psi_-^{(0)} = 0\,, \qquad (3.24b)\end{aligned}$$

and can immediately notice that $\mathcal{S}_+^{(0)} = \Gamma^{\underline{v}}\mathcal{S}_-^{(0)}$. Thus (3.24) provide only a single constraint on the coefficients $\psi_\pm^{(0)}$, fixing exactly half of the free parameters.

The first instance of pole-skipping occurs when these equations are satisfied for any values of $\psi_\pm^{(0)}$ which happens exactly at the zeroth fermionic Matsubara frequency and if the momentum is given by

$$\omega_0 = -\pi i T\,, \qquad k = im\sqrt{h(r_0)}\,, \qquad (3.25)$$

as then the terms in the square brackets in (3.24) vanish.

Other constraint equations $\mathcal{S}_\pm^{(l)} = 0$ are then used to relate higher order expansion coefficients $\psi_\pm^{(n)}$, with $n = 1, 2, \ldots$, to a linear combination of $\psi_+^{(0)}$ and $\psi_-^{(0)}$. In this way one constructs a regular solution whose value at the horizon is completely undetermined. In other words, there exist two independent regular solutions with the same behaviour at the horizon, one parametrised by $\psi_+^{(0)}$ and the other by $\psi_-^{(0)}$, and as a consequence, at (3.25) the retarded Green's function is not uniquely defined.[31]

Logarithmic Divergences

If one evaluates the equations of motion at $\omega = \omega_0$, but keeps a generic value of the momentum, then logarithmic terms appear in the near horizon expansion and make one of the solutions divergent. The leading order behaviour of the spinors in that case

[31] Note that the solution parametrized by $\psi_+^{(0)}$, for example, is *not* a solution with a well defined eigenvalue under $\Gamma^{\underline{r}}$ everywhere in the bulk. While setting $\psi_-^{(0)} = 0$ does mean that solution has a definite chirality at the horizon, all other coefficients $\psi_\pm^{(n)}$, with $n = 1, 2, \ldots$, are generically non-vanishing. The same analysis holds for $\psi_-^{(0)}$.

takes the form

$$\psi_+ = \psi_+^{(0)} + \chi_+^{(0)} \log(r - r_0) + \dots \,, \tag{3.26a}$$
$$\psi_- = \psi_-^{(0)} + \chi_-^{(0)} \log(r - r_0) + \dots \,, \tag{3.26b}$$

where $\psi_\pm^{(0)}$ and $\chi_\pm^{(0)}$ are constant spinors of definite chirality, and the dots represent subleading terms that contain no free parameters. Similarly, the expansions of the equations of motion (3.18) near the horizon to leading order become

$$\mathcal{S}_+ = \widehat{\mathcal{S}}_+^{(0)} + \widetilde{\mathcal{S}}_+^{(0)} \log(r - r_0) + \dots = 0 \,, \tag{3.27a}$$
$$\mathcal{S}_- = \widehat{\mathcal{S}}_-^{(0)} + \widetilde{\mathcal{S}}_-^{(0)} \log(r - r_0) + \dots = 0 \,, \tag{3.27b}$$

and can be solved iteratively. One finds that the leading order terms yield

$$\widehat{\mathcal{S}}_+^{(0)} = -\frac{r_0}{2\sqrt{h(r_0)}} \left(ik + m\sqrt{h(r_0)}\right) \left(\psi_+^{(0)} - \Gamma^{\underline{v}} \psi_-^{(0)}\right) + r_0^2 f'(r_0) \chi_+^{(0)} = 0 \,, \tag{3.28a}$$
$$\widehat{\mathcal{S}}_-^{(0)} = \frac{r_0}{2\sqrt{h(r_0)}} \left(ik + m\sqrt{h(r_0)}\right) \left(\psi_-^{(0)} + \Gamma^{\underline{v}} \psi_+^{(0)}\right) + r_0^2 f'(r_0) \chi_-^{(0)} = 0 \,, \tag{3.28b}$$
$$\widetilde{\mathcal{S}}_+^{(0)} = \Gamma^{\underline{v}} \widetilde{\mathcal{S}}_-^{(0)} = -\frac{r_0}{2\sqrt{h(r_0)}} \left(ik + m\sqrt{h(r_0)}\right) \left(\chi_+^{(0)} - \Gamma^{\underline{v}} \chi_-^{(0)}\right) = 0 \,. \tag{3.28c}$$

The last equation is solved by $\chi_+^{(0)} = \Gamma^{\underline{v}} \chi_-^{(0)}$, which can be inserted into (3.28a) and one notices that in this case the remaining two equations are related by $\widehat{\mathcal{S}}_+^{(0)} = \Gamma^{\underline{v}} \widehat{\mathcal{S}}_-^{(0)}$. Thus at leading order there are only two independent equations in (3.27), the solutions of which have generically $\chi_\pm^{(0)} \neq 0$. But when we impose the ingoing condition at the horizon, we pick the solution for which these coefficients vanish. So for a general value of k, we find a unique ingoing solution even at this Matsubara frequency.

If we evaluate the equations (3.28) at (3.25), then (3.28c) is automatically satisfied, but the remaining two equations become independent and naturally impose $\chi_+^{(0)} = \chi_-^{(0)} = 0$ while leaving $\psi_\pm^{(0)}$ undetermined, thus explicitly showing that at the pole-skipping location the logarithmic terms vanish and the two independent solutions are both regular at the horizon.

3.3.2 Pole-Skipping at Higher Matsubara Frequencies

There are two equivalent ways to locate the pole-skipping points at higher Matsubara frequencies. The first method uses the second order differential equations for half of the components, which is the analogue of the approach taken when analysing the scalar field, while the second technique bypasses the computational difficulties of obtaining second order equations by working directly with the Dirac equation and is the natural extension of the procedure used to identify the lowest pole-skipping point.

Using the Second Order Differential Equations

The Dirac equations (3.18) can be transformed into two decoupled second order differential equations for the spinors $\psi_\pm$. Since the following procedure is independent of whether we work with the positive or negative chirality component, we can choose to work with ψ_+, as once this spinor is known the Dirac equations completely determine ψ_-.

We begin by inserting the near-horizon expansion of ψ_+, given in (3.22), into the second order differential equation governing its radial evolution, denoted as $\mathcal{Q}_+ = 0$, which in turn can be expanded in a series as

$$\mathcal{Q}_+ = \sum_{l=0}^{\infty} \mathcal{Q}_+^{(l)} (r - r_0)^l = 0 \,. \tag{3.29}$$

The equation of motion is now solved order by order through $\mathcal{Q}_+^{(l)} = 0$ which determine the expansion coefficients of ψ_+. The first equation reads

$$\mathcal{Q}_+^{(0)} = (3\pi T - i\omega)\, \psi_+^{(1)} + \mathcal{M}_+^{(00)}(\omega, k)\, \psi_+^{(0)} = 0 \,, \tag{3.30}$$

where $\mathcal{M}_+^{(00)}(\omega, k)$ is a complicated function[32] of ω and k, whose explicit form will not be presented. For generic values of ω and k, this equation relates $\psi_+^{(1)}$ and $\psi_+^{(0)}$. Furthermore, using the higher order equations $\mathcal{Q}_+^{(l)} = 0$, one can express all other field expansion coefficients in terms of only $\psi_+^{(0)}$, and in this way explicitly construct a regular solution which is unique up to an overall spinor.

This procedure gets slightly altered if we evaluate the equations at the first fermionic Matsubara frequency

$$\omega_1 = -3\pi i T \,, \tag{3.31}$$

as in this case the prefactor of $\psi_+^{(1)}$ in (3.30) vanishes, setting $\psi_+^{(0)}$ to zero for generic values of k. However, a regular solution can still be constructed using $\psi_+^{(1)}$ as a free parameter, with the leading near-horizon behaviour of such a solution being $\psi_+ \sim (r - r_0)$.

If in addition to $\omega = \omega_1$, the momentum k is such that

$$\mathcal{M}_+^{(00)}(\omega_1, k) = 0 \,, \tag{3.32}$$

then the equation (3.30) is automatically satisfied and both $\psi_+^{(0)}$ and $\psi_+^{(1)}$ remain unconstrained. Iteratively solving the constraint equations in this case yields a regular

[32] It should be understood that all coefficients appearing in equations, such as (3.30), are proportional to the identity matrix in spinor space, unless explicitly stated otherwise.

solution with two free parameters corresponding to different near-horizon behaviours. The coefficient $\psi_+^{(0)}$ is related to a solution which is constant and finite at the horizon, while $\psi_+^{(1)}$ corresponds to a solution that vanishes with a first order zero.

Because of multiple regular solutions at these points in momentum space, the associated Green's function is not unique and one predicts pole-skipping. One should note that $\mathcal{M}_+^{(00)}(\omega_1, k)$ is a third degree polynomial in k, hence in general one expects as many pole-skipping points at $\omega = \omega_1$.

In order to locate the pole-skipping points at the second Matsubara frequency, consider the next constraint from (3.29) which reads

$$\mathcal{Q}_+^{(1)} = (5\pi T - i\omega)\,\psi_+^{(2)} + \mathcal{M}_+^{(11)}(\omega, k)\,\psi_+^{(1)} + \mathcal{M}_+^{(10)}(\omega, k)\,\psi_+^{(0)} = 0\,, \tag{3.33}$$

where $\mathcal{M}_+^{(11)}$ and $\mathcal{M}_+^{(10)}$ are complicated functions of ω and k, which we will not present explicitly. The coefficient in front of $\psi_+^{(2)}$ vanishes at $\omega = \omega_2 = -5\pi i T$, in which case the equations $\mathcal{Q}_+^{(0)} = 0$ and $\mathcal{Q}_+^{(1)} = 0$ can be written in matrix form as

$$\begin{pmatrix} \mathcal{Q}_+^{(0)} \\ \mathcal{Q}_+^{(1)} \end{pmatrix} = \mathcal{M}_+^{(2)}(\omega_2, k) \begin{pmatrix} \psi_+^{(0)} \\ \psi_+^{(1)} \end{pmatrix} \equiv \begin{pmatrix} \mathcal{M}_+^{(00)}(\omega_2, k) & -2\pi T \\ \mathcal{M}_+^{(10)}(\omega_2, k) & \mathcal{M}_+^{(11)}(\omega_2, k) \end{pmatrix} \begin{pmatrix} \psi_+^{(0)} \\ \psi_+^{(1)} \end{pmatrix} = 0. \tag{3.34}$$

Pole-skipping is predicted when the matrix $\mathcal{M}_+^{(2)}(\omega_2, k)$ is not invertible as then the resulting regular solution involves two free parameters: $\psi_+^{(2)}$ and for example $\psi_+^{(0)}$. Thus the next pole-skipping points are found for the following values of momentum and frequency

$$\omega = \omega_2\,, \qquad k = k_2\,, \qquad \det \mathcal{M}_+^{(2)}(\omega_2, k_2) = 0\,. \tag{3.35}$$

This procedure is easily generalised to higher frequency locations. At order $(n-1)$, the constraint equation from (3.29) is schematically written as

$$\mathcal{Q}_+^{(n-1)} = ((2n+1)\pi T - i\omega)\,\psi_+^{(n)} + \mathcal{M}_+^{(n-1,n-1)}\psi_+^{(n-1)} + \ldots + \mathcal{M}_+^{(n-1,0)}\psi_+^{(0)} = 0\,. \tag{3.36}$$

Generalising the procedure from above, one finds that the pole-skipping points at the n-th fermionic Matsubara frequency is located at

$$\omega = \omega_n = -2\pi i T\left(n + \frac{1}{2}\right), \qquad k = k_n\,, \qquad \det \mathcal{M}_+^{(n)}(\omega_n, k_2) = 0\,, \tag{3.37}$$

where $\det \mathcal{M}_+^{(n)}(\omega_n, k)$ is a $(2n+1)$-degree polynomial in k, predicting $(2n+1)$ pole-skipping locations at this frequency. The matrix used in the determinant is obtained by evaluating the first n constraint equations of (3.29) at $\omega = \omega_n$, and rewriting them

in matrix form. The matrix $\mathcal{M}_+^{(n)}(\omega,k)$, before we insert any particular value of the frequency, is thus given by

$$\mathcal{M}_+^{(n)}(\omega,k) \equiv \begin{pmatrix} \mathcal{M}_+^{(00)}(\omega,k) & 3\pi T - i\omega & 0 & \cdots & \cdots & 0 \\ \mathcal{M}_+^{(10)}(\omega,k) & \mathcal{M}_+^{(11)}(\omega,k) & 5\pi T - i\omega & 0 & \cdots & 0 \\ \vdots & \vdots & \vdots & \ddots & \ddots & \vdots \\ & & & & & 0 \\ & & & & & (2n-1)\pi T - i\omega \\ \mathcal{M}_+^{(n-1,0)}(\omega,k) & \cdots & \cdots & \cdots & \cdots & \mathcal{M}_+^{(n-1,n-1)}(\omega,k) \end{pmatrix} \tag{3.38}$$

Aside from making the choice $\Gamma^{\underline{vx}} = \Gamma^{\underline{r}}$, we have not used a particular representation of the gamma matrices, thus ψ_+, and therefore all expansion coefficients $\psi_+^{(k)}$, are two-component objects. Similarly all elements of (3.38) are in principle 2×2 matrices, however they are all proportional to the identity matrix in spinor space, meaning that the determinant (3.37) can be calculated as if the matrix elements were scalars.

Using the First-Order Differential Equations

One can also obtain the pole-skipping locations by analysing higher order constraints coming from the near-horizon expansions of the Dirac equations (3.23). For $l = 1$, these can be written in a matrix form as

$$\begin{pmatrix} \mathcal{S}_+^{(1)} \\ \mathcal{S}_-^{(1)} \end{pmatrix} = \widetilde{\mathcal{M}}^{(11)}(\omega,k) \begin{pmatrix} \psi_+^{(1)} \\ \psi_-^{(1)} \end{pmatrix} + \widetilde{\mathcal{M}}^{(10)}(k) \begin{pmatrix} \psi_+^{(0)} \\ \psi_-^{(0)} \end{pmatrix} = 0\,, \tag{3.39}$$

where $\widetilde{\mathcal{M}}^{(j,k)}$ are matrices whose elements are proportional either to the identity matrix or to $\Gamma^{\underline{v}}$, and thus all commute with each other. For example

$$\widetilde{\mathcal{M}}^{(11)} = \begin{pmatrix} -i\omega - \frac{mr_0}{2} - \frac{ik\,r_0}{\sqrt{h(r_0)}} + 5\pi T, & \left(-i\omega + \frac{mr_0}{2} + \frac{ik\,r_0}{\sqrt{h(r_0)}} + \pi T\right)\Gamma^{\underline{v}} \\ -\left(-i\omega - \frac{mr_0}{2} - \frac{ik\,r_0}{\sqrt{h(r_0)}} + \pi T\right)\Gamma^{\underline{v}}, & -i\omega + \frac{mr_0}{2} + \frac{ik\,r_0}{\sqrt{h(r_0)}} + 5\pi T \end{pmatrix}, \tag{3.40}$$

and it is worth noting that $\widetilde{\mathcal{M}}^{(10)}$, whose form can be seen explicitly in Appendix B, depends only on k. For generic values of ω and k, the equation (3.39) is used to completely determine $\psi_\pm^{(1)}$ in terms of the zeroth order spinor coefficients. However, if (3.40) is singular, then these equations do not provide two independent constraints on $\psi_+^{(1)}$ and $\psi_-^{(1)}$. One finds that

$$\det \widetilde{\mathcal{M}}^{(11)} = 8\pi T(3\pi T - i\omega)\,, \tag{3.41}$$

which vanishes at $\omega = \omega_1 = -3\pi i T$, in which case only a particular linear combination of $\psi_+^{(1)}$ and $\psi_-^{(1)}$ is constrained by the values of $\psi_\pm^{(0)}$, and we find that it is given by

$$\psi_c^{(1)} \equiv \psi_+^{(1)} - \Gamma^{\underline{v}}\psi_-^{(1)} \,. \tag{3.42}$$

Combining the equations (3.24) and (3.39), and evaluating them at $\omega = \omega_1$, yields a system of three independent equations which can be schematically written as (see Appendix B for the explicit form of the elements)

$$\begin{pmatrix} \mathcal{S}_+^{(0)} \\ \mathcal{S}_+^{(1)} \\ \mathcal{S}_-^{(1)} \end{pmatrix} = \widetilde{\mathcal{M}}_1(\omega_1, k) \begin{pmatrix} \psi_+^{(0)} \\ \psi_-^{(0)} \\ \psi_c^{(1)} \end{pmatrix} \equiv \begin{pmatrix} \widetilde{\mathcal{M}}_{++}^{(00)} & \widetilde{\mathcal{M}}_{+-}^{(00)} & 0 \\ \widetilde{\mathcal{M}}_{++}^{(10)} & \widetilde{\mathcal{M}}_{+-}^{(10)} & \widetilde{\mathcal{M}}_{+}^{(11)} \\ \widetilde{\mathcal{M}}_{-+}^{(10)} & \widetilde{\mathcal{M}}_{--}^{(10)} & \widetilde{\mathcal{M}}_{-}^{(11)} \end{pmatrix} \begin{pmatrix} \psi_+^{(0)} \\ \psi_-^{(0)} \\ \psi_c^{(1)} \end{pmatrix} = 0 \,. \tag{3.43}$$

At generic values of k, the matrix $\widetilde{\mathcal{M}}_1(\omega_1, k)$ is invertible and thus the above equation sets all three spinor coefficients to zero. As then $\psi_+^{(0)} = \psi_-^{(0)} = 0$, the leading behaviour of the solution at the horizon becomes $\psi \sim (r - r_0)$. Furthermore $\psi_c^{(1)} = 0$ implies that

$$\psi_+^{(1)} = \Gamma^{\underline{v}}\psi_-^{(1)} \,, \tag{3.44}$$

so, for example, $\psi_+^{(1)}$ can be taken as the free parameter of the solution which is again constructed by considering higher order constraint equations.

One obtains two independent solutions if the values of k are such that the matrix $\widetilde{\mathcal{M}}_1(\omega_1, k)$ is not invertible, or equivalently if

$$\det \widetilde{\mathcal{M}}_1(\omega_1, k) = 0 \,. \tag{3.45}$$

Since the above gives a cubic function of k, we expect three complex values for which this equation is satisfied. Having multiple ingoing solutions implies non-uniqueness of the boundary correlator, hence we predict that pole-skipping occurs at such locations in Fourier space. One can check that these results match the points predicted by the method involving the second order differential equations.

Pole-skipping points associated to even higher Matsubara frequencies are located in a similar manner. We take the equations at order n in the expansion (3.23) and write them schematically as

$$\begin{pmatrix} \mathcal{S}_+^{(n)} \\ \mathcal{S}_-^{(n)} \end{pmatrix} = \widetilde{\mathcal{M}}^{(nn)}(\omega, k) \begin{pmatrix} \psi_+^{(n)} \\ \psi_-^{(n)} \end{pmatrix} + \ldots + \widetilde{\mathcal{M}}^{(n0)}(k) \begin{pmatrix} \psi_+^{(0)} \\ \psi_-^{(0)} \end{pmatrix} = 0 \,, \tag{3.46}$$

where all $\widetilde{\mathcal{M}}^{(jk)}$ are matrices whose elements are proportional either to $\Gamma^{\underline{v}}$ or $\mathbb{I}$. Only the $\widetilde{\mathcal{M}}^{(nn)}$ depends on both the frequency and momentum while the remaining coefficients

depend only on k. One finds that for any n

$$\widetilde{\mathcal{M}}^{(nn)} = \begin{pmatrix} -i\omega - \frac{mr_0}{2} - \frac{ik\,r_0}{\sqrt{hr_0}} + (4n+1)\pi T, & \left(-i\omega + \frac{mr_0}{2} + \frac{ik\,r_0}{\sqrt{hr_0}} + \pi T\right)\Gamma^{\underline{v}} \\ -\left(-i\omega - \frac{mr_0}{2} - \frac{ik\,r_0}{\sqrt{hr_0}} + \pi T\right)\Gamma^{\underline{v}}, & -i\omega + \frac{mr_0}{2} + \frac{ik\,r_0}{\sqrt{hr_0}} + (4n+1)\pi T \end{pmatrix}, \tag{3.47}$$

whose determinant is given by $\det \widetilde{\mathcal{M}}^{(nn)} = 8\pi n T\left((2n+1)\pi T - i\omega\right)$.

We are interested in the values of the frequency and momentum at which there exist two independent ingoing solutions to the equations of motion. First we require that (3.46) provide only one constraint for $\psi_+^{(n)}$ and $\psi_-^{(n)}$ which happens at the fermionic Matsubara frequencies

$$\omega = \omega_n = -2\pi i T\left(n + \frac{1}{2}\right), \qquad n = 1, 2, 3, \ldots \tag{3.48}$$

where the determinant of (3.47) vanishes. We then construct the analogue of the equation (3.43) by evaluating all constraints of the form (3.46) with $l \leq n$ at $\omega = \omega_n$. We write them succinctly in matrix form

$$\begin{pmatrix} \mathcal{S}_+^{(0)} & \mathcal{S}_+^{(1)} & \mathcal{S}_-^{(1)} & \cdots & \mathcal{S}_-^{(n)} \end{pmatrix}^T = \widetilde{\mathcal{M}}_n \begin{pmatrix} \psi_+^{(0)} & \psi_-^{(0)} & \psi_+^{(1)} & \cdots & \psi_c^{(n)} \end{pmatrix}^T = 0\,, \tag{3.49}$$

where

$$\widetilde{\mathcal{M}}_n \equiv \begin{pmatrix} \widetilde{\mathcal{M}}_{++}^{(00)} & \widetilde{\mathcal{M}}_{+-}^{(00)} & 0 & \cdots & \cdots & \cdots & 0 \\ \widetilde{\mathcal{M}}_{++}^{(10)} & \widetilde{\mathcal{M}}_{+-}^{(10)} & \widetilde{\mathcal{M}}_{++}^{(11)} & \widetilde{\mathcal{M}}_{+-}^{(11)} & 0 & \cdots & 0 \\ \vdots & \vdots & \vdots & \vdots & \vdots & \vdots & \vdots \\ \widetilde{\mathcal{M}}_{++}^{(n0)} & \widetilde{\mathcal{M}}_{+-}^{(n0)} & \cdots & \cdots & \cdots & \cdots & \widetilde{\mathcal{M}}_{+}^{(nn)} \\ \widetilde{\mathcal{M}}_{-+}^{(n0)} & \widetilde{\mathcal{M}}_{--}^{(n0)} & \cdots & \cdots & \cdots & \cdots & \widetilde{\mathcal{M}}_{-}^{(nn)} \end{pmatrix}, \tag{3.50}$$

$$\widetilde{\mathcal{M}}_{+}^{(nn)} = -\frac{mr_0}{2} - \frac{ikr_0}{2\sqrt{h(r_0)}} + \frac{nr_0^2\,f'(r_0)}{2}\,, \tag{3.51a}$$

$$\widetilde{\mathcal{M}}_{-}^{(nn)} = \left(\frac{mr_0}{2} + \frac{ikr_0}{2\sqrt{h(r_0)}} + \frac{nr_0^2\,f'(r_0)}{2}\right)\Gamma^{\underline{v}}, \tag{3.51b}$$

and $\psi_c^{(n)} \equiv \psi_+^{(n)} - \Gamma^{\underline{v}}\psi_-^{(n)}$ is the analogue of the constrained linear combination (3.42). Pole-skipping occurs for values of k for which the determinant of the matrix $\widetilde{\mathcal{M}}_n$ vanishes

$$k = k_n\,, \qquad \det \widetilde{\mathcal{M}}_n(\omega_n, k_n) = 0\,. \tag{3.52}$$

Note that each element of $\widetilde{\mathcal{M}}_n$ is a linear function in k, hence this equation has $2n+1$ solutions, each corresponding to a pole-skipping point at the n-th fermionic Matsubara frequency. These points coincide with the locations predicted by (3.37).

3.4 Pole-Skipping in Higher Dimensions

We now generalize the results to higher dimensional spacetimes. We assume that the bulk has $D+2$ dimensions in which spinors are $N_F = 2^{\lfloor \frac{D}{2} \rfloor + 1}$ component objects. Let the background metric be given by (2.14) and choose the orthonormal frame

$$E^{\underline{v}} = \frac{1+f(r)}{2}\, r dv - \frac{dr}{r}\,, \qquad E^{\underline{r}} = \frac{1-f(r)}{2}\, r dv + \frac{dr}{r}\,, \qquad E^{\underline{i}} = \sqrt{h(r)}\, dx^i\,, \tag{3.53}$$

which is the direct generalization of the frame (3.14) used in three dimensions. As such, it has analogous properties, including

$$ds^2 = \eta_{ab} E^a\, E^b\,, \qquad \eta_{ab} = \mathrm{diag}(-1, 1, 1, \ldots, 1)\,, \tag{3.54}$$

while the spin connection components are given by

$$\begin{aligned}
\omega_{\underline{vr}} &= \frac{dr}{r} - \frac{2rf(r) + r^2 f'(r)}{2}\, dv, \\
\omega_{\underline{vi}} &= \frac{r\, h'(r)\, (1-f(r))}{4\sqrt{h(r)}}\, dx^i, \\
\omega_{\underline{ri}} &= -\frac{r\, h'(r)\, (1+f(r))}{4\sqrt{h(r)}}\, dx^i\,,
\end{aligned} \tag{3.55}$$

with all other components not related by symmetry being 0.

The manipulation of the equations of motion is conceptually the same as in section 3.3 so we don't repeat it in full and rather give the details in Appendix B. The Dirac equation in $D+2$ dimensions reads

$$\begin{aligned}
\Big\{ &\Gamma^{\underline{v}} \Big[-\frac{r(1-f(r))}{2}\, \partial_r - \frac{i\omega}{r} - \frac{1-f(r)-rf'(r)}{4} - \frac{D\, r\, (1-f(r))h'(r)}{8h(r)} \Big] \\
&+ \Gamma^{\underline{r}} \Big[\frac{r(1+f(r))}{2}\, \partial_r - \frac{i\omega}{r} + \frac{1+f(r)+rf'(r)}{4} + \frac{D\, r\, (1+f(r))h'(r)}{8h(r)} \Big] \\
&+ \frac{ik_i \Gamma^{\underline{i}}}{\sqrt{h(r)}} - m \Big\} \psi(r) = 0,
\end{aligned} \tag{3.56}$$

where we have again introduced the plane-wave ansatz $\psi(r, v, x^j) = \psi(r) e^{-i\omega v + i k_i x^i}$. Next, we separate the spinor into the positive and negative component with respect to the matrix $\Gamma^{\underline{r}}$, as in (3.8), with the only difference being that now each of $\psi_\pm$ contains

$N_F/2$ free parameters. For $D \geq 2$ the matrices $\Gamma^{\underline{r}}$ and $k_i\Gamma^{\underline{vi}}$ (with summation over i implied) are independent and commuting, and therefore we can introduce an additional decomposition ($a = \pm$)

$$\psi_a = \psi_a^{(+)} + \psi_a^{(-)}\,, \tag{3.57}$$
$$\psi_a^{(\pm)} \equiv P^{(\pm)}\psi_a\,, \qquad P^{(\pm)} \equiv \frac{1}{2}\left(1 \pm \hat{k}_i\Gamma^{\underline{vi}}\right)\,,$$

where $k_i\Gamma^{\underline{vi}}\,\psi_a^{(\pm)} = \pm k\psi_a^{(\pm)}$, and we have used $\hat{k}_i \equiv k_i/k$ with $k = \sqrt{\vec{k}\cdot\vec{k}}$. All in all, this divides ψ into four independent spinors $\psi_\pm^{(\pm)}$, each of which contains $N_F/4$ degrees of freedom and has definite eigenvalues under the action of $\Gamma^{\underline{r}}$ and $k_i\Gamma^{\underline{vi}}$.

A small remark on the nomenclature that we are going to use. The $\Gamma^{\underline{r}}$ matrix projects the spinor along the radial direction of AdS and can be considered the chirality operator, especially with respect to the boundary theory [93]. Hence we refer to $\psi_\pm$ as positive or negative *chirality* spinors. The matrix $k_i\Gamma^{\underline{vi}}$ is somewhat similar to the helicity operator as it can be considered the projection of the spinor along the direction of the momentum. Hence we refer to $\psi^{(\pm)}$ as positive or negative *helicity* spinors. For example, we refer to $\psi_+^{(-)}$ as a spinor with positive chirality but negative helicity.

With this spinor decomposition, the Dirac equation (3.56) separates into two decoupled subsystems of first order differential equations, one for $(\psi_+^{(+)}, \psi_-^{(-)})$ and one for $(\psi_+^{(-)}, \psi_-^{(+)})$, with the former being

$$\begin{aligned}\mathcal{S}_+^{(+)} \equiv &\left[\frac{r^2 f'(r)}{4} + \frac{r f(r)}{4}\left(2 + \frac{D\,r\,h'(r)}{h(r)}\right) - \frac{m\,r(1+f(r))}{2} - \frac{ikr(1-f(r))}{2\sqrt{h(r)}} - i\omega\right]\psi_+^{(+)} \\ &+ \Gamma^{\underline{v}}\left[\frac{r^2 f'(r)}{4} + \frac{m\,r(1-f(r))}{2} + \frac{ikr(1+f(r))}{2\sqrt{h(r)}} - i\omega\right]\psi_-^{(-)} + r^2 f(r)\,\partial_r\psi_+^{(+)} = 0,\end{aligned} \tag{3.58a}$$

$$\begin{aligned}\mathcal{S}_-^{(-)} \equiv &\left[\frac{r^2 f'(r)}{4} + \frac{r f(r)}{4}\left(2 + \frac{D\,r\,h'(r)}{h(r)}\right) + \frac{m\,r(1+f(r))}{2} + \frac{ikr(1-f(r))}{2\sqrt{h(r)}} - i\omega\right]\psi_-^{(-)} \\ &- \Gamma^{\underline{v}}\left[\frac{r^2 f'(r)}{4} - \frac{m\,r(1-f(r))}{2} - \frac{ikr(1+f(r))}{2\sqrt{h(r)}} - i\omega\right]\psi_+^{(+)} + r^2 f(r)\,\partial_r\psi_-^{(-)} = 0.\end{aligned} \tag{3.58b}$$

We will focus only on these equations, as the subsystem for $(\psi_+^{(-)}, \psi_-^{(+)})$ is equivalent, but with $k \to -k$ (see (B.1.11) in Appendix B), so the results of the second subsystem can be obtained by simply reversing the momentum.

The equations (3.58) are the same as (3.18), with the exception of a term that changes with the number of dimensions. Due to this similarity, the methods presented in section 3.3 easily translate to the higher dimensional case and we can locate pole-skipping points by the already known methods. Therefore, we do not repeat the

procedure in full as most of the details were already presented in the preceding section. Rather we focus only on deriving the pole-skipping locations and discussing the novelties that appear with additional dimensions.

3.4.1 Locating Pole-Skipping Points

At Zeroth Matsubara Frequency

The spinors and subsequently the Dirac equations (3.58) can be expanded in a series around the horizon as

$$\psi_+^{(+)} = \sum_{l=0}^{\infty} \left(\psi_+^{(+)}\right)^{(l)} (r-r_0)^l \,, \qquad \psi_-^{(-)} = \sum_{l=0}^{\infty} \left(\psi_-^{(-)}\right)^{(l)} (r-r_0)^l \,, \tag{3.59a}$$

$$\mathcal{S}_+^{(+)} = \sum_{l=0}^{\infty} \left(\mathcal{S}_+^{(+)}\right)^{(l)} (r-r_0)^l \,, \qquad \mathcal{S}_-^{(-)} = \sum_{l=0}^{\infty} \left(\mathcal{S}_-^{(-)}\right)^{(l)} (r-r_0)^l \,. \tag{3.59b}$$

At the horizon there is only one independent equation

$$\begin{aligned}\left(\mathcal{S}_+^{(+)}\right)^{(0)} = \Gamma^{\underline{v}} \left(\mathcal{S}_-^{(-)}\right)^{(0)} = \Gamma^{\underline{v}} \Bigg[-i\omega + \frac{r_0^2 f'(r_0)}{4} + \frac{m\, r_0}{2} + \frac{ikr_0}{2\sqrt{h(r_0)}} \Bigg] \left(\psi_-^{(-)}\right)^{(0)} \\ + \Bigg[-i\omega + \frac{r_0^2 f'(r_0)}{4} - \frac{m\, r_0}{2} - \frac{ikr_0}{2\sqrt{h(r_0)}} \Bigg] \left(\psi_+^{(+)}\right)^{(0)} = 0 \,,\end{aligned} \tag{3.60}$$

which is equivalent to (3.24a) and thus we find pole-skipping at the same locations as in the three-dimensional case. However, for $D \geq 2$ we also need to consider the subsystem $(\psi_+^{(-)}, \psi_-^{(+)})$ where pole-skipping occurs at the same value of the frequency, but at opposite momentum to (3.25). This means that all in all, for higher dimensional systems the lowest frequency pole-skipping points are located at

$$\omega = \omega_0 = -\pi i T \,, \qquad k = \pm i k_0 \,, \qquad k_0 = m\sqrt{h(r_0)} \,, \tag{3.61}$$

thus compared to asymptotically AdS_3 spaces, there exists an additional location with negative imaginary momentum. This pole-skipping point is universal as it contains no explicit dependence on the dimension of spacetime.

Notice that for $m \neq 0$, the two subsystems of equations experience pole-skipping at different points in momentum space. For example, (3.60) is trivially satisfied if $\omega = \omega_0$ and $k = +ik_0$, hence the two spinors that are governed by this equation remain unconstrained. However, because pole-skipping occurs at the opposite momentum for the other subsystem, the equation analogous to (3.60) is not identically zero at $\omega = \omega_0$ and $k = +ik_0$, and thus constrains the solutions thereby halving the number of free parameters in $\psi_+^{(-)}$ and $\psi_-^{(+)}$. This means that at (3.61) imposing the ingoing condition at the horizon reduces the number of free parameters in the spinor to $3N_F/4$.

This partial reduction of the degrees of freedom is not seen in the scalar case nor in the analysis of the spinor in three dimensions. For the latter this is due to the absence of the additional subsystem of equations as in that case the spinors are only two-component objects. On the other hand, a similar reduction can be seen for the metric perturbation, where only the δg_{vv} component experiences pole-skipping at (2.49). So it seems that this is a generic feature of many-component fields.

The massless spinor is a notable exception to this rule, as for $m = 0$ the two pole-skipping points in (3.61) merge into one, located at $\omega = \omega_0$ and $k = 0$. In this case both subsystems experience pole-skipping at the same time and thus the ingoing condition does not impose any constraints on the spinors. It would be interesting to investigate this further, especially in terms of the boundary theory interpretation.

At Higher Matsubara Frequencies

To derive the locations of higher order pole-skipping points one can use either method presented in section 3.3.2 as both easily generalize to arbitrary dimensions. We find that pole-skipping robustly occurs at the fermionic Matsubara frequencies (3.3), whereas the values of the momentum at these points vary with the number of dimensions due to the explicit factor of D in the differential equations (3.58).

All of the novelties that we have discussed in the case of pole-skipping at $\omega = \omega_0$ repeat themselves at higher frequencies. The number of special locations is doubled at each frequency because the equation (3.56) separates into two decoupled subsystems. Thus we obtain $2(2n+1)$ pole-skipping points at each frequency $\omega = \omega_n$ if the mass of the fermion is non-vanishing. Furthermore, in general at each pole-skipping point only $N_F/4$ components of the spinor are constrained by the regularity at the horizon, which is again related to the two subsystems experiencing pole-skipping at different locations in momentum space.

The massless fermion is again an exception as in this case, for an *individual* subsystem, the momentum for which pole-skipping occurs at $\omega = \omega_n$ is taken from a set that is invariant under the reversal of the momentum and can be thus schematically written as $k = \{0, \pm k_1, \pm k_2 \ldots, \pm k_n\}$.[33] Therefore in this case, the other subsystem experiences pole-skipping at the exact same locations. The number of total pole-skipping points at $\omega = \omega_n$ is then halved to $(2n+1)$, but at each such point the ingoing condition at the horizon does not impose any constraints on the spinor.

[33] While we are currently lacking a proof that this pattern continues for arbitrary n, we find no reason why this feature would cease to hold after the first few pole-skipping points, for which this was checked explicitly.

3.5 Green's Function Near the Pole-Skipping Points

In this section we show that the near-horizon equations predict that in the neighbourhood of the pole-skipping points in momentum space the fermionic Green's function takes the pole-skipping form (2.31). This signals that at such locations a line of poles and a line of zeros of the boundary correlator intersect. We perform the calculations in an asymptotically AdS_3 spacetime, as the results of the previous section suggest that the analysis in higher dimensions is analogous.

3.5.1 Near the Lowest Matsubara Frequency

At the pole-skipping point (3.25), the equations of motion have two independent ingoing solutions, hence we cannot find a unique boundary Green's function by using the prescription [49, 55]. However, one of the solutions becomes divergent as soon as we move to any infinitesimally nearby point in Fourier space.

Consider the series expansion of the equations of motion (3.23), evaluated at

$$\omega = \omega_0 + \epsilon\,\delta\omega\,, \qquad k = k_0 + \epsilon\,\delta k\,, \tag{3.62}$$

where ϵ is a small dimensionless parameter, while $\delta\omega$ and δk denote the directions in which we move away from the pole-skipping point (3.25) in momentum space.

At zeroth order in the ϵ expansion, the equations (3.24) are automatically satisfied as they are evaluated at the pole-skipping values. However, at linear order in ϵ we get a non-trivial constraint

$$\left(\delta\omega + \frac{r_0}{2\sqrt{h(r_0)}}\,\delta k\right)\psi_+^{(0)} + \left(\delta\omega - \frac{r_0}{2\sqrt{h(r_0)}}\,\delta k\right)\Gamma^{\underline{v}}\psi_-^{(0)} = 0\,, \tag{3.63}$$

which allows us to write

$$\psi_-^{(0)} = \frac{\left(\frac{\delta\omega}{\delta k}\right) + \frac{r_0}{2\sqrt{h(r_0)}}}{\left(\frac{\delta\omega}{\delta k}\right) - \frac{r_0}{2\sqrt{h(r_0)}}}\,\Gamma^{\underline{v}}\psi_+^{(0)}\,, \quad \text{or} \quad \psi_+^{(0)} = -\frac{\left(\frac{\delta\omega}{\delta k}\right) - \frac{r_0}{2\sqrt{h(r_0)}}}{\left(\frac{\delta\omega}{\delta k}\right) + \frac{r_0}{2\sqrt{h(r_0)}}}\,\Gamma^{\underline{v}}\psi_-^{(0)}\,. \tag{3.64}$$

These relations depend explicitly on the slope $(\delta\omega/\delta k)$ which can be interpreted as the additional free parameter appearing in the regular solution if the equations of motion are evaluated directly at the pole-skipping point.

A generic solution to the bulk equations of motion contains a normalisable part, which is related to the poles of the Green's function, and a non-normalizable part, related to the zeros of the correlator. However, there exist solutions that are fully normalizable $\psi^{(n)}$, and fully non-normalizable $\psi^{(nn)}$, which we can expand near the

horizon as

$$\psi^{(n)} = \psi_+^{(n)} + \psi_-^{(n)} = \left(\psi_+^{(n)}\right)^{(0)} + \left(\psi_-^{(n)}\right)^{(0)} + \dots , \tag{3.65a}$$

$$\psi^{(nn)} = \psi_+^{(nn)} + \psi_-^{(nn)} = \left(\psi_+^{(nn)}\right)^{(0)} + \left(\psi_-^{(nn)}\right)^{(0)} + \dots , \tag{3.65b}$$

where we have used the decomposition (3.8), and the dots represent higher order terms in the expansion, as in (3.22). The zeroth order coefficients are related by

$$\left(\psi_+^{(n)}\right)^{(0)} = -\frac{\left(\frac{\delta\omega}{\delta k}\right)_p - \frac{r_0}{2\sqrt{h(r_0)}}}{\left(\frac{\delta\omega}{\delta k}\right)_p + \frac{r_0}{2\sqrt{h(r_0)}}} \Gamma^{\underline{v}} \left(\psi_-^{(n)}\right)^{(0)} , \tag{3.66a}$$

$$\left(\psi_-^{(nn)}\right)^{(0)} = \frac{\left(\frac{\delta\omega}{\delta k}\right)_z + \frac{r_0}{2\sqrt{h(r_0)}}}{\left(\frac{\delta\omega}{\delta k}\right)_z - \frac{r_0}{2\sqrt{h(r_0)}}} \Gamma^{\underline{v}} \left(\psi_+^{(nn)}\right)^{(0)} , \tag{3.66b}$$

where $(\delta\omega/\delta k)_{p,z}$ denote to the directions in which we need to move away from the pole-skipping point to obtain a normalizable (subscript p) or a non-normalizable (subscript z) solution.

As already mentioned, a generic ingoing solution is a combination of the normalizable and non-normalizable components

$$\psi = \psi^{(n)} + \psi^{(nn)} , \tag{3.67}$$

which initially both contain a degree of freedom that we choose to be $\left(\psi_-^{(n)}\right)^{(0)}$ and $\left(\psi_+^{(nn)}\right)^{(0)}$ respectively. If these are left unconstrained, the solution has too many free parameters to uniquely determine the Green's function, which happens at the pole-skipping point. Away from this location, the Dirac equation relates the coefficients through

$$\left(\psi_-^{(n)}\right)^{(0)} = \mathcal{R}\left(\frac{\delta\omega}{\delta k}\right) \cdot \left(\psi_+^{(nn)}\right)^{(0)} , \tag{3.68}$$

where $\mathcal{R}(\delta\omega/\delta k)$ depends on the slope of the displacement in momentum space. Due to the prescription of [55], the boundary Green's function depends on this direction as well, as

$$G^R \propto \mathcal{R}\left(\frac{\delta\omega}{\delta k}\right) . \tag{3.69}$$

The relation (3.68) is obtained by inserting (3.67) into the Dirac equations evaluated

at the horizon. Near the pole-skipping point, at linear order in ϵ, we find the relation

$$\left(\psi_+^{(n)}\right)^{(0)} = -\frac{\left(\frac{\delta\omega}{\delta k}\right)_p + \frac{r_0}{2\sqrt{h(r_0)}}}{\left(\frac{\delta\omega}{\delta k}\right)_z - \frac{r_0}{2\sqrt{h(r_0)}}} \frac{\delta\omega - \left(\frac{\delta\omega}{\delta k}\right)_z \delta k}{\delta\omega - \left(\frac{\delta\omega}{\delta k}\right)_p \delta k} \Gamma^{\underline{v}} \left(\psi_-^{(nn)}\right)^{(0)} , \tag{3.70}$$

from which we can easily read off the proportionality factor $\mathcal{R}$. Ignoring all unimportant factors,[34] one finds

$$G^R(\omega_n + \delta\omega, k_n + \delta k) \propto \frac{\delta\omega - \left(\frac{\delta\omega}{\delta k}\right)_z \delta k}{\delta\omega - \left(\frac{\delta\omega}{\delta k}\right)_p \delta k} , \tag{3.71}$$

and thus the Green's function for fermion fields also takes on the pole-skipping form near the special locations.

This form shows that the Green's function is infinitely multi-valued at the pole-skipping points. Namely, at any finite values of $\delta\omega$ and δk, the slope of the displacement from the special locations $(\delta\omega/\delta k)$ uniquely relates the components of the spinor through (3.70), and similarly fixes the value of the correlator by (3.71). However, directly at the pole-skipping point, this slope is ill-defined and can be considered as an additional free-parameter of the solution, with the singularity structure of the Green's function given explicitly by the pole-skipping form.

From (3.70) it is clear that at (3.25) the Green's function always takes the pole-skipping form, or equivalently, is never anomalous. This can be heuristically justified by recalling that for the scalar field anomalous points usually appeared when two pole-skipping points coincided [72]. For the fermion field, there is only one such point at the frequency $\omega = \omega_0$, so there exists no other pole-skipping point with which it can collide. Therefore this pole-skipping point is never anomalous and subsequently there is always a line of zeros and a line of poles of the Green's function that intersect at (3.25).

3.5.2 Near Higher Matsubara Frequencies

To derive the form of the Green's function near the pole-skipping points at higher Matsubara frequencies, we employ the method that involves the second order differential equations due to the similarity with the scalar field case which was analysed in [72].

Without loss of generality, we work with the component ψ_+. If we evaluate the equations (3.29) at a generic point in momentum space, we can express all coefficients appearing in (3.22) in terms of $\psi_+^{(0)}$ only. Solving the equations $\mathcal{Q}_+^{(p)} = 0$ order by

[34] The prefactors in (3.70) vanish or diverge if the slope takes the values $(\delta\omega/\delta k) = \pm r_0/(2\sqrt{h(r_0)})$. These correspond to the case where the (non-)normalisable solution has a definite $\Gamma^{\underline{r}}$ chirality at the horizon (see (3.64)) and thus we are not able to take $\left(\psi_+^{(n)}\right)^{(0)}$ or $\left(\psi_-^{(nn)}\right)^{(0)}$ as the free parameter, because they vanish. However, the pole-skipping form (3.71) generically persists even in this case.

order, we find a generic relation

$$((2q+1)\pi T - i\omega)\ \psi_+^{(q)} + \frac{1}{N^{(q)}(\omega)}\ \det \mathcal{M}_+^{(q)}(\omega,k)\ \psi_+^{(0)} = 0\,, \tag{3.72}$$

where $q = 1, 2, 3, \ldots$, the matrix $\mathcal{M}_+^{(q)}$ is defined in (3.38),

$$N^{(q)} \equiv (i\omega - 3\pi T)(i\omega - 5\pi T)\ldots(i\omega - (2q-1)\pi T)\,, \tag{3.73}$$

and we have assumed that ω does not equal any of the fermionic Matsubara frequencies, *i.e.* $N^{(q)}$ does not vanish. Now evaluate this relation in the vicinity of a pole-skipping point

$$\omega = \omega_q + \epsilon\,\delta\omega\,, \qquad k = k_q + \epsilon\,\delta k\,, \tag{3.74}$$

where ω_q, k_q is the location of a pole-skipping point with $q = 1, 2, 3, \ldots$, and ϵ is a small parameter. At linear order in ϵ, the equation (3.72) reads

$$\frac{1}{N(\omega_q)}\left[\partial_k \det \mathcal{M}_+^{(q)}(\omega_q,k_q)\,\delta k + \partial_\omega \det \mathcal{M}_+^{(q)}(\omega_q,k_q)\,\delta\omega\right]\ \psi_+^{(0)} - i\delta\omega\psi_+^{(q)} = 0\,, \tag{3.75}$$

where $N(\omega_q) \equiv (q-1)!(2\pi T)^{q-1}$, from which we can obtain a relation

$$\psi_+^{(q)} = -i\,\frac{\partial_k \det \mathcal{M}_+^{(q)}(\omega_q,k_q) + \partial_\omega \det \mathcal{M}_+^{(q)}(\omega_q,k_q)\left(\dfrac{\delta\omega}{\delta k}\right)}{N(\omega_q)\left(\dfrac{\delta\omega}{\delta k}\right)}\,\psi_+^{(0)}\,, \tag{3.76}$$

which again depends explicitly on the direction in which we move away from the pole-skipping point. In particular, there exist slopes associated to normalizable ($\psi_+^{(n)}$) and non-normalizable ($\psi_+^{(nn)}$) solutions, where the above relation reads

$$\left(\psi_+^{(n)}\right)^{(q)} = -i\,\frac{\partial_k \det \mathcal{M}_+^{(q)}(\omega_q,k_q) + \partial_\omega \det \mathcal{M}_+^{(q)}(\omega_q,k_q)\left(\dfrac{\delta\omega}{\delta k}\right)_p}{N(\omega_q)\left(\dfrac{\delta\omega}{\delta k}\right)_p}\,\left(\psi_+^{(n)}\right)^{(0)}\,, \tag{3.77a}$$

$$\left(\psi_+^{(nn)}\right)^{(q)} = -i\,\frac{\partial_k \det \mathcal{M}_+^{(q)}(\omega_q,k_q) + \partial_\omega \det \mathcal{M}_+^{(q)}(\omega_q,k_q)\left(\dfrac{\delta\omega}{\delta k}\right)_z}{N(\omega_q)\left(\dfrac{\delta\omega}{\delta k}\right)_z}\,\left(\psi_+^{(nn)}\right)^{(0)}\,. \tag{3.77b}$$

A generic solution contains both a normalisable and a non-normalisable part (3.67) which are related through the Dirac equation. As before, the retarded Green's function

is proportional to the multiplicative factor relating the normalizable degree of freedom $\left(\psi_+^{(n)}\right)^{(0)}$ to the non-normalizable one $\left(\psi_+^{(nn)}\right)^{(0)}$. This is similar to (3.70), only that in this case there exist additional prefactors because we are considering two positive chirality components (see [55]). At linear order in ϵ we obtain

$$\left(\psi_+^{(n)}\right)^{(0)} = -\left(\frac{\delta\omega}{\delta k}\right)_p \left(\frac{\delta\omega}{\delta k}\right)_z^{-1} \frac{\delta\omega - \left(\frac{\delta\omega}{\delta k}\right)_z \delta k}{\delta\omega - \left(\frac{\delta\omega}{\delta k}\right)_p \delta k} \left(\psi_+^{(nn)}\right)^{(0)} , \tag{3.78}$$

and by reading off the prefactor, we can see that the correlator has the pole-skipping form (2.31) near higher-order pole-skipping points as well.

A key condition in obtaining the pole-skipping form is that the relation (3.76) depends on the slope $(\delta\omega/\delta k)$, which is not the case if $\partial_k \det \mathcal{M}_+^{(n)}(\omega_n, k_n) = 0$. Therefore, a pole-skipping point at $\omega = \omega_n$ and $k = k_n$ is anomalous if

$$\det \mathcal{M}_+^{(n)}(\omega_n, k_n) = 0\,, \qquad \text{and} \qquad \partial_k \det \mathcal{M}_+^{(n)}(\omega_n, k_n) = 0\,, \tag{3.79}$$

where the matrix $\mathcal{M}_+^{(n)}$ is defined in (3.38). These conditions are satisfied whenever we have a repeated root in the determinant, or in other words, when two pole-skipping points coincide.

3.6 Examples

In this section we look at some concrete examples. First, we consider the non-rotating BTZ black hole background [61, 62] where the fermionic Green's function is known. If the mass of the fermion (or the conformal dimension of the dual operator) is a half-integer number, the correlation function takes a special form, and we show that the near-horizon analysis perfectly agrees with the exact result even then. We also present the case of a massless fermion propagating in a Schwarzschild black hole in anti-de Sitter spacetime.

3.6.1 BTZ Black Hole

Near Horizon Analysis

For the non-spinning BTZ black hole, the two functions that appear in the metric (3.13) are given by

$$f(r) = 1 - \left(\frac{r_0}{r}\right)^2 , \qquad \text{and} \qquad h(r) = r^2\,, \tag{3.80}$$

with the Hawking temperature given by $T = r_0/2\pi$. We choose the following set of gamma matrices

$$(\Gamma^{\underline{v}}, \Gamma^{\underline{r}}, \Gamma^{\underline{x}}) = (i\sigma^2, \sigma^3, \sigma^1)\,, \tag{3.81}$$

where σ^i are the Pauli matrices, so that $\Gamma^{\underline{r}}$ is diagonal and thus its eigenvectors are given by $\psi_+^T = (\psi_+(r), 0)$ and $\psi_-^T = (0, \psi_-(r))$. The Dirac equation can hence be reduced to two coupled differential equations for scalar functions $\psi_\pm(r)$ that read

$$\left[ik - i\omega + \frac{(-ik + (m+1)r)r_0^2}{2r^2}\right]\psi_- + \left[-i\omega - (m-1)r + \frac{((m-1)r - ik)\,r_0^2}{2r^2}\right]\psi_+ + (r^2 - r_0^2)\partial_r\psi_+ = 0 \tag{3.82a}$$

$$\left[-i\omega + (m+1)r - \frac{((m+1)r - ik)\,r_0^2}{2r^2}\right]\psi_- + \left[-ik - i\omega + \frac{(ik - (m-1)r)r_0^2}{2r^2}\right]\psi_+ + (r^2 - r_0^2)\partial_r\psi_- = 0\,. \tag{3.82b}$$

Using the procedure presented in section 3.3, the first pole-skipping point is located at

$$\omega = -\frac{ir_0}{2} = -i\pi T\,, \qquad k = imr_0 = 2\pi i m T\,. \tag{3.83}$$

Either of the two methods presented in section 3.3 can be used to find the other pole-skipping points and we use this example to showcase the first order method. The equations (3.39) for this example read

$$M^{(11)}\begin{pmatrix}\psi_+^{(1)}\\ \psi_-^{(1)}\end{pmatrix} + M^{(10)}\begin{pmatrix}\psi_+^{(0)}\\ \psi_-^{(0)}\end{pmatrix} = 0\,, \tag{3.84}$$

with the two matrices being

$$M^{(11)} = \begin{pmatrix}-ik - (m-5)r_0 - 2i\omega, & ik + (m+1)r_0 - 2i\omega\\ -ik - (m-1)r_0 - 2i\omega, & ik + (m+5)r_0 - 2i\omega\end{pmatrix}\,, \tag{3.85a}$$

$$M^{(10)} = \frac{1}{r_0}\begin{pmatrix}-3(m-1)r_0 + 2ik, & -(m+1)r_0 + 2ik\\ (m-1)r_0 - 2ik, & 3(m+1)r_0 - 2ik\end{pmatrix}\,, \tag{3.85b}$$

where all elements of the above matrices are scalar functions due to our choice of the representation of the Clifford algebra (3.81). The frequency of the next pole-skipping point is given by the value at which the determinant of $M^{(11)}$, given by $\det M^{(11)} = 8r_0(3r_0 - 2i\omega)$, vanishes. This occurs at the next Matsubara frequency

$$\omega = \omega_1 \equiv -\frac{3ir_0}{2} = -3\pi i T\,. \tag{3.86}$$

ω	k	Number of pole-skipping points
$\omega_0 = -\pi i T$	$2\pi i m T$	1
$\omega_1 = -3\pi i T$	$-2\pi i m T,\ 2\pi i(m \pm 1)T$	3
$\omega_2 = -5\pi i T$	$2\pi i m T,\ -2\pi i(m \pm 1)T$ $2\pi i(m \pm 2)T$	5
$\omega_3 = -7\pi i T$	$-2\pi i m T,\ 2\pi i(m \pm 1)T$ $-2\pi i(m \pm 2)T,\ 2\pi i(m \pm 3)T$	7

Table 5: The locations of the first few pole-skipping points for a fermion in a non-spinning BTZ black hole background. At each Matsubara frequency $\omega = \omega_n$, one finds exactly $2n + 1$ pole-skipping points.

The easiest way to obtain the corresponding momenta is to set one of $\psi_{\pm}^{(1)}$ to 0, and combine (3.84) with the zeroth order equation[35] to obtain a system of three equations for three variables, which we evaluate at $\omega = \omega_1$. For example, setting $\psi_{-}^{(1)} = 0$ gives[36]

$$M^{(1)} \begin{pmatrix} \psi_{+}^{(0)} \\ \psi_{-}^{(0)} \\ \psi_{+}^{(1)} \end{pmatrix} \equiv \begin{pmatrix} -(m+2)r_0 - ik & (m-2)r_0 + ik & 0 \\ \frac{2ik}{r_0} - 3m + 3 & \frac{2ik}{r_0} - m - 1 & -(m-2)r_0 - ik \\ -\frac{2ik}{r_0} + m - 1 & -\frac{2ik}{r_0} + 3m + 3 & -(m+2)r_0 - ik \end{pmatrix} \begin{pmatrix} \psi_{+}^{(0)} \\ \psi_{-}^{(0)} \\ \psi_{+}^{(1)} \end{pmatrix} = 0. \tag{3.87}$$

Pole-skipping points are located at the values of the momentum at which the determinant of the matrix $M^{(1)}$ vanishes, which are given by

$$k = -imr_0 = -2\pi i T\,, \qquad k = i(m \pm 1)r_0 = 2\pi i T(m \pm 1)\,. \tag{3.88}$$

Finding other pole-skipping locations follows the same pattern and we collect the results for the first few points in table 5. At a particular frequency, the momenta at which pole-skipping occurs are not invariant under the transformation $k \to -k$, unlike in the case of a scalar field (see eq. (4.6) of [72]). The case of $m = 0$ is an exception as then the momentum associated to one of the pole-skipping points vanishes, while the others form pairs as $k = \pm i k_n$. This can be seen clearly in figure 6, where we depicted the first few pole-skipping points at $m = 1$ (bottom row) and $m = 0$ (top row), and the latter plot is symmetric with respect to the vertical axis.

[35] The zeroth order equation reads

$$(-ik + r_0 - mr_0 - 2i\omega)\psi_{+}^{(0)} + (ik + r_0 + mr_0 - 2i\omega)\psi_{-}^{(0)} = 0$$

[36] We can set one of $\psi_{\pm}^{(1)}$ to 0 as a consequence of the fact that at any fermionic Matsubara frequency, only the combination (3.42) is constrained, which in this case is simply $\psi_{+}^{(1)} - \psi_{-}^{(1)}$. If we set $\psi_{+}^{(1)} = 0$ and include $\psi_{-}^{(1)}$ in the matrix (3.87), the determinant only switches sign which does not change the values of the roots. This is because the coefficients multiplying $\psi_{\pm}^{(1)}$ in (3.84) differ only by a sign if they are evaluated at $\omega = \omega_1$.

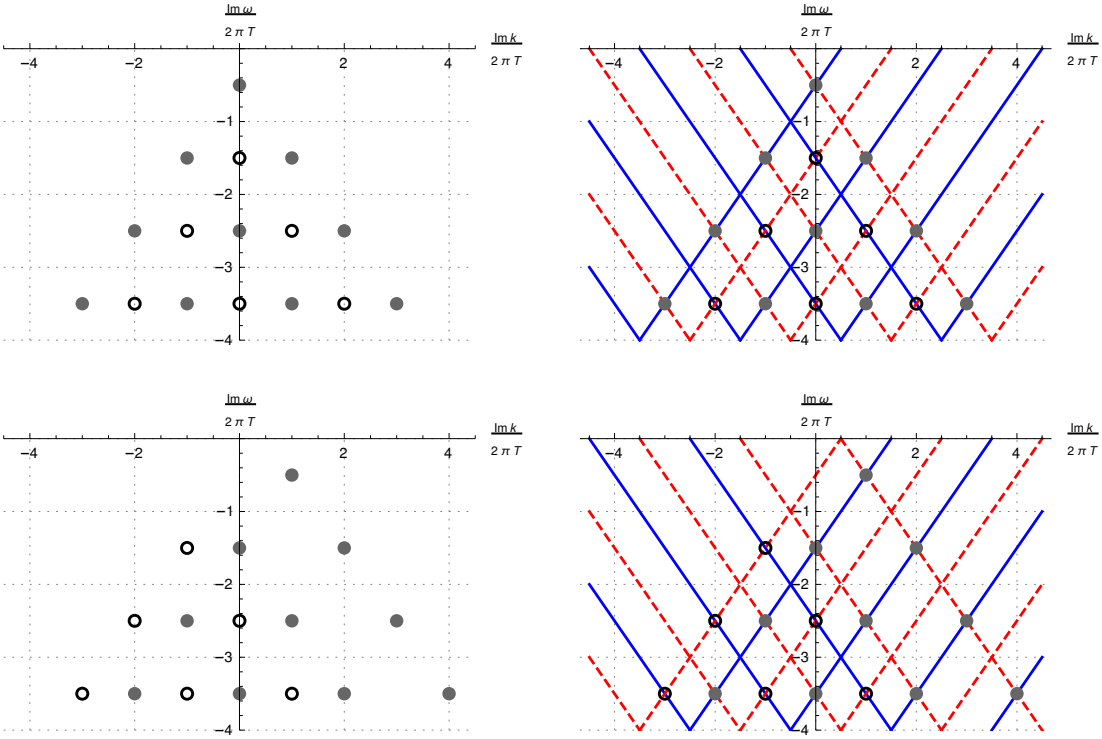

Figure 6: Plots of the locations of pole-skipping points for the fermionic Green's function in the BTZ black hole background. The top row is for $m = 0$ and the bottom row shows the locations for $m = 1$. The left column shows only the locations of the pole-skipping points as predicted from the near horizon analysis. The gray points correspond to the momentum written with a positive sign in and the hollow points correspond to the momenta with a negative sign as written in table 5. Comparing the top left and bottom left panel we notice that, by increasing the mass, the gray points get rigidly translated to the right by the value of m and the hollow points get translated by an equal amount to the left. The right column has superimposed the lines of zeros (red, dashed) from (3.6.1) and lines of poles (blue) from (3.6.1). For both values of the mass the near-horizon analysis predicts the location of the intersections of lines of zeros and lines of poles.

Comparison with the Exact Green's Function

The exact retarded Green's function for a fermion propagating in a BTZ black hole geometry was derived in [55]. For non half-integer values of the mass m, the correlator in the case of a non-spinning black hole is given by

$$G_R(\omega,k) = -i\,\frac{\Gamma\left(\frac{1}{2}-m\right)\Gamma\left(\frac{m}{2}+\frac{1}{4}+\frac{i(k-\omega)}{4\pi T}\right)\Gamma\left(\frac{m}{2}+\frac{3}{4}-\frac{i(k+\omega)}{4\pi T}\right)}{\Gamma\left(\frac{1}{2}+m\right)\Gamma\left(-\frac{m}{2}+\frac{3}{4}+\frac{i(k-\omega)}{4\pi T}\right)\Gamma\left(-\frac{m}{2}+\frac{1}{4}-\frac{i(k+\omega)}{4\pi T}\right)}\,. \tag{3.89}$$

It has a pole whenever the argument of any of the gamma functions in the numerator hits a non-positive integer. Similarly, it has a zero whenever an argument of any of the gamma functions in the denominator is equal to a non-positive integer.

Assuming that the mass is fixed and is not half-integer valued, we get two infinite families of lines of poles and two infinite families of lines of zeros in the (ω, k) plane.

The poles are located at

$$\omega_1^P = k - \pi i T(4n + 2m + 1)\,, \qquad \omega_2^P = -k - \pi i T(4n + 2m + 3)\,, \tag{3.90}$$

and the zeros can be found at

$$\omega_1^Z = k - \pi i T(4n - 2m + 3)\,, \qquad \omega_2^Z = -k - \pi i T(4n - 2m + 1)\,, \tag{3.91}$$

where in all cases $n = 0, 1, 2, \ldots$. Pole-skipping is observed whenever a line of poles and a line of zeros intersect, which happens at

$$\begin{aligned} \omega_n = -i\pi T(2n+1), \qquad k_{n,q_1} &= 2\pi i T(m + n - 2q_1), \\ k_{n,q_2} &= -2\pi i T(m + n + 1 - 2q_2), \end{aligned} \tag{3.92}$$

for any $n \in \{0, 1, \ldots\}$ and $q_1 \in \{0, \ldots, n\}$, $q_2 \in \{1, \ldots, n\}$.[37] The lines of zeros and lines of poles are shown for two values of the mass ($m = 0$ in the top row and $m = 1$ in the bottom row) in figure 6, where we can see that the intersections of these lines are in perfect agreement with the predictions from the near-horizon analysis summarised in table 5.

Green's Function at Half-Integer Conformal Dimensions

When the mass m (or equivalently the scaling dimension Δ of the dual operators) is half-integer valued, the boundary retarded Green's function takes a different form. We focus on the case of $m > 0$, or equivalently $\Delta > 1$, in which case the correlator is given by

$$\begin{aligned} G_R(\omega, k) \propto \frac{\Gamma\left(\frac{\Delta}{2} - \frac{1}{4} + i\frac{(k-\omega)}{4\pi T}\right)\Gamma\left(\frac{\Delta}{2} + \frac{1}{4} - i\frac{(k+\omega)}{4\pi T}\right)}{\Gamma\left(-\frac{\Delta}{2} + \frac{5}{4} + i\frac{(k-\omega)}{4\pi T}\right)\Gamma\left(-\frac{\Delta}{2} + \frac{3}{4} - i\frac{(k+\omega)}{4\pi T}\right)} \times \\ \left[\psi\left(\frac{\Delta}{2} - \frac{1}{4} + i\frac{(k-\omega)}{4\pi T}\right) + \psi\left(\frac{\Delta}{2} + \frac{1}{4} - i\frac{(k+\omega)}{4\pi T}\right)\right], \end{aligned} \tag{3.93}$$

where $\psi(z)$ is the digamma function and we have written the mass m in terms of the scaling dimension Δ using (3.10). The explicit derivation of this form is presented in Appendix C.

Because Δ is half-integer valued, the arguments of the gamma functions in the denominator and numerator of (3.93) differ pairwise by an integer. Thus, we can

[37] For $n = 0$, there are no solutions in the k_{n,q_2} branch of (3.92).

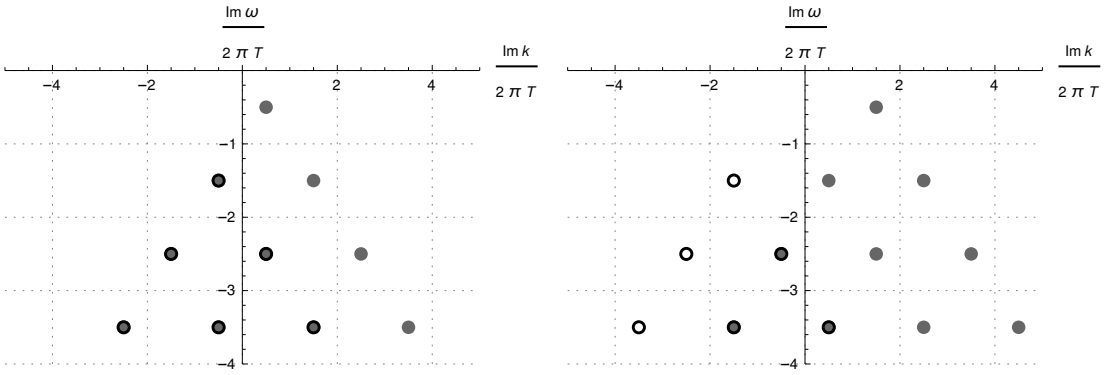

Figure 7: Pole-skipping points as predicted from the naive near-horizon analysis for half-integer mass values. The left plot depicts the locations for $m = \frac{1}{2}$ and the right plot contains the locations for $m = \frac{3}{2}$. The gray points correspond to the momentum written with a positive sign in and the hollow points correspond to the momenta with a negative sign as written in table 5. We see that at half-integer values of the mass, some of the locations overlap (black circles with gray filling). These cases correspond to so-called anomalous points and signal that a more thorough analysis of the boundary Green's function is needed.

expand the ratio of the gamma functions into a product of finitely many terms as

$$\frac{\Gamma\left(\frac{\Delta}{2}-\frac{1}{4}+\frac{i(k-\omega)}{4\pi T}\right)}{\Gamma\left(-\frac{\Delta}{2}+\frac{5}{4}+\frac{i(k-\omega)}{4\pi T}\right)}=\prod_{n=1}^{\Delta-\frac{3}{2}}\left(\frac{\Delta}{2}-\frac{1}{4}-n+\frac{i(k-\omega)}{4\pi T}\right). \tag{3.94}$$

The ratio of the other two gamma functions can be found in a similar way to be

$$\frac{\Gamma\left(\frac{\Delta}{2}+\frac{1}{4}-\frac{i(k+\omega)}{4\pi T}\right)}{\Gamma\left(-\frac{\Delta}{2}+\frac{3}{4}-\frac{i(k+\omega)}{4\pi T}\right)}=\prod_{n=0}^{\Delta-\frac{3}{2}}\left(\frac{\Delta}{2}-\frac{3}{4}-n-\frac{i(k+\omega)}{4\pi T}\right). \tag{3.95}$$

This means that the retarded Green's function has a family of $2\Delta-2$ lines of zeros, given by the equations

$$\omega_1^Z=k-2\pi iT\left(2n-\Delta+\frac{1}{2}\right), \qquad \omega_2^Z=-k-2\pi iT\left(2n-\Delta+\frac{3}{2}\right), \tag{3.96}$$

where $n\in\left\{0,1,\ldots,\Delta-\frac{3}{2}\right\}$ and there is no solution for $n=0$ in ω_1^Z.

Poles arise when the argument of any of the two digamma functions is a non-positive integer, yielding two infinite families of lines of poles located at

$$\omega_1^P=k-2\pi iT\left(2n+\Delta-\frac{1}{2}\right), \qquad \omega_2^P=-k-2\pi iT\left(2n+\Delta+\frac{1}{2}\right), \tag{3.97}$$

for $n=0,1,2,\ldots$. The intersections between the lines of zeros and the lines of poles

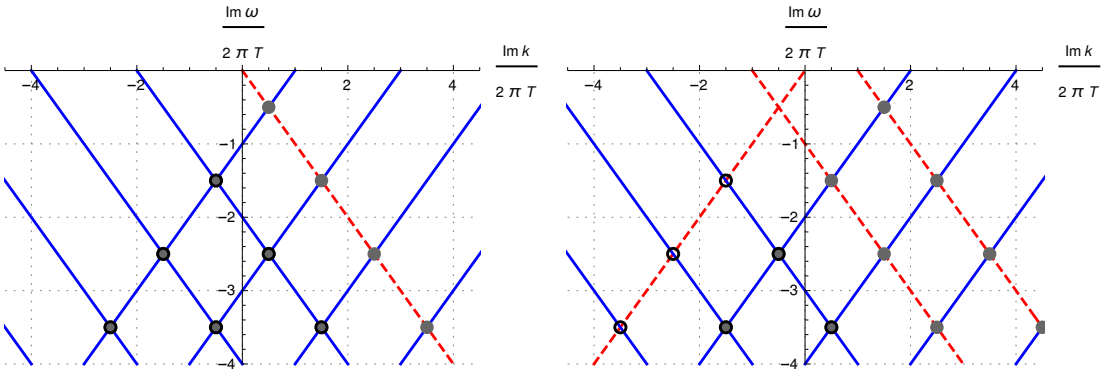

Figure 8: Comparison of the locations of the pole-skipping points predicted by the near-horizon analysis (gray and hollow points) and the locations of the intersections of the lines of poles (blue) and lines of zeros (red, dashed) of the exact boundary retarded Green's function for half-integer values of the conformal dimension. We see that the non-anomalous pole-skipping points (either hollow or gray, but not gray with black circle) perfectly match the locations of the intersections. The anomalous pole-skipping points (gray with black boundary) correspond to the locations where two lines of poles intersect. The physical interpretation of these anomalous points is still unclear.

occur at

$$\begin{aligned} \omega_n = -i\pi T(2n+1), \qquad k_{n,q_1} &= 2\pi i T(n+\Delta-2q_1-1), \\ k_{n,q_2} &= -2\pi i T(n+\Delta-2q_2), \end{aligned} \tag{3.98}$$

where $n \in \{0,1,\ldots\}$, $q_1 \in \{0,\ldots,\min\left(n,\Delta-\frac{3}{2}\right)\}$, $q_2 \in \{1,\ldots,\min\left(n,\Delta-\frac{3}{2}\right)\}$ and again there is no pole-skipping point at $n=0$ for the momenta given by k_{0,q_2}.

These special values for the intersections are predicted by considering anomalous pole-skipping points which occur when two pole-skipping points overlap, see figure 7 where we depict the naive pole-skipping points for $m=1/2$ and $m=3/2$.

For $n < m+1/2$, where m is a half-integer number, there are only non-anomalous pole-skipping points. If $n \geq m+1/2$, then the non-anomalous pole-skipping points are given by

$$k_{n,q_1} = 2\pi i T(m+n-2q_1)\,, \qquad q_1 \in \{0,1,\ldots m-1/2\}\,, \tag{3.99a}$$

$$k_{n,q_2} = -2\pi i T(m+n+1-2q_2)\,, \qquad q_2 \in \{1,2,\ldots m-1/2\}\,, \tag{3.99b}$$

where for $m=1/2$, there are no solutions in the second branch. This implies that the anomalous points are given by

$$k_{n,q_1} = 2\pi i T(m+n-2q_1)\,, \qquad q_1 \in \{m+1/2, m+3/2, \ldots n\}\,. \tag{3.100}$$

In summary, the near-horizon analysis predicts that the *non-anomalous* pole-skipping

points are located at

$$\begin{aligned} \omega_n = -i\pi T(2n+1), \qquad k_{n,q_1} &= 2\pi i T(m+n-2q_1), \\ k_{n,q_2} &= -2\pi i T(m+n+1-2q_2), \end{aligned} \tag{3.101}$$

with $n \in \{0,1,\ldots\}$ and $q_1 \in \{0,\ldots,\min\left(n, m-\frac{1}{2}\right)\}$, $q_2 \in \{1,\ldots,\min\left(n, m-\frac{1}{2}\right)\}$. Since $m = \Delta - 1$, these points coincide with intersections of the lines of poles and lines of zeros of the exact boundary retarded Green's function (see figure 8).

3.6.2 Schwarzschild Black Hole in AdS$_{D+2}$

Let us now assume that the background is the Schwarzschild-AdS black hole in $D+2$ dimensions for which the two functions appearing in the metric are

$$f(r) = 1 - \left(\frac{r_0}{r}\right)^{D+1}, \qquad h(r) = r^2, \tag{3.102}$$

with the Hawking temperature given by $(D+1)r_0 = 4\pi T$. The pole-skipping points at the lowest frequency are located at

$$\omega = \omega_0 = -\pi i T, \qquad k = \pm\frac{4\pi i}{D+1} m T, \tag{3.103}$$

which include the locations for both subsystems discussed in section 3.4. When $m = 0$ these merge into a single point with momentum $k = 0$.

In the case of a massless fermion ($m = 0$) the next few pole-skipping points are located at

$$\omega = \omega_1 = -3\pi i T, \qquad k = \begin{cases} 0, \\ k = \pm 2i\sqrt{\frac{2D}{D+1}}\,\pi T, \end{cases} \tag{3.104a}$$

$$\omega = \omega_2 = -5\pi i T, \qquad k = \begin{cases} 0, \\ \pm 2i\sqrt{\frac{5D+\sqrt{D(D+8)}}{D+1}}\,\pi T, \\ \pm 2i\sqrt{\frac{5D-\sqrt{D(D+8)}}{D+1}}\,\pi T, \end{cases} \tag{3.104b}$$

Notice that the non-zero momenta at ω_1 coincide with the pole-skipping momenta associated with first bosonic Matsubara frequency $\omega = \omega_1^B = -2\pi i T$ for the massless bosonic field in the same background [72].

3.7 Discussion

In this chapter we have investigated the near-horizon behaviour of a minimally coupled fermion field in asymptotically anti-de Sitter spacetimes. The thermal Green's function of the dual operator exhibits an ambiguity: at certain values of the frequency and the momentum there exist multiple independent solutions to the Dirac equations that are ingoing at the horizon. As a consequence the correlator is not uniquely defined at these points due to a collision between a pole and a zero of the Green's function.

The special frequencies where this happens are precisely the negative fermionic Matsubara frequencies

$$\omega_n = -2\pi i T \left(n + \frac{1}{2} \right) , \tag{3.105}$$

where n is a non-negative integer. At each of these frequencies there are in general $2(2n+1)$ associated values of the momentum at which pole-skipping takes place. Away from these special locations, the ingoing boundary condition at the horizon fixes half of the components of the spinor, whereas directly at the pole-skipping points the ingoing condition in general only fixes a quarter. Interesting exceptional cases include that of a spinor in three-dimensional spacetime and the massless spinor field in arbitrary dimension. In the latter case the number of pole-skipping points at each frequency is halved and in addition at each special location the ingoing condition does not impose any constraints – all solutions are ingoing.

The fermionic results are conceptually similar to that of scalar fields [72]. In both the near-horizon behaviour determines the boundary field theory correlators *away from the origin in Fourier space*. Furthermore, there is a similarity in that the higher the frequency of the pole-skipping point, the farther we probe away from the horizon and into the spacetime. This is manifested in the fact that the momentum values depend on higher derivatives of metric functions evaluated at the horizon.

In addition, we see that the pole-skipping points for scalar and fermionic fields have a similar structure. The frequency is determined purely by the temperature of the black hole, whereas the momentum has two general contributions, one coming from the mass term and one which depends solely on the ambient spacetime.

There are also some differences. For instance, in the scalar case there are fewer pole-skipping points: at any bosonic Matsubara frequency, i.e. $\omega_{\tilde{n}} = -2\pi i \tilde{n} T$, with $\tilde{n} = 1, 2, 3 \ldots$, there are $2\tilde{n}$ special locations, while for the fermion field at the n-th fermionic Matsubara frequency (3.105), there are $2(2n+1)$ pole-skipping points.

Another interesting novelty is the appearance of the pole-skipping point at the zeroth fermionic Matsubara frequency. This is due to the fact that spinors are multi-component objects and thus there exist two linearly independent solutions with the same behaviour at the horizon. This point is the most localized probe at the horizon,

as its location does not depend on any derivatives of the metric functions. Furthermore, it can never be anomalous and is thus a robust feature of holographic Green's functions of fermionic operators.

There are a few potential pathways in which one could generalize these results. The first is that the frequencies at which pole-skipping occurs follow a pattern depending on the spin of the field.[38] The first pole-skipping point of the graviton is located at $\omega = +2\pi iT$, for the vector field the first frequency is $\omega = 0$ [72], our analysis shows that for fermions this first frequency is $\omega = -\pi iT$, and scalar fields start to skip poles at $\omega = -2\pi iT$. It is natural to conjecture that spin-3/2 fields, described by a Rarita-Schwinger action (see for example [94–99] for the treatments of Rarita-Schwinger fields in AdS), should have their first pole-skipping point located at $\omega = +\pi iT$.

In an upcoming publication [90] we show that this is indeed the case. We hope that this indicates a certain universality of pole-skipping. It would be interesting to investigate the importance of this order on the relation between pole-skipping, chaos, and holographic theories in general.

Another interesting development comes from the analysis of 2-dimensional CFTs, where it has been shown [100] that pole-skipping is also seen for frequencies which are non-integer multiples of πiT. These are neither bosonic nor fermionic Matsubara frequencies and could be associated with non-half integer spin particles: anyons. It would be interesting to see whether there is a corresponding bulk object whose near-horizon behaviour would explain pole-skipping at such frequencies.

Our hope is that one can get a better understanding of pole-skipping by considering more complicated, yet soluble models, such as the axion model [81, 82]. This model contains an additional parameter which regulates the strength of the energy dissipation in the boundary theory. Ref. [70] discusses pole-skipping in this model for the energy density function and finds that the pole-skipping point does not change as the dissipation is increased and correctly predicts the dispersion relation of the collective excitations in the boundary for both the weakly and strongly dissipating regime. It would be interesting to see whether such statements could be translated to the scalar or spinor field case.

Similarly, one could analyse how corrections to Einstein gravity affect the pole-skipping locations in scalar and fermion fields. In [71] it was shown that the momentum value at the pole-skipping locations for the energy-density correlator correctly predicts the corrections to the butterfly velocity in such theories. Repeating the same analysis for scalars or fermions could clarify whether simpler fields can be used as a diagnostic for chaos.

Another point of interest is the interpretation of anomalous locations which occur whenever two pole-skipping points overlap. It would be interesting to see if there is

[38] We thank Richard Davison for pointing this out to us.

some additional physics that happens at such points.

The detailed analysis of the Green's functions revealed that at (bosonic or fermionic) Matsubara frequencies, the retarded and advanced Green's functions are equal. Another interesting aspect worth looking into is to see how this is manifested in the boundary theory.

An example of a spin-1/2 field in a boundary field theory is the time component of the supersymmetric current in $\mathcal{N} = 4$ SYM theory in four dimensions discussed in [101] which in the low frequency and low momentum limit gives rise to the so-called phonino mode. It would be interesting to see whether this hydrodynamic mode (or modes coming from other components of the supersymmetric current) passes through the pole-skipping point (3.25) if its dispersion relation is analytically continued to imaginary values of the frequency and momentum, as is the case for the shear or sound modes [68, 73] that pass through the bosonic pole-skipping points analysed in the previous chapter.

Finally, we have added to the literature of properties of the boundary theories that are encoded in the near-horizon region. One may wonder if there are other universal properties of holographic theories that can be seen from simple near-horizon analysis of bulk fields.

Chapter 4

Review of D1-D5-P System

In the introduction we have discussed black holes and argued that a full theory of quantum gravity may be needed in order to fully resolve some of the issues that arise in the semi-classical picture. String theory emerged as a possible framework in which one can address these questions, hence in this and the next chapter we describe a specific system comprised of a BPS configuration of D1 and D5 branes (with additional momentum charge P) in type IIB superstring theory.

We first study the supergravity description of this system and review a counting argument that reproduces the Bekenstein-Hawking entropy. Next we present the $\text{AdS}_3/\text{CFT}_2$ duality that arises from the D1-D5 system, and especially focus on the CFT at the orbifold point. We then review the *fuzzball proposal* which states that black holes are course grained averages over a vast amount of horizonless microstates and finally introduce the *microstate geometries programme* which tries to construct microstates that have a valid description within supergravity.

This chapter has some overlap with [1].

4.1 Brane Setup

We work in type IIB string theory on $\mathbb{R}^{1,4} \times S^1 \times \mathcal{M}$ where the internal space $\mathcal{M}$ is either $K3$ or T^4, but in most of what follows we use $\mathcal{M} = T^4$, except where explicitly stated otherwise. Let t denote the time coordinate, x_μ with $\mu = 1, 2, 3, 4$ denote the coordinates of $\mathbb{R}^4$, y is the coordinate of S^1 which has radius R_y, and x_i with $i = 6, 7, 8, 9$ denote the coordinates of T^4 which has volume V_4.

The system of interest is a specific configuration of D1 and D5-branes that are wrapped around the compact directions of spacetime (see table 6 for summary). Let n_1 D1-branes be wrapped along the S^1, and let n_5 D5-branes be wrapped around $S^1 \times T^4$, and in addition there is n_P units of left-moving momentum along S^1. We assume that the branes are localised in the $\mathbb{R}^4$ which we call the *base space*.

		$\mathbb{R}_t$	$\mathbb{R}^4$				S^1	T^4			
		t	x_1	x_2	x_3	x_4	y	x_6	x_7	x_8	x_9
Objects	D1	•	–	–	–	–	•	–	–	–	–
	D5	•	–	–	–	–	•	•	•	•	•
	P	•	–	–	–	–	•	–	–	–	–

Table 6: The brane configuration of the D1-D5-P system. The directions in which an object is extended is denoted by •, while – denotes the directions in which the object is localised. The D1-branes are extended only along the macroscopic S^1 direction, parametrised by the coordinate $y \in [0, 2\pi R_y)$. The D5-branes are extended along the $S^1 \times T^4$ and we add an additional momentum charge along the S^1, but all the momentum points only in one direction. In the non-compact space $\mathbb{R}^4$ all the branes are localised.

The assumption that the momentum is moving in only one direction is necessary to preserve some supersymmetries, namely if we add some right-moving momentum into the above configuration, all supersymmetries are broken. With only left-moving momentum, the system preserves 4 out of the total 32 supercharges of type IIB string theory and is thus an 1/8-BPS system [102].

Throughout the next two chapters we work the large N limit by assuming that

$$n_1, n_5 \gg 1\,, \tag{4.1.1}$$

meaning that the number of D1 and D5 branes in the system is large. Furthermore, we assume that the size of the T^4 is of the string length size and thus small. We sometimes refer to this space as the *internal space*. On the other hand, we assume that the size of the S^1 is large in string length units so that $R_y \gg l_s$.

We can look at this system in two different limits. Our main focus will be on the strong string coupling limit ($g_s \gg 1$) in which the branes gravitate. If we limit ourselves to the low energy physics, we can describe the branes in terms of a curved metric, hence we denote this regime as the *classical supergravity limit*. However, we can also study the limit $g_s \ll 1$, such that $g_s n_1 n_5 \ll 1$, where open and closed strings decouple. Thus the effective picture in this case is that of non-interacting open strings on flat branes in non-curved spacetime. This regime contains some interesting physics, especially in light of the microstates of the D1-D5-P black hole, which ultimately leads us to the *fuzzball proposal*.

4.2 Gravity Description

4.2.1 General Ansatz and System of Equations

Let us begin by introducing a system of equations that is tailored for 1/8-BPS solutions to type IIB supergravity [103]. The action (1.15) that we have presented in the introduction contains only the RR gauge field strengths F_1, F_3, and F_5, which correspond roughly to exterior derivatives of the potentials C_0, C_2 and C_4. However, D5-branes can also be thought as sources of a higher order form potential which is not included in this action.

In this case it is convenient to use the democratic formulation of supergravity [104] which introduces "high" order forms (or their field strengths) and puts them on equal footing with the "low" order ones by imposing additional constraint equations. Begin by defining an operator λ, whose action on a p-form A_p is given by

$$\lambda\left(A_p\right) = (-1)^{p(p-1)/2} A_p \,. \tag{4.2.1}$$

In the new formulation the RR gauge field content of type IIB supergravity is enhanced to $\{C_0, C_2, C_4, C_6, C_8\}$. Defining

$$H = dB \,, \tag{4.2.2}$$

where B is the usual NS-NS two-form, we define a RR p-form field strength as

$$F_p = dC_{p-1} - H \wedge C_{p-3} \,. \tag{4.2.3}$$

These satisfy

$$dF_p = H \wedge F_{p-2} \,, \tag{4.2.4}$$

which can be seen as modified Bianchi identities.

By allowing additional gauge potentials, we have almost doubled the number of degrees of freedom appearing in the C_p fields. To remedy this, we impose the self-duality constraint

$$F_p = *\lambda\left(F_{10-p}\right) \,, \tag{4.2.5}$$

where $*$ is the ten-dimensional hodge dual operator. For type IIB supergravity the above constraint can be written out explicitly as

$$F_1 = *F_9, \quad F_3 = -*F_7, \quad F_5 = *F_5, \quad F_7 = -*F_3, \quad F_9 = *F_1 \,, \tag{4.2.6}$$

which implies that F_p and F_{10-p} effectively carry the same degrees of freedom.

Using this new framework, a general 1/8-BPS solution to the equations of motion was derived in [103,105], building on previous work [106–108].[39] The assumptions made are that

1. The solutions admit a null isometry.[40]

2. The solutions are isotropic in the internal manifold, *i.e.* the fields do not depend on the coordinates of T^4 and forms can only have either no legs in this space or have a factor proportional to the volume form $\widehat{\text{vol}}_4$ of T^4.

The general solution is then given by the ansatz

$$ds_{10}^2 = \sqrt{\alpha}\, ds_6^2 + \sqrt{\frac{Z_1}{Z_2}}\, d\hat{s}_4^2, \tag{4.2.7a}$$

$$ds_6^2 = -\frac{2}{\sqrt{\mathcal{P}}}(dv+\beta)\Big[du+\omega+\frac{\mathcal{F}}{2}(dv+\beta)\Big] + \sqrt{\mathcal{P}} ds_4^2, \tag{4.2.7b}$$

$$e^{2\Phi} = \frac{Z_1^2}{\mathcal{P}}, \tag{4.2.7c}$$

$$B_2 = -\frac{Z_4}{\mathcal{P}}(du+\omega)\wedge(dv+\beta) + a_4\wedge(dv+\beta) + \delta_2, \tag{4.2.7d}$$

$$C_0 = \frac{Z_4}{Z_1}, \tag{4.2.7e}$$

$$C_2 = -\frac{\alpha}{Z_1}(du+\omega)\wedge(dv+\beta) + a_1\wedge(dv+\beta) + \gamma_2, \tag{4.2.7f}$$

$$C_4 = \frac{Z_4}{Z_2}\widehat{\text{vol}}_4 - \frac{Z_4}{\mathcal{P}}\gamma_2\wedge(du+\omega)\wedge(dv+\beta) + x_3\wedge(dv+\beta), \tag{4.2.7g}$$

$$C_6 = \widehat{\text{vol}}_4\wedge\left[-\frac{Z_1}{\mathcal{P}}(du+\omega)\wedge(dv+\beta) + a_2\wedge(dv+\beta) + \gamma_1\right] \tag{4.2.7h}$$

with

$$\alpha \equiv \frac{Z_1 Z_2}{Z_1 Z_2 - Z_4^2}, \qquad \mathcal{P} \equiv Z_1\, Z_2 - Z_4^2. \tag{4.2.8}$$

We have defined new asymptotically null coordinates u and v as

$$u \equiv \frac{1}{\sqrt{2}}(t-y), \qquad v \equiv \frac{1}{\sqrt{2}}(t+y), \tag{4.2.9}$$

which can be thought of as world-volume coordinates of the branes. In the above ansatz, ds_{10}^2 denotes the string-frame metric of the ten-dimensional spacetime, and ds_6^2 denotes the Einstein-frame metric of the six-dimensional spacetime, which is a fibration

[39] See also [109] for a recent review.

[40] Assuming a null isometry is natural in the context of the D1-D5-P solutions, as one assumes no right-moving momentum along S^1 to preserve some supersymmetry. Forming light-cone coordinates (4.2.9), one can identify the right-moving direction as the direction of the isometry.

over a 4-dimensional base $\mathcal{B}$ with metric

$$ds_4^2 = h_{\mu\nu}(x,v)dx^\mu dx^\nu\,, \tag{4.2.10}$$

where the metric components can in principle be functions of the coordinates on $\mathcal{B}$ and v. The ansatz includes scalars $Z_1, Z_2, Z_4, \mathcal{F}$; one-forms $\beta, \omega, a_1, a_2, a_4$; two-forms $\gamma_1, \gamma_2, \delta_2$; and a three-form x_3, all on $\mathcal{B}$. These quantities can depend on the coordinates of $\mathcal{B}$ and on v, but supersymmetry requires them to be independent of u. The RR potentials C_p can have an extra term proportional to a four-form $\mathcal{C}$ on $\mathcal{B}$, but it has been set to zero by using the gauge symmetries discussed in [103, 110].

There is some redundancy in the ansatz as the form of the solution is preserved by the diffeomorphism

$$v \to v + V(x)\,, \qquad u \to u + U(x,v)\,, \tag{4.2.11}$$

provided that the following transformations are taken at the same time

$$\beta \to \beta - d_4 V\,, \qquad \mathcal{F} \to \mathcal{F} - 2\dot{U}\,, \qquad \omega \to \omega - d_4 U + \dot{U}\beta\,. \tag{4.2.12}$$

In the above d_4 denotes the exterior derivative constrained to the base space $\mathcal{B}$, and the dot denotes the partial derivative with respect to v, *i.e.* $\dot{} \equiv \partial_v$. It is also convenient to introduce a gauge invariant differential operator

$$\mathcal{D} \equiv d_4 - \beta \wedge \partial_v\,. \tag{4.2.13}$$

The potentials in the ansatz (4.2.7) are not gauge invariant and thus the ansatz quantities appearing in them are also not gauge invariant. The equations of motion relate only gauge invariant quantities, which are the two-forms [103, 109]

$$\Theta_1 \equiv \mathcal{D}a_1 + \dot{\gamma}_2 - \dot{\beta} \wedge a_1\,, \qquad \Sigma_1 \equiv \mathcal{D}\gamma_2 - a_1 \wedge \mathcal{D}\beta\,, \tag{4.2.14a}$$

$$\Theta_2 \equiv \mathcal{D}a_2 + \dot{\gamma}_1 - \dot{\beta} \wedge a_2\,, \qquad \Sigma_2 \equiv \mathcal{D}\gamma_1 - a_2 \wedge \mathcal{D}\beta\,, \tag{4.2.14b}$$

$$\Theta_4 \equiv \mathcal{D}a_4 + \dot{\delta}_2 - \dot{\beta} \wedge a_4\,, \qquad \Sigma_4 \equiv \mathcal{D}\delta_2 - a_4 \wedge \mathcal{D}\beta\,, \tag{4.2.14c}$$

and an additional four-form Ξ_4 which will not be important in our discussion. Essentially these are different degrees of freedom appearing in the field strengths F_p [103, 109], and one can think of this new formalism as a particular way to nicely decouple the equations governing the different degrees of freedom appearing in the gauge fields. But note that the fields in (4.2.14) are not completely independent as one can show that they satisfy $(I = 1, 2, 4)$ [109]

$$\mathcal{D}\Sigma_I = -\Theta_I \wedge \mathcal{D}\beta, \qquad \partial_v(\Sigma_I + \beta \wedge \Theta_I) = d_4\Theta_I. \tag{4.2.15}$$

The equations of motion can be separated into three layers [103]. These can be solved in succession, with the solution of the previous layer acting as source in the next one. Most importantly, the system has a linear structure [108]: apart from the zeroth layer, the equations of motion are linear with the only non-linear part coming from the sources, which in principle are known from solving the previous layer.

Zeroth Layer

The zeroth layer determines the metric of the base space $h_{\mu\nu}$ and the one-form β. The space must be almost hyper-Kähler on which we find a set of three anti-self dual two-forms J_A, $A = 1, 2, 3$, that satisfy the following set of equations

$$*_4 J_A = -J_A \,, \tag{4.2.16a}$$

$$J_A \wedge J_B = -2\delta_{AB}\, \mathrm{vol}_4 \,, \tag{4.2.16b}$$

$$d_4 J_A = \partial_v \left(\beta \wedge J_A\right) \,, \tag{4.2.16c}$$

where $*_4$ is the hodge-dual on the base space and vol_4 is its volume form. In addition, the one-form β needs to be self-dual

$$\mathcal{D}\beta = *_4\, \mathcal{D}\beta \,. \tag{4.2.17}$$

This layer is in principle the hardest to solve as it involves non-linear differential equations (4.2.16). The solutions appear as sources in the first layer, mainly through β and the hodge-dual operator, with the exception being an anti-self dual two-form which can be constructed as

$$\psi = \frac{1}{8}\epsilon^{ABC}\, (J_A)^{\mu\nu} \left(\dot{J}_B\right)_{\mu\nu} J_C \,, \tag{4.2.18}$$

where ϵ^{ABC} is a totally anti-symmetric tensor and we take $\epsilon^{123} = +1$.

First Layer

The first layer relates the scalars Z_I with the gauge strengths Θ_I and Σ_I. In fact one can group the equations into three sets of independent equations which all have the same form

$$*_4(\mathcal{D}Z_1 + \dot{\beta} Z_1) = \Sigma_2 \,, \qquad (1 - *_4)\Theta_2 = 2 Z_1 \psi \,, \tag{4.2.19a}$$

$$*_4(\mathcal{D}Z_2 + \dot{\beta} Z_2) = \Sigma_1 \,, \qquad (1 - *_4)\Theta_1 = 2 Z_2 \psi \,, \tag{4.2.19b}$$

$$*_4(\mathcal{D}Z_4 + \dot{\beta} Z_4) = \Sigma_4 \,, \qquad (1 - *_4)\Theta_4 = 2 Z_4 \psi \,, \tag{4.2.19c}$$

and thus a solution for one set of equations is also a solution for the other two. Note that the two-form ψ coming out of the zeroth-layer is related to the failure of the two-forms Θ_I to be self dual.

There exists an equivalent set of equations in which Σ_I has been eliminated, which is given by

$$\partial_v \Big(*_4(\mathcal{D}Z_1 + \dot{\beta}Z_1)\Big) = d_4\Theta_2 - \partial_v\left(\beta \wedge \Theta_2\right) ,$$
$$\mathcal{D} *_4 \left(\mathcal{D}Z_1 + \dot{\beta}Z_1\right) = -\Theta_2 \wedge \mathcal{D}\beta\,, \tag{4.2.20a}$$
$$\partial_v \Big(*_4(\mathcal{D}Z_2 + \dot{\beta}Z_2)\Big) = d_4\Theta_1 - \partial_v\left(\beta \wedge \Theta_1\right) ,$$
$$\mathcal{D} *_4 \left(\mathcal{D}Z_2 + \dot{\beta}Z_2\right) = -\Theta_1 \wedge \mathcal{D}\beta\,, \tag{4.2.20b}$$
$$\partial_v \Big(*_4(\mathcal{D}Z_4 + \dot{\beta}Z_4)\Big) = d_4\Theta_4 - \partial_v\left(\beta \wedge \Theta_4\right) ,$$
$$\mathcal{D} *_4 \left(\mathcal{D}Z_4 + \dot{\beta}Z_4\right) = -\Theta_4 \wedge \mathcal{D}\beta\,. \tag{4.2.20c}$$

Second Layer

Finally, the second layer determines $\mathcal{F}$ and ω [105, 109]

$$(1 + *_4)\mathcal{D}\omega + \mathcal{F}\,\mathcal{D}\beta = Z_1\Theta_1 + Z_2\Theta_2 - 2Z_4\Theta_4 - 2(Z_1Z_2 - Z_4^2)\psi, \tag{4.2.21a}$$

$$\begin{aligned} &*_4\mathcal{D} *_4 L + 2\dot{\beta}_\mu L^\mu - *_4(\psi \wedge \mathcal{D}\omega) \\ &\quad = -\frac{1}{4}(Z_1Z_2 - Z_4^2)\dot{h}^{\mu\nu}\dot{h}_{\mu\nu} + \frac{1}{2}\partial_v[(Z_1Z_2 - Z_4^2)h^{\mu\nu}\dot{h}_{\mu\nu}] \\ &\qquad + (\dot{Z}_1\dot{Z}_2 - \dot{Z}_4^2) + (Z_1\ddot{Z}_2 + Z_2\ddot{Z}_1 - 2Z_4\ddot{Z}_4) \\ &\qquad - \frac{1}{2} *_4 \Big[(\Theta_1 - Z_2\psi) \wedge (\Theta_2 - Z_1\psi) - (\Theta_4 - Z_4\psi) \wedge (\Theta_4 - Z_4\psi) \\ &\qquad\qquad + (Z_1Z_2 - Z_4^2)\psi \wedge \psi\Big], \end{aligned} \tag{4.2.21b}$$

where we have defined the one-form

$$L \equiv \dot{\omega} + \frac{\mathcal{F}}{2}\dot{\beta} - \frac{1}{2}\mathcal{D}\mathcal{F}. \tag{4.2.22}$$

The equations are linear in $\mathcal{F}$ and ω, although (4.2.21b) is significantly more complicated than the equations that we encountered so far. The reason is that the equations in the first two layers (and (4.2.21a)) are derived using the supersymmetry in the system. This can be seen most easily from the fact that the equations are first rather than second order differential equations, which appear in the usual Einstein-Maxwell like equations. However, in most of the systems, solving BPS equations alone is not enough to fully specify the solutions and one has to add an additional equation of motion,

usually from either the Maxwell's or Einstein's equations [111]. Here (4.2.21b) comes from a null-null component of the Einstein equations [103].

The fact that the equations are first order differential equations is an additional advantage when looking for new solutions as these are significantly easier to solve than second order equations. Thus we are able to find solutions which were previously too difficult to obtain.

Flat Base Space

As mentioned above, the zeroth layer is the hardest to solve. However, a huge number of solutions can be found by considering a base space with a flat metric

$$h_{\mu\nu}(x,v) = \delta_{\mu\nu}\,, \tag{4.2.23}$$

and a set of v-independent two forms J_A, from which it follows that $\psi = 0$. One can make a further assumption that the one-form β is also v-independent, in which case the self duality constraint reduces to

$$d_4\beta = *_4 (d_4\beta)\ . \tag{4.2.24}$$

This simplifies the first and second layer equations significantly, as they are now given by

$$*_4\mathcal{D}\dot{Z}_1 = \mathcal{D}\Theta_2, \qquad \mathcal{D}*_4\mathcal{D}Z_1 = -\Theta_2\wedge d\beta, \qquad \Theta_2 = *_4\Theta_2, \tag{4.2.25a}$$

$$*_4\mathcal{D}\dot{Z}_2 = \mathcal{D}\Theta_1, \qquad \mathcal{D}*_4\mathcal{D}Z_2 = -\Theta_1\wedge d\beta, \qquad \Theta_1 = *_4\Theta_1, \tag{4.2.25b}$$

$$*_4\mathcal{D}\dot{Z}_4 = \mathcal{D}\Theta_4, \qquad \mathcal{D}*_4\mathcal{D}Z_4 = -\Theta_4\wedge d\beta, \qquad \Theta_4 = *_4\Theta_4, \tag{4.2.25c}$$

and

$$\mathcal{D}\omega + *_4\mathcal{D}\omega + \mathcal{F}d\beta = Z_1\Theta_1 + Z_2\Theta_2 - 2Z_4\Theta_4, \tag{4.2.26a}$$

$$*_4\,\mathcal{D}*_4\left(\dot{\omega} - \frac{1}{2}\mathcal{D}\mathcal{F}\right) = \partial_v^2(Z_1Z_2 - Z_4^2) - (\dot{Z}_1\dot{Z}_2 - (\dot{Z}_4)^2) - \frac{1}{2}*_4(\Theta_1\wedge\Theta_2 - \Theta_4\wedge\Theta_4). \tag{4.2.26b}$$

4.2.2 D1-D5-P Black Hole

We begin by considering the simplest 3-charge solution, which corresponds to setting all ansatz quantities to zero, except [105]

$$Z_1 = 1 + \frac{Q_1}{r^2}\,, \qquad Z_2 = 1 + \frac{Q_5}{r^2}\,, \qquad \frac{\mathcal{F}}{2} = -\frac{Q_p}{r^2}\,. \tag{4.2.27}$$

We also assume that the base space is $\mathbb{R}^4$ with the metric (4.2.23). This is the solution corresponding to the superposition of a stack of D1 and D5 branes localised at the origin of $\mathbb{R}^4$, with momentum charge along one direction in S^1 [102], and is thus precisely the supergravity description of the brane configuration summarized in table 6. The charges Q_1, Q_5, and Q_p are measured within supergravity and are related to the quantized numbers n_1, n_5, and n_p as [105]

$$Q_1 = \frac{(2\pi)^4 g_s l_s^6}{V_4}\, n_1\,, \qquad Q_5 = g_s l_s^2\, n_5\,, \qquad Q_p = \frac{(2\pi)^4 g_s^2 l_s^8}{V_4 R_y^2}\, n_p\,. \tag{4.2.28}$$

Inserting these values into the ansatz (4.2.7) shows that the system is described by

$$ds_{10}^2 = -\frac{2}{\sqrt{Z_1 Z_2}}\, dv\left(du + \frac{\mathcal{F}}{2} dv\right) + \sqrt{Z_1 Z_2}\, ds_4^2 + \sqrt{\frac{Z_1}{Z_2}} d\hat{s}_4^2\,, \tag{4.2.29a}$$

$$e^{2\Phi} = \frac{Z_1}{Z_2}, \qquad B = 0, \qquad C_0 = 0, \qquad C_2 = -\frac{1}{Z_1} du \wedge dv + \gamma_2,$$

$$C_4 = 0\,, \qquad C_6 = \left(-\frac{1}{Z_2} du \wedge dv + \gamma_1\right) \wedge dx^{6789}, \tag{4.2.29b}$$

where γ_1 and γ_2 are determined by the anti-self duality condition $F_3 = -*_{10} F_7$, which is equivalent to imposing

$$d\gamma_1 = *_4 dZ_1\,, \qquad d\gamma_2 = *_4 dZ_2\,. \tag{4.2.30}$$

Thus in addition to having a non-trivial metric, this solution has an excited two-form gauge potential (and a corresponding six-form potential) and a dilaton field.

Asymptotic behaviour ($r \to \infty$) In this limit both Z_1 and Z_2 tend to 1, while $\mathcal{F}$ vanishes. Using $-du\, dv = -dt^2 + dy^2$, we see that the metric at infinity corresponds to a flat metric in ten dimensions and thus (4.2.29) describes an asymptotically flat spacetime, with the asymptotic space being $\mathbb{R}^{1,4} \times S^1 \times T^4$. The remaining fields show similar behaviour in this region, as the dilaton vanishes while the components of C_2 and C_6 become constant and thus their corresponding field strengths vanish.

Near Horizon Region ($r \ll \sqrt{Q_{1,5}}$) In this limit we can neglect the factors "1" in $Z_{1,2}$. If one uses the coordinate transformation $r^2 = \widetilde{r}^2 - Q_p$ [112] the metric can be rewritten as

$$ds^2 = -\frac{\widetilde{r}^2 f(\widetilde{r})^2}{R_{\text{AdS}}^2}\, dt^2 + \frac{R_{\text{AdS}}^2}{\widetilde{r}^2 f(\widetilde{r})^2}\, d\widetilde{r}^2 + \frac{\widetilde{r}^2}{R_{\text{AdS}}^2}\left(dy + \frac{Q_p}{\widetilde{r}^2}\, dt\right)^2 + R_{\text{AdS}}^2 d\Omega_3^2 + \sqrt{\frac{Q_1}{Q_5}} d\hat{s}_4^2\,, \tag{4.2.31}$$

where

$$f(\widetilde{r}) = 1 - \frac{Q_p}{\widetilde{r}^2}\,, \tag{4.2.32}$$

$d\Omega_3^2$ is the area element of a unit sphere in three dimensions, and

$$R_{\rm AdS}^2 = \sqrt{Q_1 Q_5}\,. \tag{4.2.33}$$

This is the extremal BTZ black hole [61, 62] (satisfies $M\,R_{\rm AdS} = |J|$) together with a three-sphere with a constant radius $R_{\rm AdS}$, and a four torus with a different radius $Q_1^{\frac{1}{4}}\,Q_5^{-\frac{1}{4}}$.

We can compactify the solution along $S^1 \times T^4$ [113] to obtain [102, 114][41]

$$ds_E^2 = -\lambda^{-\frac{2}{3}}\,dt^2 + \lambda^{\frac{1}{3}}\left(dr^2 + r^2 d\Omega_3^2\right)\,, \tag{4.2.34}$$

which is written in the Einstein frame, with

$$\lambda = \left(1 + \frac{Q_1}{r^2}\right)\left(1 + \frac{Q_5}{r^2}\right)\left(1 + \frac{Q_p}{r^2}\right)\,. \tag{4.2.35}$$

This is a generalisation of the extremal Reissner–Nordström solution in 5 dimensions. The metric components diverge at $r \to 0$, however the curvature invariants (such as the Ricci scalar or Kretschmann scalar (1.6)) are finite, meaning that at this point we have a horizon rather than a singularity, and thus we can calculate the Bekenstein-Hawking entropy of this black hole through (1.12).

Since the horizon is located at $r = 0$ where λ diverges, one could assume that the area of the three-sphere S^3 either vanishes or diverges due to the factor of $r^2\,\lambda^{\frac{1}{3}}$ multiplying the part of the metric concerned with the sphere. However, there is a stabilisation due to the cancellation between the divergence of the $\lambda^{\frac{1}{3}}$ and vanishing of r^2, which fixes the radius of the sphere to $(Q_1 Q_5 Q_p)^{\frac{1}{3}}$, and consequently the area of the horizon is given by

$$A_H = 2\pi^2\sqrt{Q_1\,Q_5\,Q_p}\,. \tag{4.2.36}$$

Since the supergravity charges are related to the quantised charges via (4.2.28), the horizon area depends on the moduli of the theory, such as the value of the string coupling or the size of the compact dimensions. However, in the Bekenstein-Hawking

[41] We use (4.2.9) to go back to the $\{t, y, x_\mu\}$ coordinate system and then compactify along S^1 coordinatized by y.

entropy all moduli dependence cancels out to give

$$S_{BH} = \frac{A_H}{4G_N^{(5)}} = 2\pi\sqrt{n_1\, n_5\, n_p}\,, \tag{4.2.37}$$

where $G_N^{(5)}$ is the five-dimensional Newton's constant which can be written in terms of the parameters of the theory as [115]

$$G_N^{(5)} = \frac{8\pi^6 g_s^2\, l_s^8}{2\pi R_y\,(2\pi)^4\, V}\,. \tag{4.2.38}$$

This result is significant as it shows that contrary to the horizon area, the entropy is depends only on the number of objects in the configuration.

4.2.3 D1-D5 Black Hole

Let us briefly look at behaviour of the above system as we take the two-charge limit

$$Q_p \to 0 \qquad \Longleftrightarrow \qquad n_p \to 0\,, \tag{4.2.39}$$

so we must set $\mathcal{F} = 0$ in the metric part of (4.2.29), but leave the RR potentials and the dilaton field unchanged. The resulting solution reduces to the exact same form in the $r \to \infty$ limit as before, and is thus also asymptotically flat. On the other hand, the near horizon region changes. By taking the limit $r \ll \sqrt{Q_{1,5}}$ we observe that the metric can now be written as

$$ds^2 = -\frac{r^2}{R_{\text{AdS}}^2}\,dt^2 + \frac{R_{\text{AdS}}^2}{r^2}\,dr^2 + \frac{r^2}{R_{\text{AdS}}^2}dy^2 + R_{\text{AdS}}^2 d\Omega_3^2 + \sqrt{\frac{Q_1}{Q_5}}d\hat{s}_4^2\,, \tag{4.2.40}$$

with the radius of AdS still being given by (4.2.33). This is the metric of an extremal massless (and thus non-rotating) BTZ black hole fibered with an S^3 with a radius of R_{AdS} and a T^4 with a constant radius. The BTZ black hole is locally AdS_3, however these two spaces differ globally. The horizon is again located at $r = 0$, but in this case coincides with the position of the curvature singularity, unlike in the solution (4.2.31) where the horizon is located at $\widetilde{r} = \sqrt{Q_P}$.

The physical interpretation of this difference can be traced to the brane configuration found in table 6. Close to the branes, the spacetime transverse to the world-volume tends to expand, while the directions in which the brane is extended tend to shrink, as this lowers the energy due to the tension of the branes. Since along S^1 both D1 and D5 branes are extended, this spacetime dimension effectively vanishes where the branes are located (see that in (4.2.40) at $r = 0$ the length of the circle parametrised by y shrinks to 0).

On the contrary, momentum causes the directions along which is propagates to expand. Recall that in a compact space, the momentum is quantised in units of inverse length, so a larger space implies lower momentum excitations. Thus adding momentum along S^1 stabilises the circle at the position of the branes which leads to a non-vanishing horizon area.

It is this stabilisation that is the difference between the three and the two-charge black hole. It can be also seen after the compactification along $S^1 \times T^4$, which in the case of the two-charge black hole yields [114]

$$ds_E^2 = -\widetilde{\lambda}^{-\frac{2}{3}}\, dt^2 + \widetilde{\lambda}^{\frac{1}{3}} \left(dr^2 + r^2 d\Omega_3^2\right) , \tag{4.2.41}$$

in the Einstein frame, with

$$\widetilde{\lambda} = \left(1 + \frac{Q_1}{r^2}\right)\left(1 + \frac{Q_5}{r^2}\right) . \tag{4.2.42}$$

For this metric the curvature invariants diverge at $r \to 0$, which is also the position of the horizon. In that limit $r^2\, \lambda^{\frac{1}{3}} \sim r^{2/3}$, so the radius of S^3 and thus the horizon area vanish. Therefore classically, the D1-D5 two-charge black hole has a vanishing Bekenstein-Hawking entropy.

All in all, the two-charge solution is simpler than the three-charge one, however it is also special in the sense that the curvature singularity and the horizon overlap. Thus the two-charge black hole serves as an important toy model for the more complicated three-charge solution where the horizon is at a macroscopic distance from the singularity and thus the physics at the horizon scale is clearly distinguished from the physics near the singularity.

4.3 Brane Description

The Bekenstein-Hawking entropy for the three-charge black hole depends only on the number of D1 and D5-branes, and the number of quantized units of momentum added onto the geometry. Thus one can speculate that the same entropy can be obtained from a pure counting argument. This was confirmed by Strominger and Vafa in [116] (albeit they used $K3$ rather than T^4), where they found that a moduli invariant bound of the number of BPS states in a system which provides a dual description to the gravity picture correctly reproduces the black hole entropy.

Soon thereafter Callan and Maldacena [102] provided a more physical interpretation of how this counting can be seen from an open string perspective. Here we give a simplified account of their derivation and follow [22, 102, 115, 117].

We assume $g_s \ll 1$ and $g_s n_1 n_5 \ll 1$ so that open and closed strings decouple,

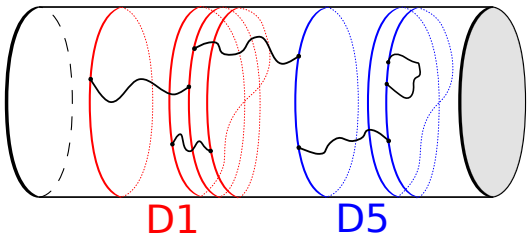

Figure 9: The schematic depiction of S_1, where we have separated the coincident branes and ignore the remaining directions. We have n_1 D1-branes (depicted in red) and n_5 D5-branes (depicted in blue), both of which can be either singly or multiply-winded. There are open strings (in black) which can end on either of the branes and carry the momentum charge of the system. In order to have a BPS system the strings have to be massless and travel in the same direction.

and thus the system is described by branes in flat ten dimensional spacetime. The momentum charge has to be carried by an object that does not break any additional supersymmetries. It turns out that these objects are massless open strings which carry momentum along one direction in S^1 [102].

Since we work in a limit where the S^1 is much larger than the T^4, we can imagine the system being described by an effective theory living on the S^1 with D5-branes reduced to one dimensional objects on the circle. The open strings can end either on the D1-brane or the D5-brane, which gives us four different options – $(1,1)$, $(1,5)$, $(5,1)$, and $(5,5)$, where each label describes the brane on which the left or right end lives, and since the strings are oriented, we need to distinguish between the left and the right end-point.

We want to show that number of configurations of such a system can reproduce the Bekenstein-Hawking entropy, to leading order. Thus we are interested only in the largest contribution which comes from the strings whose ends lie on different branes. Furthermore, it turns out that when many $(1,5)$ and $(5,1)$ strings are excited, the $(1,1)$ and $(5,5)$ become massive [102, 118] and thus putting momentum into any such string breaks the BPS condition.

Because the stacks of D1-branes and D5-branes are coinciding on S^1, and the coupling between open strings is small, these effectively behave as free massless point particles. Their wavefunction is therefore just a superposition of momentum eigenstates on a circle and can be schematically written as

$$\psi(y) \sim \sum_k e^{\frac{iky}{2\pi R_y}} \,. \tag{4.3.1}$$

Or in other words, the open strings behave as a dilute non-interacting gas in a one dimensional box of length $L = 2\pi R_y$ with periodic boundary conditions imposed.

Before we continue, we need to explain that the quantised charges n_1 and n_5 actually

refer to the total number of windings of the D1 and D5-branes around S^1. This can be achieved in multiple ways, as a brane can be multiply wound around the circle, with the two extremal cases being, in the example of D1-branes, n_1 singly wound branes and a single brane wound n_1 times. In general, the charge can be distributed over the differently wound branes in an arbitrary manner, as long as the total number of windings is n_1, which gives the constraint

$$\sum_{k=1}^{n_1} m_k\, k = n_1\,, \tag{4.3.2}$$

where m_k denotes the number of D1-branes with winding k. A similar analysis can be done for the D5-branes.

It follows that each open string has two additional labels, which we denote as $\psi(d_1, d_5)$, which indicate the position (or more precisely, the loop) in the winding of the branes on which it ends. For example, $\psi(2,3)$ denotes that the open string currently connects the second loop of the D1-brane with the third loop of the D5 brane.

The winding of the branes on which the open string ends determines the periodicity of the wavefunction (4.3.1), and one can show that if the string ends on a D1-brane with winding m_1 and a D5-brane with winding m_5, the total period of the wavefunction becomes $L_T = 2\pi m_1 m_5 R_y$.[42] Thus one can think of the open strings as living in a box with effective length L_T, where the momentum excitations are quantised in units of $1/L_T$ rather than $1/L$, which is called *momentum fractionalisation* [22].

Physically different configurations correspond to the different ways in which we can distribute the total momentum charge $P = n_p/L$ to the open strings. We are interested only in the leading contribution so we focus on the extremal case where all branes are maximally winded, i.e. $m_1 = n_1$ and $m_5 = n_5$. In this case the momentum excitations have the lowest possible value, thus we can distribute the momentum in the most number of ways, meaning that such configurations have the highest entropy [119].

Finally, we need to consider that the string carries 4 bosonic and 4 fermionic degrees of freedom, totalling to 6 bosonic degrees of freedom ($n_B + 1/2 n_F = 4 + 2$).[43] As each of these contributes to the momentum, we have to find the number of configurations

[42] Strictly speaking this is the period if m_1 and m_5 are coprime numbers. If this is not the case, we can always find a pair of numbers that are coprime and to leading order in large $m_{1,5}$ limit reproduce the same period.

[43] The bosonic degrees of freedom can be viewed as the 4 directions in T^4 along which the D5-branes are extended and the open strings can fluctuate into. This picture becomes much clearer in another duality frame [115] in which the same system is described by F1-NS5-P, where NS5 is a 5-dimensional solitonic object of string theory. In this system the momentum is carried by transverse waves of the fundamental string, which have to be contained within the 4 dimensions of the NS5-brane. The 4 fermionic degrees of freedom are the supersymmetric partners of these bosonic degrees of freedom. A much more thorough analysis of the degrees of freedom from the point of view of D1-D5-P system is carried out in [118].

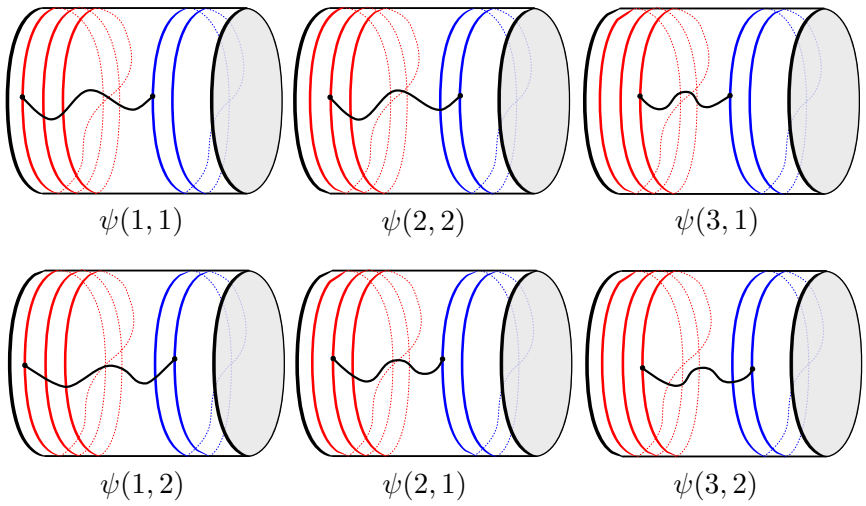

Figure 10: Massless open strings that have one end on a D1-brane (red) and the other end on a D5-brane (blue) can be effectively described by a dilute ideal gas in a one-dimensional box of length $L_T = 2\pi R_y m_1 m_5$, where m_1 and m_5 are the windings of the D1 and D5-branes respectively. In the figure, this is shown for the canonical example $m_1 = 3$ and $m_5 = 2$ [102]. The sequence starts on the top left and finishes at the bottom right, and each step shows a full rotation around S^1. Rotating starting from $\psi(3,2)$ returns $\psi(1,1)$, which shows that one has to rotate around the circle $m_1 m_5 = 6$ times in order to return to the original configuration.

satisfying the constraint (assuming equal distribution of momentum)

$$P = \frac{n_p}{L} = 6\sum_{k=1}^{\infty}\frac{k m_k}{L_T} = 6\sum_{k=1}^{\infty}\frac{k m_k}{n_1 n_5 L}\,, \tag{4.3.3}$$

which can be rearranged to

$$\frac{n_1 n_5 n_p}{6} = \sum_{k=1}^{\infty} m_k k\,, \tag{4.3.4}$$

which is the problem of partitioning the number $\frac{n_1 n_5 n_p}{6}$, which we assume to be an integer. In the limit $n_1 n_5 n_p \gg 1$ the result is given by [120]

$$\Omega \sim \left[e^{2\pi\sqrt{\frac{n_1 n_5 n_p}{36}}}\right]^6 = e^{2\pi\sqrt{n_1 n_5 n_p}}\,, \tag{4.3.5}$$

where we have used the fact that to leading order there is a six-fold degeneracy in which we can find the states. Using the Boltzmann formula (1.14), we find that the entropy associated to such a system is given by

$$S_{micro} = 2\pi\sqrt{n_1 n_5 n_p}\,, \tag{4.3.6}$$

which precisely matches the result (4.2.37) obtained using the Bekenstein-Hawking formula.[44]

4.4 AdS/CFT Duality in the D1-D5 system

Another way of analysing the microscopic behaviour of the D1-D5-P system is by using the AdS/CFT duality, which states that type IIB string theory on $\text{AdS}_3 \times S^3 \times \mathcal{M}$ (where $\mathcal{M}$ can be either T^4 or $K3$, although we take it to be the former) is equivalent to a 2D CFT with $\mathcal{N} = (4,4)$ supersymmetry, called the D1-D5 CFT [41].[45]

We are interested in the classical supergravity limit of the correspondence where the string coupling is small, and the ratio between the radius of AdS and the string length is large, with the dual theory being a strongly coupled CFT with a large central charge[46]

$$c = \bar{c} = 6N\,, \qquad \text{where} \qquad N \equiv n_1\, n_5\,. \tag{4.4.1}$$

Let us review the symmetries of the two sides of the duality. The isometry group of AdS_3 is $SO(2,2) \simeq SL(2,\mathbb{R})_L \times SL(2,\mathbb{R})_R$ which gets mapped to the global conformal symmetry group of the CFT. The two-dimensional conformal group is infinte dimensional [124], however only the finite, anomaly-free part of the Virasoro algebra is important for the duality. The isometry group of the sphere $SO(4)_E \simeq SU(2)_L \times SU(2)_R$, which from a three-dimensional gravity perspective can be seen as the gauge symmetry, is dual to the $\mathcal{R}$-symmetry of the boundary theory. Furthermore, the isometry group of the torus $SO(4)_I \simeq SU(2)_C \times SU(2)_B$ translates into an outer automorphism symmetry of the boundary superalgebra ($SU(2)_B$), and an additional custodial group ($SU(2)_C$) which is not part of the symmetry of the dual theory.

The D1-D5 two-charge black hole preserves 8 of the 32 supercharges of type IIB supergravity, but in the decoupling limit this number gets enhanced to 16. This matches the number of supersymmetry generators of the CFT [26], where we find two sets of eight Majorana-Weyl spinors, one set for the holomorphic and one for the anti-holomorphic sector. In two dimensions, each such spinor has one real degree of freedom which gives a total of 16 supercharges. In summary, combining the fermionic and bosonic symmetries, one finds that the symmetry group is given by the supergroup $SU(1,1|2)_L \times SU(1,1|2)_R$.

This holographic SCFT has a free locus in its moduli space where it can be described

[44] This matching was done only to leading order. Other methods, especially those involving the supersymmetric index have found matching at the subleading order as well. See for example [121] for a review.

[45] See *e.g.* [122, 123] for reviews of the D1-D5 CFT.

[46] The central charge effectively measures the number of degrees of freedom in a CFT. The large central charge regime is thus equivalent to taking the large N limit of $\mathcal{N} = 4$ SYM theory.

by a collection of free fields. This theory is called the *free orbifold CFT* and is described in terms of a two dimensional sigma model with a target space $(T^4)^N/S_N$, which is N copies of T^4 identified under the permutation group S_N.[47] The field theory at this point does not have a good dual supergravity description and thus there exists no generic dictionary between the gravity excitations and the fields in the free theory.[48]

Some connections can be made due to non-renormalization theorems, for example it can be shown that three-point functions of BPS operators do not change as we vary the moduli [129]. On the other hand, four-point functions are not protected by supersymmetry as seen for example in [130]. In what follows we briefly review the main contents of the free orbifold CFT that are used in the next chapter.

4.5 D1-D5 CFT at the Orbifold Point

4.5.1 Field Content

We follow the conventions of [123]. At the free orbifold point the CFT is described by a sigma model with central charge $c = \bar{c} = 6N$, whose fields map $\mathbb{R} \times S^1$ to $(T^4)^N/S_N$. One can think of the full theory as a collection of N copies of the same CFT which we label with an index $(r) = 1, 2, \dots N$. All physical states must be invariant under the action of the permutation group S_N which acts on the index (r), hence we can think of this symmetry as a discrete gauge symmetry of the theory. Each copy contains the following bosonic and fermionic fields

$$\left(X^{A\dot{A}}_{(r)}(t,y), \psi^{\alpha\dot{A}}_{(r)}(t+y), \widetilde{\psi}^{\dot{\alpha}\dot{A}}_{(r)}(t-y)\right), \tag{4.5.1}$$

where t and y are the coordinates of the boundary of AdS_3, with y being periodic with the identification $y \sim y + 2\pi R_y$. The Greek indices $\alpha, \dot{\alpha} = +, -$ are in the fundamental representation of $SU(2)_L$ and $SU(2)_R$ respectively, with $SU(2)_L \times SU(2)_R$ being the $\mathcal{R}$-symmetry of the theory. The index $A = 1, 2$ is in the fundamental representation of $SU(2)_B$, which acts as an outer automorphism on the superalgebra, while the index $\dot{A} = 1, 2$ belongs to the custodial $SU(2)_C$. Since the bosonic fields are in the $(\mathbf{2}, \mathbf{2})$ representation of $SU(2)_C \times SU(2)_B$, one can think of this group as acting on the tangent space of the target space T^4 of one boson, which is why this symmetry is related to the isometry group of the four-torus.

[47] See *e.g.* [125, 126] for a discussion on the moduli space and the position of the free orbifold point.

[48] Recently (see for example [127, 128]) it has been argued that in the large N limit the exact dual of the symmetric orbifold CFT is given by the superstring theory on $\text{AdS}_3 \times S^3 \times T^4$ with one unit of NS-NS flux ($k = 1$). This explicitly shows that the dual theory of the free orbifold point cannot be analysed by supergravity alone.

It is often more convenient to perform a Wick rotation to Euclidean time

$$t = -i\tau \,, \tag{4.5.2}$$

and transform the cylinder to a plane by

$$z \equiv e^{\frac{\tau}{R_y}+i\frac{y}{R_y}} \,, \qquad \bar{z} \equiv e^{\frac{\tau}{R_y}-i\frac{y}{R_y}} \,. \tag{4.5.3}$$

The fields then split into a holomorphic (left-moving) and an anti-holomorphic (right-moving) sector containing $(\partial X^{A\dot{A}}_{(r)}(z),\ \psi^{\alpha\dot{A}}_{(r)}(z))$ and $(\bar{\partial} X^{A\dot{A}}_{(r)}(\bar{z}),\ \tilde{\psi}^{\dot{\alpha}\dot{A}}_{(r)}(\bar{z}))$ respectively. The two sectors are completely analogous, hence we limit ourselves to the holomorphic part only, but it should be understood that equivalent statements can be made about the anti-holomorphic sector. From now on we also suppress the index labelling the copy.

CFTs are characterised by operator product expansions (OPE), and we use the conventions in which the OPEs between elementary fields are

$$\partial X_{A\dot{A}}(z_1)\partial X_{B\dot{B}}(z_2) \sim \frac{\epsilon_{AB}\epsilon_{\dot{A}\dot{B}}}{(z_1-z_2)^2} \,, \quad \psi^{\alpha\dot{A}}(z_1)\psi^{\beta\dot{B}}(z_2) \sim -\frac{\epsilon^{\alpha\beta}\epsilon^{\dot{A}\dot{B}}}{z_1-z_2}. \tag{4.5.4}$$

The periodicity of the boundary of AdS imposes the periodicity of the fields in the CFT, and while bosonic fields are always periodic, fermionic fields require a bit more care. Global AdS (5.3.13) naturally imposes anti-periodic boundary conditions on the fermions on the cylinder which are therefore in the NS sector. On the other hand, the near horizon limit of the D1-D5 system is the extremal BTZ black hole which imposes periodic boundary conditions on the fermions on the cylinder which are then in the R sector. These periodicities are exchanged when we go the complex plane as fermions pick up a non-trivial Jacobi factor. There, NS fermions are periodic with respect to a rotation around the origin, while fermions in the R sector are anti-periodic with respect to the same transformation [123].

We will mostly work in the NS sector of the theory, but there exists a transformation called the *spectral flow* [131] which allows us to map all problems in the R sector to (more tractable) problems in the NS sector. This is especially important because states representing the duals of microstate geometries are more naturally represented in the R sector.

4.5.2 Symmetry Currents and Current Algebra

The fundamental fields can be used to construct symmetry currents. In the holomorphic sector these are the stress-energy current $T(z)$ corresponding to the Virasoro symmetry, the $SU(2)_L$ current $J^i(z)$, where i is the triplet index of $SU(2)_L$, and the fermionic

Field	Conformal weight h
$\partial X^{\dot{A}A}(z)$	1
$\psi^{\alpha\dot{A}}(z)$	1/2
$T(z)$	2
$J^i(z)$	1
$G^{\alpha A}$	3/2

Table 7: Table of conformal weights for the fundamental fields and conserved currents. These values can be read off from the respective field's OPE with the stress-energy tensor (see for example Appendix A of [123]).

current $G^{\alpha A}(z)$. In a single copy of the CFT with the copy index supressed, they are given by [123]

$$T(z) = \frac{1}{2}\epsilon_{\dot{A}\dot{B}}\epsilon_{AB}\partial X^{\dot{A}A}\partial X^{\dot{B}B} + \frac{1}{2}\epsilon_{\alpha\beta}\epsilon_{\dot{A}\dot{B}}\psi^{\alpha\dot{A}}\partial\psi^{\beta\dot{B}}, \tag{4.5.5a}$$

$$J^i(z) = \frac{1}{4}\epsilon_{\dot{A}\dot{B}}\epsilon_{\alpha\beta}(\sigma^{*i})^{\beta}{}_{\gamma}\psi^{\gamma\dot{B}}, \tag{4.5.5b}$$

$$G^{\alpha A}(z) = \psi^{\alpha\dot{A}}\partial X^{\dot{B}A}\epsilon_{\dot{A}\dot{B}}, \tag{4.5.5c}$$

where $(\sigma^j)_{\beta}{}^{\alpha}$ are the Pauli matrices and all $SU(2)$ indices are lowered/raised with the ϵ satisfying[49] $\epsilon_{12} = \epsilon_{+-} = \epsilon^{21} = \epsilon^{-+} = 1$. These currents (and their anti-holomorphic counterparts) form a copy of the small $\mathcal{N} = 4$ superconformal algebra.

All fields can be expanded into modes by using

$$\mathcal{O}(z) = \sum_m \mathcal{O}_m z^{-m-h}, \qquad \mathcal{O}_m = \frac{1}{2\pi i}\oint dz\, \mathcal{O}(z) z^{h+m-1}, \tag{4.5.6}$$

where $\mathcal{O}(z)$ is a generic operator with conformal weight h. The conformal weights of the fundamental fields and the symmetry currents are listed in table 7. Note that the modes of all bosonic fields are integers. Fermion fields in the NS sector have half-integer modes, which also means that they do not have any zero modes. On the other hand R sector fermions have integer modes and thus contain zero modes which is important for the degeneracy of ground states in the R sector.

The current modes satisfy the algebra [123]

$$\left[J^i_m, J^j_n\right] = \frac{c}{12}m\delta^{ij}\delta_{m+n} + i\epsilon^{abc}J^c_{m+n}, \tag{4.5.7a}$$

$$\left[J^j_m, G^{\alpha A}_n\right] = \frac{1}{2}(\sigma^j)_{\beta}{}^{\alpha}G^{\beta A}_{m+n}, \tag{4.5.7b}$$

[49] We use $\alpha = +, -$ and $A = 1, 2$ to highlight the difference between the $\mathcal{R}$-symmetry and the outer automorphism indices.

$$\left[L_m, J_n^j\right] = -nJ_{m+n}^j, \tag{4.5.7c}$$

$$\left[L_m, G_n^{\alpha A}\right] = \left(\frac{m}{2} - n\right) G_{m+n}^{\alpha A}, \tag{4.5.7d}$$

$$[L_m, L_n] = (m-n)L_{m+n} + \frac{c}{12}m(m^2-1)\delta_{m+n}, \tag{4.5.7e}$$

$$\begin{aligned}\left\{G_m^{\alpha A}, G_n^{\beta B}\right\} = &-\frac{c}{6}\left(m^2 - \frac{1}{4}\right)\epsilon^{AB}\epsilon^{\alpha\beta}\delta_{m+n} - \epsilon^{AB}\epsilon^{\alpha\beta}L_{m+n} \\ &+ (m-n)\epsilon^{AB}(\sigma^{iT})^{\alpha}{}_{\gamma}\epsilon^{\gamma\beta}J_{m+n}^i,\end{aligned} \tag{4.5.7f}$$

which is infinite-dimensional as the mode numbers can take any of the allowed values. However, in this case the algebra is anomalous due to the appearance of central terms. For the AdS/CFT duality only the globally well defined anomaly-free part of the algebra is important. In the NS sector it is spanned by $\left(L_0, L_{\pm 1}, J_0^a, G_{\pm\frac{1}{2}}^{\alpha A}\right)$ with the explicit form of the (anti)-commutation relations being

$$\begin{aligned}&[L_m, L_n] = (m-n)L_{m+n}\,, \quad [J_0^j, J_0^k] = i\epsilon^{jkl}J_0^l\,, \quad [L_n, J_0^{\alpha\beta}] = 0\,, \\ &[J_0^j, G_m^{\alpha A}] = \frac{1}{2}G_m^{\beta A}(\sigma^j)_{\beta}{}^{\alpha}\,, \quad [L_m, G_n^{\alpha A}] = \left(\frac{m}{2} - n\right)G_{m+n}^{\alpha A}\,, \\ &\{G_m^{\alpha A}, G_n^{\beta B}\} = \epsilon^{\alpha\beta}\epsilon^{AB}L_{m+n} + (m-n)\epsilon^{AB}(\sigma^{iT})^{\alpha}{}_{\gamma}\epsilon^{\gamma\beta}J_{m+n}^i\,.\end{aligned} \tag{4.5.8}$$

4.5.3 Twist Fields

So far we have only considered operators within one copy of the CFT. However, a physical state in the D1-D5 CFT has to be invariant under the S_N group, which also means that every generator in (4.5.5) actually has to be considered in a permutation invariant sum over all indices (r).

In addition to the fields which act within one copy of the CFT, there exist *twist fields* which combine several single copies into a long component string that we call a *strand*. If no twist operators have been inserted, and all component strings have length one, we are in the *untwisted sector* of the theory. The alternative is the *twisted sector* where some of the copies are sewn together to form longer strands. These can have arbitrary length with the strings combined in various ways, subject to the condition that the overall length must be N

$$\sum_{k=1}^{\infty} kN_k = N\,, \tag{4.5.9}$$

where N_k denotes the number of strands of length k.

The action of a twist field changes the boundary conditions of other fields, as now a full rotation around S^1 lands us on a different string. After the transformation (4.5.3) this corresponds to glueing together multiple complex planes, so that after a full rotation around a point, one lands on a different sheet. For example, a bosonic

field in a strand of length k has the following identifications

$$\partial X^{A\dot{A}}_{(r)}(e^{2\pi i}z) = \partial X^{A\dot{A}}_{(r+1)}(z)\,, \qquad \text{and} \qquad \partial X^{A\dot{A}}_{(k)}(e^{2\pi i}z) = \partial X^{A\dot{A}}_{(1)}(z)\,. \tag{4.5.10}$$

It is possible to perform a change of basis in which the monodromy conditions become diagonal [132]. In this new basis, the independent fields are labelled by an index $\rho = 0, 1, \ldots k-1$, and the corresponding periodicity conditions are

$$\partial X^{1\dot{A}}_{\rho}(e^{2\pi i}z) = e^{-2\pi i\frac{\rho}{k}}\partial X^{1\dot{A}}_{\rho}(z)\,, \qquad \partial X^{2\dot{A}}_{\rho}(e^{2\pi i}z) = e^{2\pi i\frac{\rho}{k}}\partial X^{2\dot{A}}_{\rho}(z)\,. \tag{4.5.11}$$

As a consequence, the mode expansions of such fields contain fractional modes, for example [133]

$$\partial X^{1\dot{1}}_{\rho}(z) = \sum_{n\in\mathbb{Z}} \alpha^{1\dot{1}}_{\rho,n-\frac{\rho}{k}}\, z^{-n-1+\frac{\rho}{k}}\,. \tag{4.5.12}$$

4.5.4 Construction of Multiplets in the NS Sector

With these current modes, we are able to construct the multiplets in the NS sector. We closely follow [123]. The states can be labelled by the eigenvalues of the Cartan subalgebra of (4.5.8) which is spanned by L_0 and J^3_0, and whose eigenvalues we denote by h and m respectively. One can also use the eigenvalue of the Casimir operator $(J^i_0)^2$ of the $SU(2)_L$ group to give an additional index j, where

$$j \geq m \geq -j. \tag{4.5.13}$$

We define a (global-)*primary state* as a state $|\psi\rangle$ that is annihilated by all positive modes of the anomaly free algebra[50]

$$L_{+1}|\psi\rangle = G^{\alpha A}_{+\frac{1}{2}}|\psi\rangle = 0\,. \tag{4.5.14}$$

A *chiral state* $|\chi\rangle$ satisfies

$$G^{+A}_{-\frac{1}{2}}|\chi\rangle = 0\,, \tag{4.5.15}$$

which means that it is annihilated by two operators, as $A = 1, 2$. Furthermore, in a unitary theory any physical state has to obey [123]

$$h \geq j\,, \quad \rightarrow \quad h \geq |m|\,. \tag{4.5.16}$$

[50] One usually refers to a state as a *primary* if it is annihilated by all positive modes of the full algebra (4.5.7). However, as we are mainly interested in the anomaly free part (4.5.8), we wont make this distinction here. Hence, with an abuse of nomenclature, we refer to a primary as a state that satisfies (4.5.14).

A *chiral primary state* (or just chiral primary) saturates this bound by having

$$h = j = m\,, \tag{4.5.17}$$

while an *anti-chiral primary* also saturates the bound, but has

$$h = j = -m\,. \tag{4.5.18}$$

One can show that a state is a chiral primary if and only if it is both a chiral and a primary state. The conformal weights of chiral primaries are also constrained by [123]

$$\frac{k-1}{2} \leq h \leq \frac{k+1}{2}, \tag{4.5.19}$$

which can be derived by looking at fractional modes in a k-twisted sector. This bound gives the upper and lower limit on the values of the conformal weights of chiral primaries in each twisted sector.

In a generic k-twisted sector there are four chiral primaries, with the lowest conformal dimension being given by $h = m = (k-1)/2$. For the untwisted sector, where $k = 1$, this lowest state is the vacuum $|0,0\rangle$ of the NS sector, which is annihilated by all generators of the small $\mathcal{N} = 4$ algebra.[51] The vacuum state is the only state which is simultaneously a chiral primary and an anti-chrial primary.

Starting from the chiral primary with the lowest conformal dimension, in any k-twisted sector additional chiral primaries are obtained through the fermionic mode $\psi^{+\dot{A}}_{-1/2}$. Acting once gives a doublet of states, while the action with $\psi^{+\dot{1}}_{-1/2}\psi^{+\dot{2}}_{-1/2}$ gives a state with $h = m = (k+1)/2$. The four chiral primaries in the k-twisted sector are then given by

$$|c_0\rangle = \left|\frac{k-1}{2}, \frac{k-1}{2}\right\rangle, \quad \psi^{+\dot{A}}_{-\frac{1}{2}}|c_0\rangle \propto \left|\frac{k}{2}, \frac{k}{2}\right\rangle^{\dot{A}}, \quad \psi^{+\dot{1}}_{-\frac{1}{2}}\psi^{+\dot{2}}_{-\frac{1}{2}}|c_0\rangle \propto \left|\frac{k+1}{2}, \frac{k+1}{2}\right\rangle, \tag{4.5.20}$$

where we denoted a state with $|h,m\rangle$, and h and m represent the eigenvalues under the action of L_0 and J^3_0 respectively.

Chiral primaries are the highest weight states in their $SU(2)_L$ multiplet, as they saturate the bound (4.5.17). Their superdescendants are generated by the action of negative modes of the anomaly-free subalgebra. We define the usual raising and lowering operators of the $SU(2)_L$ algebra by

$$J^{\pm}_0 = J^1_0 \pm iJ^2_0, \tag{4.5.21}$$

[51] In fact, more generally the vacuum $|0,0\rangle$ satisfies $L_n|0,0\rangle = \tilde{L}_n|0,0\rangle = 0$ for any $n \geq -1$ and $G^{\alpha A}_r|0,0\rangle = \tilde{G}^{\dot{\alpha}A}_r|0,0\rangle = 0$ for $r \geq -1/2$ also $J^i_n|0,0\rangle = \tilde{J}^{\bar{i}}_n|0,0\rangle = 0$ for $n \geq -1$.

and a multiplet is generated by acting on a chiral primary repeatedly with J_0^- which decreases the J_0^3 eigenvalue by one until $m = -h$ and we reach the lowest weight state of the multiplet, the anti-chiral primary.

One can similarly act on a state with L_{-1} which increases the conformal dimension by one and leaves the $SU(2)_L$ charge unchanged. Since $[L_{-1}, J_0^+] = 0$, the action of L_{-1} maps a highest weight state of the $SU(2)_L$ into another highest weight state.

Finally, one can act on a chiral primary with $G^{-A}_{-\frac{1}{2}}$ which decreases the $SU(2)_L$ charge by one half while simultaneously increasing the conformal dimension by the same amount. Because these modes are anti-commuting, one can only obtain three new states by their repeated action. However, starting from a non-chiral primary state, which is not annihilated by $G^{+A}_{-\frac{1}{2}}$, we can actually obtain 15 new states by the repeated action of the supersymmetry current modes.

The state obtained by the action of $G^{-1}_{-\frac{1}{2}} G^{-2}_{-\frac{1}{2}}$ on a chiral primary is not completely independent of the state that is obtained by acting with $J_0^- L_{-1}$ on the same initial state. If the starting point is a chiral primary $|h, h\rangle$, one can use the algebra (4.5.8) to show that the linearly independent state is given by

$$|\psi\rangle \equiv \left(G^{-1}_{-\frac{1}{2}} G^{-2}_{-\frac{1}{2}} + \frac{1}{2h} J_0^- L_{-1} \right) |h, h\rangle, \tag{4.5.22}$$

whose eigenvalues under the action of L_0 and J_0^3 are

$$L_0|\psi\rangle = (h+1)|\psi\rangle\,, \qquad J_0^3|\psi\rangle = (h-1)|\psi\rangle\,. \tag{4.5.23}$$

This new state is the highest-weight member of its $SU(2)_L$ multiplet, despite not being a chiral primary. Thus we can again generate descendants by repeated action of J_0^- and L_{-1}, and in this way construct a new linearly independent family of states in the theory.

4.5.5 Spectral Flow

One can realise the superalgebra in equivalent ways by taking the spectral flow of the currents [123] whose modes transform as (we follow the conventions of [105])

$$L_m \mapsto L_m - 2\nu J_m^3 + \frac{c\nu^2}{6}\delta_{m,0}, \tag{4.5.24a}$$

$$J_m^3 \mapsto J_m^3 - \frac{c\nu}{2}\delta_{m,0}, \tag{4.5.24b}$$

$$J_m^\pm \mapsto J^\pm_{m\mp 2\nu}, \tag{4.5.24c}$$

$$G_m^{\pm A} \mapsto G^{\pm A}_{m\mp\nu}, \tag{4.5.24d}$$

where ν is the spectral flow parameter, and an equivalent transformation holds for the anti-holomorphic sector with an independent parameter $\bar{\nu}$. Under such a transformation, the eigenvalues change as well

$$h \mapsto h + 2\nu m + \frac{c\nu^2}{6}, \qquad m \mapsto m + \frac{c\nu}{6}. \tag{4.5.25}$$

By choosing appropriate values of ν, one can map the NS sector to the R sector and vice versa. Under a spectral flow not only do the operators change, but also the states as well. This allows us to have a one-to-one correspondence between states in the NS sector and states in the R sector.

In the next chapter we are particularly interested in anti-chiral primary states. By choosing $\nu = \bar{\nu} = -1/2$, such states flow to Ramond-Ramond ground states with charges

$$h_{\mathrm{R}} = \frac{c}{24}, \qquad j_{\mathrm{R}} = -h_{\mathrm{NS}} + \frac{c}{12}, \tag{4.5.26}$$

where we have used that for anti-chiral primary states $j_{\mathrm{NS}} = m_{\mathrm{NS}} = -h_{\mathrm{NS}}$.

4.5.6 AdS/CFT Dictionary

Let us introduce a notation that is useful when stating the correspondence between the CFT states and bulk fields [109, 126, 134]. In each k-twisted sector, there are 4 (anti-)chiral primaries in the holomorphic and 4 (anti-)chiral primaries in the anti-holomorphic sector. Since a general state is a product of the holomorphic and anti-holomorphic states, we have 16 possible (anti-)chiral primaries in each twisted sector. We denote the anti-chiral primary states as [134]

$$|\alpha\dot{\alpha}\rangle_k^{\mathrm{NS}}, \qquad h_{\mathrm{NS}} = -j_{\mathrm{NS}} = \frac{k+\alpha}{2}, \qquad \bar{h}_{\mathrm{NS}} = -\bar{j}_{\mathrm{NS}} = \frac{k+\dot{\alpha}}{2}, \tag{4.5.27a}$$

$$\left|\alpha\dot{A}\right\rangle_k^{\mathrm{NS}}, \qquad h_{\mathrm{NS}} = -j_{\mathrm{NS}} = \frac{k+\alpha}{2}, \qquad \bar{h}_{\mathrm{NS}} = -\bar{j}_{\mathrm{NS}} = \frac{k}{2}, \tag{4.5.27b}$$

$$\left|\dot{A}\dot{\alpha}\right\rangle_k^{\mathrm{NS}}, \qquad h_{\mathrm{NS}} = -j_{\mathrm{NS}} = \frac{k}{2}, \qquad \bar{h}_{\mathrm{NS}} = -\bar{j}_{\mathrm{NS}} = \frac{k+\dot{\alpha}}{2}, \tag{4.5.27c}$$

$$\left|\dot{A}\dot{B}\right\rangle_k^{\mathrm{NS}}, \qquad h_{\mathrm{NS}} = -j_{\mathrm{NS}} = \frac{k}{2}, \qquad \bar{h}_{\mathrm{NS}} = -\bar{j}_{\mathrm{NS}} = \frac{k}{2}, \tag{4.5.27d}$$

where the indices $\dot{A} = 1, 2$ come from the degeneracies of the middle states in (4.5.20), and $\alpha, \dot{\alpha} = \pm$ should be interpreted as ± 1 in the expressions for the eigenvalues. The spin of a state is given by $s = j - \bar{j}$, which means that the states (4.5.27a) and (4.5.27d) are bosonic while the remaining ones are fermionic.

We are interested in bosonic states that are invariant under the symmetry of the four-torus $SO(4)_I \simeq SU(2)_C \times SU(2)_B$, which are the states (4.5.27a) and an invariant

combination of (4.5.27d) given by

$$|00\rangle_k^{\rm NS} \equiv \frac{1}{2}\epsilon_{\dot{A}\dot{B}}\left|\dot{A}\dot{B}\right\rangle_k^{\rm NS}. \tag{4.5.28}$$

Among these states is the NS-NS vacuum, which in this notation is denoted by $|--\rangle_k^{\rm NS}$, as can be seen from its eigenvalues $h_{\rm NS} = j_{\rm NS} = \overline{h}_{\rm NS} = \overline{j}_{\rm NS} = 0$.

Under the spectral flow, all anti-chiral primaries map into ground states of the RR sector with charge $h_{\rm R} = \overline{h}_{\rm R} = k/4$, where we have used the value of the central charge of a k-twisted string $c_k = \bar{c}_k = 6k$. More specifically, the bosonic anti-chrial primaries get mapped into

$$|\alpha\dot{\alpha}\rangle_k^{\rm NS} \mapsto |-\alpha, -\dot{\alpha}\rangle_k^{\rm R}, \qquad j_{\rm R} = -\frac{\alpha}{2}, \quad \overline{j}_{\rm R} = -\frac{\dot{\alpha}}{2}, \tag{4.5.29a}$$

$$|00\rangle_k^{\rm NS} \mapsto |00\rangle_k^{\rm R}, \qquad j_{\rm R} = \overline{j}_{\rm R} = 0, \tag{4.5.29b}$$

where the indices $\alpha, \dot{\alpha} = \pm$ should be understood to mean ± 1 when appearing in $j_{\rm R}$ and $\overline{j}_{\rm R}$. For example, the NS-NS vacuum transforms as

$$|--\rangle_1^{\rm NS} \mapsto |++\rangle_1^{\rm R}, \qquad j_{\rm R} = \overline{j}_{\rm R} = \frac{1}{2}. \tag{4.5.30}$$

All in all, there are 5 distinct bosonic ground states in each twisted sector, denoted by $|\alpha\dot{\alpha}\rangle_k^{\rm R}$ and $|00\rangle_k^{\rm R}$.

According to the AdS/CFT duality, CFT states are dual to solutions in supergravity. The NS-NS vacuum state is dual to global $\mathrm{AdS}_3 \times S^3$ [26], while other (anti-)chiral primary states and their superdescendants correspond to excitations of linear supergravity around this geometry, often referred to as supergravitons [135], which were studied in [136–138]. Chiral primaries are 1/4-BPS states and thus dual to 1/4-BPS supergravitons in the bulk. By acting on such states with the symmetry generators in the holomorphic sector, while leaving the anti-holomorphic sector untouched, we create 1/8-BPS states. Such descendants of chiral primary states are dual to 1/8-BPS excitations of empty $\mathrm{AdS}_3 \times S^3$.

As we can see from (4.5.26), in the large c limit, the conformal dimension of the ground states of the RR sector, and thus also of all of their descendants, is very large. States in the RR sector are hence associated with non-trivial, asymptotically AdS geometries in the bulk with a large mass. In this case the distinction between 1/4 and 1/8-BPS states is even more profound. 1/4-BPS states, which are obtained by spectral flow from chrial primaries, are dual to smooth 1/4-BPS solutions in supergravity called Lunin-Mathur geometries [114, 139–143],[52] while the gravity duals of 1/8-BPS states

[52] To be more precise, the correct statement in the AdS/CFT dictionary is that the coherent superpositions of states (4.5.31) in the RR sector are dual to classical geometries on the bulk side. We explain how the coherent superposition is obtained in the next chapter.

are not fully known and we focus on these in the next chapter.

Finally, the complete CFT state is a permutation invariant tensor product of states in all different strands of the system and can be schematically written as [134]

$$\prod_{\psi}\prod_{k=1}^{N}(|\psi\rangle_k)^{N_k^{\psi}}\,, \tag{4.5.31}$$

where k is the strand length, the label ψ runs through all possible states in a single strand of length k, and N_k^{ψ} is the number of states ψ in a strand of length k. This form is the same in the NS-NS and the RR sector, only the states $|\psi\rangle$ that we include in the product differ. The above product must also satisfy the "strand budget" constraint

$$\sum_{\psi}\sum_{k} k\, N_k^{\psi} = N\,, \tag{4.5.32}$$

saying that the total length of all strands is equal to N.

4.6 Fuzzball Proposal

We saw that (4.2.37) and (4.3.6) agree (to leading order), despite being derived at different values of the couplings and with completely different methods. One is a result in gravity and accounts for the entropy of a region of spacetime, while the other is obtained from a pure counting argument and represents the entropy of a system with a high degeneracy and fixed macroscopic charges.

How do we interpret this equality? On one hand we have a black hole, a seemingly unique object in supergravity, while on the other hand the same system can be realised as many inequivalent physical configurations, all of which have the same charges as the black hole. Does this imply that a black hole admits a microscopical description? If so, what are the associated gravitational degrees of freedom? There are many proposals which answer these questions. For example *firewalls* [23, 144–146], where a highly energetic membrane is formed just outside the horizon. Another possible way to encode the microscopics is through *soft hair* [147, 148], where the degrees of freedom can be seen in the soft charges of a black hole. Here we focus on another resolution called the *fuzzball proposal* [114, 115, 149, 150].

To motivate this proposal, we can go back to the brane picture of the D1-D5-P system and ask what happens to individual string configurations as we increase the string coupling. One would think that as the string coupling and thus the gravitational backreaction increase, the branes shrink until they form a horizon and eventually become indistinguishable from the conventional black hole geometry. However, this is not the case, as some of the brane configurations actually expand and never form a horizon

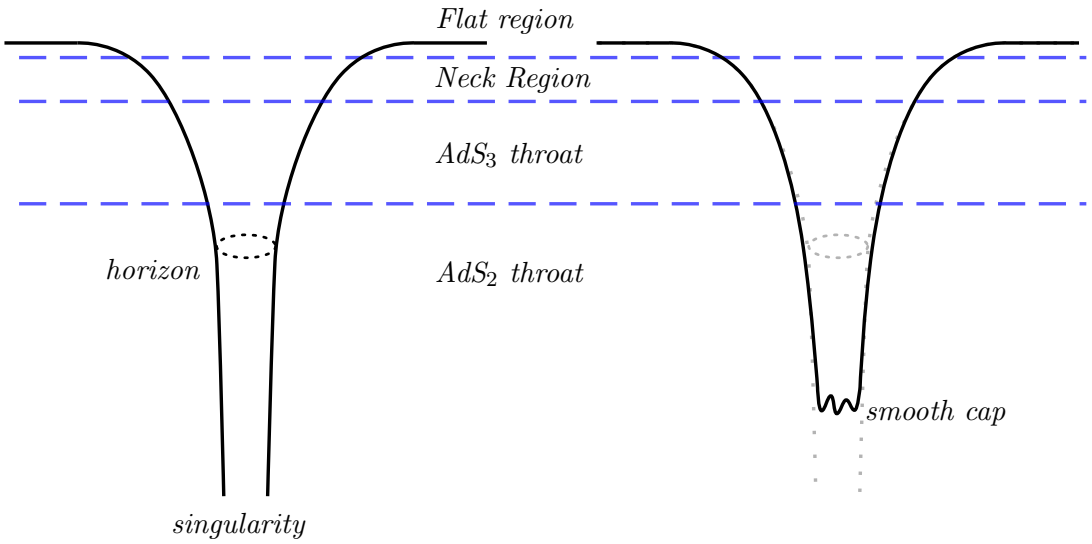

Figure 11: The difference between the classical description of an (extremal) black hole (left) and the fuzzball description if the solution can be described within supergravity (right). We start from an asymptotically flat region which is connected through the neck with the throat region. First we encounter an AdS_3 throat which can be, if $Q_p \neq 0$, further reduced to an AdS_2 throat [152] which is infinitely long and leads to a singularity. The fuzzball is undistinguishable from the classical picture up until the (would be) horizon which is now absent, but at this scale the microstates start to differ from each other and from the classical geometry. Furthermore, the throat regions may still appear, but now smoothly cap of at a finite distance without encountering a singularity.

while only being asymptotically indistinguishable from the usual black hole [151].

At its core, the fuzzball proposal says that this expanding of configurations happens generically and not just for specific examples. It claims that a black hole geometry, like the one we considered in (4.2.34), should be interpreted as an average description over many *horizonless* microstates whose total number should exactly reproduce the Bekenstein-Hawking entropy. It further asserts all microstates are indistinguishable from the usual black hole geometry far away from the centre, but at the scale of the horizon we find a new, *fuzzy* structure which is different for each microstate, but generically contains a long throat which eventually caps off without ever reaching a singularity. Thus both the horizon *and* the singularity of a black hole emerge due to the coarse graining over an ensemble of well behaved microstates.

Note that the condition that microstates have no horizons seems very natural. Consider a black hole in a particular microstate. Thus the system is in a pure state whose entropy should be 0. If a microstate were to have a horizon, then according to (1.12) it would have an entropy. This leads to a contradiction as a pure state would have a non-vanishing entropy. Thus if we want to have a consistent microscopical picture, the microstates need to be horizonless.

The appearance of new structure already at the horizon and not only around the singularity is one of the main points of the proposal as it also leads to a possible resolution of the information paradox. Namely the Hawking radiation is created in a region where the fuzzy nature of the geometry is already visible and hence could contain information about the degrees of freedom of the black hole. In this way the evaporation of a fuzzball does not differ significantly from the standard burning of coal,[53] and in principle all information could be recovered from the radiation thus making black hole evaporation a unitary process. Note that this is consistent with the arguments of [23] that we have considered in the introduction as fuzzballs do *not* satisfy all assumptions by virtue of encountering new physics at the horizon, and hence Hawking radiation can be in a pure state without any fiery ends for potential black hole explorers.

The argument for fuzzballs is further substantiated by Mathur's small correction theorem [158] which states that the information paradox cannot be resolved by summing up small corrections to Hawking's calculation. In short, something new may be needed at the horizon and we claim that this something is a fuzzball.

4.6.1 Microstate Geometries

String theory allows us to construct such fuzzy microstates which in general include arbitrary stringy modes and can be properly described only in full string theoretical framework. However, there exist some solutions with no stringy excitations that can be studied using supergravity alone and we call these *microstate geometries* [151]: They are smooth and horizonless solutions to the supergravity equations that have the same mass, angular momentum and charges as a given black hole.

Despite recent progress in the direction of generic fuzzballs [159–161], we focus mainly on microstates geometries of the D1-D5-P black hole. The microstate geometry programme has been particularly successful for supersymmetric black holes where a large number of microstate geometries have been explicitly constructed [162, 163].[54] It is still unclear how large a subset of all microstates is describable within supergravity, but even if not all microstates allow a supergravity description, explicit microstate geometries are important because they provide the only top-down, direct tool available for studying and understanding the microstate structure of black holes.

Superstrata [109, 110, 126, 177–182] represent the largest family of microstate geometries of the D1-D5-P black hole constructed thus far. As is detailed in the next chapter, superstrata are constructed based on a solution-generating technique whose holographic meaning is well-understood. Consequently, the CFT states dual to superstrata are explicitly known which makes them an ideal setup for studying precision

[53] For non-extremal black holes this was studied in [153–157].

[54] See [164–173] for explicit constructions of microstate geometries of the D1-D5-P system before the superstratum technology was developed. Recent developments include [174–176].

holography [142, 143, 183, 184].

Superstrata also give interesting clues for the physical nature of typical microstates. Although the superstrata written down thus far are not typical microstates of the black-hole ensemble, they are expected to evolve into more typical states when perturbed, and the endpoint of such a process is a subject of much physical interest [185–191].

Chapter 5

Supercharging Superstrata

In this chapter we present an explicit construction of a new class of superstrata which share the same features as the original ones constructed in [110, 126, 179], such as representing microstates of the D1-D5-P black hole and having known dual CFT states, however they are simpler in that they involve a smaller number of non-trivial fields.

The structure of the chapter is as follows. In section 5.2 we describe the family of 1/8-BPS states in the D1-D5 CFT whose dual gravitational geometries we want to construct. In section 5.3 we introduce the two-charge geometry which we use as a seed in our solution-generating technique and present the superstrata that were previously constructed in [110, 126, 179]. In section 5.4 we construct the Killing spinors of global $\mathrm{AdS}_3 \times S^3 \times T^4$ and use them to generate the fermionic variations of the supergravity fields. In section 5.5 we obtain new solutions to the BPS equations corresponding to infinitesimal deformations of $\mathrm{AdS}_3 \times S^3 \times T^4$. We derive the fully backreacted geometries in section 5.6, where we also discuss the asymptotically flat extension and calculate their conserved charges. In section 5.7 we collect our results and, in addition, present two families of solutions for which all the excited scalars and forms can be written down in an explicit way. We conclude with a brief outlook for future research directions in the final section.

There are two appendices that are relevant for this chapter. Appendix A summarises the conventions used for type IIB supergravity, while in Appendix D we discuss some technical aspects of the supersymmetry variations that are not fully covered in the main text.

The results of this chapter were published in [1].

5.1 Introduction

The original superstrata were constructed using the solution-generating technique as follows. First we take, as a seed, some 2-charge solution of linear supergravity around

$\text{AdS}_3 \times S^3$, for which the dual CFT state $|\psi\rangle$ is known and we always take it to be an anti-chiral primary. Next, we act on the seed with the generators of the $SU(1,1|2)_L \times SU(1,1|2)_R$ (super)isometry group of $\text{AdS}_3 \times S^3$ [164]. Specifically, we apply J_0^+ and L_{-1} of the bosonic subgroup[55] $SL(2,\mathbb{R})_L \times SU(2)_L \subset SU(1,1|2)_L$ m and n times respectively [110, 126, 179], which generates a new linear solution with non-vanishing momentum charge P that is dual to the CFT state $(J_0^+)^m (L_{-1})^n |\psi\rangle$. Finally, we use the structure of the BPS equations to complete the linear solution to a fully backreacted non-linear solution which in the CFT corresponds to having the same excitation many times, namely, $[(J_0^+)^m (L_{-1})^n |\psi\rangle]^{N_{mn}}$, with $N_{mn} \gg 1$.

However, the supergroup $SU(1,1|2)_L$ also includes fermionic generators $G^{+A}_{-1/2}$ and alternatively we can act with these on the seed twice to generate a completely new class of linear solutions. In addition to this, one can act on the newly obtained state with the bosonic symmetry generators to obtain $(J_0^+)^m (L_{-1})^n G^{+1}_{-1/2} G^{+2}_{-1/2} |\psi\rangle$. The non-linear completion goes much the same way as before, and produces a new set of superstrata.

The supersymmetric solutions in supergravity are parametrised by a number of scalars and forms [103, 106, 107, 110] as given in the general ansatz (4.2.7). In microstate geometries, these quantities get excited in non-trivial ways, representing the structure of the microstate. In the original superstrata, the scalar Z_4 and the 2-form Θ_4 get excited at linear order and, at quadratic order, more scalars and forms are turned on in a very specific way so that the combination that enters the metric is v-independent. This mechanism was crucial for the explicit construction of the geometry and was called "coiffuring" [192].

In contrast, in the new superstrata whose construction we present in this chapter, at linear order, only Θ_4 is excited and there is no scalar whose excitation must be cancelled by other scalars at higher order. Thus coiffuring is not necessary for the new superstrata and, consequently, they are simpler than the ones generated by using just bosonic generators. In hindsight, the existence of such a simple branch of superstrata could have been expected from the excitation spectrum of linear supergravity around $\text{AdS}_3 \times S^3$ [135–138]; However, we go beyond such linear analysis and construct fully non-linear solutions using the structure of the BPS equations.

5.2 CFT States

Let us analyse the states dual to the geometries that we are about to construct by first considering anti-chiral primary states in the NS-NS sector. A simple example of such a state in the free orbifold theory is, using the notation introduced in section 4.5.6,

[55] These are generators in the NS-NS sector.

$|00\rangle_1^{\rm NS} \equiv O^{--}|--\rangle_1^{\rm NS}$ where

$$O^{\alpha\dot\alpha} = -\frac{i}{\sqrt{2N}}\sum_{r=1}^{N}\psi_{(r)}^{\alpha\dot A}\,\tilde\psi_{(r)}^{\dot\alpha\dot B}\,\epsilon_{\dot A\dot B}\,, \tag{5.2.1}$$

which has $h=\bar h=1/2$ and we sum over all possible strands, all of which have length 1 in the above example. Recall that there is another family of anti-chiral primary operators which we denote[56] $\Sigma_{[k]}^{--}$ with $h=\bar h=\frac{k-1}{2}$ that, at the free locus, live in the twisted sectors of the orbifold. In the following, we use the anti-chiral primary $O_{[k]}^{--}$ with $h=\bar h=\frac{k}{2}$, where a strand of length k is further excited by a holomorphic and an anti-holomorphic elementary fermionic field and, for the corresponding states, we introduce the notation

$$|00\rangle_k^{\rm NS} = \lim_{z,\bar z\to 0} O_{[k]}^{--}|--\rangle_k^{\rm NS}\,. \tag{5.2.2}$$

Notice that for $k=1$ the above state reduces to (5.2.1). Acting with J_0^+, L_{-1} and $G^{+A}_{-\frac12}$ on $|00\rangle_k^{\rm NS}$ we can obtain new bosonic 1/8-BPS states in the same multiplet which we denote

$$|k,m,n,q\rangle^{\rm NS} = (J_0^+)^m (L_{-1})^n \left(G^{+1}_{-\frac12}G^{+2}_{-\frac12} + \frac{1}{k}J_0^+L_{-1}\right)^q |00\rangle_k^{\rm NS}\,, \tag{5.2.3}$$

where $m\le k-2q$, $q=0,1$, otherwise the state is trivially zero, while $n=0,1,2\ldots$ can be any non-negative integer. The eigenvalues (h,j) of L_0 and J_0^3 are $h=\frac{k}{2}+n+q$ and $j=-\frac{k}{2}+m+q$, while $(\bar h,\bar j)$ are unchanged. Notice that, due to the commutation relations (4.5.8), the order of the operators in (5.2.3) is immaterial. The combination in the parenthesis (weighted by q) is chosen so as to make the states $|k,m+1,n+1,0\rangle^{\rm NS}$ and $|k,m,n,1\rangle^{\rm NS}$ orthogonal, which means that, under the AdS/CFT dictionary, they correspond to two independent supergravity perturbations. It is straightforward to check this by using the commutation relations (4.5.8). It is easier to start with the $n=0$ case:

$$\begin{aligned}{}^{\rm NS}\langle k,m+1,1,0|k,m,0,1\rangle^{\rm NS} &= {}^{\rm NS}\langle k,m+1,0,0|\,L_1(G^{+1}_{-\frac12}G^{+2}_{-\frac12}+\frac{1}{k}J_0^+L_{-1})|k,m,0,0\rangle^{\rm NS}\\ &= {}^{\rm NS}\langle k,m+1,0,0|\left(-J_0^+ + \frac{2}{k}L_0J_0^+\right)|k,m,0,0\rangle^{\rm NS} = 0\,.\end{aligned} \tag{5.2.4}$$

This shows that $L_1|k,m,n,q\rangle^{\rm NS}\sim|k,m,n-1,q\rangle^{\rm NS}$, so we can recursively prove the orthogonality of $|k,m+1,n+1,0\rangle^{\rm NS}$ and $|k,m,n,1\rangle^{\rm NS}$ for general n. Finally notice that the state $|1,0,0,1\rangle^{\rm NS}$ is trivial[57] since it has zero norm and so all the states $|1,0,n,1\rangle^{\rm NS}$

[56] The subscript $[k]$ in the square parenthesis refers to the order of the twisted sector where the operator under discussion lives

[57] This follows form $G^{-A}_{-\frac12}|00\rangle_1^{\rm NS}=0$, while the same does not hold for states of winding $k>1$.

are zero since they are constructed from $|1,0,0,1\rangle^{\rm NS}$ by dressing it with powers of L_{-1}.

For the full "single particle" state in the NS-NS sector, assume that all strands are in the singly twisted sector on which the CFT is in the vaccum state $|--\rangle_1^{\rm NS}$, with the sole exception being a single strand of length k on which the CFT is in the state[58] $|k,m,n,q\rangle_k^{\rm NS}$ so that the full state is then given by

$$\left(|--\rangle_1^{\rm NS}\right)^{N-k}|k,m,n,q\rangle_k^{\rm NS}. \tag{5.2.5}$$

Through the spectral flow with $\nu=\bar\nu=-1/2$ these states get mapped to excited RR states that we denote as

$$\left(|++\rangle_1^{\rm R}\right)^{N-k}|k,m,n,q\rangle^{\rm R}\,,\quad\text{with}\quad h_{\rm R}=\frac{N}{4}+m+n+2q\,,\;\; j_{\rm R}=\frac{N-k}{2}+m+q\,, \tag{5.2.6}$$

where we used $c=6N$ and (4.5.30).

Here we focus on RR states that are dual to smooth supergravity solutions. A nice class of such states is obtained by starting from an NS-NS multi-particle state which is the product of N_b copies of (5.2.3), and then performing the spectral flow to the RR sector. In this chapter we consider states involving just one type of excitation which are dual to a single-mode superstrata solution and in the RR sector take the form:

$$\left(|++\rangle_1^{\rm R}\right)^{N_a}\left(|k,m,n,q\rangle^{\rm R}\right)^{N_b}\,,\quad\text{with}\quad N_a+kN_b=N\,. \tag{5.2.7}$$

To be precise, the CFT states that are dual to classical supergravity solutions are coherent sums of terms involving different numbers of elementary excitations, but in the large N_b limit the sums are sharply peaked around (5.2.7) which hence represent the dominant terms [193].[59] Here it is sufficient to say that such a coherent sum is defined in terms of two continuous parameters a^2 and b^2, related to N_a and N_b respectively, which also determine the dual gravity solution. Such a coherent sum of CFT states has charges equal to the those of the dominant term (5.2.7) which are given by the eigenvalues of the operators L_0, $\bar L_0$, J_0^3, and $\bar J_0^3$ and in the RR sector are equal to

$$h_{\rm R}=\frac{N}{4}+(m+n+2q)\,N_b\,,\quad \bar h_{\rm R}=\frac{N}{4}\,,\quad j_{\rm R}=\frac{N_a}{2}+(m+q)\,N_b\,,\quad \bar j_{\rm R}=\frac{N_a}{2}\,. \tag{5.2.8}$$

As we see in section 5.6.4, these results match precisely the momentum and the angular momenta of the dual supergravity solution.

We can give a heuristic picture of why taking $N_b\gg 1$ results in a non-trivial

[58] We can start with the 1/4-BPS state $\left(|--\rangle_1^{\rm NS}\right)^{N-k}|00\rangle_k^{\rm NS}$ and act on it with J_0^+, L_{-1} and $G^{+A}_{-\frac12}$ to obtain (5.2.3). In general the symmetry generators act on all strands equally, but because the vacuum state $|--\rangle_1^{\rm NS}$ is annihilated by all such generators, the only non-trivial state that survives is (5.2.5)

[59] For a discussion of this point in the context of three-charge states, see [126] and reference therein.

backreacted solution. Let us start in the NS sector. If $N_b = 1$, the NS state is given by (5.2.5) whose bulk dual is a linear excitation around $\mathrm{AdS}_3 \times S^3$ which one can think as a (supergraviton) particle propagating in that background. This should facilitate the interpretation that such states can be though of as single particle states of the CFT and by increasing N_b we are increasing the number of supergravitons. As long as $N_b \ll N$, these can be seen as a dilute gas in the curved background and the deformation of the AdS space is only infinitesimal [134]. As $N_b \approx N$, the number of particles becomes large enough to cause a finite backreaction, which, after spectral flowing to the RR sector, gives a geometry which differs from the usual black hole.

5.3 Supergravity Setup

Our goal is to find the supergravity solutions dual to the CFT states (5.2.7). As an illustration in this section we focus on the $q = 0$ case, *i.e.*, we review the original superstrata [110, 126, 179] which only involve bosonic generators. In later sections we generalise this approach to the $q = 1$ case, the new superstrata which involve fermionic generators.

5.3.1 Lunin-Mathur Geometries and the AdS/CFT Dictionary

The construction of three-charge black hole microstates via the superstratum technology begins with a two-charge seed solution. All two-charge solutions are known [139, 140, 143, 194] and can be obtained by a systematic procedure using an auxiliary curve in $\mathbb{R}^8$ (we are ignoring the compact nature of T^4 for now) which determines the values of the ansatz quantities in (4.2.7).

The origin of this curve can be seen by performing a series of S and T dualities, with which one can map the D1-D5 brane system into the F1-P system in which the configuration is described in terms of a multiply wound fundamental string on S^1 with P units of left-moving momentum charge [115]. This momentum is carried by transverse excitations of the string which causes it to expand in the remaining 8 directions and thus the profile of the F1 is given by a curve in $\mathbb{R}^8$.

As one increases the string coupling, the string causes the spacetime to bend and produces a metric which was derived in [195]. Using the S and T dualities one can then map the corresponding metric to the frame in which the system is described in terms of D1 and D5-branes where this auxiliary curve can be thought of as the smeared positions of the branes in the subspace $\mathbb{R}^4 \times T^4$.

We are only interested in configurations that are isotropic along T^4 and thus we restrict the 8-dimensional curve to only a 5-dimensional subspace. The profile of the curve is then given by a collection of "shape" functions $g_A(v')$, where four of the functions ($A = 1, 2, 3, 4$) correspond to the profile in the non-compact dimensions, while the

function with $A = 5$ denotes the isotropic mode along T^4. The parameter v' denotes the position along the string and has the range

$$0 \leq v' \leq L \equiv 2\pi \frac{Q_5}{R_y} \,. \tag{5.3.1}$$

The ansatz quantities of (4.2.7) that get excited by a curve with a profile $g_A(v')$ are given by [110]

$$Z_2 = 1 + \frac{Q_5}{L} \int_0^L \frac{1}{|x_\mu - g_\mu(v')|^2} dv', \qquad Z_4 = -\frac{Q_5}{L} \int_0^L \frac{\dot{g}_5(v')}{|x_\mu - g_\mu(v')|^2} dv' \tag{5.3.2a}$$

$$Z_1 = 1 + \frac{Q_5}{L} \int_0^L \frac{|\dot{g}_\mu(v')|^2 + |\dot{g}_5(v')|^2}{|x_\mu - g_\mu(v')|^2} dv', \qquad d\gamma_2 = *_4 dZ_2, \qquad d\delta_2 = *_4 dZ_4, \tag{5.3.2b}$$

$$A = -\frac{Q_5}{L} \int_0^L \frac{\dot{g}_\nu(v') dx^\nu}{|x_\mu - g_\mu(v')|^2} dv', \qquad dB = - *_4 \, dA, \qquad ds_4^2 = \delta_{\mu\nu} dx^\mu dx^\nu, \tag{5.3.2c}$$

$$\beta = \frac{-A + B}{\sqrt{2}}, \qquad \omega = \frac{-A - B}{\sqrt{2}}, \qquad \mathcal{F} = 0, \qquad a_1 = a_4 = x_3 = 0 \,, \tag{5.3.2d}$$

where the dot denotes the derivative with respect to the variable v'. The metric on $\mathbb{R}^4$ is the flat metric and the hodge dual is taken with respect to this four dimensional space. Furthermore, the D1 charge is obtained from the integral

$$Q_1 = \frac{Q_5}{L} \int_0^L \left(|\dot{g}_\mu(v')|^2 + |\dot{g}_5(v')|^2 \right) dv', \tag{5.3.3}$$

and both the D1 and the D5 charge are connected to the integer values through (4.2.28).

There is a well defined dictionary between the shape functions and the states in the RR sector of the dual CFT. We begin by expanding the profile functions into a Fourier series in each direction. Then we make the following complex linear combinations [126]

$$g_1 + i g_2 = \sum_{k=1}^{N} \left[\frac{a_k^{++}}{k} e^{\frac{2\pi i k}{L} v'} + \frac{a_k^{--}}{k} e^{-\frac{2\pi i k}{L} v'} \right] \tag{5.3.4a}$$

$$g_3 + i g_4 = \sum_{k=1}^{N} \left[\frac{a_k^{+-}}{k} e^{\frac{2\pi i k}{L} v'} + \frac{a_k^{-+}}{k} e^{-\frac{2\pi i k}{L} v'} \right] \tag{5.3.4b}$$

$$g_5 = -\mathrm{Im} \left[\sum_{k=1}^{N} \frac{a_k^{00}}{k} e^{\frac{2\pi i k}{L} v'} \right] , \tag{5.3.4c}$$

subject to the constraint

$$\sum_{k=1}^{N} \left[\left|a_k^{++}\right|^2 + \left|a_k^{--}\right|^2 + \left|a_k^{+-}\right|^2 + \left|a_k^{-+}\right|^2 + \left|a_k^{00}\right|^2 \right] = \frac{Q_1 Q_5}{R_y^2} \,. \tag{5.3.5}$$

The dictionary [110, 142, 143] then states that the mode numbers k correspond to the length of the strand on which a state is found, while the amplitudes $a_k^{\alpha\dot{\alpha}}$ and a_k^{00} are related to the number of times a particular state occurs in the full CFT state, with the relations

$$|{+}{+}\rangle_k^{\mathrm{R}} \Longleftrightarrow N_k^{++} \propto \left|a_k^{++}\right|^2, \tag{5.3.6a}$$
$$|{-}{-}\rangle_k^{\mathrm{R}} \Longleftrightarrow N_k^{--} \propto \left|a_k^{--}\right|^2, \tag{5.3.6b}$$
$$|{+}{-}\rangle_k^{\mathrm{R}} \Longleftrightarrow N_k^{+-} \propto \left|a_k^{+-}\right|^2, \tag{5.3.6c}$$
$$|{-}{+}\rangle_k^{\mathrm{R}} \Longleftrightarrow N_k^{-+} \propto \left|a_k^{-+}\right|^2, \tag{5.3.6d}$$
$$|00\rangle_k^{\mathrm{R}} \Longleftrightarrow N_k^{00} \propto \left|a_k^{00}\right|^2 . \tag{5.3.6e}$$

In that sense we see that the condition (5.3.5) gets translated into the constraint on the total number of windings (4.5.31).

5.3.2 Seed solution

The construction of the superstrata begins with a 1/4-BPS geometry we call the seed solution and is parametrised by the following shape functions

$$g_1 + ig_2 = ae^{\frac{2\pi i}{L}v'}, \qquad g_5 = -\frac{b}{k}\sin\left(\frac{2\pi k v'}{L}\right), \tag{5.3.7}$$

which means that we have taken $a_1^{++} = a$ and $a_k^{00} = b$, with all other coefficients vanishing. This corresponds to the state

$$|\psi\rangle = \left(|{+}{+}\rangle_1^{\mathrm{R}}\right)^{Na}\left(|00\rangle_k^{\mathrm{R}}\right)^{N_b}, \tag{5.3.8}$$

with $N_a \propto a^2$ and $N_b \propto b^2$, with the proportionality factors being the parameters of the theory.

We begin by considering the state with $N_b = 1$, as such a state gets mapped via spectral flow to an NS state whose dual interpretation is that of a single 1/4-BPS supergraviton propagating in $\mathrm{AdS}_3 \times S^3$. To realise this on the gravity side we take the limit $b \ll a$ and look at the geometry generated by the shape functions at linear order in b/a expansion. This geometry is sometimes called the perturbed round supertube solution [143].

We start off by parameterising the base space $\mathbb{R}^4$ with a new set of coordinates related to the Cartesian ones by

$$x_1 + ix_2 = \sqrt{r^2 + a^2}\sin\theta\, e^{i\phi}, \qquad x_3 + ix_4 = r\cos\theta\, e^{i\psi}, \tag{5.3.9}$$

where $\theta \in [0, \frac{\pi}{2}]$ and $\phi, \psi \in [0, 2\pi)$. The ansatz quantities in these coordinates are given

by[60]

$$ds_4^2 = (r^2 + a^2\cos^2\theta)\left(\frac{dr^2}{r^2+a^2} + d\theta^2\right) + (r^2+a^2)\sin^2\theta\, d\phi^2 + r^2\cos^2\theta\, d\psi^2\,, \tag{5.3.10a}$$

$$Z_1 = \frac{Q_1}{\Sigma}\,, \qquad Z_2 = \frac{Q_5}{\Sigma}\,, \tag{5.3.10b}$$

$$\beta = \frac{R\,a^2}{\sqrt{2}\,\Sigma}\,(\sin^2\theta\, d\phi - \cos^2\theta\, d\psi) \equiv \beta_0\,, \qquad \omega = \frac{R\,a^2}{\sqrt{2}\,\Sigma}\,(\sin^2\theta\, d\phi + \cos^2\theta\, d\psi) \equiv \omega_0\,, \tag{5.3.10c}$$

$$\gamma_2 = -Q_5\frac{(r^2+a^2)\cos^2\theta}{\Sigma} d\phi\wedge d\psi, \tag{5.3.10d}$$

$$Z_4 = R_y b a^k \frac{\sin^k\theta\, e^{-ik\phi}}{(r^2+a^2)^{k/2}\Sigma}\,, \tag{5.3.10e}$$

$$\delta_2 = -R_y a^k b \frac{\sin^k\theta}{(r^2+a^2)^{k/2}}\left[\frac{(r^2+a^2)\cos^2\theta\, e^{-ik\phi}}{\Sigma}\, d\phi\wedge d\psi + i\frac{\cos\theta}{\sin\theta}\, e^{-ik\phi}\, d\theta\wedge d\psi\right], \tag{5.3.10f}$$

$$\mathcal{F} = a_{1,4} = x_3 = \gamma_1 = \Theta_{1,2,4} = 0, \tag{5.3.10g}$$

where we have introduced

$$\Sigma \equiv r^2 + a^2\cos^2\theta\,,$$

and the parameter k is a positive integer. Since we have taken the parameter b to be small, we kept only the $\mathcal{O}(b)$ terms. We can think of the solution (5.3.10) as a combination of the background supertube ($b = 0$) [195–197] with an added perturbation ($b \neq 0$) which turns on the form fields B_2, C_0, and C_4. The perturbation does not change the metric at linear order in b, because Z_4 appears only quadratically in the metric (4.2.7a). In the same approximation the parameter a is related to the D-brane charges Q_1 and Q_5 via

$$a = \frac{\sqrt{Q_1 Q_5}}{R_y}. \tag{5.3.11}$$

One can check that the above ansatz satisfies the BPS equations (4.2.25) and (4.2.26) discussed in section 4.2.1 to linear order. One could also consider the finite b version of the above solution [110], but that is not necessary for our purposes.

Performing a coordinate transformation

$$\widetilde{\phi} = \phi - \frac{t}{R_y}, \qquad \widetilde{\psi} = \psi - \frac{y}{R_y}, \tag{5.3.12}$$

[60] Here we focus on the asymptotically AdS solutions, so we write Z_1 and Z_2 after taking the decoupling limit, where we drop the factors of "1".

one finds that the six-dimensional metric becomes

$$ds_6^2 = \sqrt{Q_1 Q_5}\left(-\frac{r^2+a^2}{a^2 R_y^2}dt^2 + \frac{r^2}{a^2 R_y^2}dy^2 + \frac{dr^2}{r^2+a^2} + d\theta^2 + \sin^2\theta\, d\widetilde{\phi}^2 + \cos^2\theta\, d\widetilde{\psi}^2\right), \tag{5.3.13}$$

which is that of global $\mathrm{AdS}_3 \times S^3$ with radius $R_{\mathrm{AdS}}^2 = \sqrt{Q_1 Q_5}$. Therefore, our seed solution represents $\mathrm{AdS}_3 \times S^3 \times T^4$ with a linear perturbation, which on the CFT side corresponds to the NS-NS vacuum with a small excitation.[61] Since the NS-NS vacuum is invariant under the action of $SL(2,\mathbb{C}) \cong SL(2,\mathbb{R})_L \times SL(2,\mathbb{R})_R$ and $SU(2)_L \times SU(2)_R$, acting on the excited state with the generators of these symmetries generates a new state, which is the NS-NS vacuum with a different excitation added to it. Performing the corresponding transformations on the gravity side similarly generates pure $\mathrm{AdS}_3 \times S^3 \times T^4$ with a different linear perturbation, which again satisfies the BPS equations and, in addition, we precisely know the CFT state dual to the new geometry.

The transformation (5.3.12) involves a change of the coordinates t and y, which parametrise the boundary region of AdS_3. This transformation therefore also affects the dual CFT theory and is in fact the dual of the spectral flow that changes the RR sector into the NS-NS sector on the CFT side (4.5.25). For that reason we refer to the coordinates $(r, t, y, \theta, \phi, \psi)$ as the RR coordinates and $(r, t, y, \theta, \widetilde{\phi}, \widetilde{\psi})$ as the NS-NS coordinates.

To summarize, we have generated a seed solution (5.3.10) expressed in the RR coordinates which, using the standard AdS/CFT dictionary, is dual to a RR ground state. After performing the spectral flow transformation (5.3.12) to the NS-NS coordinates, the geometry is dual to an anti-chiral primary with the conformal dimensions $h = \overline{h} = \frac{k}{2}$ and $j = \overline{j} = -\frac{k}{2}$. We thus identify the supertube ansatz expressed in the NS-NS coordinates as dual to the state (5.2.5) with $m = n = q = 0$. As usual, the gravity and the free CFT descriptions are valid in different points of the moduli space, so the dictionary mentioned above is meaningful when applied to protected quantities such as the 3-point correlators [129].

5.3.3 Original Superstrata

Our results follow up on the work of [105, 110, 126], where superstrata solutions were obtained by acting on the seed solution (5.3.10) with the gravity realisations of the bosonic symmetry generators J_0^+ and L_{-1}, thus generating the geometries dual to the CFT states (5.2.3) with $q = 0$. Below we review the construction of this class of superstrata.

[61] For this reason we refer to the case with $b = 0$ as the vacuum or the background geometry, while reserving the term seed solution for the perturbed vacuum with $b \neq 0$.

As mentioned above, the background geometry is invariant under the action of $SL(2,\mathbb{R})_L \times SL(2,\mathbb{R})_R$ and $SU(2)_L \times SU(2)_R$, while the perturbation is not. Acting on the perturbed geometry with the generators of these symmetries gives us a new, different perturbed geometry. Focusing on the left sector of the theory, one can show that the generators of the symmetry groups $SL(2,\mathbb{R})_L \times SU(2)_L$ can be explicitly realised in the in the NS-NS coordinates as [126, 135]

$$\begin{aligned} L_0 &= \frac{iR_y}{2}(\partial_t + \partial_y), \\ L_{\pm 1} &= ie^{\pm\frac{i}{R_y}(t+y)}\left[-\frac{R_y}{2}\left(\frac{r}{\sqrt{r^2+a^2}}\partial_t + \frac{\sqrt{r^2+a^2}}{r}\partial_y\right) \pm \frac{i}{2}\sqrt{r^2+a^2}\,\partial_r\right], \end{aligned} \tag{5.3.14}$$

$$J_0^3 = -\frac{i}{2}(\partial_{\tilde\phi} + \partial_{\tilde\psi}), \quad J_0^\pm = \frac{i}{2}e^{\pm i(\tilde\phi+\tilde\psi)}(\mp i\partial_\theta + \cot\theta\,\partial_{\tilde\phi} - \tan\theta\,\partial_{\tilde\psi}), \tag{5.3.15}$$

which can be shown to satisfy the algebra (4.5.8).

Acting on the seed solution (5.3.10) m times with J_0^+ and n times with L_{-1} leaves all ansatz quantities unchanged at linear order[62] in $b_4 \sim b$, except for the function Z_4 and the two-form Θ_4, which are now given by

$$Z_4 = b_4\, z_{k,m,n}\,, \qquad \Theta_4 = b_4\, \vartheta_{k,m,n}\,. \tag{5.3.16}$$

We have introduced the notation

$$z_{k,m,n} = R_y\,\frac{\Delta_{k,m,n}}{\Sigma}\,\cos\hat v_{k,m,n}, \tag{5.3.17a}$$

$$\begin{aligned} \vartheta_{k,m,n} = -\sqrt{2}\,\Delta_{k,m,n}\Bigg[&\left((m+n)\,r\sin\theta + n\left(\frac{m}{k}-1\right)\frac{\Sigma}{r\sin\theta}\right)\Omega^{(1)}\sin\hat v_{k,m,n} \\ &+\left(m\left(\frac{n}{k}+1\right)\Omega^{(2)} + \left(\frac{m}{k}-1\right)n\,\Omega^{(3)}\right)\cos\hat v_{k,m,n}\Bigg], \end{aligned} \tag{5.3.17b}$$

with

$$\begin{aligned} \Delta_{k,m,n} &\equiv \left(\frac{a}{\sqrt{r^2+a^2}}\right)^k\left(\frac{r}{\sqrt{r^2+a^2}}\right)^n\cos^m\theta\,\sin^{k-m}\theta\,, \\ \hat v_{k,m,n} &\equiv (m+n)\frac{\sqrt{2}\,v}{R_y} + (k-m)\phi - m\psi\,, \end{aligned} \tag{5.3.18}$$

and we have expanded $\vartheta_{k,m,n}$ on a basis of self-dual two-forms $\Omega^{(i)}$ $(i=1,2,3)$ on $\mathbb{R}^4$,

[62] See after (5.5.9) for a comment on the precise relation between b_4 and b.

given by:

$$\begin{aligned}\Omega^{(1)} &\equiv \frac{dr\wedge d\theta}{(r^2+a^2)\cos\theta}+\frac{r\sin\theta}{\Sigma}d\phi\wedge d\psi\,,\\ \Omega^{(2)} &\equiv \frac{r}{r^2+a^2}dr\wedge d\psi+\tan\theta\, d\theta\wedge d\phi\,,\\ \Omega^{(3)} &\equiv \frac{dr\wedge d\phi}{r}-\cot\theta\, d\theta\wedge d\psi\,.\end{aligned} \tag{5.3.19}$$

The above solution-generating technique allows us to generate a family of solutions, parametrised by the quantum numbers (k,m,n). One of the important aspects of such solutions is that they depend on the variable v, unlike the seed solution (5.3.10). Although (5.3.16) only involve one mode at a time, using the linearity of the first-layer BPS equations, we can write down the general solution given by an arbitrary superposition of modes with different quantum numbers. This superposition does not only solve the first-layer BPS equations for the Z_4 and Θ_4, but also for the other two pairs (Z_1,Θ_2) and (Z_2,Θ_1), because the structure of their equations is identical. Hence the general class of solutions with $q=0$ for the first-layer equations are given by

$$\begin{aligned} Z_1 &= \frac{Q_1}{\Sigma}+\sum_{k,m,n} b_1^{k,m,n}\, z_{k,m,n}\,, \quad \Theta_2 = \sum_{k,m,n} b_1^{k,m,n}\,\vartheta_{k,m,n}\,,\\ Z_2 &= \frac{Q_5}{\Sigma}+\sum_{k,m,n} b_2^{k,m,n}\, z_{k,m,n}\,, \quad \Theta_1 = \sum_{k,m,n} b_2^{k,m,n}\,\vartheta_{k,m,n}\,,\\ Z_4 &= \sum_{k,m,n} b_4^{k,m,n}\, z_{k,m,n}\,, \qquad\quad \Theta_4 = \sum_{k,m,n} b_4^{k,m,n}\,\vartheta_{k,m,n}\,, \end{aligned} \tag{5.3.20}$$

where Z_1 and Z_2 also include the zero modes, which appear in the seed solution. In these superpositions the coefficients $b_I^{k,m,n}$ are still taken to be infinitesimal. They therefore generate second-order source terms on the right-hand side of the second-layer BPS equations, which govern the change of $\mathcal{F}$ and ω. Thus to linear order in the perturbation parameter, these two ansatz quantities remain the same.

However, we can again use the linearity of the first-layer BPS equation to make all the coefficients $b_I^{k,m,n}$ finite, and (5.3.20) still remains a solution to the first-layer equations. With the coefficients being finite, we have non-vanishing source terms on the right-hand side of the second-layer BPS equations. Solving these represents a challenge and in [126], a general solution to the second-layer equations for single-mode superstrata was found. These solutions correspond to configurations with a single non-trivial coefficients $b_4^{k,m,n}$ in (5.3.20). The lesson from the non-linear solution-generating technique employed in [103, 105] is that the descendant states have $b_2^{k,m,n}=0$ for all values of k,m,n and this is also the case for the single-mode superstrata, where one can consistently set $b_2=0$ [126]. Furthermore, b_1 was determined by "coiffuring", which in the single-mode case requires that the v-dependent source terms on the right-hand side of second-layer equations vanish. In the case of $b_2=0$, this corresponds to setting

$b_1 = b_4^2$, thus having the solutions to the first layer given by

$$Z_1 = \frac{Q_1}{\Sigma} + \frac{b_4^2 R_y^2}{2Q_5}\frac{\Delta_{2k,2m,2n}}{\Sigma}\cos\hat{v}_{2k,2m,2n}\,, \qquad Z_2 = \frac{Q_5}{\Sigma}\,,$$
$$Z_4 = R_y\, b_4 \frac{\Delta_{k,m,n}}{\Sigma}\cos\hat{v}_{k,m,n}, \tag{5.3.21a}$$
$$\Theta_1 = 0\,, \qquad \Theta_2 = \frac{b_4^2 R_y}{2Q_5}\vartheta_{2k,2m,2n}\,, \qquad \Theta_4 = b_4\,\vartheta_{k,m,n}\,. \tag{5.3.21b}$$

By using these in the source terms of the second-layer equations, one finds that the second-layer quantities are given by

$$\omega^{\rm orig}_{k,m,n} = \omega_0 + \omega^{\rm orig,RMS}_{k,m,n}\,, \qquad \mathcal{F} = \mathcal{F}^{\rm orig}_{k,m,n}\,, \tag{5.3.22}$$

where we further decompose

$$\omega^{\rm orig,RMS}_{k,m,n} = \mu^{\rm orig}_{k,m,n}(d\widetilde{\psi} + d\widetilde{\phi}) + \nu^{\rm orig}_{k,m,n}(d\widetilde{\psi} - d\widetilde{\phi})\,. \tag{5.3.23}$$

One can show that the solutions for the second-layer equations are given by

$$\mathcal{F}^{\rm orig}_{k,m,n} = 4b_4^2\left[\frac{m^2(k+n)^2}{k^2}F_{2k,2m,2n} + \frac{n^2(k-m)^2}{k^2}F_{2k,2m+2,2n-2}\right], \tag{5.3.24}$$
$$\mu^{\rm orig}_{k,m,n} = \frac{R_y\, b_4^2}{\sqrt{2}}\left[\frac{(k-m)^2(k+n)^2}{k^2}F_{2k,2m+2,2n} + \frac{m^2n^2}{k^2}F_{2k,2m,2n-2}\right.$$
$$\left. - \frac{r^2 + a^2\,\sin^2\theta}{4\,\Sigma}\,b_4^{-2}\mathcal{F}_{k,m,n} - \frac{\Delta_{2k,2m,2n}}{4\,\Sigma} + \frac{x_{k,m,n}}{4\,\Sigma}\right], \tag{5.3.25}$$

where the function $F_{2k,2m,2n}$ is defined in (5.6.7), and the functions $\nu^{\rm orig}_{k,m,n}$ are given by differential equations [126, (4.13)], and can be solved for each case individually. We have put the superscript "orig" to distinguish these original superstrata solutions from the new superstrata we are presenting below. The solutions obtained this way are asymptotically $\mathrm{AdS}_3 \times S^3 \times T^4$. To obtain asymptotically flat solutions, one needs to add "1" to the warp factors Z_1 and Z_2. This alters the right-hand side of second-layer equations and induces new v-dependent terms into $\mathcal{F}$ and ω [126]. As it turns out, our new superstrata do not generate these additional v-dependent terms in the asymptotically flat case, hence the asymptotically flat extension of the new solutions is simpler than those of the original superstrata.

5.4 Killing Spinors of the $\mathbf{AdS_3 \times S^3}$ Background

We now proceed to the construction of new superstrata, which have $q = 1$ and involve the action of fermionic generators $G^{+A}_{-\frac{1}{2}}$. In supergravity, these fermionic generators

correspond to the Killing spinors of the $\mathrm{AdS}_3 \times S^3 \times T^4$ background. To begin with, in this section, we work out the explicit form of these Killing spinors, and give a precise map between their components and the fermionic generators $G^{\alpha A}_{\pm\frac{1}{2}}$ in the CFT.

5.4.1 Supersymmetry Variations

From [104, (2.17)], the supersymmetry transformations for bosonic fields in type IIB supergravity are given by[63]

$$\delta e^a_M = \bar{\epsilon}\,\Gamma^a\,\psi_M, \tag{5.4.1a}$$

$$\delta B_{MN} = 2\bar{\epsilon}\,\Gamma_{[M}\sigma_3\psi_{N]}, \tag{5.4.1b}$$

$$\delta\phi = \frac{1}{2}\bar{\epsilon}\,\lambda, \tag{5.4.1c}$$

$$\begin{aligned}\delta C^{(2n-1)}_{M_1\ldots M_{2n-1}} = &-e^{-\phi}\bar{\epsilon}\,\Gamma_{[M_1\ldots M_{2n-2}}\mathcal{P}_n\left((2n-1)\psi_{M_{2n-1}]} - \frac{1}{2}\Gamma_{M_{2n-1}]}\lambda\right)\\ &+ (n-1)(2n-1)C^{(2n-3)}_{[M_1\ldots M_{2n-3}}\delta B_{M_{2n-2}M_{2n-1}]}\,.\end{aligned} \tag{5.4.1d}$$

In type IIB supergravity, each fermionic field appears in two copies, which we combine into a doublet, for example $\epsilon \equiv (\epsilon^1, \epsilon^2)$. The Pauli matrices σ^i in the variations above act on the doublet indices which will be made explicit in the following calculations when relevant. With that in mind, the variations of the gravitino $\psi^{1,2}_M$ and dilatino fields $\lambda^{1,2}$ read

$$\delta\psi_M = \left(\partial_M + \frac{1}{4}\not{\omega}_M + \frac{1}{8}\mathcal{P}H_{MNR}\Gamma^{NR}\right)\epsilon + \frac{1}{16}e^{\phi}\sum_n \frac{1}{(2n)!}\not{F}_{2n}\Gamma_M\mathcal{P}_n\epsilon, \tag{5.4.2}$$

$$\delta\lambda = \left(\not{\partial}\phi + \frac{1}{12}\not{H}\mathcal{P}\right)\epsilon + \frac{1}{8}e^{\phi}\sum_n(-1)^{2n}\frac{5-2n}{(2n)!}\not{F}_{2n}\mathcal{P}_n\epsilon, \tag{5.4.3}$$

where $n = 1/2, \ldots, 9/2$,

$$\mathcal{P} = -\sigma^3, \qquad \mathcal{P}_n = \begin{cases}\sigma^1 & n+1/2\text{: even}\\ i\sigma^2 & n+1/2\text{: odd}\end{cases}, \tag{5.4.4}$$

and we have also introduced the slashed notation

$$\not{A}_p = \frac{1}{p!}A_{M_1\ldots M_p}\Gamma^{M_1\ldots M_p}\,, \tag{5.4.5}$$

where every form index is contracted with a gamma matrix. Using the Γ-matrix algebra and the self-duality relations of the RR field strengths, one can write the variations

[63] For spinor conventions used see Appendix A.

(5.4.2) explicitly as

$$\delta\psi^1_M = \left(\nabla_M - \frac{1}{8}H_{MNP}\Gamma^{NP}\right)\epsilon^1 + \frac{1}{8}e^{\phi}\left(+\not{F}_1 + \not{F}_3 + \frac{1}{2}\not{F}_5\right)\Gamma_M\epsilon^2\,, \tag{5.4.6a}$$

$$\delta\psi^2_M = \left(\nabla_M + \frac{1}{8}H_{MNP}\Gamma^{NP}\right)\epsilon^2 + \frac{1}{8}e^{\phi}\left(-\not{F}_1 + \not{F}_3 - \frac{1}{2}\not{F}_5\right)\Gamma_M\epsilon^1\,, \tag{5.4.6b}$$

$$\delta\lambda^1 = \left(d\phi - \frac{1}{2}H\right)\epsilon^1 + \frac{1}{4}e^{\phi}(-4\not{F}_1 - 2\not{F}_3)\epsilon^2\,, \tag{5.4.6c}$$

$$\delta\lambda^2 = \left(d\phi + \frac{1}{2}H\right)\epsilon^2 + \frac{1}{4}e^{\phi}(+4\not{F}_1 - 2\not{F}_3)\epsilon^1\,, \tag{5.4.6d}$$

where $\nabla_M = \partial_M + \frac{1}{4}\omega_{Mab}\Gamma^{ab}$ ith ω_M the spin connection 1-form. In deriving the above relations, we also used the fact that $\epsilon^{1,2}$ are Majorana-Weyl spinors with positive chirality. These variations can be written in a more compact way as

$$\delta\lambda = \left(\not{d}\phi - \frac{1}{2}\not{H}\,\sigma^3 - e^{\phi}\not{F}_1\,(i\sigma^2) - \frac{1}{2}e^{\phi}\not{F}_3\,\sigma^1\right)\epsilon\,, \tag{5.4.7a}$$

$$\delta\psi_M = \left[\nabla_M - \frac{1}{8}H_{MNP}\Gamma^{NP}\,\sigma^3 + \frac{1}{8}e^{\phi}\left(\not{F}_1\,(i\sigma^2) + \not{F}_3\,\sigma^1 + \frac{1}{2}\not{F}_5\,(i\sigma^2)\right)\Gamma_M\right]\epsilon\,. \tag{5.4.7b}$$

The variations (5.4.7) hold in a generic coordinate system in Type IIB supergravity. In our previous discussion, we have introduced two parametrisations of the unperturbed background: the NS-NS and the RR coordinates. In what follows we focus on the NS-NS description and derive an explicit expression for the Killing spinors (5.4.17).[64]

As mentioned before, in the seed (5.3.10), the metric, the dilaton, and C_2 do not change at $\mathcal{O}(b)$, while B_2, C_0, C_4 get excited at $\mathcal{O}(b)$. In the NS-NS coordinates, the $\mathcal{O}(b^0)$ fields are the metric and

$$e^{2\Phi} = \frac{Q_1}{Q_5}, \tag{5.4.8a}$$

$$C_2 = -\frac{r^2+a^2}{Q_1}du\wedge dv - Q_5\cos^2\theta\, d\widetilde{\phi}\wedge d\widetilde{\psi} - \frac{Q_5}{\sqrt{2}R_y}(du-dv)\wedge d\widetilde{\phi}, \tag{5.4.8b}$$

while the $\mathcal{O}(b)$ fields are

$$B_2 = -b\Delta_{k,0,0}\,e^{-i\hat{v}_{k,0,0}}\left[\frac{r^2+a^2}{R_y a^2}du\wedge dv + \frac{1}{\sqrt{2}}(du-dv)\wedge\left(\frac{i\cos\theta\, d\theta}{\sin\theta} + d\widetilde{\phi}\right)\right.$$
$$\left. + R_y\cos\theta\left(\frac{i\, d\theta}{\sin\theta} + \cos\theta d\widetilde{\phi}\right)\wedge d\widetilde{\psi}\right], \tag{5.4.8c}$$

[64] The Killing spinors in RR coordinates and the map between the two sets of solutions is presented in Appendix D of [1].

$$C_0 = \frac{bQ_5}{a^2 R_y}\Delta_{k,0,0}\, e^{-i\hat{v}_{k,0,0}}, \tag{5.4.8d}$$

$$C_4 = \frac{b}{a^2 R_y}\Delta_{k,0,0}\, e^{-i\hat{v}_{k,0,0}}\left[Q_1\widehat{\mathrm{vol}}_4 + Q_5(r^2+a^2)\cos^2\theta\, du\wedge dv\wedge d\widetilde{\phi}\wedge d\widetilde{\psi}\right] \tag{5.4.8e}$$

where

$$\hat{v}_{k,0,0} = k\left(\frac{u+v}{\sqrt{2}R_y} + \widetilde{\phi}\right). \tag{5.4.9}$$

On the other hand, the field strengths are $F_3 = \mathcal{O}(b^0)$; $H_3, F_1, F_5 = \mathcal{O}(b)$; and $d\phi = \mathcal{O}(b^2)$. Therefore, the supersymmetry variations (5.4.7) for the seed solution (5.3.10) split into the $\mathcal{O}(b^0)$ part

$$\delta\lambda_0 = -\frac{1}{2}e^{\phi}\not{F}_3\,\sigma^1\,\epsilon\,, \tag{5.4.10a}$$

$$\delta\psi_{M,0} = \nabla_M\epsilon + \frac{1}{8}e^{\phi}\not{F}_3\Gamma_M\sigma^1\epsilon\,, \tag{5.4.10b}$$

and the $\mathcal{O}(b)$ part

$$\delta\lambda_b = -\frac{1}{2}\not{H}\,\sigma^3\epsilon - e^{\phi}\not{F}_1\,(i\sigma^2)\epsilon\,, \tag{5.4.10c}$$

$$\delta\psi_{M,b} = -\frac{1}{8}H_{MNP}\Gamma^{NP}\,\sigma^3\epsilon + \frac{1}{8}e^{\phi}\left(\not{F}_1 + \frac{1}{2}\not{F}_5\right)\Gamma_M\,(i\sigma^2)\epsilon\,. \tag{5.4.10d}$$

In this section, we are interested in the Killing spinors in the unperturbed ($b = 0$) background, which in the NS-NS coordinates is given by the metric (5.3.13) and is nothing but $\mathrm{AdS}_3\times S^3\times T^4$. We work in the u, v coordinates (4.2.9) where

$$ds_6^2 = \sqrt{Q_1Q_5}\left[-\frac{a^2du^2 + 2(a^2+2r^2)du\,dv + a^2dv^2}{2a^2R_y^2} + \frac{dr^2}{r^2+a^2}\right.$$
$$\left. + d\theta^2 + \sin^2\theta d\widetilde{\phi}^2 + \cos^2\theta d\widetilde{\psi}^2\right], \tag{5.4.11}$$

which suggests the following choice of 10-dimensional vielbeine

$$E^{\underline{u}} = \frac{1}{2\sqrt{aR_y}}\left[\left(\sqrt{r^2+a^2}+r\right)du + \left(\sqrt{r^2+a^2}-r\right)dv\right], \tag{5.4.12a}$$

$$E^{\underline{v}} = \frac{1}{2\sqrt{aR_y}}\left[\left(\sqrt{r^2+a^2}-r\right)du + \left(\sqrt{r^2+a^2}+r\right)dv\right], \tag{5.4.12b}$$

$$E^{\underline{r}} = \sqrt{aR_y}\,\frac{dr}{\sqrt{r^2+a^2}}, \qquad E^{\underline{\theta}} = \sqrt{aR_y}\,d\theta, \tag{5.4.12c}$$

$$E^{\underline{\widetilde{\phi}}} = \sqrt{aR_y}\,\sin\theta\,d\widetilde{\phi}, \qquad E^{\underline{\widetilde{\psi}}} = \sqrt{aR_y}\,\cos\theta\,d\widetilde{\psi}, \tag{5.4.12d}$$

$$E^{\underline{k}} = \left(\frac{Q_1}{Q_5}\right)^{\frac{1}{4}}dx^k, \tag{5.4.12e}$$

where x^k, $k = 6, 7, 8, 9$ are the coordinates of the internal T^4. With this choice the metric can be written as

$$ds_{10}^2 = -2E^{\underline{u}}E^{\underline{v}} + \delta_{\underline{ab}}E^{\underline{a}}E^{\underline{b}}, \tag{5.4.13}$$

with $a = r, \theta, \widetilde{\phi}, \widetilde{\psi}, 6, 7, 8, 9$. The variations (5.4.10a) and (5.4.10b) can be written out explicitly as

$$\delta\lambda_0^1 = \frac{1}{\sqrt{aR_y}}\Gamma^{\underline{r}}\Gamma^{\underline{uv}}\left(1 - \Gamma^{\underline{6789}}\right)\epsilon^2, \tag{5.4.14a}$$

$$\begin{aligned}\delta\psi_{u,0}^1 = \partial_u\epsilon^1 &+ \frac{1}{8aR_y}\left(\sqrt{r^2+a^2} - r\right)\Gamma^{\underline{ur}}\left[2\epsilon^1 + \Gamma^{\underline{uv}}\left(1 + \Gamma^{\underline{6789}}\right)\epsilon^2\right] \\ &- \frac{1}{8aR_y}\left(\sqrt{r^2+a^2} + r\right)\Gamma^{\underline{vr}}\left[2\epsilon^1 - \Gamma^{\underline{uv}}\left(1 + \Gamma^{\underline{6789}}\right)\epsilon^2\right],\end{aligned} \tag{5.4.14b}$$

$$\begin{aligned}\delta\psi_{v,0}^1 = \partial_v\epsilon^1 &+ \frac{1}{8aR_y}\left(\sqrt{r^2+a^2} - r\right)\Gamma^{\underline{vr}}\left[2\epsilon^1 + \Gamma^{\underline{uv}}\left(1 + \Gamma^{\underline{6789}}\right)\epsilon^2\right] \\ &- \frac{1}{8aR_y}\left(\sqrt{r^2+a^2} + r\right)\Gamma^{\underline{ur}}\left[2\epsilon^1 - \Gamma^{\underline{uv}}\left(1 + \Gamma^{\underline{6789}}\right)\epsilon^2\right],\end{aligned} \tag{5.4.14c}$$

$$\delta\psi_{r,0}^1 = \partial_r\epsilon^1 - \frac{1}{4\sqrt{r^2+a^2}}\Gamma^{\underline{uv}}\left(1 + \Gamma^{\underline{6789}}\right)\epsilon^2, \tag{5.4.14d}$$

$$\delta\psi_{\theta,0}^1 = \partial_\theta\epsilon^1 - \frac{1}{4}\Gamma^{\underline{r\theta}}\Gamma^{\underline{uv}}\left(1 + \Gamma^{\underline{6789}}\right)\epsilon^2, \tag{5.4.14e}$$

$$\delta\psi_{\widetilde{\phi},0}^1 = \partial_{\widetilde{\phi}}\,\epsilon^1 + \frac{\cos\theta}{2}\Gamma^{\underline{\widetilde{\phi}\theta}}\,\epsilon^1 - \frac{\sin\theta}{4}\Gamma^{\underline{r\widetilde{\phi}}}\Gamma^{\underline{uv}}\left(1 + \Gamma^{\underline{6789}}\right)\epsilon^2, \tag{5.4.14f}$$

$$\delta\psi_{\widetilde{\psi},0}^1 = \partial_{\widetilde{\psi}}\,\epsilon^1 - \frac{\sin\theta}{2}\Gamma^{\underline{\widetilde{\psi}\theta}}\,\epsilon^1 - \frac{\cos\theta}{4}\Gamma^{\underline{r\widetilde{\psi}}}\Gamma^{\underline{uv}}\left(1 + \Gamma^{\underline{6789}}\right)\epsilon^2, \tag{5.4.14g}$$

$$\delta\psi_{k,0}^1 = \partial_k\epsilon^1 - \frac{Q_1^{\frac{1}{4}}Q_5^{-\frac{1}{4}}}{4\sqrt{aR_y}}\Gamma^{\underline{uvrk}}\left(1 - \Gamma^{\underline{6789}}\right)\epsilon^2. \tag{5.4.14h}$$

In these equations we have made the doublet index of the fermionic fields explicit. We have only given the variations for $\delta\lambda_0^1$ and $\delta\psi_{M,0}^1$, as the variations for $\delta\lambda_0^2$ and $\delta\psi_{M,0}^2$ can be obtained simply by interchanging the doublet indices $1 \leftrightarrow 2$ on all fermions in the above variations.

5.4.2 The Killing Spinors

Killing spinors of the $\mathrm{AdS}_3 \times S^3 \times T^4$ background are non-trivial spinors that satisfy the equations

$$\delta\lambda^{1,2} = \delta\psi_M^{1,2} = 0. \tag{5.4.15}$$

We find that the spinors that solve the equations (5.4.15) are given by

$$\epsilon^1 = \frac{1}{2} R_- \, Y_- \, (\widetilde{\eta} + \eta) + \frac{1}{2} R_+ \, Y_+ \, (\widetilde{\xi} + \xi) \,, \tag{5.4.16a}$$

$$\epsilon^2 = \frac{1}{2} R_- \, Y_- \, (\widetilde{\eta} - \eta) + \frac{1}{2} R_+ \, Y_+ \, (\widetilde{\xi} - \xi) \,, \tag{5.4.16b}$$

where in the above spinors, the following definitions are used[65]

$$Y_\pm(\theta, \widetilde{\phi}, \widetilde{\psi}) \equiv \exp\left(\pm\frac{1}{2}\theta\Gamma^{r\theta}\right) \exp\left(\frac{1}{2}\widetilde{\phi}\Gamma^{\theta\widetilde{\phi}}\right) \exp\left(\pm\frac{1}{2}\widetilde{\psi}\Gamma^{r\widetilde{\psi}}\right) , \tag{5.4.17a}$$

$$R_\pm(r) \equiv \left(\frac{\sqrt{r^2+a^2} \pm r}{a}\right)^{\frac{1}{2}} , \tag{5.4.17b}$$

$$\widetilde{\xi}(u) = \widetilde{\zeta}_+ e^{-\frac{iu}{\sqrt{2}R_y}} + \widetilde{\zeta}_- e^{\frac{iu}{\sqrt{2}R_y}} , \quad \widetilde{\eta}(u) = i\widehat{\Gamma}^{ru}\Big(\widetilde{\zeta}_- e^{-\frac{iu}{\sqrt{2}R_y}} - \widetilde{\zeta}_+ e^{\frac{iu}{\sqrt{2}R_y}}\Big), \tag{5.4.17c}$$

$$\xi(v) = \zeta_- e^{-\frac{iv}{\sqrt{2}R_y}} + \zeta_+ e^{\frac{iv}{\sqrt{2}R_y}} , \quad \eta(v) = i\widehat{\Gamma}^{rv}\Big(\zeta_- e^{-\frac{iv}{\sqrt{2}R_y}} - \zeta_+ e^{\frac{iv}{\sqrt{2}R_y}}\Big), \tag{5.4.17d}$$

and we have defined

$$\widehat{\Gamma}^{rv} \equiv \frac{1}{\sqrt{2}}\Gamma^{rv}, \qquad \widehat{\Gamma}^{ru} \equiv \frac{1}{\sqrt{2}}\Gamma^{ru} . \tag{5.4.18}$$

The spinors $\zeta_\pm, \widetilde{\zeta}_\pm$ are constant spinors that do not depend on any coordinates. As standard in type IIB supergravity, the $\epsilon^{1,2}$ in (5.4.16) are Majorana-Weyl spinors. The Weyl condition is

$$\Gamma_{(10)} \, \epsilon^{1,2} = \epsilon^{1,2} \,, \tag{5.4.19}$$

with $\Gamma_{(10)} \equiv \Gamma^{uvr\theta\widetilde{\phi}\widetilde{\psi}6789}$. In our convention in which the charge conjugation matrix is $\mathcal{C} = \Gamma^t$, the Majorana condition reads

$$\epsilon^* = \epsilon \,. \tag{5.4.20}$$

We can now spell out the constraints following from (5.4.20) on the spinors in (5.4.16) and (5.4.17). The factors $Y_\pm(\theta, \widetilde{\phi}, \widetilde{\psi})$ and $R_\pm(r)$ are real functions containing the explicit dependence of the spinors on the angular and radial parts respectively. Then in order for $\epsilon^{1,2}$ to be real, spinors $\zeta_\pm$, $\widetilde{\zeta}_\pm$ must satisfy

$$\zeta_\pm^* = \zeta_\mp \,, \qquad \widetilde{\zeta}_\pm^* = \widetilde{\zeta}_\mp \,. \tag{5.4.21}$$

[65] In (5.4.16) we suppress the functional dependencies to avoid cluttering. Note that the angular parts can be solved with the help techniques developed in [198,199], where similar differential equations have been considered, however in a different coordinate system.

This means that $\zeta_\pm$ and $\widetilde{\zeta}_\pm$ are complex. On the other hand, $\xi(v)$, $\eta(v)$, $\widetilde{\xi}(u)$ and $\widetilde{\eta}(u)$ are real spinors. Therefore, $\xi(0)$, $\eta(0)$, $\widetilde{\xi}(0)$ and $\widetilde{\eta}(0)$ are constant, real spinors, each containing 4 independent real degrees of freedom and can be used to parametrise the variations.

Furthermore the dilatino variation and the variation in the T^4 subspace impose

$$\Gamma^{\underline{6789}}\,\epsilon^{1,2} = \epsilon^{1,2}\,. \tag{5.4.22}$$

All spinors in (5.4.16) and (5.4.17), $\xi, \widetilde{\xi}, \eta, \widetilde{\eta}, \zeta_\pm, \widetilde{\zeta}_\pm$, must satisfy the conditions (5.4.19) and (5.4.22). In addition, they have the following chirality for the matrix $\Gamma^{\underline{uv}}$:

$$\begin{aligned} &\Gamma^{\underline{uv}}\,\xi(v) = -\xi(v)\,, \qquad \Gamma^{\underline{uv}}\,\eta(v) = +\eta(v)\,, \qquad \Gamma^{\underline{uv}}\,\zeta_\pm = -\zeta_\pm\,, \\ &\Gamma^{\underline{uv}}\,\widetilde{\xi}(u) = +\widetilde{\xi}(u)\,, \qquad \Gamma^{\underline{uv}}\,\widetilde{\eta}(u) = -\widetilde{\eta}(u)\,, \qquad \Gamma^{\underline{uv}}\,\widetilde{\zeta}_\pm = +\widetilde{\zeta}_\pm\,. \end{aligned} \tag{5.4.23}$$

As mentioned above each one of $\eta, \widetilde{\eta}, \xi, \widetilde{\xi}$ contains 4 real degrees of freedom. On the other hand, each one of $\zeta_\pm, \widetilde{\zeta}_\pm$ contains 4 complex degrees of freedom, but only half of them are independent. Therefore, either way, each spinor $\epsilon^{1,2}$ contains 8 real degrees of freedom, combining to 16 in total. This is what we expected, as global $\mathrm{AdS}_3 \times S^3$ should preserve half of the total 32 supercharges.

In order to generate new solutions, we need to identify the spinor components that correspond to different modes of the fermionic generators $G^{\alpha A}_{\pm\frac{1}{2}}$ and $\widetilde{G}^{\dot{\alpha} A}_{\pm\frac{1}{2}}$. We are only interested in generating left-moving excitations, which are generated by G and not $\widetilde{G}$, hence we limit ourselves only to the discussion around the left-moving sector. However, the discussion on the right-moving sector is completely analogous. The relation between the supergravity Killing spinors $\zeta^{\alpha A}_\pm$ and the CFT supercurrent $G^{\alpha A}_{\pm\frac{1}{2}}$ can be encoded in terms of the projectors

$$\mathcal{P}^\pm_S \equiv \frac{1}{2} \pm J_{\widetilde{\psi}}\,, \qquad \mathcal{P}^A_T \equiv \frac{1 + (-1)^A i\Gamma^{\underline{67}}}{2}, \quad A = 1, 2, \tag{5.4.24}$$

where $J_{\widetilde{\psi}}$ is defined in (D.1.3a). We leave the discussion of this point to Appendix D.1 and here quote just the final result

$$\zeta^{\alpha A}_\pm \equiv \mathcal{P}^A_T\,\mathcal{P}^\alpha_S\,\zeta_\pm \quad \longleftrightarrow \quad G^{\alpha A}_{\pm\frac{1}{2}}, \qquad \alpha = \pm, \quad A = 1, 2. \tag{5.4.25}$$

With this identification we can proceed to generate the supergravity solution corresponding to the state (5.2.3) in CFT.

5.5 Fermionically Generated Superstrata: Linear Analysis

In this section we derive a linearised classical solution to the supergravity equations using the Killing spinors for $\mathrm{AdS}_3 \times S^3 \times T^4$ obtained in the previous section. We do so by performing two supersymmetry variations, generated by the spinors corresponding to $G^{\alpha A}_{-\frac{1}{2}}$, on the $b \neq 0$ seed solution (5.3.10). Single variations of bosonic fields vanish, as these are proportional to the fermionic fields, which are set to zero for classical supergravity solutions. Double variations of the bosonic fields, however, are non-vanishing, as these include terms which are proportional to the variations of the fermionic fields. Note that, by definition, Killing spinors are non-trivial spinors for which the variations of fermionic fields vanish. However, here we use the Killing spinors for the unperturbed case ($b = 0$) on the perturbed background ($b \neq 0$), which generate fermionic variations that are non-vanishing. We limit ourselves to terms at linear order in parameter b. Using these non-vanishing fermionic variations we can generate new solutions at linear order in the parameter b.

This section gives a step-by-step procedure on how to obtain the new solutions. We begin by presenting the variations of the fermionic fields of the seed solution, generated by the Killing spinors (5.4.16). We then present the double variations of the bosonic fields generated, thus obtaining the solution dual to the state $G^{+1}_{-\frac{1}{2}} G^{+2}_{-\frac{1}{2}} |00\rangle^{\mathrm{NS}}_k$. In this derivation we treat the complex spinors $\zeta^{\alpha A}_+$ and $\zeta^{\alpha A}_-$ as independent, although they really are not, due to the relation (5.4.21). Because of this, the spinors $\epsilon^{1,2}$ become complex and we obtain a complex-valued perturbation: as usual, at the linear level, we can derive a standard supergravity solution by taking the real part of the final result. While this is indeed a new solution to the first-layer BPS equation it is not linearly independent from the ones already known, as discussed in section 5.2. We therefore present the new, linearly independent solution, dual to the state $\big(G^{+1}_{-\frac{1}{2}} G^{+2}_{-\frac{1}{2}} + \frac{1}{k} J^+_0 L_{-1}\big)|00\rangle^{\mathrm{NS}}_k$, and further give the solution dual to the state (5.2.3) with $q = 1$.

5.5.1 Variations of Fermionic Fields

As a preliminary step, we use the Killing spinors found in the previous section to calculate the supersymmetry variations of the fermionic fields. The result can be used later when we consider double variations of bosonic fields. Furthermore, it also serves as a consistency check of the identification (5.4.25) between the fermionic generators in supergravity and CFT.

As discussed in previous sections, the seed solution (5.3.10) expressed in the NS-NS coordinates is dual to an anti-chiral primary state, which should be annihilated by $G^{-A}_{-\frac{1}{2}}$ but not by $G^{+A}_{-\frac{1}{2}}$. According to the identification (5.4.25), this implies that

the supersymmetry variation of the seed by ζ_-^{-A} vanishes while the supersymmetry variation by ζ_-^{+A} does not. In performing this check, we set $\zeta_+^{\alpha A}=0$ and look at the variations of the fermionic fields generated by the components in the spinor $\zeta_-^{\alpha A}$. With this choice, the Killing spinor (5.4.16) simplifies to

$$\epsilon^1=-\epsilon^2=\frac{1}{2}\left(R_+-iR_-\widehat{\Gamma}^{\underline{vr}}\right)e^{-\frac{iv}{\sqrt{2}R_y}}\,Y_+\zeta_-^{\alpha A}\,. \tag{5.5.1}$$

The dilatino variation generated by this spinor is given by

$$\begin{aligned}\delta\lambda_b^1=\delta\lambda_b^2=&\frac{ba^k\,k\sin^{k-1}\theta}{\sqrt{aR_y}\,(a^2+r^2)^{\frac{k+1}{2}}}\\&\times\left(R_--iR_+\widehat{\Gamma}^{\underline{vr}}\right)e^{-ik\left(\frac{u+v}{\sqrt{2}R_y}+\widetilde{\phi}\right)-\frac{iv}{\sqrt{2}R_y}}\left(\cos\theta\,\Gamma^{\underline{\theta}}+\sin\theta\,\Gamma^{\underline{r}}-i\Gamma^{\underline{\widetilde{\phi}}}\right)Y_+\zeta_-^{\alpha A}\,.\end{aligned} \tag{5.5.2}$$

This expression is correct for a generic component $\zeta_-^{\alpha A}$. However, as discussed above, this variation should distinguish between the ζ_-^{+A} and the ζ_-^{-A} components of the spinor. Indeed, this is the case here, as one can see from the factors that contain the gamma matrices with components along S^3. Using the definition of Y_+ in (5.4.17) one can show that

$$\left(\cos\theta\,\Gamma^{\underline{\theta}}+\sin\theta\,\Gamma^{\underline{r}}-i\Gamma^{\underline{\widetilde{\phi}}}\right)Y_+\zeta_-^{\alpha A}=2\Gamma^{\underline{\theta}}\,e^{-\theta\Gamma^{\underline{r\theta}}}\,Y_+\zeta_-^{+A} \tag{5.5.3}$$

because, when we commute the factor in the brackets through Y_+, we generate a projector $\mathcal{P}_S^+$, which projects out the ζ_-^{-A} component. Therefore, as expected, the supersymmetry variation of the seed by ζ_-^{-A} vanishes, while the supersymmetry variation by ζ_-^{+A} does not. The variations of the gravitino components ψ_M are calculated in the same manner and discussed in Appendix D.

5.5.2 Solution-Generating Technique

The first step to finding the geometry dual to the state (5.2.3) with $q=1$ is to find the geometry dual to $G^{+1}_{-\frac{1}{2}}G^{+2}_{-\frac{1}{2}}|00\rangle^{\rm NS}_k$. In order to do so, we do a double variation of the bosonic fields. These variations generically have two kinds of terms: either they are proportional to fermionic fields or the variation of fermionic fields. In a classical solution, fermionic fields vanish and hence we are left only with the second type of terms. Using the variations summarised in Appendix A, we get that, for example, the variation of the axion field C_0 is given by

$$\delta'\delta C_0=\frac{1}{2}e^{-\phi}\,\epsilon^T\Gamma^{\underline{t}}(i\sigma^2)\delta'\lambda \tag{5.5.4}$$

where δ denotes the variation generated by spinors $\epsilon^{1,2}$ and δ' denotes the variation with different spinors $\epsilon'^{1,2}$. In our case the constant components of these spinors are ζ_-^{+1} for the variation δ and $\zeta_-'^{+2}$ for the variation δ'. Following the procedure of [110, 126] we are interested in calculating the infinitesimal deformation from the seed solution in the ansatz function Z_4 and the two-form Θ_4. The physical fields in which these two quantities are appearing are the axion C_0 and the NS-NS gauge B-field, so we are interested in their variations. Since these two calculations are analogous, we only present the detailed calculation for the axion field, while the results of the B-field can be found in Appendix D.

As mentioned at the beginning of this section, because we treat complex spinors $\zeta_+^{\alpha A}$ and $\zeta_-^{\alpha A}$ as independent, the spinor ϵ becomes complex. This is justified with the understanding that we take the real part in the final result. In the intermediate calculations, although $\epsilon^{1,2}$ are really complex, we still treat them as real spinors. In writing down (5.5.4), we used the relation (A.2.8), which is valid only for real (Majorana) spinors, in order to rewrite $\bar{\epsilon}$ appearing in the formula (5.4.1d) in terms of ϵ^T. Another way to justify this manipulation is that, because the first variation parameter ϵ and the second one ϵ' are on an equal footing, it is not possible for ϵ to enter in the variation $\delta'\delta C_0$ being complex conjugated and ϵ' without being complex conjugated. They must both enter without being complex conjugated, as in (5.5.4).

The variations we consider are generated by the Killing spinors (5.5.1). As mentioned above, the first variation is generated by the component ζ_-^{+1} and the second by $\zeta_-'^{+2}$. In this case, as we have seen in (5.5.1), we have $\epsilon^1 = -\epsilon^2$. Furthermore, the variations are such that $\delta\lambda_0 = 0$ and $\delta\lambda_b^1 = \delta\lambda_b^2$. With these, the axion variation (5.5.4) simplifies to

$$\delta'\delta C_0 = e^{-\phi}\,(\epsilon^1)^T\Gamma^{\underline{t}}\delta'\lambda_b^1\,. \tag{5.5.5}$$

We insert the spinor (5.5.1) and the variation (5.5.2) (since we use only ζ_-^{+A} we use the projection (5.5.3) in the variation) into this expression to obtain

$$\begin{aligned}\delta'\delta C_0 &= b\frac{\sqrt{aR_y}}{Q_1}\frac{ka^k\sin^{k-1}\theta}{(a^2+r^2)^{\frac{k+1}{2}}}e^{-i\left[k\left(\frac{u+v}{\sqrt{2}}+\widetilde{\phi}\right)+\sqrt{2}v-(\widetilde{\phi}+\widetilde{\psi})\right]}\\ &\quad\times\left(\zeta_-^{+1}\right)^T e^{-\frac{\theta}{2}\Gamma^{r\theta}}\left(R_+ + iR_-\widehat{\Gamma}^{\underline{vr}}\right)\left(\widehat{\Gamma}^{\underline{v}}+\widehat{\Gamma}^{\underline{u}}\right)\left(R_- - iR_+\widehat{\Gamma}^{\underline{vr}}\right)\Gamma^{\underline{\theta}}e^{-\frac{\theta}{2}\Gamma^{r\theta}}\zeta_-'^{+2}\\ &= 2kba^{k-1}\frac{\sqrt{aR_y}}{Q_1}\frac{r\sin^{k-1}\theta\,\cos\theta}{(a^2+r^2)^{\frac{k+1}{2}}}e^{-i\left[k\left(\frac{u+v}{\sqrt{2}R_y}+\widetilde{\phi}\right)+\sqrt{2}\frac{v}{R_y}-(\widetilde{\phi}+\widetilde{\psi})\right]}\left[\left(\zeta_-^{+1}\right)^T i\Gamma^{\underline{r\theta}}\zeta_-'^{+2}\right].\end{aligned} \tag{5.5.6}$$

In the second equality we have used the properties of the Clifford algebra and the $R_\pm$ functions together with the fact that $\Gamma^{\underline{uv}}\zeta_-^{\alpha A} = -\zeta_-^{\alpha A}$ and hence $\Gamma^{\underline{u}}\zeta_-^{\alpha A} = (\zeta_-^{\alpha A})^T\Gamma^{\underline{v}} =$

$-(\Gamma^{\underline{u}}\zeta_-)^T = 0$. Furthermore, one uses the fact that $(\Gamma^{\underline{r\theta}})^2 = -1$ to expand

$$\Gamma^{\underline{r\theta}} e^{-\theta\Gamma^{\underline{r\theta}}} = \cos\theta\,\Gamma^{\underline{r\theta}} + \sin\theta. \tag{5.5.7}$$

Finally noting that due to the projector property $(\mathcal{P}_S^+)^T = \mathcal{P}_S^-$, we have $(\zeta_-^{+1})^T\zeta_-'^{+2} = 0$, which leaves us with the result (5.5.6). The calculation for the B-field follows along the same lines; see (D.4.2) for the final result.

After the inverse spectral flow coordinate transformation (the inverse transformation of (5.3.12)), one finds that the double variation leaves all ansatz quantities unchanged at linear order in b, except for Z_4 and Θ_4, which are now given by[66]

$$Z_4^f = bkR_y\frac{\Delta_{k,1,1}}{\Sigma}\cos\hat{v}_{k,1,1}\,, \tag{5.5.8a}$$

$$\Theta_4^f = -\sqrt{2}bk\Delta_{k,1,1}\left[\left((k-1)\frac{\Sigma}{r\sin\theta} + 2r\sin\theta\right)\Omega^{(1)}\sin\hat{v}_{k,1,1} + \left((k+1)\Omega^{(2)} + (k-1)\Omega^{(3)}\right)\cos\hat{v}_{k,1,1}\right], \tag{5.5.8b}$$

where we have again expanded Θ_4 in the self-dual basis (5.3.19). As in mentioned above, in the final result, we selected the real part of the perturbation. We also normalised the spinors as follows: $[(\zeta_-^{+1})^T i\Gamma^{\underline{r\theta}}\zeta_-'^{+2}] \to \frac{1}{2}\sqrt{aR_y}$, which is natural since in our conventions, spinors have a mass dimension of $-1/2$ and so a spinor bilinear should have mass dimension -1 or should have units of length. One can check explicitly that the result (5.5.8a) satisfies the first-layer BPS equations (4.2.25).

To get a feeling for this solution we can compare it with the old superstrata solution (5.3.16), for $(k,m,n) = (k,1,1)$, which is obtained by using the bosonic symmetry generators (5.3.15) and (5.3.14) only. The solutions are similar and this may not be unexpected, as they both introduce the same amount of momentum and angular momentum into the geometry. We notice that the form of the function Z_4 is the same, while Θ_4 slightly differs in the relative factors multiplying the basis elements $\Omega^{(i)}$.

As shown on the CFT side, the state $G^{+1}_{-\frac{1}{2}}G^{+2}_{-\frac{1}{2}}|00\rangle^{\rm NS}_k$ is not linearly independent from the state $J_0^+L_{-1}|00\rangle^{\rm NS}_k$. The proper combination which contains the information about the new, linearly independent CFT state is given by the combination

$$\left(G^{+1}_{-\frac{1}{2}}G^{+2}_{-\frac{1}{2}} + \frac{1}{k}J_0^+L_{-1}\right)|00\rangle^{\rm NS}_k\,. \tag{5.5.9}$$

In order to write the supergravity solution dual to (5.5.9), let us briefly discuss the relation between the parameter b_4 in (5.3.16) and the original parameter b appearing in the seed solution. By keeping track of the overall normalisation when acting with

[66] The superscript f is to denote that these solutions are obtained by acting with fermionic generators only and hence the state that this solution is dual to is $G^{+1}_{-\frac{1}{2}}G^{+2}_{-\frac{1}{2}}|00\rangle^{\rm NS}_k$.

bosonic generators (5.3.15) and (5.3.14), we have $b_4 = (-1)^n k \frac{(k+(n-1))!}{(k-m)!} b$. Because for $m = n = 1$ this gives $b_4 = -k^2 b$, one finds that the solution dual to the state (5.5.9) is given by the following new linear perturbation

$$Z_4 = 0, \tag{5.5.10a}$$

$$\Theta_4 = -\sqrt{2}\,\widehat{b}\,\Delta_{k,1,1}\left[\frac{\Sigma}{r\sin\theta}\Omega^{(1)}\sin\hat{v}_{k,1,1} + \left(\Omega^{(2)} + \Omega^{(3)}\right)\cos\hat{v}_{k,1,1}\right], \tag{5.5.10b}$$

where we introduced $\widehat{b} = (k^2 - 1)b$. The new solution has a vanishing Z_4 function, which means that both the axion field C_0 and also the component B_{uv} of the B-field are vanishing. However, because Θ_4 is non-vanishing, the components of $B_{\mu\nu}$ with one leg in AdS_3 and one in S^3 are non-vanishing, which agrees with the spectrum calculated by [136]. One can show that Z_4 and Θ_4 given in (5.5.10) satisfy the first-layer of BPS equations (4.2.25). The solution is dual to the CFT state with quantum numbers $(k, m, n, q) = (k, 0, 0, 1)$. Notice that for $k = 1$ both the above supergravity perturbation and the corresponding CFT state are trivial, which provides a further check on the identification proposed.

We can generalise this approach and use the geometry (5.5.10) as a new seed solution and act on it with the bosonic symmetry generators (5.3.14) and (5.3.15) to obtain the geometry dual to the state $(k, m, n, q = 1)$. One finds that the geometry dual to the state (5.2.3) with $q = 1$ is again unchanged at linear order from the original seed solution (5.3.10) in all the ansatz quantities except for[67]

$$Z_4 = 0\,, \qquad \Theta_4 = \widehat{b}_4^{k,m,n}\,\widehat{\vartheta}_{k,m,n}\,, \tag{5.5.11}$$

with

$$\widehat{\vartheta}_{k,m,n} = \Delta_{k,1+m,1+n}\left[\frac{\Sigma}{r\sin\theta}\Omega^{(1)}\sin\hat{v}_{k,1+m,1+n} + \left(\Omega^{(2)} + \Omega^{(3)}\right)\cos\hat{v}_{k,1+m,1+n}\right]. \tag{5.5.12}$$

Again it is not difficult to show explicitly that these satisfy the first-layer BPS equations. Also in this more general case Z_4 remains trivial and the structure of Θ_4 is the same as in (5.5.10), apart from a change in the argument $\hat{v}_{k,1+m,1+n}$ of the trigonometric functions and in the quantum numbers in the $\Delta_{k,1+m,1+n}$ function.

5.6 Non-Linear Completion

In the previous sections we generated new solutions to the BPS equations at linear order in the perturbation parameter b. Since the first-layer BPS equations are linear, any linear combination of solutions (5.3.16) and (5.5.11), with an allowed combination

[67] We reabsorb all overall normalisations in the parameter $\widehat{b}_4^{k,m,n}$.

of the quantum numbers (k, m, n), is also a solution of these equations. This general bulk configuration correspond to a CFT state containing various excitations (5.2.3) with different values of (k, m, n, q). Up to this point we have taken the coefficients $b_I^{k,m,n}$ and $\widehat{b}_I^{k,m,n}$ to be infinitesimally small, making any solution only an infinitesimal deformation of the empty $\mathrm{AdS}_3 \times S^3 \times T^4$ space. In principle we could promote all these coefficients to be finite[68], which corresponds, on the CFT side, to taking many copies of the same excitation. With the parameters $\widehat{b}_I^{k,m,n}$ being finite, the scalars Z_I and the two-forms Θ_I become sources on the right-hand sides of the second-layer equations. Thus, once we have a finite solution to the first-layer equations, we can determine the deformation of $\mathcal{F}$ and ω from their seed values by solving the second-layer equations.

Here we do not tackle this general problem and focus on a single-mode superstratum, *i.e.*, we make a single, arbitrary mode coefficient to be finite and the solve the second-layer equations with the corresponding source terms. We find that a special feature of this new class of non-linear solutions is that their extension to asymptotically flat solutions is trivial. We close this section by calculating the conserved charges of the newly obtained solutions and comparing them to the CFT states (5.2.3) to find perfect agreement between the two results.

5.6.1 Solving the Second-Layer Equations

The second-layer equations (4.2.26) are in general coupled second-order partial differential equations for the components of the anti-self-dual one-form ω and the scalar $\mathcal{F}$. These quantities encode the information about the conserved charges of the geometry, *i.e.*, the momentum charge Q_p and the angular momenta J and $\widetilde{J}$. As mentioned above, our goal here is to calculate the backreaction on ω and $\mathcal{F}$ that the new finite deformations cause on the geometry. We limit ourselves to the case of single-mode superstrata involving the new $q = 1$ excitations, meaning that our initial ansatz for the finite first-layer solution is

$$\begin{aligned} Z_1 &= \frac{Q_1}{\Sigma}\,, & \Theta_1 &= \widehat{b}_2^{k,m,n}\,\widehat{\vartheta}_{k,m,n}\,, \\ Z_2 &= \frac{Q_5}{\Sigma}\,, & \Theta_2 &= \widehat{b}_1^{k,m,n}\,\widehat{\vartheta}_{k,m,n}\,, \\ Z_4 &= 0\,, & \Theta_4 &= \widehat{b}_4^{k,m,n}\,\widehat{\vartheta}_{k,m,n}\,, \end{aligned} \tag{5.6.1}$$

where $\widehat{b}_{1,2}^{k,m,n}$ should be determined as a function of $\widehat{b}_4^{k,m,n}$, which, in turn, is related to number of excitations (5.2.3) in the corresponding CFT state. We further simplify our ansatz by recalling that the bosonic descendants of an anti-chiral primary state have a trivial Θ_1 [105]. The same feature is shared by the bosonic superstrata obtained by using

[68] See [126] for discussion on the technical difficulty in superposing modes with completely general (k_1, m_1, n_1) and (k_2, m_2, n_2).

the excitations (5.2.3) with $q = 0$ [126]. We assume that a similar property holds also for $q = 1$ excitations and set to zero the coefficients $\widehat{b}_2^{k,m,n}$. Furthermore, in all previous work [110,126,200], the coefficients $\widehat{b}_1^{k,m,n}$ were tuned in such a way that the singularity-causing v-dependent terms vanished. This procedure was called "coiffuring". However, we find that, with the solutions generated with the new solution-generating technique, the right-hand sides of the second-layer equations are automatically v-independent. For this reason, we assume that all $\widehat{b}_1^{k,m,n}$ are also vanishing. In this case the only non-trivial source in the second-layer equations is $\Theta_4 \wedge \Theta_4$ which takes the simple form written on the right-hand side of (5.6.4). Since there are no potentially dangerous terms to be taken care of by coiffuring, the ansatz we use for the first-layer solution of a single-mode superstrata is simply

$$Z_1 = \frac{Q_1}{\Sigma}\,, \quad Z_2 = \frac{Q_5}{\Sigma}\,, \quad Z_4 = 0\,, \tag{5.6.2a}$$

$$\Theta_1 = \Theta_2 = 0\,, \qquad \Theta_4 = \widehat{b}\,\widehat{\vartheta}_{k,m,n}. \tag{5.6.2b}$$

We now want to solve the second-layer equations where the source on the right-hand side is determined by (5.6.2). By following [126] we take the following ansatz for $\mathcal{F}$ and ω

$$\mathcal{F} = \mathcal{F}^{\mathrm{RMS}}(r,\theta), \qquad \omega = \omega_0 + \omega^{\mathrm{RMS}}(r,\theta), \tag{5.6.3}$$

where ω_0 is given in (5.3.10), and the RMS superscript denotes that the ansatz functions are independent of the coordinate v and are thus non-oscillating. We assume that $\mathcal{F}^{\mathrm{RMS}}$ and the components of ω^{RMS} only depend on the coordinates r and θ and that $\omega_r^{\mathrm{RMS}} = \omega_\theta^{\mathrm{RMS}} = 0$. Using (5.6.2) on the right-hand side of the second-layer equations, we see that the RMS parts of (5.6.3) are governed by the differential equations

$$d_4\omega^{\mathrm{RMS}} + *_4 d_4\omega^{\mathrm{RMS}} + \mathcal{F}^{\mathrm{RMS}} d\beta = 0, \tag{5.6.4a}$$

$$\widehat{\mathcal{L}}\mathcal{F}^{\mathrm{RMS}} = 4\,\widehat{b}^2\,\frac{\Delta_{2k,2m+2,2n+2} + \Delta_{2k,2m+4,2n}}{(r^2+a^2)\cos^2\theta\;\Sigma}\,, \tag{5.6.4b}$$

where we have used the fact that $d_4\omega_0$ is anti-self-dual and have introduced $\widehat{\mathcal{L}} \equiv -\,*_4\, d_4\, *_4\, d_4$ as the Laplace operator in the four-dimensional Euclidean base space. Notice that the top differential equation has a vanishing right-hand side, which was not the case in previously known examples.

One can show that when acting on a scalar function that depends only on r and θ, the Laplace operator can be written as

$$\widehat{\mathcal{L}}F \equiv \frac{1}{r\Sigma}\,\partial_r\big(r(r^2+a^2)\,\partial_r F\big) + \frac{1}{\Sigma\sin\theta\cos\theta}\partial_\theta\big(\sin\theta\cos\theta\,\partial_\theta F\big)\,. \tag{5.6.5}$$

We then note that the differential equation of the form

$$\widehat{\mathcal{L}}F_{2k,2m,2n} = \frac{\Delta_{2k,2m,2n}}{(r^2+a^2)\cos^2\theta\ \Sigma} \tag{5.6.6}$$

is solved by the function[69]

$$F_{2k,2m,2n} = -\sum_{j_1,j_2,j_3=0}^{j_1+j_2+j_3\leq k+n-1} \binom{j_1+j_2+j_3}{j_1,j_2,j_3} \frac{\binom{k+n-j_1-j_2-j_3-1}{k-m-j_1,m-j_2-1,n-j_3}^2}{\binom{k+n-1}{k-m,m-1,n}^2} \times \frac{\Delta_{2(k-j_1-j_2-1),2(m-j_2-1),2(n-j_3)}}{4(k+n)^2(r^2+a^2)}\,, \tag{5.6.7}$$

with

$$\binom{j_1+j_2+j_3}{j_1,j_2,j_3} \equiv \frac{(j_1+j_2+j_3)!}{j_1!\,j_2!\,j_3!}\,. \tag{5.6.8}$$

Notice that (5.6.4b) is already in the form (5.6.6), and can be thus solved by a linear combination of the F functions.

To get the solution for ω, we introduce the ansatz[70] [126]

$$\omega^{\rm RMS} = \mu_{k,m,n}(d\psi + d\phi) + \nu_{k,m,n}(d\psi - d\phi)\,, \tag{5.6.9}$$

and define a new function

$$\widehat{\mu}_{k,m,n} \equiv \mu_{k,m,n} + \frac{R_y}{4\sqrt{2}}\frac{r^2+a^2\sin^2\theta}{\Sigma}\mathcal{F}_{k,m,n}, \tag{5.6.10}$$

where $\mathcal{F}_{k,m,n} \equiv \mathcal{F}$ is the solution of (5.6.4b). One can show that $\widehat{\mu}_{k,m,n}$ satisfies the differential equation

$$\widehat{\mathcal{L}}\widehat{\mu}_{k,m,n} = \frac{\widehat{b}^2 R_y}{\sqrt{2}}\frac{\Delta_{2k,2m+2,2n}+\Delta_{2k,2m+4,2n+2}}{(r^2+a^2)\cos^2\theta\ \Sigma}\,, \tag{5.6.11}$$

which can be again solved by a linear combination of the functions (5.6.7). One is thus able to determine $\mathcal{F}_{k,m,n}$ and $\widehat{\mu}_{k,m,n}$ as the solution of their respective second-order differential equations. By following the same approach of [126], one can show that the explicit forms of the ansatz quantities are given by

$$\mathcal{F}_{k,m,n} = 4\widehat{b}^2\,(F_{2k,2m+2,2n+2} + F_{2k,2m+4,2n})\,, \tag{5.6.12a}$$

[69] For the proof see Appendix A of [126].

[70] Notice that in previous work $\nu_{k,m,n}$ was named $\zeta_{k,m,n}$. Here we change the notation to avoid confusion with the complex spinor components $\zeta_{\pm}^{\alpha A}$.

$$\mu_{k,m,n} = \frac{\widehat{b}^2 R_y}{\sqrt{2}} \Bigg[F_{2k,2m+2,2n} + F_{2k,2m+4,2n+2} - \frac{r^2 + a^2 \sin^2\theta}{\Sigma} \left(F_{2k,2m+2,2n+2} + F_{2k,2m+4,2n} \right) + \frac{\widehat{x}_{k,m,n}}{4\Sigma} \Bigg], \quad (5.6.12b)$$

where in (5.6.12b) we have added an additional harmonic piece that is left undetermined by the differential equations. Its form is chosen so that the solution is regular at the centre of the coordinate system and is determined in the next subsection. The remaining $\nu_{k,m,n}$ functions are obtained by solving first-order differential equations, which contain $\mathcal{F}_{k,m,n}$ and $\mu_{k,m,n}$ as sources. These equations are

$$\partial_r \nu_{k,m,n} = -\frac{\left(a^2 + r^2\right) \sin^2\theta - r^2 \cos^2\theta}{r^2 + a^2 \sin^2\theta} \partial_r \mu_{k,m,n} - \frac{2r \sin\theta \cos\theta}{r^2 + a^2 \sin^2\theta} \partial_\theta \mu_{k,m,n} - \frac{\sqrt{2} a^2 R_y \left(a^2 + 2r^2\right) r \sin^2\theta \cos^2\theta}{\left(r^2 + a^2 \sin^2\theta\right) \Sigma^2} \mathcal{F}_{k,m,n}, \quad (5.6.13a)$$

$$\partial_\theta \nu_{k,m,n} = \frac{2\left(a^2 + r^2\right) r \sin\theta \cos\theta}{r^2 + a^2 \sin^2\theta} \partial_r \mu_{k,m,n} + \frac{r^2 \cos^2\theta - \left(a^2 + r^2\right) \sin^2\theta}{r^2 + a^2 \sin^2\theta} \partial_\theta \mu_{k,m,n} + \frac{\sqrt{2} a^2 R_y \left(a^2 + r^2\right) r^2 \sin\theta \cos\theta \cos 2\theta}{\left(r^2 + a^2 \sin^2\theta\right) \Sigma^2} \mathcal{F}_{k,m,n} \,. \quad (5.6.13b)$$

These equations can be solved by integration on a case-by-case basis for each set of quantum numbers.

5.6.2 Regularity

We want our solutions to be free of any singularities. However, the coordinates introduced in (5.3.9), which are used to describe the solutions, have points at which they degenerate. Hence using these coordinates we have to take special care of the functions and components of the forms in order for our solutions to be regular. There are regions of the base manifold at which the coordinates degenerate. The first one is at $\theta = 0$, where the ϕ circle degenerates. The second one is at $\theta = \frac{\pi}{2}$, where the ψ circle shrinks. Finally at the locus $(r = 0, \theta = 0)$ the entire sphere $S^3_{\theta\phi\psi}$ shrinks. Imposing regularity at these regions imposes constraints on our solutions. We look at each of the constraints separately. Since now the scalar functions Z_1 and Z_2 are the same as the seed solutions and Z_4 is vanishing, we only focus on the regularity of the forms. The standard procedure to check the regularity is to express the forms in a coordinate system without any degenerate points. However, we instead impose the equivalent condition that form components along $d\phi$ and $d\psi$ vanish at a degenerate locus.

We start by looking at the region where $(r = 0, \theta = 0)$. Focus on the regularity of the 1-form ω, especially on the $d\psi + d\phi$ component, which explicit expression is given in (5.6.12b). In order to cancel out the singularity caused by the form legs, $\mu_{k,m,n}$

needs to vanish at the point of interest. This determines the constant multiplying the harmonic term in $\mu_{k,m,n}$, which must be

$$\widehat{x}_{k,m,n} = k\frac{(k-m-2)!\,m!\,n!}{(k+n+1)!}\,. \tag{5.6.14}$$

Again the $\widehat{x}$ notation is used to distinguish the normalisation from the $q = 0$ case. The same analysis needs to be repeated for the $d\psi - d\phi$ component of the one-form, which also needs to be vanishing at the centre of the base manifold. However, as we are currently lacking a closed expression for generic quantum numbers, the analysis needs to be done on a case-by-case basis.

Let us now look at the points of the location of the supertube, namely ($\theta = \frac{\pi}{2}$). This is the same as looking at $\Sigma = 0$, where the scalars Z_1 and Z_2 diverge. To check the regularity of the solution, we look at the $(d\phi + d\psi)^2$ component of the metric and demand that it is regular at the position of the supertube. Imposing regularity at this locus of spacetime changes the relation between the brane charges Q_1, Q_5 and the parameters defining the supertube ansatz a and b, which is now given by

$$\frac{Q_1 Q_5}{R_y^2} = a^2 + \frac{\widehat{b}^2}{2}\widehat{x}_{k,m,n}\,, \tag{5.6.15}$$

where $\widehat{x}_{k,m,n}$ is defined in (5.6.14).

5.6.3 Asymptotically Flat Solution

Up to this point, the solutions we presented are asymptotically $\mathrm{AdS}_3 \times S^3 \times T^4$, which allows for the identification with the dual CFT states discussed in section 5.2. It turns out that these solutions can be extended to asymptotically flat configurations (in our case that is asymptotically equal to $\mathbb{R}^{4,1} \times S^1 \times T^4$) in a straightforward way and so can be identified with microstates of asymptotically flat black holes. As usual, this is done by adding back "1" in the functions Z_1 and Z_2. By introducing this extra constant, one usually obtains additional v-dependence on the right-hand side of second-layer equations. The effect of these additional terms is that we get new v-dependent terms in (5.6.3), with the differential equations determining these new terms usually being cumbersome to solve. Luckily, the novel feature of the solution (5.6.2) is that including the constant term in $Z_{1,2}$ does not add any additional source terms into the second-layer equations.

Thus focusing on the single-mode superstrata, the asymptotically flat extension of the solution (5.6.2),

$$Z_1 = 1 + \frac{Q_1}{\Sigma}, \qquad Z_2 = 1 + \frac{Q_5}{\Sigma}, \qquad Z_4 = 0\,, \tag{5.6.16a}$$

$$\Theta_1 = \Theta_2 = 0, \qquad \Theta_4 = \widehat{b}\,\widehat{\vartheta}_{k,m,n}\,, \tag{5.6.16b}$$

gives the same second-layer equations for $\mathcal{F}$ and ω as in the asymptotically AdS case. So, both the asymptotically AdS and the full asymptotically flat solution are v-independent.

5.6.4 Conserved Charges

One can extract the conserved charges of our new solutions from their large-distance behaviour. This gives a consistency check of the proposed identification between the new superstrata and the CFT states (5.2.7).

The angular momentum charges J and $\widetilde{J}$ associated with the left-moving and right-moving sector of the CFT respectively are related to the J_ϕ and J_ψ components of the supergravity angular momentum through

$$J = \frac{J_\phi + J_\psi}{2}\,, \qquad \widetilde{J} = \frac{J_\phi - J_\psi}{2}\,. \tag{5.6.17}$$

These charges can be found by analysing the $g_{\phi\psi}$ component of the ten-dimensional metric. In our ansatz, this component is obtained by looking at the $\phi + \psi$ components of the one-forms β and ω. It is straightforward to adapt the general prescription of [201] to this case (see for instance [105]), and one obtains

$$\beta_\phi + \beta_\psi + \omega_\phi + \omega_\phi \sim \sqrt{2}\,\frac{J - \widetilde{J}\,\cos 2\theta}{r^2} + \mathcal{O}(r^{-3})\,. \tag{5.6.18}$$

Thus it is possible to read off the angular momenta of our newly obtained solutions from the knowledge of β (which is unchanged from (5.3.10a)) and μ (5.6.12b). One finds that these are given by

$$J = \frac{R_y}{2}\left(a^2 + \widehat{b}^2\frac{m+1}{k}\widehat{x}_{k,m,n}\right)\,, \qquad \widetilde{J} = \frac{R_y a^2}{2}\,. \tag{5.6.19}$$

Similarly, the momentum charge Q_p can be extracted from the large-distance behaviour of the function $\mathcal{F}$:

$$\mathcal{F} \sim -\frac{2Q_p}{r^2} + \mathcal{O}(r^{-3})\,. \tag{5.6.20}$$

For our new solutions, we find

$$Q_p = \widehat{b}^2\frac{m+n+2}{2k}\widehat{x}_{k,m,n}\,. \tag{5.6.21}$$

Finally, we note that the brane charges Q_1 and Q_5 that appear in the scalar functions Z_1 and Z_2 do not change, as the two functions remain unchanged from the seed solutions

(5.3.10).

The supergravity charges calculated above are proportional to the quantised charges calculated on the CFT side. The brane charges Q_1 and Q_5 are related to the D-brane numbers n_1 and n_5 through

$$Q_1 = \frac{(2\pi)^4 g_s \alpha'^3}{V_4} n_1 \quad , \qquad Q_5 = g_s \alpha' n_5 \, , \tag{5.6.22}$$

with V_4 being the coordinate volume of T^4, g_s the string coupling, and α' the Regge slope. The relation between the Q_p obtained in (5.6.20) and the quantised momentum number n_p is

$$Q_p = \frac{(2\pi)^4 g_s^2 \alpha'^4}{V_4 R_y^2} n_p \ = \frac{Q_1 Q_5}{R_y^2 N} n_p . \tag{5.6.23}$$

The angular momenta J, $\tilde{J}$ obtained from the supergravity calculation in (5.6.18) are related to the quantised ones j, $\bar{j}$ by

$$J = \frac{(2\pi)^4 g_s^2 \alpha'^4}{V_4 \, R_y} j = \frac{Q_1 Q_5}{R_y N} j \, , \qquad \tilde{J} = \frac{(2\pi)^4 g_s^2 \alpha'^4}{V_4 \, R_y} \bar{j} = \frac{Q_1 Q_5}{R_y N} \bar{j} \, . \tag{5.6.24}$$

We are now able to compare the charges obtained from the supergravity solutions with the ones calculated on the CFT side. The latter are given by (5.2.8). The crucial point at this step is to identify the supergravity constraint obtained from the regularity condition at the position of the supertube (5.6.15) and the CFT constraint for the total number of strands (5.2.7). The parameter a is connected with the number of untwisted strands N_a and the number of twisted strands N_b with the parameter b. We find that these quantities are connected by

$$a^2 = \frac{Q_1 Q_5}{R_y^2} \frac{N_a}{N} \, , \qquad b^2 = \frac{2 Q_1 Q_5}{R_y^2} \frac{k N_b}{N} \widehat{x}^{-1}_{k,m,n} \, . \tag{5.6.25}$$

Using this identification together with the relations between the supergravity and quantised momenta, we get that the CFT charges corresponding to the supergravity solutions obtained above are given by[71]

$$\bar{j}_{\mathrm{R}} = \frac{R_y N}{Q_1 Q_5} \widetilde{J} = \frac{N_a}{2} \, , \tag{5.6.26a}$$

$$j_{\mathrm{R}} = \frac{R_y N}{Q_1 Q_5} J = \frac{N_a}{2} + (m+1) N_b \, , \tag{5.6.26b}$$

[71] We reinstated the subscript R for j and h to stress that we are listing the results in the in Ramond sector.

for the angular momenta, and using that the momentum charge $n_p = h_{\rm R} - \bar{h}_{\rm R}$, we get

$$n_p = \frac{R_y^2 N}{Q_1 Q_5} Q_p = (m+n+2) N_b \,. \tag{5.6.27}$$

We see that in all three cases these charges agree with the ones given in (5.2.8), if we set $q = 1$, as we should for our new supergravity solutions. This provides a check that the newly obtained solutions really are dual to the CFT states (5.2.3), with $q = 1$.

5.7 Compendium of Formulas and Explicit Solutions

Here we collect the expressions for the new superstrata that we constructed in this chapter.

The new superstrata represent supersymmetric solutions of supergravity, whose 10-dimensional fields are given by the ansatz (4.2.7). The quantities that enter the ansatz satisfy two layers of BPS equations, which are differential equations on a four-dimensional base, which we took to be flat $\mathbb{R}^4$. The ansatz quantities that solve the first-layer equations (4.2.25) are

$$Z_1 = \frac{Q_1}{\Sigma}\,, \quad Z_2 = \frac{Q_5}{\Sigma}\,, \quad Z_4 = 0\,, \quad \Theta_1 = \Theta_2 = 0\,, \tag{5.7.1a}$$

$$\Theta_4 = \widehat{b}_4^{k,m,n}\, \Delta_{k,1+m,1+n} \left[\frac{\Sigma}{r\sin\theta} \Omega^{(1)} \sin \hat{v}_{k,1+m,1+n} + \left(\Omega^{(2)} + \Omega^{(3)} \right) \cos \hat{v}_{k,1+m,1+n} \right] , \tag{5.7.1b}$$

where the definitions of $\Delta_{k,m,n}$ and $\hat{v}_{k,m,n}$ can be found in (5.3.18) and the self-dual two-forms $\Omega^{(i)}$ are given in (5.3.19). The range of the integers (k,m,n) is $k \geq 1$, $0 \leq m \leq k-2$, $n \geq 0$.

Due to the linearity the BPS equations, an arbitrary superposition of solutions (5.7.1) is still a solution of the first-layer equations (see (5.6.1)). However, in this chapter, we limited ourselves to single-mode superstrata, for which only one of the coefficients $\widehat{b}_4^{k,m,n} \equiv \widehat{b}$ is non-vanishing. In this case, the ansatz quantites that solve the second-layer BPS equations (4.2.26) are given by

$$\mathcal{F} = \mathcal{F}^{\rm RMS}(r,\theta), \qquad \omega = \omega_0 + \omega^{\rm RMS}(r,\theta)\,, \tag{5.7.2}$$

where ω_0 is defined in (5.3.10c),

$$\omega^{\rm RMS} = \mu_{k,m,n}(d\psi + d\phi) + \nu_{k,m,n}(d\psi - d\phi)\,, \tag{5.7.3}$$

and

$$\mathcal{F}^{\rm RMS} = \mathcal{F}_{k,m,n} = 4\widehat{b}^2 \left(F_{2k,2m+2,2n+2} + F_{2k,2m+4,2n}\right) , \tag{5.7.4a}$$

$$\mu_{k,m,n} = \frac{\widehat{b}^2 R_y}{\sqrt{2}} \Bigg[F_{2k,2m+2,2n} + F_{2k,2m+4,2n+2} - \frac{r^2 + a^2 \sin^2\theta}{\Sigma} \left(F_{2k,2m+2,2n+2} + F_{2k,2m+4,2n}\right) + \frac{\widehat{x}_{k,m,n}}{4\Sigma} \Bigg] , \tag{5.7.4b}$$

while $\nu_{k,m,n}$ has to be calculated on a case-by-case basis using the differential equations (5.6.13). The functions $F_{2k,2m,2n}$ are given by (5.6.7) and the coefficient $\widehat{x}_{k,m,n}$ is fixed by regularity of the solution to be (5.6.14).

In the dual CFT, the single-mode superstrata correspond to states of the form

$$|{+}{+}\rangle^{N_a} \left(|k,m,n,q\rangle^{\rm R}\right)^{N_b} , \quad \text{with} \quad N_a + kN_b = N \tag{5.7.5}$$

where $|k,m,n,q\rangle^{\rm R}$ is the spectral flow to the R sector of the NS state

$$|k,m,n,q\rangle^{\rm NS} = (J_0^+)^m (L_{-1})^n \left(G^{+1}_{-\frac{1}{2}} G^{+2}_{-\frac{1}{2}} + \frac{1}{k} J_0^+ L_{-1}\right)^q |00\rangle^{\rm NS}_k . \tag{5.7.6}$$

with $q = 0, 1$. States with $q = 1$ are dual to the new superstrata while the states with $q = 0$ are dual to the original superstrata constructed in [126]. The relation between the supergravity parameters a, b and the CFT parameters N_a, N_b is given by (5.7.5).

The above solutions are asymptotically AdS_3 but by simply setting

$$Z_1 \to Z_1 + 1 , \qquad Z_2 \to Z_2 + 1 , \tag{5.7.7}$$

the solutions become asymptotically flat. Such a transformation does not spoil the second-layer equations, meaning that the $\mathcal{F}_{k,m,n}$ and $\omega_{k,m,n}$ are still valid solutions, even in the asymptotically flat case. In contrast, extending the original superstrata to asymptotically flat ones required a non-trivial step of solving differential equations [126].

5.7.1 Explicit Examples

The solutions above are valid for any allowed set of quantum numbers $(k, m, n, q = 1)$. However, $\mathcal{F}_{k,m,n}$ and $\mu_{k,m,n}$ contain linear combinations of $F_{2k,2m,2n}$, which include non-trivial sums and are generically hard to evaluate. However, in certain cases, these sums can be evaluated explicitly, which then makes it possible to find solutions to the second-layer BPS equations in a closed form. Here we present the explicit expression for $\mathcal{F}_{k,m,n}, \omega_{k,m,n}$ for two classes of solutions.

$(k, m, n, q) = (k, 0, 0, 1)$ class of solutions

The simplest class of solutions is parametrised by the quantum numbers $(k, m, n, q) = (k, 0, 0, 1)$, with k being an arbitrary positive integer. These geometries already carry three charges, as momentum is added through the action of the fermionic generators. They are given by

$$\mathcal{F}_{k,0,0} = -\frac{\widehat{b}^2}{k(k^2-1)^2(X-1)^3(a^2+r^2)}\left[P^{(0)}_{\mathcal{F}}(X;k) + P^{(1)}_{\mathcal{F}}(X;k)\ Z\right], \tag{5.7.8a}$$

$$\begin{aligned}\omega_{k,0,0} = \frac{\widehat{b}^2\, R_y}{\sqrt{2}\, k^2(k^2-1)^2(X-1)^4\Sigma}\ \Big[&\Big(P^{(1)}_{\psi}(X;k)\, Z + P^{(2)}_{\psi}(X;k)\, Z^2\Big)\cos^2\theta\, d\psi \\ &+ \Big(P^{(0)}_{\phi}(X;k) + P^{(1)}_{\phi}(X;k)\, Z + P^{(2)}_{\phi}(X;k)\, Z^2\Big)\sin^2\theta\, d\phi\Big]\,,\end{aligned} \tag{5.7.8b}$$

where we introduced the notation

$$X = \frac{a^2\sin^2\theta}{r^2+a^2}\,, \qquad Z = \frac{r^2}{r^2+a^2}\,, \tag{5.7.9}$$

and $P^{(l)}_{\mathcal{F}}$, $P^{(l)}_{\psi}$, and $P^{(l)}_{\phi}$ denote polynomial functions in the variable X with the parameter k. They are given by

$$\begin{aligned}P^{(0)}_{\mathcal{F}}(X;k) &= 2(X-1)(X+1)(X^k-1) - k(X-1)^2(1+3X)X^{k-1} \\ &\quad - 2k^2(X-1)^2(X^{k-1}-1) + k^3(X-1)^3X^{k-1}\,,\end{aligned} \tag{5.7.10a}$$

$$\begin{aligned}P^{(1)}_{\mathcal{F}}(X;k) &= 4(X+1)(X^k-1) - k(X-1)(1+6X+X^2)X^{k-1} \\ &\quad + 2k^2(X-1)^2(X+1)X^{k-1} - k^3(X-1)^3X^{k-1}\,,\end{aligned} \tag{5.7.10b}$$

$$\begin{aligned}P^{(0)}_{\phi}(X;k) &= -2(X-1)^2(X^k-1) - k(X-1)^2(X+1)(X^{k-1}-1) \\ &\quad + 2k^2(X-1)^3X^{k-1} + k^3(X-1)^3(X^{k-1}-1)\,,\end{aligned} \tag{5.7.10c}$$

$$\begin{aligned}P^{(1)}_{\phi}(X;k) &= -4(X-1)(X+2)(X^k-1) + 2k(X-1)(2X - X^{k-1} - 4X^k + 3X^{k+1}) \\ &\quad + 4k^2(X-1)^2X^{k-1} - 2k^3(X-1)^3X^{k-1}\,,\end{aligned} \tag{5.7.10d}$$

$$\begin{aligned}P^{(2)}_{\phi}(X;k) &= -6(X+1)(X^k-1) + k(X-1)(2 + X^{k-1} + 8X^k + X^{k+1}) \\ &\quad - 2k^2(X-1)^2(X+1)X^{k-1} + k^3(X-1)^3X^{k-1}\,,\end{aligned} \tag{5.7.10e}$$

$$\begin{aligned}P^{(1)}_{\psi}(X;k) &= -2(X-1)(1+2X)(X^k-1) + 2k^2(X-1)^2X^k - k^3(X-1)^3 + k(X-1) \\ &\quad (-1+2X+X^2-4X^k+2X^{k+1})\,,\end{aligned} \tag{5.7.10f}$$

$$\begin{aligned}P^{(2)}_{\psi}(X;k) &= -2(1+4X+X^2)(X^k-1) + 2k(X-1)(X+1)(1+2X^k) \\ &\quad - 2k^2(X-1)^2X^k\,.\end{aligned} \tag{5.7.10g}$$

The above gives regular solutions for any $k > 1$.

It is interesting to see what happens for $k = 1$. If we treat k as a continuous

parameter, one can notice that all functions P in (5.7.10) vanish linearly as $k \to 1$, and so $\mathcal{F}_{k,0,0}$ and $\omega_{k,0,0}$ have a simple pole at this value of k. This means that the solution is ill-defined for $k = 1$, which is consistent with the CFT result in section 5.2 that the states $|1, 0, n, 1\rangle^{\rm NS}$ are unphysical. One may think that one could multiply $\widehat{b}^2$ by $(k-1)$ to start with in order to cancel this pole and get a physical solution. However, one can show that the solution with such modified normalisation would contain a logarithmic divergence at $\theta \to 0$ and does not represent a phyically allowed geometry.

$(k, m, n, q) = (2, 0, n, 1)$ class of solutions

The next simplest, physically meaningful class of three-charge examples is given by the quantum numbers $(k, m, n, q) = (2, 0, n, 1)$, where $n = 0, 1, 2, \ldots$. In the case where $n = 0$ the momentum charge is coming purely from fermionic generators, whereas for $n \neq 0$ the momentum charge is also added through the action of bosonic generators. One finds that for generic values of n the solutions for the second-layer equations are given by

$$\begin{aligned}\mathcal{F}_{2,0,n} = \frac{\widehat{b}^2}{a^2\,(n+1)^2(n+2)(n+3)^2}\Bigg\{\Bigg[-4\,\frac{1-Z^{n+1}}{1-Z} - 2(n+1)(n+3) \\ + (n+1)\left((n+3)(n+4)+2\right)Z^{n+1} - (n+1)^2(n+4)Z^{n+2}\Bigg] - \Bigg[4 - 8\,\frac{1-Z^{n+1}}{1-Z} \\ + (n^3+8n^2+21n+10)Z^{n+1} - 2(n+1)^2(n+4)Z^{n+2} + (n+1)^2(n+2)Z^{n+3}\Bigg]\sin^2\theta\Bigg\},\end{aligned} \tag{5.7.11a}$$

$$\begin{aligned}\omega_{2,0,n} = \frac{\widehat{b}^2\,R_y}{\sqrt{2}a^2}\,\frac{1}{Z\sin^2\theta+\cos^2\theta}\,\frac{1}{(n+1)^2(n+2)(n+3)^2} \\ \times\Bigg\{\Bigg[4Z\,\frac{1-Z^{n+1}}{1-Z} - (n+1)(n+5)\,Z^{n+2} + (n+1)^2Z^{n+3}\Bigg](\cos^2\theta\,d\psi - \sin^2\theta\,d\phi) \\ + 2\,(n+1)(n+3)(1-Z)\sin^2\theta d\phi\Bigg\},\end{aligned} \tag{5.7.11b}$$

where we have used the same variable Z as defined in (5.7.9).

5.8 Conclusions

In this chapter we have presented the explicit construction of new superstrata using the fermionic symmetries of the $SU(1,1|2)_L \times SU(1,1|2)_R$ (super)isometry group of $\mathrm{AdS}_3 \times S^3$. The new solutions are simpler than the ones known previously as only Θ_4

is excited and there is no scalar field that must be cancelled by other scalars excited at higher order.

Due to their simplicity, studying the structure of the solutions is easier for the new superstrata than for the original ones. For example, although the solution-generating technique can only produce asymptotically AdS_3 solutions, we can trivially extend the new superstrata to asymptotically flat solutions, as we do in section 5.6.3. In contrast, extending the original superstrata to asymptotically flat ones required a non-trivial step of solving differential equations [126].

Also, in the original superstrata, there was a technical difficulty in constructing solutions that involve two modes with completely different quantum numbers (k_1, m_1, n_1), (k_2, m_2, n_2) [126]. Subsequent results have shown that the geometries generated in this chapter were precisely the missing piece to making generic mulit-mode superstrata without restricting them to only a subspace of the phase space, as is the case if one considers the original superstrata alone [182].

Investigating physical aspects of this new class of superstrata, such as the integrability of the geometry [189] and precision holography [142, 143, 183, 184] would be very interesting. As mentioned above, possible instabilities of microstate geometries have attracted much interest lately [185–191]. In particular, it has been argued [185] that supersymmetric microstate geometries are non-linearly unstable when a small amount of energy is added, leading to a formation of a near-extremal black hole. The metric of the original superstrata in the asymptotically-flat setting [126] has no isometry in the v direction, which violates one of the assumptions in the analysis of [185]. However, the asymptotically-flat version of the new single-mode superstrata (5.6.16) is v-independent metrically, and it would be interesting to examine their possible instability and its endpoint.

Chapter 6

Outlook

Where do we go from here? Despite giving some outlook on future research in the relevant chapters, it may be worthwhile to further outline some of the more interesting directions in which one can expand this work.

Pole-Skipping

One of the main issues with pole-skipping is the lack of interpretation of the results. By now we have a good understanding of the near-horizon origin of this peculiar behaviour, yet a generic interpretation on the boundary side is still lacking. Some progress in this direction has been made in two-dimensional CFTs [83, 100], however we have seen that pole-skipping occurs regardless of the dimension of spacetime and thus a boundary interpretation should not be limited to the (special) two-dimensional case. Similarly, the effective hydrodynamic mode considered in [69] explains only the behaviour of the particular pole-skipping point at the positive imaginary frequency of the energy density correlator, but it does not trivially extend to other pole-skipping points or to Green's functions of other fields. One hopes that there exists a more universal mechanism that explains pole-skipping for all fields.

A further hint at the existence of such a general mechanism comes from the accumulation of results [2, 68–70, 72, 90], which show that the most positive (imaginary) frequency at which pole-skipping occurs for fields with spin s, is given by

$$\omega = 2\pi i T(s-1)\,. \tag{6.0.1}$$

This is a highly non-trivial result which currently lacks a proper interpretation.[72] A possible clarification may come by considering a specific top-down model, for example a near-extremal black hole in type IIB supergravity, where the interplay between fields

[72] This was first observed by Richard Davison.

of different spin is more apparent. It should be noted that the result (6.0.1) has been obtained without any *explicit* supersymmetry methods which might explain this kind of symmetry.

Furthermore, pole-skipping is still mysterious in the limit where the black hole becomes extremal. In this case the blackening factor $f(r)$ has a double zero at the horizon which increases the singularity of the equations of motion at this point. This fundamentally changes the near-horizon expansion of the bulk fields and therefore a more careful analysis is needed for such backgrounds. However, there are known Green's functions for extremal systems, such as the fermionc correlator in an extremal BTZ black hole [55], which should serve as useful guides in obtaining new results.

An additional interesting observation that follows from the near-horizon analysis is the equivalence of the advanced and retarded Green's functions at the Matsubara frequencies. Recall that at such frequencies, one of the solutions becomes irregular in the ingoing Eddington-Finkelstein coordinates due to logarithmic terms appearing in the near-horizon expansion. As a consequence, the remaining regular solution needs to be chosen when calculating both the advanced and the retarded correlator in holography (see section C.1.3 Appendix C for the more details). While this relation has not been fully developed yet, one can mention a comment of [72] where the same equivalence of the advanced and retarded Green's functions was observed for scalar fields at bosonic Matsubara frequencies. Namely, in order to respect causality at real values of the momentum the advanced Green's function must not have any poles in the lower half frequency plane. Since the equivalence holds at the negative Matsubara frequencies and away from the pole-skipping points:

$$G^A(\omega=\omega_n,k)=G^R(\omega=\omega_n,k)\,,\qquad \omega_n=-2\pi iT\left(n-\frac{1}{2}\right),k\neq k_n,\quad n=1,2,\dots \tag{6.0.2}$$

it follows that for real k, the retarded Green's function has no poles at $\omega=\omega_n$ besides the poles which get pole-skipped at $k=k_n$. In [72] they have investigated a similar statement for *positive* imaginary Matsubara frequencies in which case one can make a similar statement about the locations of poles of the advanced Green's function at positive imaginary Mastubara frequencies but away from the pole-skipping momentum. It would be interesting to further investigate this avenue, especially in light of the constraints from causality.

Finally, we need to clarify the relation between the pole-skipping locations and the chaotic properties of the theories. While our current understanding suggests that the pole-skipping point at the positive imaginary frequency in the energy density correlator is related to chaos, which has been demonstrated in a wide variety of systems [69–71, 202, 203], it also seems that other pole-skipping points are not related to chaos in

general. Understanding the conditions under which a connection is present (if it is present at all) might allow us to use pole-skipping as a "cheap" diagnostic for chaos in holographic systems.

Black Hole Microstates

In chapter 5 we have presented the construction of a new family of smooth microstates of the supersymmetric D1-D5-P black hole. With that we have added to an already large number of known microstates of this black hole, yet we are still far away from having a complete microscopic picture.

As it was shown in [134], the number of currently known superstrata cannot account for the full entropy of the D1-D5-P black hole, thus we know that there exist other microstates that are not yet constructed or accounted for. From the spectrum of linearised gravity around $\mathrm{AdS}_3 \times S^3$ [136–138] we know that there exist other smooth excitations that might result in superstrata. It is expected that these geometries have a deformed base space which makes them computationally harder to construct, however this means that the obstacles are more of a technical than a conceptual nature. Research in this direction is ongoing and recently new pathways have opened up, containing holomorphic techniques [175] and perhaps more promisingly, it was found that some of the superstrata can be reduced to only three dimensions [176]. One hopes that by using this reduction, one can generate solutions in three dimensions which can then be uplifted to six dimensions, where they would represent a new class of smooth microstates.

However, superstrata are very atypical microstates as they correspond to coherent superpositions of excitations (see for example [204] for a discussion on typicality) and an open question is what a typical microstate looks like. One may expect that such a state is not fully captured by supergravity and may in general contain stringy excitations [159–161, 205]. This may give an additional motivation for the construction of all possible microstate geometries as it should show whether supergravity is enough to describe the microscopic degrees of freedom of a black hole.

Furthermore, so far we have only constructed the microstates of a supersymmetric black hole and one may ask to what extent do the results from the supersymmetric configurations translate to the non-supersymmetric sector? In fact, generating non-supersymmetric black holes is also one of the (long-term) goals of the programme, as such black holes are dynamical and evaporate. Some results are already known [206,207] yet a finite-temperature superstratum is currently unavailable.

Another interesting avenue is the probing of the known microstate geometries to analyse the differences with respect to the conventional black hole. As we have noted above, the three-point correlation functions are protected by supersymmetry [129],

hence four-point functions are the simplest non-trivial correlators that involve novel information about the geometry. A very interesting class of such correlators is the HHLL correlator with two parametrically heavy operators (H) whose conformal dimensions scale with the large central charge, and two light operators (L) with conformal dimensions that do not scale with the central charge. Such correlators can be thought of as describing a process in which a light particle L is scattering off a heavy microstate H. Their interaction is then encoded in the behaviour of correlator from which we can read off some of the details of the geometry of the heavy state.

Such an analysis was performed for example in [130, 132, 183, 208] and indeed deviations from the conventional black hole geometry were observed, for example in the absence of a decay at large Lorentzian times [209]. It would be interesting to see how much knowledge about the microscopic degrees of freedom is encoded in these correlators. An interesting novel direction is, for example, the study of the Regge limit of such correlators. In addition recently, using these HHLL results, generic four-point correlators of light particles in $\mathrm{AdS}_3 \times S^3$ were constructed [210, 211] (see also [212]), bypassing the usual difficulties one encounters when working with Witten Diagrams in AdS_3.

There are other methods with which one can probe the geometries. For example, using a hybrid WKB method the quasinormal modes of the superstata were obtained in [213, 214]. Similarly, in [215] the null geodesics of these geometries were used to determine the behaviour of massless probes near the photosphere of the solutions – the nearest distance from the centre where a circular orbit is still stable. All of these results allow us to build up an arsenal of differences between the conventional black holes and the microstates. The optimistic hope is that these differences would be visible in some refined signal from a black hole related experimental observation, for example the gravitational wave ringdown of a black hole merger as measured at LIGO (see for example [216]), but at the moment such observations are still out of reach.

Finally, while the two topics presented in this thesis are somewhat disjoint, one may wonder whether one could perform a pole-skipping analysis of microstate geometries. One obvious problem is that such geometries lack a horizon, so a new set of boundary conditions would have to be imposed. Similarly, the superstrata have a vanishing Hawking temperature for which pole-skipping is not yet known. All in all, the combination of these two ideas seems rather distant at the moment. But it is fun to speculate of what lies ahead.

Appendix A

Conventions

Here we present a brief summary of the conventions used throughout the document.[73]

A.1 Form Conventions

Assume that a D-dimensional spacetime is spanned locally by coordinates x^M and that the line element can then be written as

$$ds^2 = g_{MN}\, dx^M dx^N\,, \tag{A.1.1}$$

where we use the mostly-positive signature for the metric g_{MN}. We can introduce an orthonormal frame E^a which can be used to rewrite the metric as

$$ds^2 = \eta_{ab}\, E^a E^b\,, \tag{A.1.2}$$

with $\eta_{ab} = \mathrm{diag}(-,+,\ldots,+)$. As in these two line elements, throughout the document we denote curved indices with upper-case Latin letters $M, N, \ldots$, while flat space indices are denoted by lower-case Latin letters $a, b, \ldots$. Since some particular values of these indices can be the same in curved and flat space, we denote the latter as underlined. For example, X^t denotes the t-component of a vector field X in curved spacetime, while $X^{\underline{t}}$ denotes the t-component of the field in flat spacetime. Of course, these two can be related through the orthonormal frame.

A differential form of degree p or a p-form is defined as

$$A_p = \frac{1}{p!}\, A_{M_1\ldots M_p}\, dx^{M_1} \wedge \ldots \wedge dx^{M_p} = \frac{1}{p!}\, A_{a_1\ldots a_p}\, E^{a_1} \wedge \ldots \wedge E^{a_p}\,. \tag{A.1.3}$$

[73] We mostly follow the conventions used in [103], summarized in the Appendix A of that paper.

Throughout the text the following operators acting on the forms are used

$$*A_p = \frac{1}{k!(D-k)!}\epsilon_{a_1\ldots a_{D-k}a_{D-k+1}\ldots a_D}A^{a_{D-k+1}\ldots a_D}\,E^{a_1}\wedge\ldots E^{a_{D-k}}\,, \tag{A.1.4a}$$

$$\lambda\left(A_p\right) = (-1)^{p(p-1)/2}A_p\,, \tag{A.1.4b}$$

$$\not{A}_p = \frac{1}{p!}A_{M_1\ldots M_p}\Gamma^{M_1\ldots M_p}\,, \tag{A.1.4c}$$

where in (A.1.4a) we have used the totally antisymmetric symbol and we use the convention with $\epsilon_{\underline{01}\ldots\underline{D-1}} = 1$.

A.2 Spinor conventions

The introduction of the orthonormal frame allows us to define gamma matrices in curved spacetimes. We begin by defining gamma matrices in flat space which satisfy the Clifford algebra relations

$$\left\{\Gamma^a,\Gamma^b\right\} = 2\eta^{ab}\,. \tag{A.2.1}$$

In particular this means that the gamma matrix associated with the time direction[74] squares to -1 while the gamma matrices associated to the spatial directions square to 1. Using the components of the vielbein, we can define curved space gamma matrices as

$$\Gamma^M = E_a{}^M\,\Gamma^a\,, \tag{A.2.2}$$

which satisfy the algebra

$$\left\{\Gamma^M,\Gamma^N\right\} = 2g^{MN}\,. \tag{A.2.3}$$

In chapter 3 we work with Dirac spinors which in D dimensions[75] transform in a representation with $2^{\lfloor\frac{D}{2}\rfloor}$ components, where $\lfloor q\rfloor$ denotes the highest integer that is less than or equal to q. For such a spinor there are no additional constraints and thus each component is in general a complex number.

The fermion fields in type IIB supergravity are a pair of gravitinos $\psi_M^{1,2}$ and a pair of dilatinos $\lambda^{1,2}$, which are all Majorana-Weyl spinors in ten dimensions. The chiral matrix in ten dimensions is given by

$$\Gamma_{(10)} \equiv \Gamma^{\underline{t}}\cdots\Gamma^{\underline{9}}\,, \tag{A.2.4}$$

[74] Either $\Gamma^{\underline{t}}$ or $\Gamma^{\underline{v}}$

[75] Note that the number of bulk dimensions in chapter 3 was $D+2$.

with the order of multiplication in the above definition following the order of directions from left to right in table 6. For the coordinate system used in (4.2.7) and (5.3.10) the chirality matrix is defined as

$$\Gamma_{(10)} \equiv \Gamma^{\underline{uvr\theta\tilde{\phi}\tilde{\psi}6789}}. \tag{A.2.5}$$

In type IIB supergravity the chirality of the fermionic fields is given by

$$\Gamma_{(10)}\psi^I_M = +\psi^I_M, \qquad \Gamma_{(10)}\lambda^I = -\lambda^I, \tag{A.2.6}$$

where in both cases $I = 1, 2$. Spinors in supergravity also satisfy the Majorana condition. We take the charge conjugation matrix $\mathcal{C}$ to be given by

$$\mathcal{C} = \Gamma^{\underline{t}}, \tag{A.2.7}$$

so that the Majorana condition for a spinor χ reads

$$\bar{\epsilon} \equiv \chi^\dagger \Gamma^{\underline{t}} = \chi^T \mathcal{C}, \tag{A.2.8}$$

which implies that the components of the spinor are real numbers

$$\chi^* = \chi. \tag{A.2.9}$$

Note that for the choice (A.2.7) the conjugate of a Majorana spinor can be written as

$$\bar{\chi} = \chi^T \Gamma^{\underline{t}}. \tag{A.2.10}$$

The supersymmetry variations of the fields in type IIB supergravity ((5.4.1) and (5.4.2)) are generated by a doublet of Majorana-Weyl spinors $\epsilon^{1,2}$ with

$$\Gamma_{(10)}\, \epsilon^{1,2} = \epsilon^{1,2}\,. \tag{A.2.11}$$

We can count of the number of real degrees of freedom contained in the spinor pair. A Dirac spinor in ten dimensions has 2^5 complex or $2^6 = 64$ real free parameters. Imposing the Majorana or the Weyl condition halves the number of real degrees of freedom in a spinor, and imposing both leaves us with only a quarter, hence each ϵ^I contains 16 real parameters. Thus there are 32 real degrees of freedom in total which are the supersymmetry generators of type IIB supergravity.

In chapter 5 we use the coordinates u and v defined as

$$u \equiv \frac{1}{\sqrt{2}}(t - y), \qquad v \equiv \frac{1}{\sqrt{2}}(t + y), \tag{A.2.12}$$

It is then convenient to express $\Gamma^{\underline{t}}$ as

$$\Gamma^{\underline{t}} = \frac{1}{\sqrt{2}}\left(\Gamma^{\underline{u}} + \Gamma^{\underline{v}}\right) \equiv \widehat{\Gamma}^{\underline{u}} + \widehat{\Gamma}^{\underline{v}}, \quad \text{where} \quad \widehat{\Gamma}^{\underline{v}} \equiv \frac{1}{\sqrt{2}}\Gamma^{\underline{v}}, \quad \widehat{\Gamma}^{\underline{u}} \equiv \frac{1}{\sqrt{2}}\Gamma^{\underline{u}}. \tag{A.2.13}$$

The newly defined gamma matrices satisfy

$$\widehat{\Gamma}^{\underline{u}T} = \widehat{\Gamma}^{\underline{u}\dagger} = -\widehat{\Gamma}^{\underline{v}}, \qquad \widehat{\Gamma}^{\underline{v}T} = \widehat{\Gamma}^{\underline{v}\dagger} = -\widehat{\Gamma}^{\underline{u}}, \tag{A.2.14}$$

where we used the hermiticity properties of the Γ matrices,

$$\Gamma^{\underline{t}\dagger} = -\Gamma^{\underline{t}}, \qquad \Gamma^{\underline{i}\dagger} = \Gamma^{\underline{i}}, \qquad i \neq t. \tag{A.2.15}$$

Appendix B

Details of the Pole-Skipping calculations

In the main text we have only considered the detailed derivation of pole-skipping for asymptotically AdS_3 spaces where the spinors are two-component objects. The derivation in spacetimes that are asymptotically AdS_{D+2} is analogous, but contains some novelties that we want to present here. Ultimately, our goal here is to arrive at (3.58) and their $(\psi_+^{(-)}, \psi_-^{(+)})$ analogues. By doing so, we repeat some of the steps from the main text in order to make this calculation more or less self-contained.

We also give some explicit expressions for the matrix elements appearing in section 3.3.2.

B.1 Analysis in Asymptotically AdS_{D+2} Spacetimes

We work with the background metric in the ingoing Eddington-Finkelstein coordinates given by

$$ds^2 = -r^2 f(r) dv^2 + 2dv\, dr + h(r) d\vec{x}^2 \,. \tag{B.1.1}$$

We choose the orthonormal frame to be

$$E^{\underline{v}} = \frac{1+f(r)}{2}\, r dv - \frac{dr}{r}\,, \qquad E^{\underline{r}} = \frac{1-f(r)}{2}\, r dv + \frac{dr}{r}\,, \qquad E^{\underline{i}} = \sqrt{h(r)}\, dx^i\,, \tag{B.1.2}$$

so that

$$ds^2 = \eta_{ab} E^a\, E^b\,, \qquad \eta_{ab} = \mathrm{diag}(-1, 1, 1, \ldots, 1)\,. \tag{B.1.3}$$

The spin connections for this frame are given by

$$\omega_{\underline{vr}} = \frac{dr}{r} - \frac{2rf(r) + r^2 f'(r)}{2}\, dv, \tag{B.1.4a}$$

$$\omega_{\underline{vi}} = \frac{r\, h'(r)\ (1 - f(r))}{4\sqrt{h(r)}}\, dx^i, \tag{B.1.4b}$$

$$\omega_{\underline{ri}} = -\frac{r\, h'(r)\, (1 + f(r))}{4\sqrt{h(r)}}\, dx^i\,, \tag{B.1.4c}$$

with all other components, which are not related by symmetry to the ones above, being 0. Using these spin connections, one can calculate the Dirac equation to be

$$\begin{aligned}\Bigg[&\left(\frac{r(1+f(r))}{2}\,\Gamma^{\underline{r}} - \frac{r(1-f(r))}{2}\,\Gamma^{\underline{v}}\right)\partial_r + \frac{\Gamma^{\underline{r}} + \Gamma^{\underline{v}}}{r}\partial_v + \frac{\Gamma^{\underline{i}}}{\sqrt{h(r)}}\,\partial_i \\ &+ \frac{1 + f(r) + rf'(r)}{4}\,\Gamma^{\underline{r}} - \frac{1 - f(r) - rf'(r)}{4}\,\Gamma^{\underline{v}} - \frac{D\, r\,(1-f(r))h'(r)}{8h(r)}\,\Gamma^{\underline{v}} \\ &+ \frac{D\, r\,(1+f(r))h'(r)}{8h(r)}\,\Gamma^{\underline{r}} - m\Bigg]\psi(r, v, x^j) = 0\,.\end{aligned} \tag{B.1.5}$$

Inserting the plane wave ansatz $\psi(r, v, x^j) = \psi(r)e^{-i\omega v + ik_i x^i}$ gives

$$\begin{aligned}\Bigg\{ &\Gamma^{\underline{v}}\left[-\frac{r(1-f(r))}{2}\,\partial_r - \frac{i\omega}{r} - \frac{1 - f(r) - rf'(r)}{4} - \frac{D\, r\,(1-f(r))h'(r)}{8h(r)}\right] + \frac{ik_i\Gamma^{\underline{i}}}{\sqrt{h(r)}} \\ &+ \Gamma^{\underline{r}}\left[\frac{r(1+f(r))}{2}\,\partial_r - \frac{i\omega}{r} + \frac{1 + f(r) + rf'(r)}{4} + \frac{D\, r\,(1+f(r))h'(r)}{8h(r)}\right] - m\Bigg\}\psi(r) = 0\,.\end{aligned} \tag{B.1.6}$$

Next, we decouple these differential equations. We start by separating the spinors according to their eigenvalues under the action of the $\Gamma^{\underline{r}}$ matrix. Exactly half of the eigenvalues of $\Gamma^{\underline{r}}$ are $+1$ while the other half are -1, since $(\Gamma^{\underline{r}})^2 = 1$ and $\mathrm{Tr}(\Gamma^{\underline{r}}) = 0$. Therefore, we introduce

$$\psi = \psi_+ + \psi_-\,, \qquad \Gamma^{\underline{r}}\psi_\pm = \pm\psi_\pm\,, \qquad P_\pm \equiv \frac{1}{2}\left(1 \pm \Gamma^{\underline{r}}\right)\,, \tag{B.1.7}$$

and insert this decomposition into (B.1.6). After a bit of algebra, the two independent equations read

$$\begin{aligned}\Bigg[&-i\omega + \frac{r^2 f'(r)}{4} + \frac{rf(r)}{4}\left(2 + \frac{D\, r\, h'(r)}{h(r)}\right) - \frac{m\, r(1+f(r))}{2} - \frac{r(1-f(r))}{2\sqrt{h(r)}}\, ik_i\Gamma^{\underline{vi}}\Bigg]\psi_+ \\ &+ \Gamma^{\underline{v}}\Bigg[-i\omega + \frac{r^2 f'(r)}{4} + \frac{m\, r(1-f(r))}{2} - \frac{r(1+f(r))}{2\sqrt{h(r)}}\, ik_i\Gamma^{\underline{vi}}\Bigg]\psi_- + r^2 f(r)\,\partial_r\psi_+ = 0\,,\end{aligned} \tag{B.1.8a}$$

$$\Big[-i\omega+\frac{r^2f'(r)}{4}+\frac{rf(r)}{4}\Big(2+\frac{D\,r\,h'(r)}{h(r)}\Big)+\frac{m\,r(1+f(r))}{2}-\frac{r(1-f(r))}{2\sqrt{h(r)}}\,ik_i\Gamma^{\underline{vi}}\Big]\psi_-$$
$$-\Gamma^{\underline{v}}\Big[-i\omega+\frac{r^2f'(r)}{4}-\frac{m\,r(1-f(r))}{2}-\frac{r(1+f(r))}{2\sqrt{h(r)}}\,ik_i\Gamma^{\underline{vi}}\Big]\psi_++r^2f(r)\,\partial_r\psi_-=0\,. \tag{B.1.8b}$$

Observe that for $D\geq 2$, the two matrices $\Gamma^{\underline{r}}$ and $\Gamma^{\underline{vi}}$ are independent and commuting[76]. The matrix

$$\hat{k}_i\Gamma^{\underline{vi}}\equiv\frac{k_i}{k}\,\Gamma^{\underline{vi}},\quad\text{with}\quad k=\sqrt{\sum_{i=1}^{D}k_ik_i}\,, \tag{B.1.9}$$

squares to unity and is traceless. Since it is commuting with $\Gamma^{\underline{r}}$, we can find common eigenvectors. Thus, we define

$$\psi_a=\psi_a^{(+)}+\psi_a^{(-)}\,,\qquad \hat{k}_i\Gamma^{\underline{vi}}\,\psi_a^{(\pm)}=\pm\psi_a^{(\pm)}\,,\qquad P^{(\pm)}\equiv\frac{1}{2}\Big(1\pm\hat{k}_i\Gamma^{\underline{vi}}\Big)\,, \tag{B.1.10}$$

where $a=\pm$. Inserting this decomposition into (B.1.8) and separating each of the equations with the projectors defined in (B.1.10), gives four independent equations

$$\Big[-i\omega+\frac{r^2f'(r)}{4}+\frac{rf(r)}{4}\Big(2+\frac{D\,r\,h'(r)}{h(r)}\Big)-\frac{m\,r(1+f(r))}{2}-\frac{ikr(1-f(r))}{2\sqrt{h(r)}}\Big]\psi_+^{(+)}$$
$$+\Gamma^{\underline{v}}\Big[-i\omega+\frac{r^2f'(r)}{4}+\frac{m\,r(1-f(r))}{2}+\frac{ikr(1+f(r))}{2\sqrt{h(r)}}\Big]\psi_-^{(-)}+r^2f(r)\,\partial_r\psi_+^{(+)}=0\,, \tag{B.1.11a}$$

$$+\Big[-i\omega+\frac{r^2f'(r)}{4}+\frac{rf(r)}{4}\Big(2+\frac{D\,r\,h'(r)}{h(r)}\Big)+\frac{m\,r(1+f(r))}{2}+\frac{ikr(1-f(r))}{2\sqrt{h(r)}}\Big]\psi_-^{(-)}$$
$$-\Gamma^{\underline{v}}\Big[-i\omega+\frac{r^2f'(r)}{4}-\frac{m\,r(1-f(r))}{2}-\frac{ikr(1+f(r))}{2\sqrt{h(r)}}\Big]\psi_+^{(+)}+r^2f(r)\,\partial_r\psi_-^{(-)}=0\,, \tag{B.1.11b}$$

$$\Big[-i\omega+\frac{r^2f'(r)}{4}+\frac{rf(r)}{4}\Big(2+\frac{D\,r\,h'(r)}{h(r)}\Big)-\frac{m\,r(1+f(r))}{2}+\frac{ikr(1-f(r))}{2\sqrt{h(r)}}\Big]\psi_+^{(-)}$$
$$+\Gamma^{\underline{v}}\Big[-i\omega+\frac{r^2f'(r)}{4}+\frac{m\,r(1-f(r))}{2}-\frac{ikr(1+f(r))}{2\sqrt{h(r)}}\Big]\psi_-^{(+)}+r^2f(r)\,\partial_r\psi_+^{(-)}=0\,, \tag{B.1.11c}$$

[76] For $D=1$, which is the asymptotically AdS_3 case, we have $\Gamma^{\underline{vi}}=\pm\Gamma^{\underline{r}}$, as $(\mathbb{I},\Gamma^{\underline{v}},\Gamma^{\underline{i}},\Gamma^{\underline{r}})$ provide a complete basis for any 2×2 matrix.

$$\left[-i\omega + \frac{r^2 f'(r)}{4} + \frac{r f(r)}{4}\left(2 + \frac{D\, r\, h'(r)}{h(r)}\right) + \frac{m\, r(1+f(r))}{2} - \frac{ikr(1-f(r))}{2\sqrt{h(r)}} \right] \psi_-^{(+)}$$
$$- \Gamma^{\underline{v}} \left[-i\omega + \frac{r^2 f'(r)}{4} - \frac{m\, r(1-f(r))}{2} + \frac{ikr(1+f(r))}{2\sqrt{h(r)}} \right] \psi_+^{(-)} + r^2 f(r)\, \partial_r \psi_-^{(+)} = 0\,. \tag{B.1.11d}$$

These split into two decoupled subsystems. The equations describing the pair $\psi_+^{(+)}$ and $\psi_-^{(-)}$ are (B.1.11a) and (B.1.11b), while the equations governing the spinors $\psi_+^{(-)}$ and $\psi_-^{(+)}$ are (B.1.11c) and (B.1.11d). Furthermore, the equations (B.1.11a) and (B.1.11c) are related by changing $k \to -k$. The same can be said for the pair (B.1.11b) and (B.1.11d). This allows us to focus on solving only one of the subsystems while the solutions of the other are obtained by changing k into $-k$.

It is pretty straightforward to obtain a decoupled and diagonal second order differential equation for a single spinor, and as a check one can expand the equations around the boundary $r \to \infty$ and look for the leading behaviour of the spinors. One finds that

$$\psi_+^{(\pm)} \sim r^{-\frac{D+1}{2}+m} + r^{-\frac{D+3}{2}-m}\,, \qquad \psi_\pm^{(-)} \sim r^{-\frac{D+3}{2}+m} + r^{-\frac{D+1}{2}-m}\,, \tag{B.1.12}$$

which is in agreement with the results obtained in [55].

B.2 Explicit Series Expansion Coefficients

In section 3.3.2 we have presented two methods with which one can calculate the higher order pole-skipping points for fermionic fields. In the analysis we have refrained from giving explicit values for the coefficients appearing in series expansions of equations of motion, such as (3.32), as these become long expressions very quickly, without offering much insight. For completeness, in this appendix we list some of these coefficients explicitly. We still do not give any of the coefficients appearing in the method involving second order differential equations, as these terms provide almost no insight, but are also straightforward to obtain.

In equation (3.39) there are two matrix coefficients, $\widetilde{\mathcal{M}}^{(11)}$ is given in (3.40), while the elements of $\widetilde{\mathcal{M}}^{(10)}$ are given by

$$\widetilde{\mathcal{M}}^{(10)}_{++} = \frac{1}{4h(r_0)^{\frac{3}{2}}}\Big[2ikh(r_0)\left(r_0 f'(r_0) - 1\right) + ikr_0 h'(r_0) + r_0^2\sqrt{h(r_0)} f'(r_0) h'(r_0)$$
$$+ h(r_0)^{\frac{3}{2}}\left(-2m - 2(m-2) r_0 f'(r_0) + r_0^2 f''(r_0)\right)\Big]\,, \tag{B.2.1a}$$
$$\widetilde{\mathcal{M}}^{(10)}_{+-} = \frac{1}{4h(r_0)^{\frac{3}{2}}}\Gamma^{\underline{v}}\Big[2ikh(r_0)\left(r_0 f'(r_0) + 1\right) - ikr_0 h'(r_0) + h(r_0)^{\frac{3}{2}} \times$$
$$\times \left(2m - 2(m-1) r_0 f'(r_0) + r_0^2 f''(r_0)\right)\Big]\,, \tag{B.2.1b}$$

$$\widetilde{\mathcal{M}}^{(10)}_{-+} = \frac{1}{4h(r_0)^{\frac{3}{2}}}\Gamma^{\underline{v}}\Big[2ikh(r_0)\left(r_0 f'(r_0)+1\right) - ikr_0h'(r_0) - h(r_0)^{\frac{3}{2}}\times \\ \times\left(-2m+2(m+1)r_0f'(r_0)+r_0^2f''(r_0)\right)\Big], \tag{B.2.1c}$$

$$\widetilde{\mathcal{M}}^{(10)}_{--} = \frac{1}{4h(r_0)^{\frac{3}{2}}}\Big[-2ikh(r_0)\left(r_0f'(r_0)-1\right) - ikr_0h'(r_0) + r_0^2\sqrt{h(r_0)}f'(r_0)h'(r_0) \\ +h(r_0)^{\frac{3}{2}}\left(2m-2(m+2)r_0f'(r_0)+r_0^2f''(r_0)\right)\Big], \tag{B.2.1d}$$

where

$$\widetilde{\mathcal{M}}^{(10)} = \begin{pmatrix}\widetilde{\mathcal{M}}^{(10)}_{++} & \widetilde{\mathcal{M}}^{(10)}_{+-}\\ \widetilde{\mathcal{M}}^{(10)}_{-+} & \widetilde{\mathcal{M}}^{(10)}_{--}\end{pmatrix}. \tag{B.2.2}$$

Note that the elements above also occur in the matrix (3.43). In that matrix we also find the following coefficients

$$\widetilde{\mathcal{M}}^{(00)}_{++} = -\frac{mr_0}{2} - \frac{ikr_0}{2\sqrt{h(r_0)}} - \frac{r_0^2\,f'(r_0)}{2}, \tag{B.2.3a}$$

$$\widetilde{\mathcal{M}}^{(00)}_{--} = \left(\frac{mr_0}{2} + \frac{ikr_0}{2\sqrt{h(r_0)}} - \frac{r_0^2\,f'(r_0)}{2}\right)\Gamma^{\underline{v}}, \tag{B.2.3b}$$

$$\widetilde{\mathcal{M}}^{(11)}_{+} = -\frac{mr_0}{2} - \frac{ikr_0}{2\sqrt{h(r_0)}} + \frac{r_0^2\,f'(r_0)}{2}, \tag{B.2.3c}$$

$$\widetilde{\mathcal{M}}^{(11)}_{-} = \left(\frac{mr_0}{2} + \frac{ikr_0}{2\sqrt{h(r_0)}} + \frac{r_0^2\,f'(r_0)}{2}\right)\Gamma^{\underline{v}}, \tag{B.2.3d}$$

which are coefficients that have already been evaluated at $\omega = -3\pi iT$, whereas (B.2.1) are independent of the frequency. Note that the last two coefficients of (B.2.3) are merely $n = 1$ versions of (3.51). As a check, one can show that

$$\det\widetilde{\mathcal{M}}_1(\omega_1,k) \propto \widetilde{\mathcal{M}}^{(00)}_{+}(\omega_1,k), \tag{B.2.4}$$

which means that we get the same pole-skipping points with both methods presented in section 3.3.2. Elements appearing in the matrix (3.50) can be obtained in a similar manner, however their expressions are rather cumbersome so we do not give them explicitly.

Appendix C

Fermionic Green's Function for BTZ Black Hole

The retarded Green's function for fermion fields in the BTZ black hole background [61, 62] was first derived in [55]. However, the result (3.89) needs to be modified if the bulk fermion's mass is a half integer number (in multiples of the AdS radius), or equivalently, if the conformal dimension of the dual operator is a half-integer.

In this appendix we derive this new form of the correlator by using the prescription of [55]. The result is given by (3.93) and in chapter 3 we have shown that the pole-skipping points and the anomalous locations are correctly predicted by the near-horizon analysis.

C.1 Green's Function at Generic Conformal Dimension

C.1.1 Retarded Green's Function

We begin by reviewing the extraction of the Green's function for femionic fields of generic mass m in the BTZ black hole. We closely follow the derivation of [55].

The metric of a rotating BTZ black hole [61, 62] can be written as

$$ds^2 = -\frac{(r^2-r_+^2)(r^2-r_-^2)}{r^2}\,dt^2 + \frac{r^2 dr^2}{(r^2-r_+^2)(r^2-r_-^2)} + r^2\left(d\phi - \frac{r_+ r_-}{r^2}\,dt\right)^2, \tag{C.1.1}$$

where ϕ is an angular coordinate with a period of 2π. The black hole has mass M and angular momentum J given by

$$M = \frac{r_+^2 + r_-^2}{8G}, \qquad J = \frac{r_+ r_-}{4G}, \tag{C.1.2}$$

where G denotes the Newton constant in three dimensions. The black hole has two

associated temperatures named the left and right-moving temperature[77] given by

$$T_L = \frac{r_+ - r_-}{2\pi}\,, \qquad T_R = \frac{r_+ + r_-}{2\pi}\,. \tag{C.1.3}$$

There exists a nice set of coordinates, defined by

$$r^2 = r_+^2 \cosh^2\rho - r_-^2 \sinh^2\rho\,, \tag{C.1.4a}$$
$$T + X = (r_+ - r_-)(t + \phi)\,, \tag{C.1.4b}$$
$$T - X = (r_+ + r_-)(t - \phi), \tag{C.1.4c}$$

in which the metric takes the diagonal form

$$ds^2 = -\sinh^2\rho\, dT^2 + \cosh^2\rho\, dX^2 + d\rho^2. \tag{C.1.5}$$

We can then choose the orthonormal frame

$$E^T = -\sinh\rho\, dT\,, \qquad E^X = \cosh\rho\, dX\,, \qquad E^\rho = d\rho\,, \tag{C.1.6}$$

in which the non-trivial spin connection components are given by

$$\begin{aligned} \omega_{T\rho} &= -\cosh\rho\, dT \\ \omega_{X\rho} &= -\sinh\rho\, dX. \end{aligned} \tag{C.1.7}$$

In the new coordinates, the metric components depend only on the coordinate ρ (in the old coordinates the metric depends only on r), hence we can expand the solutions in the basis of plane waves as

$$\psi(T, X, \rho) = e^{-ik_T T + ik_X X}\psi(\rho, k_\mu) = e^{-i\omega t + ik\phi}\psi(\rho, k_\mu)\,. \tag{C.1.8}$$

The derivation proceeds naturally for the momentum values k_T and k_X, but in the final result we are interested in the Green's function expressed in terms of the "natural" momenta ω and k. One finds that the connection between these variables is given by

$$k_T + k_X = \frac{\omega + k}{2\pi T_R}, \qquad k_T - k_X = \frac{\omega - k}{2\pi T_L}. \tag{C.1.9}$$

The Dirac equation in Fourier space is then

$$\left[\Gamma^{\underline{\rho}}\left(\partial_\rho + \frac{1}{2}\left(\frac{\cosh\rho}{\sinh\rho} + \frac{\sinh\rho}{\cosh\rho}\right)\right) + i\left(\frac{k_X\Gamma^{\underline{X}}}{\cosh\rho} - \frac{k_T\Gamma^{\underline{T}}}{\sinh\rho}\right) - m\right]\psi = 0, \tag{C.1.10}$$

[77] In the main text we have considered the case where $T_L = T_R$ and thus $r_- = 0$, which is the non-rotating BTZ black hole. However, the retarded Green's function can be derived for the generic spinning black hole, so we do not need to make such an assumption in this derivation.

where all the gamma matrices appearing in the expression are flat space matrices. Following [55], we then make a convenient choice of gamma matrices $\Gamma^{\underline{\rho}} = \sigma^3$, $\Gamma^{\underline{T}} = i\sigma^2$, $\Gamma^{\underline{X}} = \sigma^1$, in which case we can write the spinor as $\psi = (\psi_+, \psi_-)^T$, with the subscript of the components denoting their eigenvalue under the action of the $\Gamma^{\underline{\rho}}$ matrix. Following [217], we rescale the two degrees of freedom by introducing

$$\psi_\pm \equiv \sqrt{\frac{\cosh\rho \pm \sinh\rho}{\cosh\rho\sinh\rho}}\,(\chi_1 \pm \chi_2)\,, \qquad z = \tanh^2\rho\,. \tag{C.1.11}$$

In the coordinate z, the asymptotic boundary is located at $z = 1$ and the horizon of the black hole is at $z = 0$. After some algebra the Dirac equations can be written as

$$2(1-z)\sqrt{z}\partial_z\chi_1 - i\left(\frac{k_T}{\sqrt{z}} + k_X\sqrt{z}\right)\chi_1 = \left(m - \frac{1}{2} + i(k_T + k_X)\right)\chi_2 \tag{C.1.12a}$$

$$2(1-z)\sqrt{z}\partial_z\chi_2 + i\left(\frac{k_T}{\sqrt{z}} + k_X\sqrt{z}\right)\chi_2 = \left(m - \frac{1}{2} - i(k_T + k_X)\right)\chi_1. \tag{C.1.12b}$$

It is straightforward to transform these two equations into second order differential equations for a single variable. One finds that the solutions to these equations are the hypergeometric functions ${}_2F_1(a,b,c;z)$. As we wish to calculate the retarded correlator, we follow [49] and choose the solutions that are ingoing at the horizon. These are of the form

$$\chi_1(z) = \left(\frac{a-c}{c}\right) z^{\frac{1}{2}+\alpha}(1-z)^\beta {}_2F_1(a, b+1; c+1; z) \tag{C.1.13a}$$

$$\chi_2(z) = z^\alpha(1-z)^\beta {}_2F_1(a,b;c;z)\,, \tag{C.1.13b}$$

with

$$\alpha = -\frac{ik_T}{2}, \tag{C.1.14a}$$

$$\beta = -\frac{1}{4} + \frac{m}{2}\,, \tag{C.1.14b}$$

$$a = \frac{1}{2}\left(m + \frac{1}{2}\right) - \frac{i}{2}\,(k_T - k_X)\,, \tag{C.1.14c}$$

$$b = \frac{1}{2}\left(m - \frac{1}{2}\right) - \frac{i}{2}\,(k_T + k_X)\,, \tag{C.1.14d}$$

$$c = \frac{1}{2} - ik_T. \tag{C.1.14e}$$

These solutions give us the following asymptotic behaviour

$$\psi_+ \sim A(1-z)^{\frac{1}{2}-\frac{m}{2}} + B(1-z)^{1+\frac{m}{2}}\,, \quad \psi_- \sim C(1-z)^{1-\frac{m}{2}} + D(1-z)^{\frac{1}{2}+\frac{m}{2}}. \tag{C.1.15}$$

Assuming $m > 0$, the source is taken to be A and the expectation value is D. The retarded Green's function is then given by their ratio

$$G^R = i\frac{D}{A} = -i\,\frac{\Gamma\left(\frac{1}{2}-m\right)\Gamma\left(\frac{m}{2}+\frac{1}{4}+\frac{i(k-\omega)}{4\pi T_L}\right)\Gamma\left(\frac{m}{2}+\frac{3}{4}-\frac{i(k+\omega)}{4\pi T_R}\right)}{\Gamma\left(\frac{1}{2}+m\right)\Gamma\left(-\frac{m}{2}+\frac{3}{4}+\frac{i(k-\omega)}{4\pi T_L}\right)\Gamma\left(-\frac{m}{2}+\frac{1}{4}-\frac{i(k+\omega)}{4\pi T_R}\right)}\,. \tag{C.1.16}$$

This is the result (81) of [55]. In the case of $T_L = T_R$ we obtain the result (3.89) presented in the main text.

C.1.2 Advanced Green's Function

To calculate the *advanced* Green's function, we need the solutions that are outgoing at the horizon. These take on the same form as (C.1.11), only that $\chi_1(z) \leftrightarrow \chi_2(z)$ and the parameters in the solutions are now

$$\alpha = \frac{ik_T}{2}, \qquad \beta = -\frac{1}{4}+\frac{m}{2}\,, \tag{C.1.17}$$

and

$$a = \frac{1}{2}\left(m+\frac{1}{2}\right)+\frac{i}{2}\left(k_T-k_X\right), \tag{C.1.18a}$$

$$b = \frac{1}{2}\left(m-\frac{1}{2}\right)+\frac{i}{2}\left(k_T+k_X\right), \tag{C.1.18b}$$

$$c = \frac{1}{2}+ik_T. \tag{C.1.18c}$$

Following the same steps as in the calculation of the retarded Green's function, the advanced Green's function works out to be

$$G^A = i\,\frac{\Gamma\left(\frac{1}{2}-m\right)\Gamma\left(\frac{m}{2}+\frac{1}{4}-\frac{i(k-\omega)}{4\pi T_L}\right)\Gamma\left(\frac{m}{2}+\frac{3}{4}+\frac{i(k+\omega)}{4\pi T_R}\right)}{\Gamma\left(\frac{1}{2}+m\right)\Gamma\left(-\frac{m}{2}+\frac{3}{4}-\frac{i(k-\omega)}{4\pi T_L}\right)\Gamma\left(-\frac{m}{2}+\frac{1}{4}+\frac{i(k+\omega)}{4\pi T_R}\right)}\,. \tag{C.1.19}$$

C.1.3 Equivalence at Matsubara Frequencies

The hypergeometric functions in (C.1.13) are well-defined at generic values of their arguments. The exception is when c is equal to a non-positive integer which is the case if $ik_T \to \frac{1}{2}+n$, where $n \in \{0,1,\dots\}$. This corresponds to taking the frequency to be equal to the (negative imaginary) Matsubara frequencies $\omega_n = -i\pi T(2n+1)$. By taking this limit we can investigate what happens to the ingoing solutions near such points.

It turns out that the ingoing solutions blow up as $ik_T \to \frac{1}{2}+n$, so we divide by

another infinite factor to extract the finite piece

$$\widetilde{\psi}_{\text{in}}(z) \equiv \lim_{ik_T \to \frac{1}{2}+n} \frac{\psi_{\text{in}}(z)}{\Gamma\left(\frac{1}{2} - ik_T\right)}. \tag{C.1.20}$$

It turns out that in this limit the ingoing and outgoing solutions are degenerate

$$\widetilde{\psi}_{\text{in}}(z) = \frac{\Gamma\left(\frac{\Delta+n-ik_X}{2}\right)\Gamma\left(\frac{\Delta+1+n+ik_X}{2}\right)}{\Gamma(1+n)\,\Gamma\left(\frac{\Delta-n-ik_X}{2}\right)\Gamma\left(\frac{\Delta-1-n+ik_X}{2}\right)}\,\psi_{\text{out}}(z)\,, \tag{C.1.21}$$

where we have used the fact that the mass and the conformal dimension of dual fields are related by

$$\Delta = \frac{D+1}{2} + m, \tag{C.1.22}$$

which in the case of the BTZ black hole ($D = 1$) gives

$$\Delta = 1 + m\,. \tag{C.1.23}$$

Since the ingoing and outgoing solutions are proportional to each other with their ratio independent of z, we conclude that the retarded and advanced Green's functions are equivalent at these Matsubara frequencies.

C.2 Green's Functions at Half-Integer Conformal Dimension

At half-integer values of the mass m, calculating the Green's function is not as straightforward because the exponents in (C.1.15) differ by an integer, which results in logarithms appearing in the expansion near the boundary. The expansion of the hypergeometric function that is appropriate to use here is

$$\begin{aligned}
&{}_2F_1(a,b;a+b-n;z) = \\
&\frac{(n-1)!\Gamma(a+b-n)}{\Gamma(a)\Gamma(b)}\sum_{j=0}^{n-1}\frac{(a-n)_j(b-n)_j(1-z)^{j-n}}{j!(1-n)_j} + (-1)^n\frac{\Gamma(a+b-n)}{\Gamma(a-n)\Gamma(b-n)}\times \\
&\sum_{j=0}^{\infty}\frac{(a)_j(b)_j}{j!(j+n)!}(1-z)^j\Big[\psi(j+1)+\psi(j+n+1)-\log(1-z)-\psi(a+j)-\psi(b+j)\Big],
\end{aligned} \tag{C.2.1}$$

where the arguments are given in (C.1.13), $n = \Delta - \frac{3}{2}$ and is an integer, $(x)_j \equiv \frac{\Gamma(x+j)}{\Gamma(x)}$ is the Pochhammer symbol and $\psi(x)$ is the digamma function.

C.2.1 Retarded Green's Function

We can truncate the sum at $j = 0$ which yields the overall coefficient of the leading and subleading contributions that are important in the computation of the retarded Green's function. The terms in the expansion of the prefactors of (C.1.13) only contribute to the contact terms so we can ignore them.[78] After inserting the solutions (C.1.13) into (C.1.11) we can read off the expectation value and the source term in the boundary theory. The former is given by

$$D = (-1)^n \left(\frac{a-c}{c}\right) \frac{\Gamma(a+b+1-n)}{\Gamma(a-n)\Gamma(b+1-n)} \frac{1}{n!} \left[\psi(1)+\psi(n+1)-\psi(a)-\psi(b+1)\right] \\ -(-1)^n \frac{\Gamma(a+b-n)}{\Gamma(a-n)\Gamma(b-n)} \frac{1}{n!} \left[\psi(1)+\psi(n+1)-\psi(a)-\psi(b)\right] \tag{C.2.2}$$

where the first term comes from $\chi_1(z)$ and the second from $\chi_2(z)$. The source is

$$A = \left(\frac{a-c}{c}\right) \frac{(n-1)!\Gamma(a+b+1+n)}{\Gamma(a)\Gamma(b+1)} + \frac{(n-1)!\Gamma(a+b-n)}{\Gamma(a)\Gamma(b)}, \tag{C.2.3}$$

where again the first term comes from $\chi_1(z)$ and the second from $\chi_2(z)$. The retarded Green's function is then given by

$$G^R(\omega,k) \propto \frac{\Gamma\left(\frac{\Delta}{2}-\frac{1}{4}+i\frac{(k-\omega)}{4\pi T}\right)\Gamma\left(\frac{\Delta}{2}+\frac{1}{4}-i\frac{(k+\omega)}{4\pi T}\right)}{\Gamma\left(-\frac{\Delta}{2}+\frac{5}{4}+i\frac{(k-\omega)}{4\pi T}\right)\Gamma\left(-\frac{\Delta}{2}+\frac{3}{4}-i\frac{(k+\omega)}{4\pi T}\right)} \times \\ \left[\psi\left(\frac{\Delta}{2}-\frac{1}{4}+i\frac{(k-\omega)}{4\pi T}\right)+\psi\left(\frac{\Delta}{2}+\frac{1}{4}-i\frac{(k+\omega)}{4\pi T}\right)\right], \tag{C.2.4}$$

up to contact terms.

[78] The prefactors z^α and $z^{\frac{1}{2}+\alpha}$ in (C.1.13) have contributions to the overall expansion of $\psi_\pm$ and can typically be expanded near the boundary in the following way

$$z^\gamma = \sum_{j=0}^{\infty} \frac{1}{j!} \frac{\Gamma(\gamma+1)}{\Gamma(\gamma-j+1)} (z-1)^j.$$

In our analysis, we do not take into account these additional terms.

C.2.2 Advanced Green's Function

Following the same steps as above but keeping in mind that $\chi_1(z) \leftrightarrow \chi_2(z)$ in the case of the outgoing solutions, the advanced Green's function turns out to be

$$G^A(\omega,k) \propto \frac{\Gamma\left(\frac{\Delta}{2}+\frac{1}{4}-i\frac{(k-\omega)}{4\pi T}\right)\Gamma\left(\frac{\Delta}{2}-\frac{1}{4}+i\frac{(k+\omega)}{4\pi T}\right)}{\Gamma\left(\frac{3}{4}-\frac{\Delta}{2}-i\frac{(k-\omega)}{4\pi T}\right)\Gamma\left(\frac{5}{4}-\frac{\Delta}{2}+i\frac{(k+\omega)}{4\pi T}\right)}\times \left[\psi\left(\frac{\Delta}{2}+\frac{1}{4}-\frac{i(k-\omega)}{4\pi T}\right)+\psi\left(\frac{\Delta}{2}-\frac{1}{4}+\frac{i(k+\omega)}{4\pi T}\right)\right], \tag{C.2.5}$$

up to contact terms.

Appendix D

Explicit Results in the NS-NS Sector

In this Appendix we collect some results that are omitted in chapter 5.

We begin by identifying which Killing spinors of global $\mathrm{AdS}_3 \times S^3 \times T^4$ correspond to which supersymmetry generators of the CFT. In section 5.4 we have calculated the variations of the dilatino fields generated by the Killing spinor $\zeta_-^{\alpha A}$. Here we present the variations of the components of the gravitino fields obtained by acting with the same spinor and discuss the subtleties arising in the calculation. Furthermore, we give the variation of the fermionic fields generated by the spinor $\zeta_+^{\alpha A}$ and discuss the issues arising in this case. Finally we present the explicit results of the double variations of the components of the B-field in the NS-NS coordinates, which we omitted in the main text.

D.1 Identifying Killing Spinors and CFT Fermionic Generators

Here we present a justification for the identification (5.4.24) and (5.4.25) between the components of the Killing spinors $\zeta_\pm$ and the CFT fermionic generators $G^{\alpha A}_{\pm\frac{1}{2}}$.

As we can see from (5.4.16) and (5.4.17), the spinors $\zeta_\pm$ and $\widetilde{\zeta}_\pm$ are related to the u- and v-dependent part of the Killing spinors, respectively. So they are naturally linked with the left-moving (G) and right-moving ($\widetilde{G}$) sectors of CFT. Therefore, we henceforth focus on the identification in the left-moving sector between $\zeta_\pm$ and $G^{\alpha A}_{\pm\frac{1}{2}}$. From the v-dependence in (5.4.17d), we have the tentative identification

$$\zeta_\pm \longleftrightarrow G^{\alpha A}_{\pm\frac{1}{2}}. \tag{D.1.1}$$

The next issue is to relate the $SU(2)_L \times SU(2)_R$ R-symmetry on the CFT side and

the $SO(4) \cong SU(2)_L \times SU(2)_R$ symmetry of the sphere S^3 on the supergravity side. It is clear that these symmetry groups are to be identified with each other but we would like to "align" them by identifying the "J^3" generators on the two sides.

On the supergravity side, we can write down a set of $SU(2)_L \times SU(2)_R$ generators acting on spinors as

$$J_a = -\frac{i}{4}\left(\Gamma^{\underline{ra}} + \frac{1}{2}\epsilon^{\underline{abc}}\Gamma^{\underline{bc}}\right), \qquad \widetilde{J}_a = -\frac{i}{4}\left(\Gamma^{\underline{ra}} - \frac{1}{2}\epsilon^{\underline{abc}}\Gamma^{\underline{bc}}\right), \tag{D.1.2}$$

or, more explicitly,

$$J_\theta = -\frac{i}{4}\left(\Gamma^{\underline{r\theta}} + \Gamma^{\underline{\widetilde{\phi}\widetilde{\psi}}}\right), \qquad J_{\widetilde{\phi}} = -\frac{i}{4}\left(\Gamma^{\underline{r\widetilde{\phi}}} + \Gamma^{\underline{\widetilde{\psi}\theta}}\right), \qquad J_{\widetilde{\psi}} = -\frac{i}{4}\left(\Gamma^{\underline{r\widetilde{\psi}}} + \Gamma^{\underline{\theta\widetilde{\phi}}}\right), \tag{D.1.3a}$$

$$\widetilde{J}_\theta = -\frac{i}{4}\left(\Gamma^{\underline{r\theta}} - \Gamma^{\underline{\widetilde{\phi}\widetilde{\psi}}}\right), \qquad \widetilde{J}_{\widetilde{\phi}} = -\frac{i}{4}\left(\Gamma^{\underline{r\widetilde{\phi}}} - \Gamma^{\underline{\widetilde{\psi}\theta}}\right), \qquad \widetilde{J}_{\widetilde{\psi}} = -\frac{i}{4}\left(\Gamma^{\underline{r\widetilde{\psi}}} - \Gamma^{\underline{\theta\widetilde{\phi}}}\right). \tag{D.1.3b}$$

These matrices satisfy the commutation relations

$$[J_a, J_b] = i\epsilon_{abc}J_c, \qquad [\widetilde{J}_a, \widetilde{J}_b] = i\epsilon_{abc}\widetilde{J}_c, \qquad [J_a, \widetilde{J}_b] = 0, \tag{D.1.4}$$

and have Casimir operators given by

$$J^2 = \left(J_\theta^2 + J_{\widetilde{\phi}}^2 + J_{\widetilde{\psi}}^2\right) = \frac{3}{8}\left(1 - \Gamma^{\underline{r\theta\widetilde{\phi}\widetilde{\psi}}}\right), \quad \widetilde{J}^2 = \left(\widetilde{J}_\theta^2 + \widetilde{J}_{\widetilde{\phi}}^2 + \widetilde{J}_{\widetilde{\psi}}^2\right) = \frac{3}{8}\left(1 + \Gamma^{\underline{r\theta\widetilde{\phi}\widetilde{\psi}}}\right). \tag{D.1.5}$$

We turn our focus to the action of these matrices on the spinors $\zeta_\pm$. Recall that these spinors must satisfy the conditions (5.4.19) and (5.4.22). Combining these two implies that they must satisfy

$$\Gamma^{\underline{uvr\theta\widetilde{\phi}\widetilde{\psi}}}\zeta_\pm = \zeta_\pm. \tag{D.1.6}$$

From this condition together with (5.4.23), we find that

$$\Gamma^{\underline{r\theta\widetilde{\phi}\widetilde{\psi}}}\zeta_\pm = -\zeta_\pm\,. \tag{D.1.7}$$

From the Casimir operators (D.1.5), we conclude that $\zeta_\pm$ transform in the $(\mathbf{2},\mathbf{1})$ representation under the $SU(2)_L \times SU(2)_R$ generated by $J_a, \widetilde{J}_a$. This is as expected, because $\zeta_\pm$ is to be identified with $G^{\alpha A}_{\pm\frac{1}{2}}$ which transform in the same representation under the R-symmetry.

We need to identify which of the operators in (D.1.2) corresponds to the "J^3" operator of the $SU(2)_L$ algebra on the CFT side. This operator allows us to distinguish

between the spinor components corresponding to $G^{+A}_{\pm\frac{1}{2}}$ and $G^{-A}_{\pm\frac{1}{2}}$. In order to see that, we look at the spinor (5.4.16). By setting $\widetilde{\zeta}_{\pm}=0$, we obtain a spinor with terms that contain the combination $Y_+\zeta_\pm$. Using the constraint (D.1.7) one can show that the combination appearing in the spinor can be rewritten as

$$Y_+\zeta_\pm = e^{\frac{\theta}{2}\Gamma^{r\theta}}\Big(e^{i\frac{\tilde{\phi}+\tilde{\psi}}{2}}\mathcal{P}^+_S + e^{-i\frac{\tilde{\phi}+\tilde{\psi}}{2}}\mathcal{P}^-_S\Big)\zeta_\pm\,, \tag{D.1.8}$$

where $\mathcal{P}^\pm_S$ is the projection operator onto the $J_{\tilde{\psi}}=\pm\frac{1}{2}$ eigenspace defined in (5.4.24). Because the algebra (4.5.8) says that $\{G^{\pm A}_{\frac{1}{2}}, G^{\pm B}_{-\frac{1}{2}}\}\sim J^\pm_0$, a double variation by $\zeta_\pm$ should reproduce the bosonic symmetry $J^\pm_0$ whose realisation is given in (5.3.15). Since $J^\pm_0$ include a prefactor of $e^{\pm i(\tilde{\phi}+\tilde{\psi})}$, we conclude that the $J_{\tilde{\psi}}=\pm\frac{1}{2}$ eigenspaces, multiplied by $e^{\pm i\frac{\tilde{\phi}+\tilde{\psi}}{2}}$ in (D.1.8), are precisely the $J_3=\pm\frac{1}{2}$ eigenspaces. Namely, $J_{\tilde{\psi}}$ can be identified with J^3_0 on the CFT side. This leads to a finer identification

$$\mathcal{P}^\alpha_S\zeta_\pm \;\longleftrightarrow\; G^{\alpha A}_{\pm\frac{1}{2}}. \tag{D.1.9}$$

One can repeat the procedure for the $SU(2)_B\times SU(2)_C$ symmetry on the CFT side, which is to be identified with the symmetry of the internal T^4 on the supergravity side. We can write down a set of supergravity generators of $SU(2)_B\times SU(2)_C$ in the spinor representation as follows:

$$\begin{aligned}
B_1 &= -\frac{i}{4}\left(\Gamma^{\underline{78}}-\Gamma^{\underline{69}}\right), \qquad B_2 = -\frac{i}{4}\left(\Gamma^{\underline{86}}-\Gamma^{\underline{79}}\right), \qquad B_3 = -\frac{i}{4}\left(\Gamma^{\underline{67}}-\Gamma^{\underline{89}}\right),\\
C_1 &= -\frac{i}{4}\left(\Gamma^{\underline{78}}+\Gamma^{\underline{69}}\right), \qquad C_2 = -\frac{i}{4}\left(\Gamma^{\underline{86}}+\Gamma^{\underline{79}}\right), \qquad C_3 = -\frac{i}{4}\left(\Gamma^{\underline{67}}+\Gamma^{\underline{89}}\right),
\end{aligned} \tag{D.1.10a}$$

which again satisfy the commutation relations

$$[B_i,B_j]=i\epsilon_{ijk}B_k, \qquad [C_i,C_j]=i\epsilon_{ijk}C_k, \qquad [B_i,C_j]=0\,, \tag{D.1.11}$$

and have Casimir operators

$$B^2=\frac{3}{8}\left(1+\Gamma^{\underline{6789}}\right), \qquad C^2=\frac{3}{8}\left(1-\Gamma^{\underline{6789}}\right). \tag{D.1.12}$$

Since our spinors satisfy the condition (5.4.22), we see that $\zeta_\pm$ both transform in the $(\mathbf{2},\mathbf{1})$ representation under $SU(2)_B\times SU(2)_C$ generated by B_i, C_i. This is accordance with the fact that $G^{\alpha A}_{\pm\frac{1}{2}}$ transform in the same representation under $SU(2)_B\times SU(2)_C$.

However, unlike the case of $SU(2)_L\times SU(2)_R$, there is no unique way to align the $SU(2)_B\times SU(2)_C$ groups between supergravity and CFT, because our ansatz (4.2.7) does not distinguish the four directions inside the internal T^4. As a result, in the Killing

spinors (5.4.16), no Γ matrix with legs in the T^4 appear, and all $\Gamma^{\underline{k}}$ with $k = 6, 7, 8, 9$ are on an equal footing. Therefore, we can choose the "J^3" direction of $SU(2)_B$ as we like. Specifically, we define the projectors $\mathcal{P}^A_T$, $A = 1, 2$ by (5.4.24) and identify its A index with the A index of $G^{\alpha A}_{\pm\frac{1}{2}}$. This leads to the final identification

$$\zeta^{\alpha A}_{\pm} = \mathcal{P}^{\alpha}_S \mathcal{P}^A_T \zeta_{\pm} \;\longleftrightarrow\; G^{\alpha A}_{\pm\frac{1}{2}} \tag{D.1.13}$$

which is (5.4.25) in the main text.

D.2 Gravitino Variations Generated by $\zeta^{\alpha A}_{-}$

One finds that the variations of the components of the gravitino field generated by the spinor (5.5.1) are given by

$$\begin{aligned}
\delta\psi^1_{u,b} = &-\frac{ba^k \sin^{k-1}\theta}{4\sqrt{2}R_y \left(r^2+a^2\right)^{\frac{k+1}{2}}} e^{-i\beta_1}\Bigg[k\left(iR_- + R_+\widehat{\Gamma}^{\underline{vr}}\right)\left(\cos\theta\Gamma^{\underline{r\theta}} - i\Gamma^{\underline{r\widetilde{\phi}}} + \sin\theta\right) \\
&- i\frac{\sqrt{r^2+a^2}}{a}\left(R_+\left(R^4_- + k\right) - iR_-\widehat{\Gamma}^{\underline{vr}}\left(R^4_+ + k\right)\right)\sin\theta\Bigg] Y_+ \zeta^{\alpha A}_-\,, \qquad \text{(D.2.1a)} \\
\delta\psi^1_{v,b} = &-\frac{ba^k \sin^{k-1}\theta}{4\sqrt{2}R_y \left(r^2+a^2\right)^{\frac{k+1}{2}}} e^{-i\beta_1}\Bigg[k\left(iR^3_+ + R^3_-\widehat{\Gamma}^{\underline{vr}}\right)\left(\cos\theta\Gamma^{\underline{r\theta}} - i\Gamma^{\underline{r\widetilde{\phi}}} + \sin\theta\right) \\
&- (ik+i)\frac{\sqrt{r^2+a^2}}{a}\left(R_+ - iR_-\widehat{\Gamma}^{\underline{vr}}\right)\sin\theta\Bigg] Y_+ \zeta^{\alpha A}_-\,, \qquad \text{(D.2.1b)} \\
\delta\psi^1_{r,b} = &-\frac{ba^k \sin^{k-1}\theta}{4\left(r^2+a^2\right)^{\frac{k+2}{2}}} e^{-i\beta_1}\Bigg[k\left(-R_- - iR_+\widehat{\Gamma}^{\underline{vr}}\right)\left(\cos\theta\Gamma^{\underline{r\theta}} - i\Gamma^{\underline{r\widetilde{\phi}}} + \sin\theta\right) \\
&+ \frac{\sqrt{r^2+a^2}}{a}\left(R_+\left(1 - \frac{kr}{\sqrt{1+r^2}}\right) + iR_-\left(1 + \frac{kr}{\sqrt{1+r^2}}\right)\widehat{\Gamma}^{\underline{vr}}\right)\sin\theta\Bigg] Y_+ \zeta^{\alpha A}_-\,, \qquad \text{(D.2.1c)} \\
\delta\psi^1_{\theta,b} = &-\frac{ba^k \sin^{k-1}\theta}{4\left(r^2+a^2\right)^{\frac{k+1}{2}}} e^{-i\beta_1}\Bigg[k\left(R_- - iR_+\widehat{\Gamma}^{\underline{vr}}\right)\Gamma^{\underline{r\theta}}\left(\cos\theta\Gamma^{\underline{r\theta}} - i\Gamma^{\underline{r\widetilde{\phi}}} + \sin\theta\right) \\
&+ \frac{\sqrt{r^2+a^2}}{a}\left(R_+ - iR_-\widehat{\Gamma}^{\underline{vr}}\right)\left(k\cos\theta + \sin\theta\Gamma^{\underline{r\theta}}\right)\Bigg] Y_+ \zeta^{\alpha A}_-\,, \qquad \text{(D.2.1d)} \\
\delta\psi^1_{\widetilde{\phi},b} = &-\frac{ba^k \sin^{k}\theta}{4\left(r^2+a^2\right)^{\frac{k+1}{2}}} e^{-i\beta_1}\Bigg[k\left(R_- - iR_+\widehat{\Gamma}^{\underline{vr}}\right)\Gamma^{\underline{r\widetilde{\phi}}}\left(\cos\theta\Gamma^{\underline{r\theta}} - i\Gamma^{\underline{r\widetilde{\phi}}} + \sin\theta\right) \\
&+ \frac{\sqrt{r^2+a^2}}{a}\left(R_+ - iR_-\widehat{\Gamma}^{\underline{vr}}\right)\left(\sin\theta\Gamma^{\underline{r\widetilde{\phi}}} - ik\right)\Bigg] Y_+ \zeta^{\alpha A}_-\,, \qquad \text{(D.2.1e)} \\
\delta\psi^1_{\widetilde{\psi},b} = &-\frac{ba^k \sin^{k-1}\theta\cos\theta}{4\left(r^2+a^2\right)^{\frac{k+1}{2}}} e^{-i\beta_1}\Bigg[k\left(R_- - iR_+\widehat{\Gamma}^{\underline{vr}}\right)\Gamma^{\underline{r\widetilde{\psi}}}\left(\cos\theta\Gamma^{\underline{r\theta}} - i\Gamma^{\underline{r\widetilde{\phi}}} + \sin\theta\right) \\
&+ \frac{\sqrt{r^2+a^2}}{a}\left(R_+ - iR_-\widehat{\Gamma}^{\underline{vr}}\right)\sin\theta\Gamma^{\underline{r\widetilde{\psi}}}\Bigg] Y_+ \zeta^{\alpha A}_-\,, \qquad \text{(D.2.1f)}
\end{aligned}$$

$$\delta\psi^1_{k,b} = 0\,, \qquad k = 6,7,8,9, \tag{D.2.1g}$$

where

$$\beta_1 \equiv k\Big(\frac{u+v}{\sqrt{2}R_y} + \widetilde{\phi}\Big) + \frac{v}{\sqrt{2}R_y} = \hat{v}_{k,0,\frac{1}{2}}\,. \tag{D.2.2}$$

Note that, for the variations generated by spinor (5.5.1), we have $\delta\psi^1_{M,b} = \delta\psi^2_{M,b}$ for all M. We find that the gravitino variations (D.2.1) generically have two parts. The first one is analogous to the dilatino variation, as it contains the combination $(\cos\theta\Gamma^{r\theta} - i\Gamma^{r\widetilde{\phi}} + \sin\theta)$, which when acting on the combination $(Y_+\zeta^{\alpha A}_-)$ projects out the ζ^{-A}_- components of the spinor. This part is again expected from the fact that the perturbed geometry is dual to an anti-chiral primary state. The second part of the variations (given in the second lines of the respective variations) does not distinguish between the ζ^{+A}_- and ζ^{-A}_- components of the spinors. We believe that these extra factors are related to the residual gauge freedom that we have in our system and one should be able to consistently ignore these extra factors. This claim is further strengthened by the fact that once we use these fermionic variations to calculate the double variations of bosonic fields, these additional terms consistently cancel out and thus do not contribute to any observable fields.

D.3 Fermionic Variations Generated by $\zeta^{\alpha A}_+$

The claim that the extra terms found in (D.2.1) can be set to zero by gauge transformation is further supported by calculating the variations of fermionic fields generated by the Killing spinor components $\zeta^{\alpha A}_+$. Since these are dual to the modes $G^{\alpha A}_{+\frac{1}{2}}$, the variations should vanish. Furthermore, one should not obtain any terms that would distinguish between the ζ^{+A}_+ and ζ^{-A}_+ components as now variations generated by both should vanish. If we set $\zeta^{\alpha A}_- = 0$ and make $\zeta^{\alpha A}_+$ arbitrary, the spinor that generates the variation is given by

$$\epsilon^1 = -\epsilon^2 = \frac{1}{2}\left(iR_-\widehat{\Gamma}^{\underline{vr}} + R_+\right) Y_+\zeta^{\alpha A}_+ e^{\frac{iv}{\sqrt{2}R_y}}\,. \tag{D.3.1}$$

Using this spinor as the generator of the solutions, one obtains that the explicit variations of the fermionic fields are given by

$$\delta\lambda^1_b = 0, \tag{D.3.2a}$$

$$\delta\psi^1_{u,b} = -\frac{ba^{k-1}\sin^k\theta}{4\sqrt{2}R_y\left(a^2+r^2\right)^{k/2}} e^{-i\beta_2}\left[\left(iR^4_+ - ik\right) iR_-\widehat{\Gamma}^{\underline{vr}} + \left(iR^4_- - ik\right) R_+\right] Y_+\zeta^{\alpha A}_+ \tag{D.3.2b}$$

$$\delta\psi^1_{v,b} = -\frac{ba^{k-1}\sin^k\theta}{4\sqrt{2}R_y\left(a^2+r^2\right)^{k/2}}e^{-i\beta_2}(i-ik)\left(iR_-\widehat{\Gamma}^{\underline{vr}}+R_+\right)Y_+\zeta_+^{\alpha A} \tag{D.3.2c}$$

$$\begin{aligned}\delta\psi^1_{r,b} = -\frac{ba^{k-1}\sin^k\theta}{4\left(a^2+r^2\right)^{\frac{k+1}{2}}}e^{-i\beta_2}\Bigg[&\left(-1-\frac{kr}{\sqrt{a^2+r^2}}\right)iR_-\widehat{\Gamma}^{\underline{vr}}\\&+\left(1-\frac{kr}{\sqrt{a^2+r^2}}\right)R_+\Bigg]Y_+\zeta_+^{\alpha A}\end{aligned} \tag{D.3.2d}$$

$$\delta\psi^1_{\theta,b} = -\frac{ba^{k-1}\sin^{k-1}\theta}{4\left(a^2+r^2\right)^{k/2}}e^{-i\beta_2}\left(R_+ + iR_-\widehat{\Gamma}^{\underline{vr}}\right)\left(k\cos\theta+\sin\theta\Gamma^{\underline{r\theta}}\right)Y_+\zeta_+^{\alpha A} \tag{D.3.2e}$$

$$\delta\psi^1_{\widetilde{\phi},b} = -\frac{ba^{k-1}\sin^k\theta}{4\left(a^2+r^2\right)^{k/2}}e^{-i\beta_2}\left(R_+ + iR_-\widehat{\Gamma}^{\underline{vr}}\right)\left(-ik+\sin\theta\Gamma^{\underline{r\widetilde{\phi}}}\right)Y_+\zeta_+^{\alpha A} \tag{D.3.2f}$$

$$\delta\psi^1_{\widetilde{\psi},b} = -\frac{ba^{k-1}\sin^k\theta\cos\theta}{4\left(a^2+r^2\right)^{k/2}}e^{-i\beta_2}\left(R_+ + iR_-\widehat{\Gamma}^{\underline{vr}}\right)\Gamma^{\underline{r\psi}}Y_+\zeta_+^{\alpha A}\,, \tag{D.3.2g}$$

$$\delta\psi^1_{k,b} = 0\,, \qquad k=6,7,8,9\,, \tag{D.3.2h}$$

where

$$\beta_2 \equiv k\Big(\frac{u+v}{\sqrt{2}R_y}+\widetilde{\phi}\Big)-\frac{v}{\sqrt{2}R_y} = \hat{v}_{k,0,-\frac{1}{2}}, \tag{D.3.3}$$

and $\delta\lambda^1_b = \delta\lambda^2_b$, $\delta\psi^1_{M,b} = \delta\psi^2_{M,b}$. We see that the variations of the dilatino fields vanish, as expected. On the other hand, the variations of the components of the gravitino fields do not vanish. However, note that these variations only contain the terms which we deemed as a consequence of the gauge freedom in our system and lacks the term which would distinguish between the two $SU(2)_L$ components. Since these variations should be trivial, we get another confirmation that these terms appearing in the gravitino variations are not physical.

D.4 Variations of the B-Field

The non-vanishing term in the double B-field variation is given by

$$\delta'\delta B_{\mu\nu} = 2\bar{\epsilon}\,\Gamma_{[\mu}\sigma^3\delta'\widetilde{\psi}_{\nu]} = 2\left(\epsilon_1\right)^T\Gamma^{\underline{t}}\left(\Gamma_\mu\delta\widetilde{\psi}^1_\nu-\Gamma_\nu\delta'\widetilde{\psi}^1_\mu\right)\,, \tag{D.4.1}$$

where in the last term we again used the fact that the only non-zero spinor components used to generate the variations are ζ_-^{+A}. The variations of the individual components of the B-field in the NS-NS sector are then given by

$$B_{uv} = -2bka^{k-\frac{5}{2}}R_y^{-\frac{3}{2}}\frac{r\sin^{k-1}\theta\cos\theta}{\left(r^2+a^2\right)^{\frac{k-1}{2}}}\,e^{-i\beta_3}\mathcal{A} \tag{D.4.2a}$$

$$B_{ur} = B_{vr} = -\sqrt{2}ibka^{k-\frac{1}{2}}R_y^{-\frac{1}{2}}\frac{\sin^{k-1}\theta\cos\theta}{\left(r^2+a^2\right)^{\frac{k+1}{2}}}\,e^{-i\beta_3}\mathcal{A} \tag{D.4.2b}$$

$$B_{u\widetilde{\psi}} = -B_{v\widetilde{\psi}} = \sqrt{2}bka^{k-\frac{1}{2}}R_y^{-\frac{1}{2}}\frac{\sin^{k-1}\theta\cos\theta}{(r^2+a^2)^{\frac{k+1}{2}}}\,e^{-i\beta_3}\mathcal{A} \tag{D.4.2c}$$

$$B_{r\widetilde{\psi}} = -2ibka^{k-\frac{1}{2}}R_y^{\frac{1}{2}}\frac{\sin^{k-1}\theta\,\cos\theta}{(r^2+a^2)^{\frac{k+1}{2}}}\,e^{-i\beta_3}\mathcal{A} \tag{D.4.2d}$$

$$B_{\widetilde{\phi}\widetilde{\psi}} = 2bka^{k-\frac{1}{2}}R_y^{\frac{1}{2}}\frac{r\sin^{k+1}\theta\cos\theta}{(r^2+a^2)^{\frac{k+1}{2}}}\,e^{-i\beta_3}\mathcal{A} \tag{D.4.2e}$$

$$B_{u\theta} = -B_{v\theta} = \sqrt{2}ibkR_y^{-\frac{1}{2}}a^{k-\frac{1}{2}}\frac{r\sin^{k}\theta}{(r^2+a^2)^{\frac{k+1}{2}}}\,e^{-i\beta_3}\mathcal{A} \tag{D.4.2f}$$

$$B_{\theta\widetilde{\phi}} = -2ibkR_y^{\frac{1}{2}}a^{k-\frac{1}{2}}\frac{r\sin^{k}\theta}{(r^2+a^2)^{\frac{k+1}{2}}}\,e^{-i\beta_3}\mathcal{A} \tag{D.4.2g}$$

$$B_{r\theta} = 2bka^{k-\frac{1}{2}}R_y^{\frac{1}{2}}\frac{\sin^{k}\theta}{(r^2+a^2)^{\frac{k+1}{2}}}\,e^{-i\beta_3}\mathcal{A} \tag{D.4.2h}$$

$$B_{u\widetilde{\phi}} = B_{v\widetilde{\phi}} = B_{\theta\widetilde{\psi}} = B_{r\widetilde{\phi}} = 0 \tag{D.4.2i}$$

where

$$\beta_3 \equiv k\Big(\frac{u+v}{\sqrt{2}R_y} + \widetilde{\phi}\Big) + \sqrt{2}\frac{v}{R_y} - (\widetilde{\phi}+\widetilde{\psi}), \tag{D.4.3}$$

$$\mathcal{A} = \Big[\big(\zeta_-^{+1}\big)^T i\Gamma^{\overline{r\theta}}\zeta_-'^{+2}\Big]. \tag{D.4.4}$$

Bibliography

[1] N. Čeplak, R. Russo and M. Shigemori, *Supercharging Superstrata*, *JHEP* **03** (2019) 095 [1812.08761].

[2] N. Ceplak, K. Ramdial and D. Vegh, *Fermionic pole-skipping in holography*, 1910.02975.

[3] H. Young, R. Freedman, T. Sandin and A. Ford, *Sears and Zemansky's University Physics*, no. v. 1 in Addison-Wesley series in physics. Addison-Wesley, 2000.

[4] K. Blundell, *Black Holes: A Very Short Introduction*, Very Short Introductions. OUP Oxford, 2015.

[5] A. Celotti, J. C. Miller and D. W. Sciama, *Astrophysical evidence for the existence of black holes*, *Class. Quant. Grav.* **16** (1999) A3 [astro-ph/9912186].

[6] A. M. Ghez et al., *Measuring Distance and Properties of the Milky Way's Central Supermassive Black Hole with Stellar Orbits*, *Astrophys. J.* **689** (2008) 1044 [0808.2870].

[7] LIGO Scientific, Virgo collaboration, *Observation of Gravitational Waves from a Binary Black Hole Merger*, *Phys. Rev. Lett.* **116** (2016) 061102 [1602.03837].

[8] Event Horizon Telescope collaboration, *First M87 Event Horizon Telescope Results. I. The Shadow of the Supermassive Black Hole*, *Astrophys. J.* **875** (2019) L1 [1906.11238].

[9] R. Penrose, *Gravitational collapse and space-time singularities*, *Phys. Rev. Lett.* **14** (1965) 57.

[10] S. Hawking and R. Penrose, *The Singularities of gravitational collapse and cosmology*, *Proc. Roy. Soc. Lond. A* **A314** (1970) 529.

[11] S. W. Hawking and G. F. R. Ellis, *The Large Scale Structure of Space-Time*. Cambridge University Press.

[12] R. M. Wald, *General Relativity*, p. 212, Chicago Univ. Pr., (1984).

[13] R. Kippenhahn and A. Weigert, *Stellar Structure and Evolution*. 1990.

[14] S. Hawking and J. Hartle, *Energy and angular momentum flow into a black hole*, *Commun. Math. Phys.* **27** (1972) 283.

[15] J. M. Bardeen, B. Carter and S. Hawking, *The Four laws of black hole mechanics*, *Commun. Math. Phys.* **31** (1973) 161.

[16] J. D. Bekenstein, *Black holes and entropy*, *Phys. Rev.* **D7** (1973) 2333.

[17] S. W. Hawking, *Particle Creation by Black Holes*, *Commun. Math. Phys.* **43** (1975) 199.

[18] B. Carter, *Axisymmetric Black Hole Has Only Two Degrees of Freedom*, *Phys.Rev.Lett.* **26** (1971) 331.

[19] D. Robinson, *Uniqueness of the Kerr black hole*, *Phys.Rev.Lett.* **34** (1975) 905.

[20] D. N. Page, *Information in black hole radiation*, *Phys. Rev. Lett.* **71** (1993) 3743 [hep-th/9306083].

[21] D. N. Page, *Time Dependence of Hawking Radiation Entropy*, *JCAP* **1309** (2013) 028 [1301.4995].

[22] I. Bena, S. El-Showk and B. Vercnocke, *Black Holes in String Theory*, *Springer Proc.Phys.* **144** (2013) 59.

[23] A. Almheiri, D. Marolf, J. Polchinski and J. Sully, *Black Holes: Complementarity or Firewalls?*, *JHEP* **1302** (2013) 062 [1207.3123].

[24] R. Blumenhagen, D. Lüst and S. Theisen, *Basic concepts of string theory*, Theoretical and Mathematical Physics. Springer, Heidelberg, Germany, 2013, 10.1007/978-3-642-29497-6.

[25] M. Ammon and J. Erdmenger, *Gauge/gravity duality: Foundations and applications*. Cambridge University Press, Cambridge, 4, 2015.

[26] O. Aharony, S. S. Gubser, J. M. Maldacena, H. Ooguri and Y. Oz, *Large N field theories, string theory and gravity*, *Phys. Rept.* **323** (2000) 183 [hep-th/9905111].

[27] J. Polchinski, *Dirichlet-Branes and Ramond-Ramond Charges*, *Phys. Rev. Lett.* **75** (1995) 4724 [hep-th/9510017].

[28] S. Majumdar, *A class of exact solutions of Einstein's field equations*, *Phys. Rev.* **72** (1947) 390.

[29] A. Papapetrou, *Einstein's theory of gravitation and flat space*, *Proc. Roy. Irish Acad. A* **52A** (1948) 11.

[30] C. V. Johnson, *D-branes*.

[31] H. Nastase, *Introduction to the ADS/CFT Correspondence*. Cambridge University Press, 9, 2015.

[32] E. Witten, *Anti-de Sitter space and holography*, *Adv. Theor. Math. Phys.* **2** (1998) 253 [hep-th/9802150].

[33] D. J. Gross and E. Witten, *Superstring Modifications of Einstein's Equations*, *Nucl. Phys. B* **277** (1986) 1.

[34] M. T. Grisaru, A. van de Ven and D. Zanon, *Four Loop beta Function for the N=1 and N=2 Supersymmetric Nonlinear Sigma Model in Two-Dimensions*, *Phys. Lett. B* **173** (1986) 423.

[35] M. T. Grisaru and D. Zanon, *σ Model Superstring Corrections to the Einstein-hilbert Action*, *Phys. Lett. B* **177** (1986) 347.

[36] D. A. Galante and R. C. Myers, *Holographic Renyi entropies at finite coupling*, *JHEP* **08** (2013) 063 [1305.7191].

[37] S. s. Grozdanov, N. Kaplis and A. O. Starinets, *From strong to weak coupling in holographic models of thermalization*, *JHEP* **07** (2016) 151 [1605.02173].

[38] R. C. Myers, M. F. Paulos and A. Sinha, *Quantum corrections to eta/s*, *Phys. Rev. D* **79** (2009) 041901 [0806.2156].

[39] S. S. Gubser, I. R. Klebanov and A. A. Tseytlin, *Coupling constant dependence in the thermodynamics of N=4 supersymmetric Yang-Mills theory*, *Nucl. Phys. B* **534** (1998) 202 [hep-th/9805156].

[40] J. Pawelczyk and S. Theisen, *AdS(5) x S**5 black hole metric at O(alpha-prime**3)*, *JHEP* **09** (1998) 010 [hep-th/9808126].

[41] J. M. Maldacena, *The large N limit of superconformal field theories and supergravity*, *Adv. Theor. Math. Phys.* **2** (1998) 231 [hep-th/9711200].

[42] O. Aharony, O. Bergman, D. L. Jafferis and J. Maldacena, *N=6 superconformal Chern-Simons-matter theories, M2-branes and their gravity duals*, *JHEP* **10** (2008) 091 [0806.1218].

[43] I. Heemskerk, J. Penedones, J. Polchinski and J. Sully, *Holography from Conformal Field Theory*, *JHEP* **10** (2009) 079 [0907.0151].

[44] O. DeWolfe, *TASI Lectures on Applications of Gauge/Gravity Duality*, *PoS* **TASI2017** (2018) 014 [1802.08267].

[45] J. Penedones, *TASI lectures on AdS/CFT*, in *Proceedings, Theoretical Advanced Study Institute in Elementary Particle Physics: New Frontiers in Fields and Strings (TASI 2015): Boulder, CO, USA, June 1-26, 2015*, pp. 75–136, 2017, DOI [1608.04948].

[46] E. D'Hoker and D. Z. Freedman, *Supersymmetric gauge theories and the AdS / CFT correspondence*, in *Strings, Branes and Extra Dimensions: TASI 2001: Proceedings*, pp. 3–158, 1, 2002, hep-th/0201253.

[47] E. Witten, *Anti-de Sitter space, thermal phase transition, and confinement in gauge theories*, *Adv. Theor. Math. Phys.* **2** (1998) 505 [hep-th/9803131].

[48] S. S. Gubser, I. R. Klebanov and A. M. Polyakov, *Gauge theory correlators from non-critical string theory*, *Phys. Lett.* **B428** (1998) 105 [hep-th/9802109].

[49] D. T. Son and A. O. Starinets, *Minkowski space correlators in AdS / CFT correspondence: Recipe and applications*, *JHEP* **09** (2002) 042 [hep-th/0205051].

[50] G. T. Horowitz and V. E. Hubeny, *Quasinormal modes of AdS black holes and the approach to thermal equilibrium*, *Phys. Rev.* **D62** (2000) 024027 [hep-th/9909056].

[51] C. P. Herzog and D. T. Son, *Schwinger-Keldysh propagators from AdS/CFT correspondence*, *JHEP* **03** (2003) 046 [hep-th/0212072].

[52] K. Skenderis and B. C. van Rees, *Real-time gauge/gravity duality*, *Phys. Rev. Lett.* **101** (2008) 081601 [0805.0150].

[53] K. Skenderis and B. C. van Rees, *Real-time gauge/gravity duality: Prescription, Renormalization and Examples*, *JHEP* **05** (2009) 085 [0812.2909].

[54] D. T. Son and D. Teaney, *Thermal Noise and Stochastic Strings in AdS/CFT*, *JHEP* **07** (2009) 021 [0901.2338].

[55] N. Iqbal and H. Liu, *Real-time response in AdS/CFT with application to spinors*, *Fortsch. Phys.* **57** (2009) 367 [0903.2596].

[56] B. C. van Rees, *Real-time gauge/gravity duality and ingoing boundary conditions*, *Nucl. Phys. Proc. Suppl.* **192-193** (2009) 193 [0902.4010].

[57] P. Glorioso, M. Crossley and H. Liu, *A prescription for holographic Schwinger-Keldysh contour in non-equilibrium systems*, 1812.08785.

[58] H. Liu and J. Sonner, *Holographic systems far from equilibrium: a review*, 1810.02367.

[59] J. de Boer, M. P. Heller and N. Pinzani-Fokeeva, *Holographic Schwinger-Keldysh effective field theories*, *JHEP* **05** (2019) 188 [1812.06093].

[60] N. Birrell and P. Davies, *Quantum Fields in Curved Space*, Cambridge Monographs on Mathematical Physics. Cambridge Univ. Press, Cambridge, UK, 2, 1984, 10.1017/CBO9780511622632.

[61] M. Banados, M. Henneaux, C. Teitelboim and J. Zanelli, *Geometry of the (2+1) black hole*, *Phys. Rev.* **D48** (1993) 1506 [gr-qc/9302012].

[62] M. Banados, C. Teitelboim and J. Zanelli, *The Black hole in three-dimensional space-time*, *Phys. Rev. Lett.* **69** (1992) 1849 [hep-th/9204099].

[63] J. Kapusta and C. Gale, *Finite-temperature field theory: Principles and applications*, Cambridge Monographs on Mathematical Physics. Cambridge University Press, 2011, 10.1017/CBO9780511535130.

[64] D. Birmingham, *Choptuik scaling and quasinormal modes in the AdS / CFT correspondence*, *Phys. Rev.* **D64** (2001) 064024 [hep-th/0101194].

[65] V. Cardoso and J. P. S. Lemos, *Scalar, electromagnetic and Weyl perturbations of BTZ black holes: Quasinormal modes*, *Phys. Rev.* **D63** (2001) 124015 [gr-qc/0101052].

[66] D. Birmingham, I. Sachs and S. N. Solodukhin, *Conformal field theory interpretation of black hole quasinormal modes*, *Phys. Rev. Lett.* **88** (2002) 151301 [hep-th/0112055].

[67] P. Kovtun, D. T. Son and A. O. Starinets, *Viscosity in strongly interacting quantum field theories from black hole physics*, *Phys. Rev. Lett.* **94** (2005) 111601 [hep-th/0405231].

[68] S. Grozdanov, K. Schalm and V. Scopelliti, *Black hole scrambling from hydrodynamics*, *Phys. Rev. Lett.* **120** (2018) 231601 [1710.00921].

[69] M. Blake, H. Lee and H. Liu, *A quantum hydrodynamical description for scrambling and many-body chaos*, *JHEP* **10** (2018) 127 [1801.00010].

[70] M. Blake, R. A. Davison, S. Grozdanov and H. Liu, *Many-body chaos and energy dynamics in holography*, *JHEP* **10** (2018) 035 [1809.01169].

[71] S. Grozdanov, *On the connection between hydrodynamics and quantum chaos in holographic theories with stringy corrections*, *JHEP* **01** (2019) 048 [1811.09641].

[72] M. Blake, R. A. Davison and D. Vegh, *Horizon constraints on holographic Green's functions*, 1904.12883.

[73] S. Grozdanov, P. K. Kovtun, A. O. Starinets and P. Tadić, *The complex life of hydrodynamic modes*, 1904.12862.

[74] M. Natsuume and T. Okamura, *Holographic chaos, pole-skipping, and regularity*, 1905.12014.

[75] M. Natsuume and T. Okamura, *Nonuniqueness of Green's functions at special points*, 1905.12015.

[76] J. Maldacena, S. H. Shenker and D. Stanford, *A bound on chaos*, *JHEP* **08** (2016) 106 [1503.01409].

[77] S. H. Shenker and D. Stanford, *Black holes and the butterfly effect*, *JHEP* **03** (2014) 067 [1306.0622].

[78] S. H. Shenker and D. Stanford, *Multiple Shocks*, *JHEP* **12** (2014) 046 [1312.3296].

[79] S. H. Shenker and D. Stanford, *Stringy effects in scrambling*, *JHEP* **05** (2015) 132 [1412.6087].

[80] D. A. Roberts, D. Stanford and L. Susskind, *Localized shocks*, *JHEP* **03** (2015) 051 [1409.8180].

[81] T. Andrade and B. Withers, *A simple holographic model of momentum relaxation*, *JHEP* **05** (2014) 101 [1311.5157].

[82] R. A. Davison and B. Gouteraux, *Momentum dissipation and effective theories of coherent and incoherent transport*, *JHEP* **01** (2015) 039 [1411.1062].

[83] F. M. Haehl and M. Rozali, *Effective Field Theory for Chaotic CFTs*, *JHEP* **10** (2018) 118 [1808.02898].

[84] Y. Gu, X.-L. Qi and D. Stanford, *Local criticality, diffusion and chaos in generalized Sachdev-Ye-Kitaev models*, *JHEP* **05** (2017) 125 [1609.07832].

[85] R. A. Davison, W. Fu, A. Georges, Y. Gu, K. Jensen and S. Sachdev, *Thermoelectric transport in disordered metals without quasiparticles: The Sachdev-Ye-Kitaev models and holography*, *Phys. Rev.* **B95** (2017) 155131 [1612.00849].

[86] M. Blake and A. Donos, *Diffusion and Chaos from near AdS_2 horizons*, *JHEP* **02** (2017) 013 [1611.09380].

[87] M. Blake, *Universal Diffusion in Incoherent Black Holes*, *Phys. Rev.* **D94** (2016) 086014 [1604.01754].

[88] M. Blake, *Universal Charge Diffusion and the Butterfly Effect in Holographic Theories*, *Phys. Rev. Lett.* **117** (2016) 091601 [1603.08510].

[89] M. Blake, R. A. Davison and S. Sachdev, *Thermal diffusivity and chaos in metals without quasiparticles*, *Phys. Rev.* **D96** (2017) 106008 [1705.07896].

[90] N. Ceplak and D. Vegh, *To appear*, .

[91] M. Henningson and K. Sfetsos, *Spinors and the AdS / CFT correspondence*, *Phys. Lett.* **B431** (1998) 63 [hep-th/9803251].

[92] W. Mueck and K. S. Viswanathan, *Conformal field theory correlators from classical field theory on anti-de Sitter space. 2. Vector and spinor fields*, *Phys. Rev.* **D58** (1998) 106006 [hep-th/9805145].

[93] N. Iqbal and H. Liu, *Universality of the hydrodynamic limit in AdS/CFT and the membrane paradigm*, *Phys. Rev.* **D79** (2009) 025023 [0809.3808].

[94] S. Corley, *The Massless gravitino and the AdS / CFT correspondence*, *Phys. Rev.* **D59** (1999) 086003 [hep-th/9808184].

[95] A. Volovich, *Rarita-Schwinger field in the AdS / CFT correspondence*, *JHEP* **09** (1998) 022 [hep-th/9809009].

[96] R. C. Rashkov, *Note on the boundary terms in AdS / CFT correspondence for Rarita-Schwinger field*, *Mod. Phys. Lett.* **A14** (1999) 1783 [hep-th/9904098].

[97] A. S. Koshelev and O. A. Rytchkov, *Note on the massive Rarita-Schwinger field in the AdS / CFT correspondence*, *Phys. Lett.* **B450** (1999) 368 [hep-th/9812238].

[98] P. Matlock and K. S. Viswanathan, *The AdS / CFT correspondence for the massive Rarita-Schwinger field*, *Phys. Rev.* **D61** (2000) 026002 [hep-th/9906077].

[99] J. T. Liu, L. A. Pando Zayas and Z. Yang, *Small Treatise on Spin-3/2 Fields and their Dual Spectral Functions*, *JHEP* **02** (2014) 095 [1401.0008].

[100] S. Das, B. Ezhuthachan and A. Kundu, *Real Time Dynamics in Low Point Correlators*, 1907.08763.

[101] G. Policastro, *Supersymmetric hydrodynamics from the AdS/CFT correspondence*, *JHEP* **02** (2009) 034 [0812.0992].

[102] C. G. Callan and J. M. Maldacena, *D-brane Approach to Black Hole Quantum Mechanics*, *Nucl. Phys.* **B472** (1996) 591 [hep-th/9602043].

[103] S. Giusto, L. Martucci, M. Petrini and R. Russo, *6D microstate geometries from 10D structures*, *Nucl.Phys.* **B876** (2013) 509 [1306.1745].

[104] E. Bergshoeff, R. Kallosh, T. Ortin, D. Roest and A. Van Proeyen, *New formulations of D = 10 supersymmetry and D8 - O8 domain walls*, *Class. Quant. Grav.* **18** (2001) 3359 [hep-th/0103233].

[105] S. Giusto and R. Russo, *Superdescendants of the D1D5 CFT and their dual 3-charge geometries*, *JHEP* **1403** (2014) 007 [1311.5536].

[106] J. B. Gutowski, D. Martelli and H. S. Reall, *All supersymmetric solutions of minimal supergravity in six dimensions*, *Class. Quant. Grav.* **20** (2003) 5049 [hep-th/0306235].

[107] M. Cariglia and O. A. P. Mac Conamhna, *The General form of supersymmetric solutions of N=(1,0) U(1) and SU(2) gauged supergravities in six-dimensions*, *Class. Quant. Grav.* **21** (2004) 3171 [hep-th/0402055].

[108] I. Bena, S. Giusto, M. Shigemori and N. P. Warner, *Supersymmetric Solutions in Six Dimensions: A Linear Structure*, *JHEP* **1203** (2012) 084 [1110.2781].

[109] M. Shigemori, *Superstrata*, 2002.01592.

[110] I. Bena, S. Giusto, R. Russo, M. Shigemori and N. P. Warner, *Habemus Superstratum! A constructive proof of the existence of superstrata*, *JHEP* **05** (2015) 110 [1503.01463].

[111] N. P. Warner, *Lectures on Microstate Geometries*, 1912.13108.

[112] S. Hyun, *U duality between three-dimensional and higher dimensional black holes*, *J. Korean Phys. Soc.* **33** (1998) S532 [hep-th/9704005].

[113] J. Maharana and J. H. Schwarz, *Noncompact symmetries in string theory*, *Nucl. Phys. B* **390** (1993) 3 [hep-th/9207016].

[114] K. Skenderis and M. Taylor, *The fuzzball proposal for black holes*, *Phys. Rept.* **467** (2008) 117 [0804.0552].

[115] S. D. Mathur, *The fuzzball proposal for black holes: An elementary review*, *Fortsch. Phys.* **53** (2005) 793 [hep-th/0502050].

[116] A. Strominger and C. Vafa, *Microscopic Origin of the Bekenstein-Hawking Entropy*, *Phys. Lett.* **B379** (1996) 99 [hep-th/9601029].

[117] J. M. Maldacena, *Black holes and D-branes*, *NATO Sci. Ser. C* **520** (1999) 219 [hep-th/9705078].

[118] J. M. Maldacena, *Black holes in string theory*, hep-th/9607235.

[119] J. M. Maldacena and L. Susskind, *D-branes and Fat Black Holes*, *Nucl. Phys.* **B475** (1996) 679 [hep-th/9604042].

[120] G. Andrews, *The Theory of Partitions*, Cambridge mathematical library. Cambridge University Press, 1998.

[121] A. Sen, *Microscopic and Macroscopic Entropy of Extremal Black Holes in String Theory*, *Gen. Rel. Grav.* **46** (2014) 1711 [1402.0109].

[122] J. R. David, G. Mandal and S. R. Wadia, *Microscopic formulation of black holes in string theory*, *Phys. Rept.* **369** (2002) 549 [hep-th/0203048].

[123] S. G. Avery, *Using the D1D5 CFT to Understand Black Holes*, 1012.0072.

[124] P. Di Francesco, P. Mathieu and D. Senechal, *Conformal Field Theory*, Graduate Texts in Contemporary Physics. Springer-Verlag, New York, 1997, 10.1007/978-1-4612-2256-9.

[125] F. Larsen and E. J. Martinec, *U(1) charges and moduli in the D1-D5 system*, *JHEP* **06** (1999) 019 [hep-th/9905064].

[126] I. Bena, S. Giusto, E. J. Martinec, R. Russo, M. Shigemori, D. Turton et al., *Asymptotically-flat supergravity solutions deep inside the black-hole regime*, *JHEP* **02** (2018) 014 [1711.10474].

[127] L. Eberhardt, M. R. Gaberdiel and R. Gopakumar, *The Worldsheet Dual of the Symmetric Product CFT*, *JHEP* **04** (2019) 103 [1812.01007].

[128] L. Eberhardt, M. R. Gaberdiel and R. Gopakumar, *Deriving the AdS_3/CFT_2 correspondence*, *JHEP* **02** (2020) 136 [1911.00378].

[129] M. Baggio, J. de Boer and K. Papadodimas, *A non-renormalization theorem for chiral primary 3-point functions*, *JHEP* **07** (2012) 137 [1203.1036].

[130] A. Bombini, A. Galliani, S. Giusto, E. Moscato and R. Russo, *Unitary 4-point correlators from classical geometries*, 1710.06820.

[131] A. Schwimmer and N. Seiberg, *Comments on the N=2, N=3, N=4 Superconformal Algebras in Two-Dimensions*, *Phys.Lett.* **B184** (1987) 191.

[132] A. Galliani, S. Giusto and R. Russo, *Holographic 4-point correlators with heavy states*, *JHEP* **10** (2017) 040 [1705.09250].

[133] I. Bena, E. Martinec, D. Turton and N. P. Warner, *Momentum Fractionation on Superstrata*, *JHEP* **05** (2016) 064 [1601.05805].

[134] M. Shigemori, *Counting Superstrata*, *JHEP* **10** (2019) 017 [1907.03878].

[135] J. M. Maldacena and A. Strominger, *AdS(3) black holes and a stringy exclusion principle*, *JHEP* **12** (1998) 005 [hep-th/9804085].

[136] S. Deger, A. Kaya, E. Sezgin and P. Sundell, *Spectrum of D = 6, N = 4b supergravity on AdS(3) x S(3)*, *Nucl. Phys.* **B536** (1998) 110 [hep-th/9804166].

[137] F. Larsen, *The Perturbation spectrum of black holes in N=8 supergravity*, *Nucl. Phys.* **B536** (1998) 258 [hep-th/9805208].

[138] J. de Boer, *Six-dimensional supergravity on S**3 x AdS(3) and 2-D conformal field theory*, *Nucl. Phys.* **B548** (1999) 139 [hep-th/9806104].

[139] O. Lunin and S. D. Mathur, *AdS/CFT duality and the black hole information paradox*, *Nucl. Phys.* **B623** (2002) 342 [hep-th/0109154].

[140] O. Lunin, J. M. Maldacena and L. Maoz, *Gravity solutions for the D1-D5 system with angular momentum*, hep-th/0212210.

[141] M. Taylor, *General 2 charge geometries*, *JHEP* **03** (2006) 009 [hep-th/0507223].

[142] I. Kanitscheider, K. Skenderis and M. Taylor, *Holographic anatomy of fuzzballs*, *JHEP* **04** (2007) 023 [hep-th/0611171].

[143] I. Kanitscheider, K. Skenderis and M. Taylor, *Fuzzballs with internal excitations*, *JHEP* **06** (2007) 056 [0704.0690].

[144] A. Almheiri, D. Marolf, J. Polchinski, D. Stanford and J. Sully, *An Apologia for Firewalls*, *JHEP* **09** (2013) 018 [1304.6483].

[145] S. D. Mathur and D. Turton, *The flaw in the firewall argument*, *Nucl.Phys.* **B884** (2014) 566 [1306.5488].

[146] J. Maldacena and L. Susskind, *Cool horizons for entangled black holes*, *Fortsch. Phys.* **61** (2013) 781 [1306.0533].

[147] S. W. Hawking, M. J. Perry and A. Strominger, *Soft Hair on Black Holes*, *Phys. Rev. Lett.* **116** (2016) 231301 [1601.00921].

[148] S. Haco, S. W. Hawking, M. J. Perry and A. Strominger, *Black Hole Entropy and Soft Hair*, *JHEP* **12** (2018) 098 [1810.01847].

[149] I. Bena and N. P. Warner, *Black holes, black rings and their microstates*, *Lect. Notes Phys.* **755** (2008) 1 [hep-th/0701216].

[150] S. D. Mathur, *Fuzzballs and the information paradox: A Summary and conjectures*, 0810.4525.

[151] I. Bena and N. P. Warner, *Resolving the Structure of Black Holes: Philosophizing with a Hammer*, 1311.4538.

[152] A. Strominger, *AdS(2) quantum gravity and string theory*, *JHEP* **01** (1999) 007 [hep-th/9809027].

[153] V. Cardoso, O. J. C. Dias, J. L. Hovdebo and R. C. Myers, *Instability of non-supersymmetric smooth geometries*, *Phys. Rev.* **D73** (2006) 064031 [hep-th/0512277].

[154] B. D. Chowdhury and S. D. Mathur, *Radiation from the non-extremal fuzzball*, *Class. Quant. Grav.* **25** (2008) 135005 [0711.4817].

[155] B. D. Chowdhury and S. D. Mathur, *Pair creation in non-extremal fuzzball geometries*, *Class. Quant. Grav.* **25** (2008) 225021 [0806.2309].

[156] B. D. Chowdhury and S. D. Mathur, *Non-extremal fuzzballs and ergoregion emission*, *Class. Quant. Grav.* **26** (2009) 035006 [0810.2951].

[157] S. G. Avery and B. D. Chowdhury, *Emission from the D1D5 CFT: Higher Twists*, *JHEP* **1001** (2010) 087 [0907.1663].

[158] S. D. Mathur, *The information paradox: A pedagogical introduction*, *Class. Quant. Grav.* **26** (2009) 224001 [0909.1038].

[159] E. J. Martinec and S. Massai, *String Theory of Supertubes*, 1705.10844.

[160] E. J. Martinec, S. Massai and D. Turton, *String dynamics in NS5-F1-P geometries*, *JHEP* **09** (2018) 031 [1803.08505].

[161] E. J. Martinec, S. Massai and D. Turton, *Little Strings, Long Strings, and Fuzzballs*, *JHEP* **11** (2019) 019 [1906.11473].

[162] I. Bena and N. P. Warner, *Bubbling supertubes and foaming black holes*, *Phys. Rev.* **D74** (2006) 066001 [hep-th/0505166].

[163] P. Berglund, E. G. Gimon and T. S. Levi, *Supergravity microstates for BPS black holes and black rings*, *JHEP* **0606** (2006) 007 [hep-th/0505167].

[164] S. D. Mathur, A. Saxena and Y. K. Srivastava, *Constructing 'hair' for the three charge hole*, *Nucl. Phys.* **B680** (2004) 415 [hep-th/0311092].

[165] O. Lunin, *Adding momentum to D1-D5 system*, *JHEP* **04** (2004) 054 [hep-th/0404006].

[166] S. Giusto, S. D. Mathur and A. Saxena, *Dual geometries for a set of 3-charge microstates*, *Nucl. Phys.* **B701** (2004) 357 [hep-th/0405017].

[167] S. Giusto, S. D. Mathur and A. Saxena, *3-charge geometries and their CFT duals*, *Nucl. Phys.* **B710** (2005) 425 [hep-th/0406103].

[168] S. Giusto, S. D. Mathur and Y. K. Srivastava, *A microstate for the 3-charge black ring*, *Nucl. Phys.* **B763** (2007) 60 [hep-th/0601193].

[169] J. Ford, S. Giusto and A. Saxena, *A class of BPS time-dependent 3-charge microstates from spectral flow*, *Nucl. Phys.* **B790** (2008) 258 [hep-th/0612227].

[170] S. D. Mathur and D. Turton, *Microstates at the boundary of AdS*, *JHEP* **05** (2012) 014 [1112.6413].

[171] S. D. Mathur and D. Turton, *Momentum-carrying waves on D1-D5 microstate geometries*, *Nucl.Phys.* **B862** (2012) 764 [1202.6421].

[172] O. Lunin, S. D. Mathur and D. Turton, *Adding momentum to supersymmetric geometries*, *Nucl.Phys.* **B868** (2013) 383 [1208.1770].

[173] S. Giusto, O. Lunin, S. D. Mathur and D. Turton, *D1-D5-P microstates at the cap*, *JHEP* **1302** (2013) 050 [1211.0306].

[174] P. Heidmann, *Four-center bubbled BPS solutions with a Gibbons-Hawking base*, *JHEP* **10** (2017) 009 [1703.10095].

[175] P. Heidmann, D. R. Mayerson, R. Walker and N. P. Warner, *Holomorphic Waves of Black Hole Microstructure*, *JHEP* **02** (2020) 192 [1910.10714].

[176] D. R. Mayerson, R. A. Walker and N. P. Warner, *Microstate Geometries from Gauged Supergravity in Three Dimensions*, 2004.13031.

[177] I. Bena, J. de Boer, M. Shigemori and N. P. Warner, *Double, Double Supertube Bubble*, *JHEP* **10** (2011) 116 [1107.2650].

[178] S. Giusto and R. Russo, *Perturbative superstrata*, *Nucl.Phys.* **B869** (2013) 164 [1211.1957].

[179] I. Bena, S. Giusto, E. J. Martinec, R. Russo, M. Shigemori, D. Turton et al., *Smooth horizonless geometries deep inside the black-hole regime*, *Phys. Rev. Lett.* **117** (2016) 201601 [1607.03908].

[180] I. Bena, E. Martinec, D. Turton and N. P. Warner, *M-theory Superstrata and the MSW String*, *JHEP* **06** (2017) 137 [1703.10171].

[181] E. Bakhshaei and A. Bombini, *Three-charge superstrata with internal excitations*, 1811.00067.

[182] P. Heidmann and N. P. Warner, *Superstratum Symbiosis*, *JHEP* **09** (2019) 059 [1903.07631].

[183] S. Giusto, E. Moscato and R. Russo, *AdS_3 holography for 1/4 and 1/8 BPS geometries*, *JHEP* **11** (2015) 004 [1507.00945].

[184] J. Garcia i Tormo and M. Taylor, *Correlation functions in the D1-D5 orbifold CFT*, *JHEP* **06** (2018) 012 [1804.10205].

[185] F. C. Eperon, H. S. Reall and J. E. Santos, *Instability of supersymmetric microstate geometries*, *JHEP* **10** (2016) 031 [1607.06828].

[186] J. Keir, *Wave propagation on microstate geometries*, 1609.01733.

[187] D. Marolf, B. Michel and A. Puhm, *A rough end for smooth microstate geometries*, *JHEP* **05** (2017) 021 [1612.05235].

[188] F. C. Eperon, *Geodesics in supersymmetric microstate geometries*, *Class. Quant. Grav.* **34** (2017) 165003 [1702.03975].

[189] I. Bena, D. Turton, R. Walker and N. P. Warner, *Integrability and Black-Hole Microstate Geometries*, *JHEP* **11** (2017) 021 [1709.01107].

[190] A. Tyukov, R. Walker and N. P. Warner, *Tidal Stresses and Energy Gaps in Microstate Geometries*, 1710.09006.

[191] I. Bena, E. J. Martinec, R. Walker and N. P. Warner, *Early Scrambling and Capped BTZ Geometries*, 1812.05110.

[192] I. Bena, S. F. Ross and N. P. Warner, *Coiffured Black Rings*, *Class.Quant.Grav.* **31** (2014) 165015 [1405.5217].

[193] K. Skenderis and M. Taylor, *Fuzzball solutions and D1-D5 microstates*, *Phys. Rev. Lett.* **98** (2007) 071601 [hep-th/0609154].

[194] O. Lunin, S. D. Mathur and A. Saxena, *What is the gravity dual of a chiral primary?*, *Nucl. Phys.* **B655** (2003) 185 [hep-th/0211292].

[195] O. Lunin and S. D. Mathur, *Metric of the multiply wound rotating string*, *Nucl. Phys.* **B610** (2001) 49 [hep-th/0105136].

[196] V. Balasubramanian, J. de Boer, E. Keski-Vakkuri and S. F. Ross, *Supersymmetric conical defects: Towards a string theoretic description of black hole formation*, *Phys. Rev.* **D64** (2001) 064011 [hep-th/0011217].

[197] J. M. Maldacena and L. Maoz, *De-singularization by rotation*, *JHEP* **12** (2002) 055 [hep-th/0012025].

[198] H. Lu, C. N. Pope and P. K. Townsend, *Domain walls from anti-de Sitter space-time*, *Phys. Lett.* **B391** (1997) 39 [hep-th/9607164].

[199] H. Lu, C. N. Pope and J. Rahmfeld, *A Construction of Killing spinors on S**n*, *J. Math. Phys.* **40** (1999) 4518 [hep-th/9805151].

[200] B. E. Niehoff and N. P. Warner, *Doubly-Fluctuating BPS Solutions in Six Dimensions*, *JHEP* **1310** (2013) 137 [1303.5449].

[201] R. C. Myers and M. Perry, *Black Holes in Higher Dimensional Space-Times*, *Annals Phys.* **172** (1986) 304.

[202] N. Abbasi and J. Tabatabaei, *Quantum chaos, pole-skipping and hydrodynamics in a holographic system with chiral anomaly*, 1910.13696.

[203] Y. Liu and A. Raju, *Quantum Chaos in Topologically Massive Gravity*, 2005.08508.

[204] S. Raju and P. Shrivastava, *A Critique of the Fuzzball Program*, 1804.10616.

[205] E. J. Martinec, S. Massai and D. Turton, *Stringy Structure at the BPS Bound*, 2005.12344.

[206] V. Jejjala, O. Madden, S. F. Ross and G. Titchener, *Non-supersymmetric smooth geometries and D1-D5-P bound states*, *Phys. Rev.* **D71** (2005) 124030 [hep-th/0504181].

[207] A. Bombini and S. Giusto, *Non-extremal superdescendants of the D1D5 CFT*, *JHEP* **10** (2017) 023 [1706.09761].

[208] A. Bombini and A. Galliani, *AdS_3 four-point functions from $\frac{1}{8}$ -BPS states*, *JHEP* **06** (2019) 044 [1904.02656].

[209] J. M. Maldacena, *Eternal black holes in anti-de Sitter*, *JHEP* **04** (2003) 021 [hep-th/0106112].

[210] S. Giusto, R. Russo and C. Wen, *Holographic correlators in AdS_3*, *JHEP* **03** (2019) 096 [1812.06479].

[211] S. Giusto, R. Russo, A. Tyukov and C. Wen, *Holographic correlators in AdS_3 without Witten diagrams*, *JHEP* **09** (2019) 030 [1905.12314].

[212] S. Giusto, R. Russo, A. Tyukov and C. Wen, *The CFT_6 origin of all tree-level 4-point correlators in $AdS_3 \times S^3$*, 2005.08560.

[213] I. Bena, P. Heidmann, R. Monten and N. P. Warner, *Thermal Decay without Information Loss in Horizonless Microstate Geometries*, *SciPost Phys.* **7** (2019) 063 [1905.05194].

[214] I. Bena, F. Eperon, P. Heidmann and N. P. Warner, *The Great Escape: Tunneling out of Microstate Geometries*, 2005.11323.

[215] M. Bianchi, A. Grillo and J. F. Morales, *Chaos at the rim of black hole and fuzzball shadows*, *JHEP* **05** (2020) 078 [2002.05574].

[216] K. Fransen, G. Koekoek, R. Tielemans and B. Vercnocke, *Modeling and detecting resonant tides of exotic compact objects*, 2005.12286.

[217] S. Das and A. Dasgupta, *Black hole emission rates and the AdS / CFT correspondence*, *JHEP* **10** (1999) 025 [hep-th/9907116].